Selective Salt Recovery from Reverse Osmosis Concentrate Using Interstage Ion Exchange

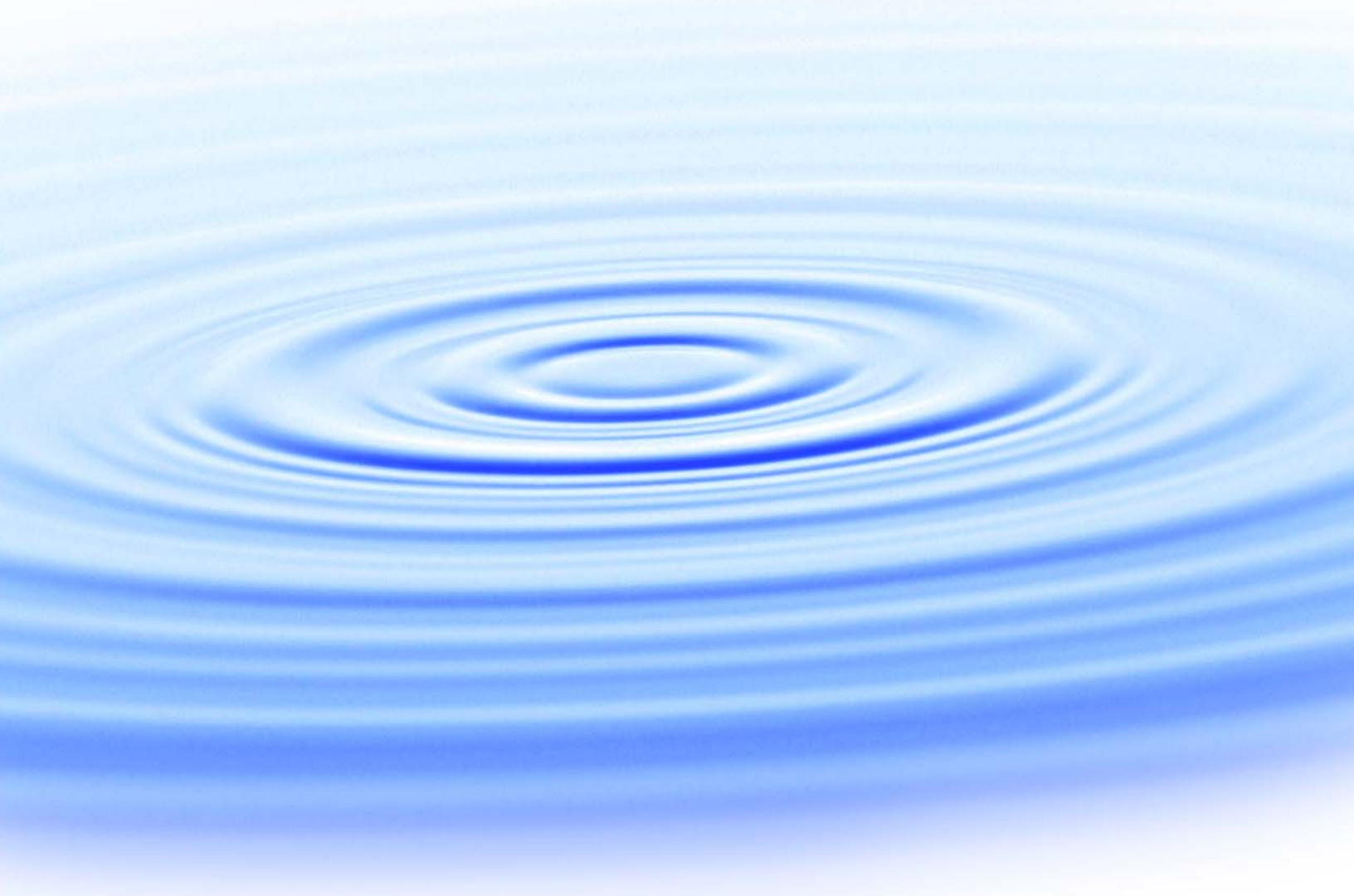

WateReuse Research Foundation

Selective Salt Recovery from Reverse Osmosis Concentrate Using Interstage Ion Exchange

About the WateReuse Research Foundation

The mission of the WateReuse Research Foundation is to conduct and promote applied research on the reclamation, recycling, reuse, and desalination of water. The Foundation's research advances the science of water reuse and supports communities across the United States and abroad in their efforts to create new sources of high quality water through reclamation, recycling, reuse, and desalination while protecting public health and the environment.

The Foundation sponsors research on all aspects of water reuse, including emerging chemical contaminants, microbiological agents, treatment technologies, salinity management and desalination, public perception and acceptance, economics, and marketing. The Foundation's research informs the public of the safety of reclaimed water and provides water professionals with the tools and knowledge to meet their commitment of increasing reliability and quality.

The Foundation's funding partners include the Bureau of Reclamation, the California State Water Resources Control Board, the California Energy Commission, and the California Department of Water Resources. Funding is also provided by the Foundation's Subscribers, water and wastewater agencies, and other interested organizations.

Selective Salt Recovery from Reverse Osmosis Concentrate Using Interstage Ion Exchange

Joshua E. Goldman
University of New Mexico

Kerry J. Howe
University of New Mexico

Bruce M. Thomson
University of New Mexico

Robert Fowlie
CDM Smith

Cosponsors

Bureau of Reclamation
California Department of Water Resources
Sandia National Laboratories

WateReuse Research Foundation
Alexandria, VA

Disclaimer

This report was sponsored by the WateReuse Research Foundation, the Bureau of Reclamation, the Department of Water Resources (CA), and Sandia National Laboratories. The Foundation and its Board Members assume no responsibility for the content of this publication or for the opinions or statements of facts expressed in the report. The mention of trade names of commercial products does not represent or imply the approval or endorsement of the WateReuse Research Foundation or its Board Members. This report is published solely for informational purposes.

For more information, contact:

WateReuse Research Foundation
1199 North Fairfax Street, Suite 410
Alexandria, VA 22314
703-548-0880
703-548-5085 (fax)
www.WateReuse.org/Foundation

WateReuse Research Foundation Project Number: WRF-06-010E
WateReuse Research Foundation Product Number: 06-010E-1

ISBN: 978-1-934183-89-2
Library of Congress Control Number: 2013950006

Printed in the United States of America

Printed on Recycled Paper

Contents

List of Figures ix
List of Tables xii
List of Acronyms xiv
Foreword xv
Acknowledgments xvi
Executive Summary xvii

Chapter 1. Introduction 1
1.1 Introduction 1
1.1.1 Background 1
1.1.2 Objectives 2
1.1.3 Proposed Treatment 2
1.2 Literature Review 6
1.2.1 Ion Exchange 6
1.2.1.1 Selectivity 7
1.2.1.2 Selectivity Modeling 9
1.2.1.3 Column Processes 10
1.2.1.4 Modeling of Column Processes 12
1.2.2 Chemical Precipitation 13

Chapter 2. Modeling 17
2.1 Chapter Objectives 17
2.2 Chapter Summary 17
2.3 Modeling 17

Chapter 3. Dependence of Resin Selectivity on Ionic Strength and Solution Composition 25
3.1 Chapter Objectives 25
3.2 Chapter Summary 25
3.3 Methods 25
3.4 Results 27
3.4.1 Cation Exchange Isotherms 27
3.4.2 Anion Exchange Isotherms 36

Chapter 4. Phase 2—Column Testing for Selectivity Verification and Ion Separation 39
4.1 Chapter Objectives 39
4.2 Chapter Summary 39
4.3 Methods 39
4.3.1 Observed Column Compared with Predictions 40
4.3.2 Separation of Ions by Varying Regeneration Conditions 44
4.3.3 Recovery of Specific Ions from a Loaded Column 45
4.4 Results 46
4.4.1 Column Performance Compared with Predictions 46
4.4.2 Separation of Ions by Varying Regeneration Conditions 50
4.4.3 Recovery of Specific Ions from a Loaded Column 53

Chapter 5. Phase 3—Salt Precipitation 57
5.1 Chapter Objectives 57
5.2 Chapter Summary 57
5.3 Methods 57
5.4 Results 61

Chapter 6. Phase 4—Pilot-Scale Process Testing in Brighton, CO 71
6.1 Pilot Design and Experimental Methods 71
6.1.1 Daily Operation 79
6.1.2 Week 1 79
6.1.3 Week 2 80
6.1.4 Weeks 3 and 4 80
6.1.5 Week 5 80
6.1.6 Week 6 80
6.1.7 Week 7 80
6.1.8 Detailed Data Collection and Analysis Procedures 80
6.2 Pilot Results 87
6.2.1 Mass Analysis 87
6.2.2 Conclusions from Investigation of Precipitate 101
6.2.3 Determination of Most Concentrated Regeneration Solution Fraction 102
6.3 Effect of Antiscalant on Resin Capacity 106
6.4 Optimization of Operation Cycle Length 109
6.5 Reverse Osmosis System Performance in Treating Pilot Effluent 111

Chapter 7. Discussion and Conclusions 115
7.1 Conclusions 115
7.1.1 Ions of Interest Can Be Recovered from Higher-Ionic-Strength Solutions Using Ion Exchange 115

7.1.2 Breakthrough Curves Can Be Predicted Using Separation Factor Regression Relationships and Modeling 116
7.1.3 Calcium and Magnesium Selectivity Are Too Similar for Ion Separation by Regeneration 116
7.1.4 Gypsum Can Be Recovered from a Mixture of Cation and Anion Regeneration Solutions 117
7.2 Discussion 117

References 119

Appendix A. Utility Survey 123
Appendix B. Salt Market Analysis 129
Appendix C. Pilot Data Collection Forms 167
Appendix D. ESPA-2 Datasheet 187

Figures

1.1 Proposed reverse osmosis concentrate treatment train 3
1.2 Research schedule 4
1.3 Ideal resin phase concentration profile from Helfferich (1962) 11
1.4 Loading and regeneration of an ion exchange column (Zagorodni, 2007) 11

2.1 Model scheme 18
2.2 Response to pulse tracer input for tanks-in-series models using different numbers of tanks (Fogler, 1999) 19
2.3 Effluent concentration curves from tanks-in-series models using different numbers of tanks 20
2.4 Effluent concentration curve from MATLAB models using different numbers of segments 20
2.5 Graphical user interface for MATLAB model 21
2.6 Example column snapshot from model 22
2.7 Example breakthrough curve from model 22
2.8 Comparison of column snapshots with different numbers of segments 24

3.1 Resin samples 26
3.2 Atomic absorption spectrometer (left) and ion chromatography system (right) 26
3.3 Calcium separation factors versus equivalent fraction of calcium 29
3.4 Calcium separation factors versus solution ionic strength 29
3.5 Predicted calcium separation factors versus measured calcium separation factors 31
3.6 Modeled breakthrough curves for systems with separation factors ranging from 1.5 to 6 31
3.7 Bed volumes to breakthrough as a function of calcium separation factor 32
3.8 Separation factor as a function of ionic strength and equivalent ionic fraction of calcium 33
3.9 Magnesium separation factors versus. equivalent fraction of magnesium 33
3.10 Magnesium separation factors vs. ionic strength 34
3.11 Predicted magnesium separation factors versus measured magnesium separation factors 35
3.12 Surface plot showing changing separation factor with ionic strength and equivalent ionic fraction 35
3.13 Sulfate separation factor as a function of ionic strength 36
3.14 Sulfate separation factor as a function of ionic fraction 37
3.15 Carbonate separation factor as a function of ionic strength 37
3.16 Carbonate separation factor as a function of equivalent fraction 37

4.1 Phase 2 setup—front (left), back (right) 40
4.2 Modeled breakthrough curves for varied separation factors 40
4.3 Relationship between separation factor and column efficiency 41
4.4 Sulfate separation factor as a function of ionic strength 42
4.5 Specially designed research column with ports 46
4.6 Breakthrough curve from Test #14 48
4.7 Correlation between calculated and measured numbers of bed volumes to calcium breakthrough 48
4.8 Correlation between calculated and measured numbers of bed volumes to magnesium breakthrough 49
4.9 Calcium elution curves measured during standard regeneration 51
4.10 Magnesium elution curves measured during standard regeneration 51
4.11 Elution curves for regeneration variation tests 53
4.12 Resin phase concentration compared to equilibrium resin phase concentration 55
4.13 Distribution of ions in the resin phase axially through a column 55

5.1 Calcite saturation index as a function of pH 58
5.2 SEM image (top 2 graphs) and EDS data (bottom 4 graphs) from Experiments 2A and 4 62
5.3 XRD spectrum from Experiment 2A 63
5.4 Results from liquid analysis of Experiments 2A and 4 64
5.5 SEM images from Experiments 3 and 5–7 65
5.6 EDS data from Experiments 3 and 5–7 66
5.7 XRD spectra from Experiments 3 and 5–7 68
5.8 Estimated salt precipitation for Tests 3, 5 and 6 based on ion concentrations 69

6.1 Pilot schematic 73
6.2 Pilot equipment on site 76
6.3 Pilot equipment including timer, power supply, titration setup, and regeneration pump 77
6.4 Solenoid valves at tops of columns 77
6.5 Solenoid valves at bottoms of columns 78
6.6 Control sequence at pilot input including pressure reducer, solenoid valve, pressure gauge, needle valve, and pressure relief valve 78
6.7 Pilot project schedule 79
6.8 SEM images of precipitate under ambient-pH conditions 89
6.9 SEM images of precipitate from low pH conditions 92
6.10 Semiquantification of EDS spectra showing % composition of spheres identified by SEM 94
6.11 Semiquantification of EDS spectra showing % composition of needles identified by SEM 95
6.12 SEM image showing possible amorphous material 96

6.13 XRD spectra of precipitate samples 97
6.14 Overlaid spectra from XRD analysis 98
6.15 Calculated salt yield per cubic meter of reverse osmosis concentrate for each week at ambient pH 100
6.16 Calculated salt yield per cubic meter of reverse osmosis concentrate for each week at low pH 100
6.17 Difference in yield between precipitation under ambient- and low-pH conditions .. 101
6.18 Elution curve for Week 2 104
6.19 Normalized elution curve for Week 2 104
6.20 Elution curve for Week 5 105
6.21 Normalized elution curve for Week 5 105
6.22 Concentration of Cl, NO_3, and SO_4 on resin stripped (meq/g) 107
6.23 Change in concentration of ions and TOC on anion exchange resin over time 108
6.24 Change in normalized concentration of ions and TOC on anion exchange resin over time 109
6.25 Breakthrough curve from extended operation cycle in Week 3 110
6.26 Normalized permeate flux (from Hydranautics spreadsheet) 112

7.1 Regression relationship for calcium selectivity with ionic fraction and ionic strength 115
7.2 Overlapping concentration curves of calcium and magnesium during regeneration 116
7.3 Comparison between reverse osmosis system at high recovery and reverse osmosis at lower recovery combined with ion exchange 118

Tables

1.1 Reverse Osmosis Parameters 4
1.2 Cations and Anions in Feed Water 4
1.3 Salt Balance 5
1.4 Resin Characteristics 5
1.5 Solubility Constants for Common Precipitates 13

3.1 Matrix of Isotherm Experiments (Ratios Are Based on Molarity) 27
3.2 Cation Exchange Isotherm Tests 28
3.3 Regression Equation and Associated Statistics for Calcium Separation Factors 30
3.4 Parameters for Modeling the Bed Volumes to Breakthrough for Different Separation Factors 30
3.5 Regression Equation and Associated Statistics for Magnesium Separation Factors 34
3.6 Anion Exchange Isotherm Tests 36

4.1 Size of Mass Transfer Zone and Efficiency of Column at Varied Separation Factors 42
4.2 Solution Ion Concentrations and Predicted Values for Selectivity Verification 43
4.3 Ion Concentrations in Solutions Used to Load Column Prior to Regeneration Experiments 45
4.4 Regeneration Operating Conditions 45
4.5 Feed Solution Ion Concentrations and Number of Bed Volumes 46
4.6 Updated versus Original Separation Factor Predictions for Column Tests 47
4.7 Predicted versus Measured Number of Bed Volumes to Breakthrough for Column Tests 49
4.8 Resin Phase Ion Concentrations Measured from Stripped Resin 54
4.9 Solution Concentration and Calculated Separation Factors 54

5.1 Anion and Cation Regeneration Solution Concentrations 59
5.2 Experimental Matrix for Phase 3 59
5.3 Samples Collected from Phase 3 Experiments 60
5.4 Notes for Phase 3 Experiments 60

6.1 Pilot Feed Water Ion Concentrations 72
6.2 Legend for Schematic Diagram 74
6.3 Sampling and Analysis Plan (Objective 1): 83
6.4 Sampling and Analysis Plan (Objective 2): 84
6.5 Sampling and Analysis Plan (Objective 3) 85
6.6 Sampling and Analysis Plan (Breakthrough Curve for Week 3) 86
6.7 Sampling and Analysis Plan for Objective 5 86
6.8 Data Forms and File Names Located in Appendix D 86

6.9 Average Ion Concentrations in the Cation Regeneration Solution 87
6.10 Average Ion Concentrations in the Anion Regeneration Solution 88
6.11 Concentration Factors for Each Ion for Weeks in Which the Entire Regeneration Cycle Was Captured.....88
6.12 Precipitate Mass from Each Week from Ambient- and Low-pH Techniques.....99
6.13 Amount of Cl, NO_3, and SO_4 on Resin Stripped with NaOH (meq/g).....108
6.14 Average Concentrations Ratio (eq) between Calcium and Magnesium.....110
6.15 RO Data Recorded during System Operation 113

Acronyms

AA	atomic absorption
AAS	atomic absorption spectroscopy
DI	deionized water
EDS	energy-dispersive spectroscopy
GUI	graphical user interface
IAP	ion activity product
IC	ion chromatography system
IS	ionic strength
IX	ion exchange
MTZ	mass transfer zone
ppm	parts per million
RO	reverse osmosis
SAC	strong acid cation
SBA	strong base anion
SEM	scanning electron microscopy
SI	saturation index
TDS	total dissolved solids
TIS	tanks in series
TOC	total organic carbon
XRD	X-ray diffraction

Foreword

The WateReuse Research Foundation, a nonprofit corporation, sponsors research that advances the science of water reclamation, recycling, reuse, and desalination. The Foundation funds projects that meet the water reuse and desalination research needs of water and wastewater agencies and the public. The goal of the Foundation's research is to ensure that water reuse and desalination projects provide high-quality water, protect public health, and improve the environment.

An Operating Plan guides the Foundation's research program. Under the plan, a research agenda of high-priority topics is maintained. The agenda is developed in cooperation with the water reuse and desalination communities including water professionals, academics, and Foundation subscribers. The Foundation's research focuses on a broad range of water reuse research topics including:

- Defining and addressing emerging contaminants
- Public perceptions of the benefits and risks of water reuse
- Management practices related to indirect potable reuse
- Groundwater recharge and aquifer storage and recovery
- Evaluation and methods for managing salinity and desalination
- Economics and marketing of water reuse

The Operating Plan outlines the role of the Foundation's Research Advisory Committee (RAC), Project Advisory Committees (PACs), and Foundation staff. The RAC sets priorities, recommends projects for funding, and provides advice and recommendations on the Foundation's research agenda and other related efforts. PACs are convened for each project and provide technical review and oversight. The Foundation's RAC and PACs consist of experts in their fields and provide the Foundation with an independent review, which ensures the credibility of the Foundation's research results. The Foundation's Project Managers facilitate the efforts of the RAC and PACs and provide overall management of projects.

Concentrate management is a major concern for inland users of reverse osmosis because of cost and environmental regulations. Treating concentrates with cation and anion exchange media has the dual benefit of removing sparingly soluble salts and concentrating them within the media. Concentrates treated by ion exchange can be sent to a second reverse osmosis system without the potential of membrane scaling, and the resulting concentrate can be used to regenerate the ion exchange media. The regeneration solutions from the cation and anion exchange media can be captured and mixed to spontaneously precipitate salts. This process improves overall water recovery and generates a usable product from a source normally considered to be waste.

Richard Nagel
Chair
WateReuse Research Foundation

G. Wade Miller
Executive Director
WateReuse Research Foundation

Acknowledgments

This project was funded by the WateReuse Research Foundation with the sopprt of the Bureau of Reclamation, the Department of Water Resources (CA), and Sandia National Laboratories.

The project team would like to thank Robert Fowlie of CDM for preparing the salt market analysis, Abdul-Mehdi S. Ali for maintaining the analytical instrumentation and helping to developing measurement methods, and Lana Mitchell for assisting with lab analyses.

Principal Investigator
Kerry J. Howe, *University of New Mexico.*

Project Team
Joshua E. Goldman, *University of New Mexico*
Kerry J. Howe, *University of New Mexico*
B. M. Thomson, *University of New Mexico*

Participating Agencies
Robert Fowlie, *CDM Smith*
East Cherry Creek Valley Water and Sanitation District

Project Advisory Committee
Jennifer Wong, *CA Department of Water Resources*
Anthony J. Tarquin, *University of Texas at El Paso*
Malynda Cappelle, *The University of Texas at El Paso (formerly with Sandia National Laboratories)*
Jeff Johnson, Southern *Nevada Water Authority*
Scott Irvine, *Bureau of Reclamation*
Pat Brady, *Sandia National Laboratories*

Executive Summary

Background

Concentrate management is a major concern for inland users of reverse osmosis (RO) because of cost and environmental regulations. A seawater RO facility may be able to discharge its concentrate stream into the ocean, but inland brackish water RO facilities must use alternative disposal options. Traditional concentrate disposal methods include discharge to surface water, evaporation, discharge to wastewater treatment plants, and deep well injection. High costs are driving RO users to look for better options, such as the recovery of salts for beneficial reuse. The sale of such products may subsidize the RO process and the reduction in fouling potential allows water to be treated further by RO or another process, resulting in increased water recovery.

This project tested the use of sequential cation and anion exchange between two RO stages. The goals of interstage ion exchange are (1) to remove sparingly soluble salts from RO concentrate so that it can be treated by another RO stage without scaling, and (2) to concentrate sparingly soluble salts during ion exchange column regeneration so that they will spontaneously precipitate when cation and anion exchange regeneration solutions are mixed. Bench- and pilot-scale tests were performed to prove the concepts behind this idea. The overall research objectives were

- To examine the effect of ionic strength and ion proportions on resin selectivity, because RO concentrate has higher ionic strength than waters typically treated by ion exchange.
- To develop a computer model using MATLAB to simulate ion distribution in an ion exchange column based on separation factors found in the resin selectivity investigation.
- To characterize the spatial distribution of ions in an ion exchange column by analysis of resin along the length of an exhausted column.
- To recover selected salts with potential resale value or recyclability by precipitation from mixed regeneration solutions from ion exchange columns.
- To examine the feasibility of using the sodium chloride solution produced by sequential ion exchange as an ion exchange regeneration solution.
- To examine the feasibility of marketing recovered salts in different regions of the United States.

Approach

The effect of ionic strength and ionic composition on resin selectivity was examined through bench scale isotherm tests. A strong acid cation resin (ResinTech) and a strong base anion resin (Purolite) were selected for use. Resins were equilibrated with prepared solutions containing ions typical of RO concentrate, including calcium, magnesium, carbonate, bicarbonate, and sulfate at a range of concentrations. Separation factors were calculated by measuring initial and final (equilibrated) ion concentrations.

MATLAB was used to develop a mathematical model to describe the ion exchange process in a column. The model uses a discretized mass balance approach in which solution and resin equilibrium are found simultaneously using a nonlinear solver. The model works by looping over time and space to produce solution and resin phase ion concentrations (equivalents) for each time step in every column segment. Advective dispersion is not included in the model. Numerical dispersion is inherent in the model, but the effect is reduced as the number of column segments is increased. This phenomenon was used to calibrate the model to match the level of physical dispersion within a column. Model results were compared with lab-scale column tests.

Lab-scale column tests were performed to (1) correlate column performance with selectivity values measured in batch isotherms for similar conditions; (2) separate chromatographic peaks of ions during regeneration by varying regeneration flow rate, concentration, and direction; and (3) recover specific ions from a column by regeneration of a specific portion of a column. Resin phase concentrations of ions in a loaded column were measured using a specially designed column that allowed access to the resin along its longitudinal axis. Resin samples from along the column's length were analyzed to determine the concentrations of ions at each location.

Simulated cation and anion regeneration solutions were mixed in the laboratory to test salt precipitation characteristics. Solution pH was varied during mixing to control carbonate precipitation. Precipitates were analyzed by scanning electron microscopy (SEM), energy-dispersive spectroscopy (EDS), and X-ray diffraction (XRD) to determine their characteristics and mineralogy.

Finally, a pilot study was conducted at a water treatment facility in Brighton, Colorado. The pilot system was run continuously between June 6 and July 7, 2011. The objectives of the pilot study were to

- Determine the consistency of the mass and purity of the recovered salt products.
- Determine the best fraction of the regenerant solution to use for salt recovery. For example, if the first and last quarter of the regeneration process yield low ion concentrations, it may be more useful to collect only the fluid from the middle portion of the process in order to increase the solubility index and precipitate a greater quantity of salt.
- Determine the effect of antiscalant addition on the resin capacity.
- Optimize the operation cycle length to maximize ion concentrations in regeneration solutions and minimize unused cation exchange capacity.
- Determine if pilot effluent recycling affects the performance of the second-stage RO system.

Results

Selectivity

Bench-scale ion exchange isotherms showed that resin selectivity decreased for all divalent ions as ionic strength increased. Some correlation was also found between ionic ratio and selectivity, but the strongest correlation came from a multivariate regression on separation factor as a function of ionic strength and ionic ratio. Regression relationships were developed for calcium, magnesium, and sodium. Although a selectivity decrease was observed,

selectivity remained adequate for a sequential ion exchange process treating most concentrates from a brackish water RO process.

Modeling

The mathematical model developed in MATLAB was able to predict breakthrough curves in laboratory column tests using separation factors based on regression developed from isotherm tests. The output arrays can also be queried in several useful ways to produce snapshots of the entire column and resin- or solution-phase concentrations at any time and location within the column.

Lab-Scale Column Testing

Separation factors calculated from lab-scale column tests correlated well with those measured during isotherm testing. Ion concentration measurements taken during standard regeneration (25 mL/min, 12.5 % NaCl) showed significant overlap of chromatographic peaks. Although flow rate, flow direction, and NaCl concentration were varied to increase peak separation, these methods were not successful. Resin-phase ion concentrations within a loaded column were measured using a column containing multiple ports for resin sampling. Results showed that ions did not form discreet layers during loading, so regeneration of a specific portion of the column would not be useful for single-ion capture.

Precipitation

Equilibrium modeling using Visual MINTEQ showed that that several salts are supersaturated in a mixture of cation and anion regeneration solutions and that adjusting pH can control the precipitation of carbonate salts. When simulated cation and anion regeneration solutions were mixed without pH adjustment, a precipitate containing a heterogeneous mix of phases including halite, bassanite, bassirite, bischofite, and calcium carbonate ($CaCO_3$) was formed. Calcium sulfate precipitated in mixtures in which the pH of the anion regeneration solution was reduced below pH 5 prior to mixing with cation regeneration solution. Precipitates were examined using scanning electron microscopy and crystal phases were determined by X-ray diffraction.

Pilot Study

Mixing pilot-generated cation and anion solutions produced results similar to those found in the laboratory. Calcium sulfate and calcium carbonate were precipitated separately by controlling the pH. When the system was optimized for calcium and sulfate recovery, pH adjustment was not necessary for gypsum precipitation. Regardless of the ionic strength of the mixed cation and anion regeneration solutions (0.6 M to 2.5 M), precipitation occurred spontaneously.

The most concentrated fraction of the regeneration cycle was determined by sampling during the cycle and measuring ion concentrations and conductivity. Peak concentrations were found to occur between 0.67 and 1.17 bed volumes. The operation cycle was optimized to 28 bed volumes, based on breakthrough curves of calcium, magnesium, and sulfate. When collection was limited to the most concentrated fraction and operation cycle length was optimized, salt yield increased almost sixfold. It was possible to generate 12 kg of salt per cubic meter of regeneration solution and to recover approximately 45% of the calcium and approximately 28% of the sulfate from the mixed regeneration solution during this pilot study. This

corresponds to a total recovery of 15% of the possible gypsum contained in the RO concentrate influent to the pilot.

No decrease in anion exchange capacity was found that could be attributed to fouling by antiscalants. The duration of the pilot was too short to make final conclusions about antiscalant effect.

Concentrate from the second-stage RO system was used to regenerate the ion exchange columns. Because it was a low-pressure, single-element unit, the maximum sodium chloride concentration in its concentrate was approximately 1%. Salt was added to increase the sodium chloride concentration to 10% prior to its use for regeneration, and no issues were encountered during this process. The second-stage RO system had several problems during the pilot that made it difficult to determine the effect of treating pilot effluent, although a decrease in specific flux was observed. Further study is required to determine the effect of antiscalant and the effect of treating pilot effect on a second-stage RO system.

Recovering dry salts and or/brine would also be of economic benefit to utilities, as it would reduce the costs of disposal. However, there are challenges to overcome in marketing the salts, such as the existence and size of the local market, salt purity requirements, and treatment costs. The possibility of recovering concentrate salts and/or brine could be evaluated to offset the operations and maintenance cost of operating the plant or as a by-product of a ZLD process incorporated into the design to recover as much water as possible from the plant. It is important to note that the feasibility of selective salt recovery is site-specific, as water quality varies from site to site, and a suitable market may not be available in the vicinity of the proposed treatment plant. Selective salt recovery and maximizing water recovery are also a sustainable solution for concentrate disposal, which is an issue facing every RO treatment plant. The full salt market analysis is located in Appendix B.

Conclusions

Sequential ion exchange has the potential to generate salts from RO concentrate and to increase water recovery from RO systems. Bench-scale tests showed that ions of interest can be recovered from higher-ionic-strength solutions using ion exchange, despite some selectivity decrease. Modeling and regression relationships developed from batch isotherms tests can be used to predict breakthrough curves. Calcium and magnesium selectivity are too similar for ion separation by regeneration variation, but gypsum can be recovered by mixing cation and anion regeneration solutions from an optimized system.

Chapter 1

Introduction

1.1 Introduction

Across the United States and the world, the issue of water scarcity is gaining importance as communities struggle to provide water to their members. The RO treatment process removes dissolved salts from water, producing drinking water from sources that cannot be treated conventionally. However, it is more wasteful than conventional treatment and can typically only recover 50% to 90% of the water diverted to the treatment process. RO recovery is limited by total dissolved salt concentration and the presence of sparingly soluble salts in the water. RO concentrate, as the waste volume is called, is difficult to treat or dispose of because it contains high concentrations of dissolved salts. The National Research Council identified concentrate management as an area in which significant research is needed (Committee on Advancing Desalination Technology, 2008). As water demand increases for limited water resources, RO treatment will become more widespread, especially in arid areas where water resources are already scarce.

Regulatory and economic constraints on traditional concentrate disposal methods are driving research on alternate concentrate management strategies. This report describes development of a treatment process for RO concentrate to recover salts for beneficial reuse and increase water recovery.

1.1.1 Background

The principle behind the RO process is that saltwater and freshwater are separated by a membrane that is more permeable to water than it is to salts. In a nonpressurized system, freshwater would diffuse into the saltwater solution to equilibrate salt concentrations on both sides of a semipermeable membrane. In the RO process, pressure is applied to the saltwater side of the semipermeable membrane, overcoming the osmotic pressure and forcing water through the membrane to the freshwater side. As a result, the saltwater becomes saltier and freshwater is recovered.

There are two main aspects of the RO process that limit recovery. First, as the salt concentration in the RO feed water increases, more pressure is required to push freshwater through the membrane. A mechanical limit exists at approximately 1200 psi, above which the pressure differential will damage the membrane. This limit is significant in seawater applications in which feed water salt concentrations can reach 35,000 mg/L or higher, requiring feed pressures near or above 1000 psi. The second limiting factor is the scaling potential. As freshwater is recovered from the feed water, the salt concentration in the concentrate increases. Scaling occurs when mineral deposits form on the membrane surface as salts reach their solubility limit. Recoveries from hard and brackish water applications are typically around 75%.

Concentrate management is a major challenge in the RO process. A seawater RO facility may be able to discharge the concentrate stream into the ocean, but inland brackish water RO facilities must use alternative disposal options. Traditional concentrate disposal methods include discharge to surface water, evaporation, discharge to wastewater treatment plants, and deep well

injection(Jordahl, 2006). High costs are driving municipalities to look for better options, such as the recovery of salts for beneficial reuse. The sale of such products may subsidize the RO process. In addition, the reduction in fouling potential allows water to be treated further by RO or another process, resulting in increased water recovery.

1.1.2 Objectives

The goal of this project was to develop a complete treatment train for RO concentrate using sequential ion exchange (IX) and chemical precipitation in order to recover selected salts for beneficial reuse and increase water recovery.

The overall goal of the project has been met through focus on the following specific objectives:

- The effect of ionic strength and ion proportions on resin selectivity was examined, because RO concentrate has higher ionic strength than waters typically treated by IX.
- A computer model using MATLAB was developed to simulate ion distribution in an IX column based on separation factors found in the resin selectivity investigation. Visual MINTEQ was used to calculate saturation indices in mixed cation and anion regeneration solutions.
- The spatial distribution of ions in an IX column was characterized by analysis of resin along the length of an exhausted column.
- Selected salts with potential resale value or recyclability were recovered by precipitation from mixed regeneration solutions from IX columns.
- Sodium chloride solution produced by sequential IX and passed through a second RO stage was recycled for use as an IX regeneration solution. This second-stage RO concentrate was evaluated for its effectiveness as IX regeneration solution.

In addition, project partner CDM, Inc. evaluated the national salt market to determine the feasibility of marketing recovered salts in the different regions of the United States.

1.1.3 Proposed Treatment

The fundamentals of the treatment train outlined in Figure 1.1 were verified experimentally by this research, and the entire process was evaluated by pilot-scale testing.

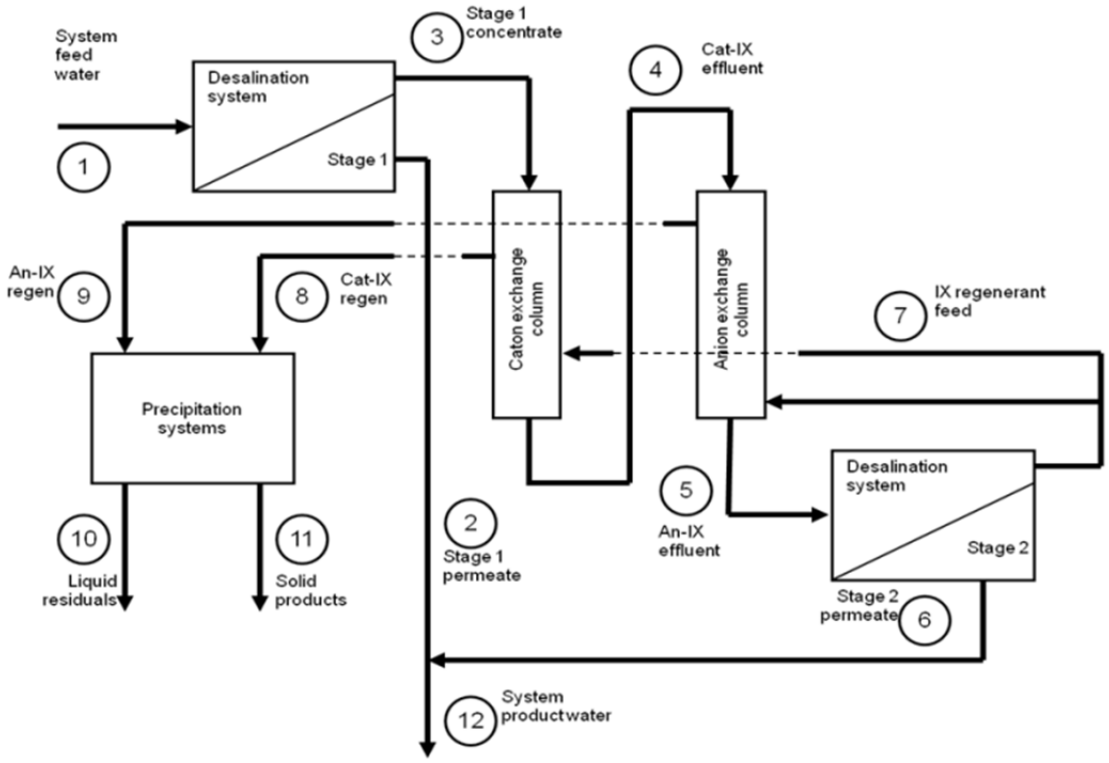

Figure 1.1. Proposed reverse osmosis concentrate treatment train.

Each of the unit processes in the proposed treatment train is in widespread use in water treatment, but the particular sequence and suggested operation are novel. This study investigated sequential IX to remove all cations and anions from an RO concentrate stream and replace them with sodium and chloride. The benefit of ion replacement is that sodium and chloride are highly soluble, so the concentrated sodium chloride effluent solution can more easily pass through some form of volume reduction using RO, membrane distillation, or another process to produce more potable water. The resulting brine solution may be concentrated enough to be used as a regeneration solution. As the IX columns are regenerated, they will release the cations and anions from the resin phase, resulting in a concentrated solution of cations and chloride from one column and a concentrated solution of anions and sodium from the other column. Depending on the constituents, it may be possible to recover commercially valuable salts by combining these solutions.

To determine the feasibility of the process, a mass balance was performed to calculate the likely sodium chloride concentration of the Stage 2 RO concentrate for use as an IX regeneration solution. Table 1.1 lists the input parameters for the RO stages. The model assumes that the cations and anions listed in Table 1.2 are present in the feed water. Their concentrations are meant to be representative of brackish groundwater. Preliminary experiments showed that a 10% sodium chloride solution will effectively regenerate a cation exchange column. The sodium chloride concentration in the IX effluent is a function of the initial feed water ion concentrations. If calcium and magnesium are present at 200 and 100 mg/L, respectively, in the initial feed water, the initial sodium concentration must be greater than or equal to 580 mg/L to produce brine that can be further treated to produce usable IX regeneration solution without further salt addition. Table 1.3 shows the water flow and ion concentrations at each stage of the process. The process numbers correspond to those in Figure 1.1.

Table 1.1. Reverse Osmosis Parameters

Stage 1 recovery	0.75
Stage 1 rejection	0.99
Stage 2 recovery	0.9
Stage 2 rejection	0.99

Table 1.2. Cations and Anions in Feed Water

Ion	Sodium	Calcium	Magnesium	Chloride	Sulfate	Carbonate
Concentration (mg/L)	580	200	100	894	479	247

This project investigated the use of sequential cation and anion exchange followed by chemical precipitation to recover selected salts from RO concentrate. The following section provides a background on these technologies and discusses their potential for this usage.

The experimental methods and results for this research are divided into four phases, and each is presented as a separate chapter. Chapter 2 describes a mathematical model developed to describe column loading based on resin selectivity and influent ion concentrations. Chapter 3 describes batch isotherm tests done to characterize IX resin selectivity with changing ionic strength and ionic ratio to determine its feasibility for use in treatment of RO concentrate. Regression relationships were developed for separation factors as a function of ionic strength and equivalent fraction of exchanging ion. Chapter 4 presents the results of column testing to verify the regression developed in Chapter 3 and to verify the model described in Chapter 2. It also reports on column tests to separate resin-phase ions chromatographically during regeneration and to characterize the distribution of ions within a loaded IX column. Chapter 5 presents the results of experiments designed to precipitate selected salts from laboratory simulated mixed regeneration solutions from cation and anion exchange columns. Chapter 6 is a report on pilot-scale testing of the proposed process. The pilot testing was conducted in conjunction with CDM at a water treatment facility operated by East Cherry Creek Valley Water and Sanitation District, located in Brighton, CO. The experimental work was completed according to the timetable in Figure 1.2. All experimental work and analysis were performed at the UNM environmental engineering laboratories, except for the pilot. IX resins were donated by ResinTech and Purolite (see Table 1.4 for characteristics).

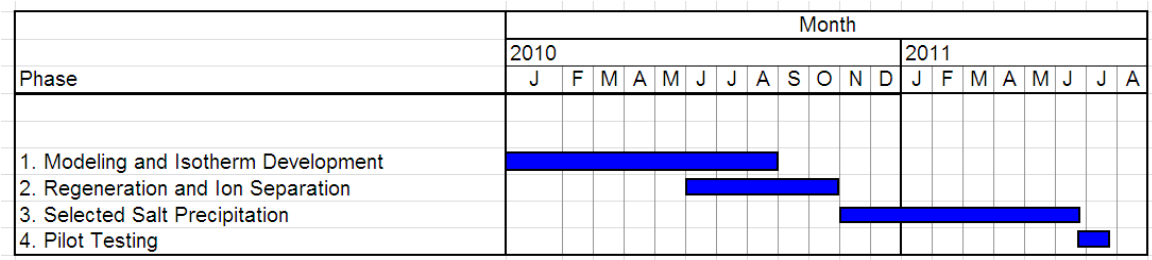

Figure 1.2. Research schedule.

Table 1.3. Salt Balance

			Cations		
			Sodium	Calcium	Magnesium
Flow	Description	Water Flow (m^3/d)	Conc. (meq/L)	Conc. (meq/L)	Conc. (meq/L)
1	System feed	1000.00	25.23	9.98	8.23
2	Stage 1 permeate	750.00	0.25	0.10	0.08
3	Stage 1 concentrate	250.00	100.16	39.62	32.67
4	Cat-IX effluent	250.00	172.45	0.00	0.00
5	An-IX effluent	250.00	172.45	0.00	0.00
6	Stage 2 permeate	225.00	1.72	0.00	0.00
7	IX regeneration feed	25.00	1709.00	0.00	0.00
8	Cat-IX regen waste	12.50	263.09	792.42	653.50
9	An-IX regen waste	12.50	1709.00	0.00	0.00
10	Liquid residuals	25.00	850.30	24.00	21.00
11	Solid products	0.00	--	--	--
12	System product water	975.00	0.59	0.08	0.06

			Anions		
			Chloride	Sulfate	Carbonate
Flow	Description	Water Flow (m3/d)	Conc. (meq/L)	Conc. (meq/L)	Conc. (meq/L)
1	System feed	1000.00	25.23	9.98	8.23
2	Stage 1 permeate	750.00	0.25	0.10	0.08
3	Stage 1 concentrate	250.00	100.16	39.62	32.67
4	Cat-IX effluent	250.00	100.16	39.62	32.67
5	An-IX effluent	250.00	172.45	0.00	0.00
6	Stage 2 permeate	225.00	1.72	0.00	0.00
7	IX regeneration feed	25.00	1714.46	0.00	0.00
8	Cat-IX regen waste	12.50	1714.46	0.00	0.00
9	An-IX regen waste	12.50	268.54	792.42	653.50
10	Liquid residuals	25.00	852.70	244.00	2.00
11	Solid products	0.00	--	--	--
12	System product water	975.00	0.59	0.08	0.06

Table 1.4. Resin Characteristics

Name	Manufacturer	Type	Important Properties
CG-10	ResinTech	Strong acid cation	High capacity, gelular, sulfonated
SBG-1	ResinTech	Strong base anion	High capacity, gelular, type 1
SST65	Purolite	Strong acid cation	Gel polystyrene cross-linked with divinylbenzene, sulfonated
A850	Purolite	Strong base anion	Gel polyacrylic cross-linked with divinylbenzene, quaternary ammonium function groups

Equation 1.1: Ion Exchange Reaction

$$2(\text{R-Na}^{+}) + \text{Ca}^{2+} \rightarrow \text{R}_2\text{-Ca}^{2+} + 2\text{Na}^{+}$$

Equation 1.2: Separation Factor, α (Equivalent based)

$$\alpha_A^B = \frac{(X_B)_r \times (X_A)_S}{(X_A)_r \times (X_B)_S}$$

Equation 1.3: Ion Exchange Chemical Reaction

$$z_B RA^{Z_A} + z_A B^{Z_B} \rightarrow z_A RB^{Z_B} + z_B A^{Z_A}$$

Equation 1.4: Selectivity Coefficient

$$K_A^B = \frac{\left[RB^{Z_B}\right]^{Z_A}\left[A^{Z_A}\right]^{Z_B}}{\left[B^{Z_B}\right]^{Z_A}\left[RA^{Z_A}\right]^{Z_B}}$$

Equation 1.5: Conversion Between Separation Factor and Selectivity Coefficient

$$\left(\alpha_A^B\right)^{Z_B} = K_A^B \left(\frac{\left[RB^{Z_B}\right]}{\left[B^{Z_B}\right]}\right)^{Z_B - Z_A}$$

1.2 Literature Review

1.2.1 Ion Exchange

Synthetic IX resins have been engineered specifically for water treatment since the 1950s. These resins contain charged functional groups on their surfaces, which attract oppositely charged "counter-ions" from a solution. The functional groups on the resin are presaturated by contact with a solution containing a high concentration of ions that have relatively low affinity for the resin. IX occurs when counter-ions in a solution displace the ions on the resin (Helfferich, 1962; Harland, 1994; Crittenden and Montgomery Watson Harza (Firm), 2005; Zagorodni, 2007). This is shown in Equation 1.1 where R indicates an active site on the resin. When all exchange sites are filled to capacity, an IX resin can be "regenerated" by immersion in a highly concentrated acid, base, or salt solution. During regeneration, counter-ions removed from the treated solution are displaced by the presaturant ion in the concentrated solution.

There are four categories of synthetic resins, which are distinguished by the types of functional groups on the resin surface. Strong acid cation (SAC) resins usually contain sulfonate groups, which exchange over a large pH range, whereas weak acid cation resins tend to contain carboxylic groups which only exchange within a limited pH range (Crittenden and Montgomery Watson Harza (Firm), 2005). Weak acid resins can be regenerated by a less concentrated solution than strong acid resins (Crittenden and Montgomery Watson Harza (Firm), 2005). Strong base anion resins often contain quaternary amine groups, which exchange over a large pH range, whereas weak base anion resins contain tertiary amine groups, which exchange over a limited pH range. The tertiary amine groups act as Lewis bases. In solution, they release a hydroxide and take up another anion in its place. Strong base anion resins are not as stable as strong acid resins and are often characterized by a fishy odor (Crittenden and Montgomery Watson Harza (Firm), 2005). IX resin particles have diameters ranging from 0.04 to 1.0 mm, and their uniformity coefficient usually lies between 1.4 and 1.6 (Crittenden and Montgomery Watson Harza (Firm), 2005).

1.2.1.1 Selectivity

The affinity of a particular resin for a particular ion can be described mechanistically or operationally. The operational description of ion affinity is called the separation factor and is represented by the Greek character α. The separation factor is described by Equation 1.2, which is based on solution and resin phase concentrations (Harland, 1994). Rational ionic fractions in each phase can also be used to calculate this factor. The separation factor is simply a ratio between phase distribution coefficients for the two ions in question (see Equation 1.3). It does not account for any other variables in a system such as ionic strength or ionic ratio and is therefore system specific. It is generally used in practical applications in which solution characteristics are unlikely to change. The selectivity coefficient (Equation 1.4), on the other hand, is used to quantify selectivity based on the mass action law. It is the equilibrium constant of a mass action equation describing an IX reaction (Equation 1.3; Harland, 1994). Because the selectivity coefficient is based on a chemical equation, in principle it has a thermodynamic significance and can represent equilibria at high ionic strength.

For systems in which ions of the same valence are being exchanged, the separation factor and the selectivity coefficient are identical. In systems in which the valances of the exchange ions are different, Equation 1.5 can be used to convert between the two.

IX resin selectivity is complicated by its dependence on several parameters, but there are some general trends that can be recognized. Resins tend to have more affinity for ions with greater charge because of increased electrostatic attraction. For ions with equal charge, ions with a smaller hydrated radius are preferred. Hydrated radius is dependent on the size-to-charge ratio of the ion. Larger ions have a greater surface area over which to distribute charge density, which reduces the field strength. For this reason, they do not coordinate with water molecules as strongly as ions with lower size-to-charge ratios, which tend to have larger relative hydrated radii (Crittenden and Montgomery Watson Harza (Firm), 2005; Howe unpublished). This physical explanation fits well with thermodynamic data from Marton and Inczédy (1988) showing the dependence of parameters g_0 and g_1 (which affect resin phase molar excess free energies) from Equation 2.9).

The effect of ionic strength on selectivity can be difficult to predict because of competing processes. When higher concentrations of ions exist in solution, neutral complexes can form, reducing the concentrations of ions free to interact. Charged complexes may also form, which could have the effect of increasing or decreasing interactions with the resin, depending on the charge. Increased ionic strength also has the effect of reducing double layer thickness, requiring ions to move closer to reactants in order to interact. If water activity becomes very low, ions may not be able to form a full hydration shell, reducing the size of the hydrated radii. The combined outcome of all these effects is that high ionic strength selectivity is difficult to model (Harland, 1994). An extreme example is that which occurs during regeneration. A resin is contacted by a very-high-ionic-strength solution containing monovalent lower-selectivity ions. The activity of divalent and trivalent ions decreases more with ionic strength than that of monovalent ions, so the selectivity of the monovalent ion increases. This selectivity reversal, combined with the overwhelming concentration of the monovalent ion, reverses the direction of IX.

Temperature has also been shown to increase IX selectivity for calcium and magnesium over sodium. A study of real and laboratory simulated seawater exchange with two weak acid resins found a significant increase in calcium and magnesium selectivity as the temperature increased from 10 to 80 °C (Muraviev et al., 1996). However, varying temperature for water treatment purposes is impractical.

Surface modification of IX resins has been a popular area of research. Research indicates that modification of an anion exchange resin surface by addition of an anionic polyelectrolyte lowers the rate of reaction with divalent ions in comparison to that with monovalent ions. This has an overall effect of increasing affinity for nitrate over sulfate. The change in selectivity was thought to be caused by size exclusion and electrostatic repulsion (Matsusaki, 1997). In another experiment, a cation exchange resin was modified by exposure to polyethyleneimine, resulting in an increased affinity for heavy metals over alkaline metals. Researchers concluded that the change in selectivity was due to an increased chelating capacity of the modified resin, which tended to favor ions that formed complexes with an amine group (Amara and Kerdjoudj, 2003). Surface modifications tend to increase the separation potential for ions with specific chemical properties, such as bond formation with amines, or physical properties, such as molecular size, but have not been developed to separate ions with similar properties, such as calcium and magnesium.

Equation 1.6 Gibbs Energy Calculation for Ion Exchange Reaction

$$\Delta G^o = -RT \ln K^T = \overline{\mu}_B^o - z\overline{\mu}_A^o + z\mu_A^o - \mu_B^o$$

Equation 1.7 Calculation of Chemical Potential for Ions in Solution Phase

$$\mu_i = \mu_i^o + RT \ln a_i$$

Equation 1.8 Calculation of Chemical Potential for Ions in Resin Phase

$$\overline{\mu}_i = \overline{\mu}_i^o + RT \ln \overline{x}_i + \overline{\mu}_i^E$$

Equation 1.9 Calculation of Excess Free Energy Change

$$\Delta\overline{G}^E = -RT\overline{x}_A\overline{x}_B\left[g_o + g_1\left(\overline{x}_A - \overline{x}_B\right)\right]$$

Equation1.10 Excess molar partial free energy of Ion A in Resin Phase

$$\overline{\mu}_A^E = \Delta\overline{G}^E + \left(1 - \overline{x_A}\right)\left(\frac{\partial\Delta\overline{G}^E}{\partial\overline{x_A}}\right)_{T,I,\overline{x_B}}$$

Equation 1.11 Excess molar partial free energy of Ion B in Resin Phase

$$\frac{\overline{\mu}_B^E}{z} = \Delta\overline{G}^E + \left(\overline{x_A}\right)\left(\frac{\partial\Delta\overline{G}^E}{\partial\overline{x_A}}\right)_{T,I,\overline{x_B}}$$

Equation 1.12 Selectivity Function from Marina

$$K_A^B = K_A^{OB}\left[\frac{\left(\overline{y}_{AR}y_{BX}\right)}{\left(\overline{y}_{BR}y_{AX}\right)}\right]\exp\left[-\pi\left(\frac{\overline{V}_{BR} - \overline{V}_{AR}}{RT}\right)\right]$$

Equation 1.13 Dependence of Activity Coefficient on Water Activity

$$y = f\frac{(a_w)}{\sigma}$$

Equation 1.14 Water Activity as a Function of Swelling Pressure

$$\frac{\overline{a_w}}{a_w} = \exp\left(\frac{-\pi V_w}{RT}\right)$$

1.2.1.2 Selectivity Modeling

The thermodynamic approach to predicting IX selectivity is based on the fact that the change in Gibbs energy at equilibrium is equal to zero. Equation 1.6 shows the pertinent Gibbs energy calculation for a standard IX reaction (Marton and Inczédy, 1988). The terms in the equation are the chemical potentials of the ions in the solution and resin phases. These can be calculated for the solution phase using Equation 1.7 and for the resin phase using Equation 1.8 (Marton and Inczédy, 1988). Resin phase partial molar excess free energies in Equation 1.8 can be calculated using the concentrated electrolyte solution model. Equation 1.9 describes the calculation of the excess Gibbs free energy of the whole system, which is then used to calculate the partial molar free energies in a two-component system by Equations 1.10 and 1.11.

The thermodynamic model of selectivity described previously and other similar methods work well as approximations of to the selectivity of a resin, but they do not take into account the specific qualities of the resin such as the degree of cross-linking (Marina et al., 1992). Depending on the method used, they may not account well for the low activity of ions in the solution and resin phases and the effects of different ionic ratios in solution. Other methods have been developed to deal with these parameters by including the swelling pressure due to high degrees of cross-linking and the low activity of water in highly concentrated solutions in the calculations (Marina et al., 1992; Christensen and Thomsen, 2005). Marina et al. developed a model to predict selectivity based on the degree of cross linking of the resin, the water activity of the solution, and the concentration ratio of the two counter-ions. He related these parameters to selectivity using Equation 1.12, where K_A^B is the selectivity coefficient with regard to ions B and A, K_A^{OB} is the thermodynamic constant of IX, $\overline{y}$ and y are the activity coefficients of the species in the resin and solution phases, respectively, π is the resin phase swelling pressure, and *V* is the partial molar volume. The activity coefficients are functions of water activity as shown by Equation 1.13, where a_w is the water activity and σ is the total concentration of dissolved species in solution. The water activity is a function of swelling pressure, as shown by Equation 1.14, where V_w is the partial molar volume of water and a_w and $\overline{a_w}$ are the water activities in the solution and resin phases, respectively. He found that water activity in the solution was an important parameter in controlling selectivity.

In dilute solutions, activities are very similar to molar concentrations and may be assumed to be unity, but for higher-ionic-strength solutions, activity coefficients must be calculated using a model. The extended Debye–Hückel model can be used to predict activity coefficients for solutions with ionic strength up to 0.1 M, and the Davies model can be used for solutions with ionic strength up to 0.5 M. Activity coefficients in solutions with ionic strengths greater than 0.5 M can be calculated using the specific interaction model, which takes into account the interaction between ions in the solution (Benjamin, 2002). The Bromley method also considers the interactions of all cations and anions in solution and can be used for solutions with ionic strengths up to 6 mol/kg (Ostroski et al., 2011).

The calculation of resin phase activities can be performed using the Wilson model, which was originally proposed in 1964 for liquid–vapor equilibrium but was first applied to resin-phase activities by Smith and Woodburn in 1978 and has since been used in many studies (Mehablia et al., 1994; Vo and Shallcross, 2003). This model requires binary interaction parameters to be known to calculate activities, and several methods have been developed over the years since then to determine them more accurately (Mehablia et al., 1994). Melis et al. proposed an entirely

different approach by considering IX as a phase equilibrium rather than a mass action law. In this model, the resin phase contains a statistical distribution of ideally behaving active sites with different adsorption energies. Adsorption at each site can be described by a simple Langmuir isotherm (Melis et al., 1996).

1.2.1.3 Column Processes

The determination of selectivity properties for a particular resin is often done using batch reactor experiments, but most operational configurations utilize a column because of the increased efficiency it provides. Column processes can be thought of as series of batch reactors in which the solution continually encounters a fresh resin bed. This forces the equilibrium reaction in a favorable direction (Zagorodni, 2007). As the solution passes through the column, the resin in contact with the solution becomes exhausted. The mass transfer zone (MTZ), the area in the column in which the exchange reaction is occurring at a specific time, moves through the column in the direction of flow until it exits the column at breakthrough. Process efficiency, as defined here, is the fraction of the column in equilibrium with the influent solution at the time of breakthrough. This fraction is determined by the length of the MTZ. If hydrodynamics, column dimensions, and ion concentrations are held constant, the length of the MTZ is primarily dependent on the selectivity of a particular ion. Consider the lengths of the MTZs of high- and low-selectivity ions moving through a column. A larger fraction of the high-selectivity ion concentration will exchange with the resin in the column segment, resulting in a smaller fraction being passed to the next segment. Therefore, fewer reactors are required to completely remove the high-selectivity ion than the low-selectivity ion (Zagorodni, 2007). Resin in which the MTZ has already been passed is completely exhausted for a particular ion, so long MTZs result in poorer column efficiency (Helfferich, 1962; Zagorodni, 2007). For an ion with infinitely high selectivity in a column in which diffusion and dispersion are neglected, the MTZ would be infinitely small, which would result in a perfectly rectangular plug front. Dispersion and diffusion will cause curve broadening of the MTZ (Zagorodni, 2007).

Because of differences in selectivity, ions move through IX columns at different rates and have breakthrough curves with different shapes (Letterman and American Water Works Association, 1999). The least selective ion is the first to exit the column at breakthrough (Zagorodni, 2007). Higher-selectivity ions concentrate at the column inlet, and the result is a banding effect in which plugs of ions form in a column, in the direction of flow, according to the selectivity sequence. In an infinitely long column, in which wave fronts have time to separate based on selectivity, the concentration profile of ions in the resin during loading would resemble Figure 1.3. Later in the column process, the resin at the topmost portion of the column is in equilibrium with the influent solution, and the resin contains the equilibrium concentrations of ions predicted by the separation factor.

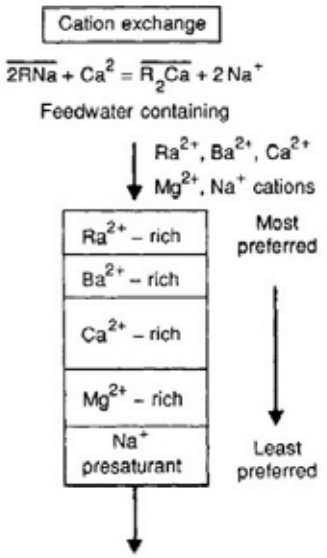

Figure 1.3. Ideal resin phase concentration profile from Helfferich (1962).

Ions are eluted from an exhausted column through one of two processes. Regeneration is done by flowing a concentrated acid, base, or salt solution through the column to drive all ions into the solution phase and out of the column. This process is used when the ions in the column are not intended for recovery. Elution is the process of removing ions of interest from the column (Zagorodni, 2007). A variety of solutions can be used to achieve this end, but they are all based on the process of exchanging ions in the solution phase for one or more ions in the resin phase. This can be done either with a concentrated solution or with a solution containing ions that are more highly selective than those on the resin. Figure 1.4 shows the loading and regeneration of an IX column. Note the ion banding effect and the displacement of the lower selectivity ions, A and B, by ion C.

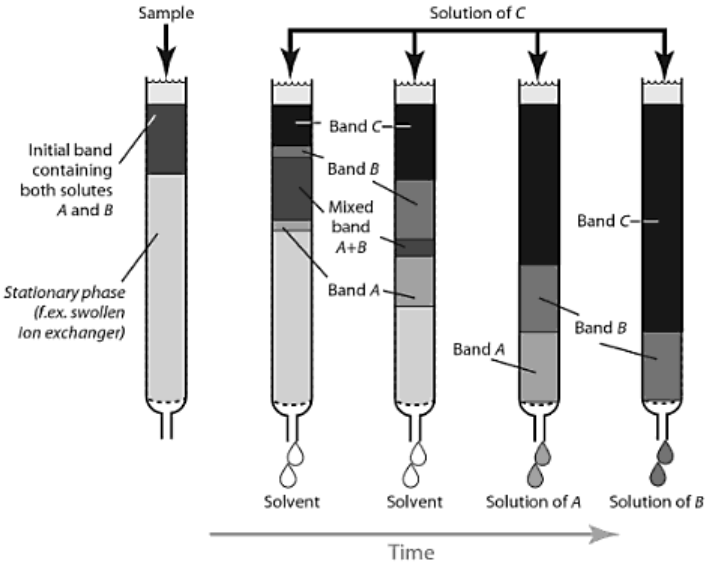

Figure 1.4. Loading and regeneration of an ion exchange column (Zagorodni, 2007).

1.2.1.4 Modeling of Column Processes

The modeling of IX processes in a column is a complex problem. Helfferich (1962) thought a rigorous solution to be hardly feasible. Over the intervening years, however, many column models have emerged. Column models can be divided into two main categories: equilibrium models and rate-based models. Equilibrium models assume that equilibrium between the resin and liquid phases is attained instantaneously as they come into contact. Column operation is modeled by dividing the column into segments that come into equilibrium in succession as the liquid moves through the column. This type of model may or may not consider the effects of advection. Equilibrium models have the advantage of simplicity, but the disadvantage is that the number of segments is an empirical quantity that cannot be predicted. The model must be calibrated to each set of specific column conditions (Helfferich, 1962). Rate-based models take into account nonequilibrium conditions, making them much more mathematically intense (Helfferich, 1962). They have the advantage of being predictable from fundamental data and need no empirical correlation. Rate-based models account for diffusion rates as well as material balances and IX equilibrium.

The model proposed by Wilson in 1986 is an equilibrium model that works by dividing a column into a number of theoretical plates (Wilson, 1986). As Wilson contends, there is no simple interpretation of the number of theoretical plates used. Each segment is assumed to be well mixed, and it is noted that numerical dispersion occurs that results in front broadening. A nonlinear numerical solver was written to solve for concentrations in each segment based on concentration, selectivity, and electroneutrality. Selectivity was assumed to be constant, although Wilson noted that a function to solve for selectivity based on solution concentrations could be added later. Wilson noted that the relationship between the broadness of the front and the number of segments is such that decreasing front width by a factor of $1/x$ requires increasing the number of segments by x^2. Increasing the number of segments also requires the use of very small time segments, resulting in increased processing costs. In response to this problem, several simplified algorithms were developed to represent advection, and the required number of segments was decreased. By today's processing standards, these modifications are not necessary, and equilibrium models such as this one can be run with many segments without excessive computer processing.

Computer processing costs are rarely considered to be a major factor in model development any more. Modern modeling efforts are much more focused on accurate prediction based on fundamental data. Ostroski et al. (2011) developed a model for column processes including mass transfer kinetics. Their model defined selectivity by the mass action equation, including activities. The activities in the solution phase were estimated using the Bromley method (Bromley, 1973) and resin phase activities were estimated using the Wilson model (Wilson, 1964). The column was divided into equal-sized elements in which a mass balance equation including bed density, interstitial velocity, axial dispersion mass transfer coefficient, total voidage, time, and space was included. The equation also included mass transfer terms for the external liquid film and the inside of a particle of resin. Mass transfer was modeled as having two distinct parts: (1) the movement of ions from the bulk phase through the liquid film and (2) the diffusion of ions into the micropores of the resin. The exchange reaction itself was considered to be instantaneous. The finite volume method was used to solve the mass balance equations. His results matched well to experimental data on IX columns in which zinc was exchanged for sodium. He concluded that the initial stage of mass transfer is controlled mainly by film resistance but the overall mass transfer process is interparticle resistance.

Nakamura et al. (2010) modeled a column containing a hydrogen–sodium–ammonia system. They defined selectivity in terms of molarity and divided the column into equal-volume segments. In their model, total resin capacity and selectivity were determined as fitting parameters, and they found that the exchange rate depended on the overall liquid phase mass transfer coefficient and the surface area of the particle. Film diffusion resistance was found to control the overall rate of mass transfer.

Another application of the mass action law to models of IX in a fixed-bed column was put forth by Borba et al. (2011). This model considered thermodynamic equilibrium at the liquid–solid interface, the external mass transfer resistance and internal diffusion resistance (in series), and the concentration profile within pores described by linear driving force to predict IX capacity. The column was divided into equal-volume segments and the following calculations were completed for each segment using the finite-volume method: liquid phase mass balance, external film mass transfer, liquid phase charge balance, diffusion of species within particles, resin phase charge balance, and mass balance between external mass transfer and diffusion mass transfer. The Langmuir and the mass action law of equilibrium were compared to see which fit the data better, and both were found to fit the data well.

A column model general enough to predict performance over a wide range of solutions, resins, and geometries has not yet been developed.

1.2.2 Chemical Precipitation

The process of chemical precipitation involves adjusting the chemical and physical parameters of a solution to form solids from dissolved species. The chemical principles are well understood, and chemical precipitation has been used in water treatment for more than a hundred years. A familiar water treatment example is the use of lime softening, the removal of calcium carbonate by increasing solution pH to promote calcium carbonate precipitation. This was discovered in 1841 by Thomas Clark, a professor of chemistry at Aberdeen University in Scotland. It was endorsed by the British Water Commission on Water Supply in 1869 and has been widely used in the United States since the 1940s (Hendricks, 2006).

The equilibrium of dissolved ions in solution with a solid precipitate occurs when the Gibbs energy of reaction is equal to zero (see Equation 1.15. Relating equilibrium to Gibbs energy allows the solubility constant to be determined based upon thermodynamics rather than by empirical correlation. The solubility product (Equation 1.15) depends on temperature and is a function of the enthalpy of the solubility reaction. The ion activity product (IAP) (Equation 1.16) uses the activities of ions in the mass action equation and, when compared to the equilibrium constant, indicates the degree of saturation. The logarithm of the ratio of the IAP to the equilibrium constant is the saturation index (SI) (Equation 1.17).

If the SI is greater than zero, precipitation will occur (Hendricks, 2006). Table 1.5 shows the pK_{SO} values of some common salt precipitates.

Table 1.5. Solubility Constants for Common Precipitates

Solid	pK_{SO}
$CaCO_3$	8.48
$CaSO_4$	4.36
$MgCO_3$	7.46
$MgSO_4 \cdot 7H_2O$	2.13

Equation 1.15 Solubility Constant	$\Delta\overline{G}_r = RT\ln(K_{SO})$
Equation 1.16 Ion Activity Product	$IAP = \{Cation\}\{Anion\}$ where $Cation + Anion \rightarrow Solid$
Equation 1.17 Saturation Index	$SI = \log\left(\frac{IAP}{K_{SO}}\right)$

There are two cases in which the solubility of a mineral is a function of pH: (1) if one of the ions reacting to form the precipitate is H^+ or OH^-; (2) if one of the ions is a weak acid or base, such as carbonate.

Precipitation may not occur instantaneously even if the SI indicates that a particular salt is supersaturated. The rate of precipitation depends on reaction kinetics, mass transfer, and available surface area for reaction. For crystals to form in suspension, small particles must exist in the suspension for crystals to grow around. Tiny crystals will eventually form spontaneously as ion concentrations increase, but this could occur at concentrations much above those specified by the solubility constant. Providing tiny particles or crystals for this purpose is called seeding and is common practice in precipitation processes(Rahardianto et al., 2007).

Complexes forming in solution may affect solubility. Complexes are dissolved species in waters consisting of a metal and a ligand. Ligands are ions or molecules that form bonds with a central metal atom. These bonds may be electrostatic, covalent, or other types such as van der Waals or dipole–dipole, for example. Metal ligand complexes also exist in equilibrium with the free ions and precipitated salt in the system (Benjamin, 2002). The mass of ions contained in these complexes at equilibrium cannot be neglected in considering solubility.

Precipitation in Combination with Reverse Osmosis

Precipitation has been used in water treatment for more than a hundred years, but more recently, as RO treatment has become widespread, it has been optimized to pretreat water to limit membrane fouling. Membrane fouling generally takes one of four forms, depending on the nature of the foulant: colloidal, organic, biological, or scaling (Wang, 2011). Scaling in RO is most commonly caused by the precipitation of sparingly soluble salts on the membrane surface. This occurs as the salts reach their solubility limit. Precipitation can be used to reduce the scaling potential by removing the sparingly soluble salts from the water before it undergoes RO treatment.

Intermediate precipitation was proposed by Gabelich et al. (2007) as another way to increase RO recovery. In this process, precipitation of hardness ions is an intermediate step between two RO stages (Gabelich et al., 2007). Precipitation was induced by pH adjustment only. Gabelich observed some interesting trends in this study. First, the presence of noncarbonate hardness resulted in lower calcium removal. Second, there was a high degree of mixed salt precipitation, such as barium and strontium precipitating with calcium. Third, general cation removal increased with increasing pH (Gabelich et al., 2007). Fourth, antiscalants were needed to prevent scaling in the secondary RO process.

The SAL-PROC system has been developed by Geo-Processors, Inc. over the last 15 years (Ahmed et al., 2003). The goal of the process is to produce usable and possibly marketable salts and slurries from RO concentrates through accelerated precipitation. Many details of the process are proprietary, but it is reported to include heating, cooling, and chemical addition (Ahmed et al., 2003). According to product literature, the process utilizes sequential concentration steps, which may include further RO treatment or evaporation. The SAL-PROC process relies entirely on chemical precipitation to recover salts. For this reason, pH control, temperature control, and chemical addition are essential to the process.

A study by Heijman in 2009 proposed a system combining precipitation with sedimentation, IX, and nanofiltration to treat groundwater to zero liquid discharge. A cation exchanger was used to remove any hardness ions not removed by chemical precipitation. The study concluded that the combination of the two technologies reduced the amount of chemicals required for treatment and increased water recovery to 97% (Heijman et al., 2009).

The accelerated precipitation softening process includes primary RO treatment followed by pH increase and calcite seeding, microfiltration to remove crystals, pH decrease, and secondary RO treatment. No recoverable salts are created in the process, and it requires extensive treatment for pH adjustment and scale protection, but 98% water recovery was reported for the process (Rahardianto et al., 2007).

Chapter 2

Modeling

One of the objectives of this project was to develop a mathematical model to describe IX in a column over time. Modeling is a convenient way to see the effects of changes in selectivity, solution characteristics, and operation time on the column process. The model is described in the first section because results from each phase of the project are compared with model predictions.

2.1 Chapter Objectives

The purpose of this chapter is to describe the mathematical model developed to describe the IX column process. The inner workings of the program will be explained in terms of computer language, functions, inputs, and outputs. The goal of this section is to impart an understanding of the model and its results, so they can be compared with experimental results in a meaningful way in later sections.

2.2 Chapter Summary

The key results and conclusions from this chapter are as follows:

1. Model assumptions:
   a. The model is based on charge balances and selectivity only. Kinetics and hydrodynamic dispersion were not included.
   b. One bed volume of operation occurs when the number of time steps is equal to the number of segments.
2. Model inputs include solution-phase ion concentrations, resin separation factors, column dimensions, the number of segments in the column, and time steps.
3. The model outputs two three-dimensional arrays. The first includes time, segment number, and resin phase ion concentration. The second includes time, segment number, and solution phase ion concentration. The arrays can be queried in several useful ways to produce snapshots of the entire column, resin phase concentration at any time, and breakthrough curves.
4. The model code was written in MATLAB.

2.3 Modeling

The model was developed using MATLAB, in cooperation with Angela Montoya, a programmer and graduate student at the University of New Mexico. It is a discretized mass balance model in which solution and resin equilibrium are found simultaneously using a nonlinear solver.

The model is based on Equation 2.1, which combines the charge balance equations and the separation factor equations to solve for solution phase composition simultaneously for all ions in the system (see Figure 2.1). The equation solver fsolve was used to solve the system of nonlinear equations. Resin phase ion equivalents, R, are solved for by subtracting the solution phase ion equivalents from the total ion equivalents in the system (Equation 2.2). The simulated column is split into a number of segments defined by the user. The equation works by looping over time and

space to produce solution and resin phase ion equivalents for each time step in every column segment. Resin phase and solution phase ion equivalent totals are converted to concentrations by dividing by the segment volume (Equation 2.3). At the beginning of each time step, total ion equivalents are calculated by adding the equivalents on the resin to the equivalents in solution. At the next time step, solutions are advanced down the column to the next segment and used as influent initial ion concentrations for the equilibrium calculation for that time step.

The column is modeled similarly to a "tanks in series" (TIS) arrangement. It is split into a number of segments (user defined, *n*) containing an equal volume (Equation 2.4). As the number of elements increases, a closer and closer approximation of plug flow is reached. This can be seen in Figure 2.2, in which a tracer concentration is plotted as a function of the normalized time (time divided by average residence time; see Fogler, 1999). The TIS model is an alternative and somewhat limited (one-parameter) method of modeling dispersion in reactors in systems with small deviations from plug flow (Levenspiel, 1962).

In an ideal plug flow column, ion sorption fronts are sharp, even for ions with low separation factors, although ions with higher separation factors will always have sharper curves than those with lower separation factors. In real columns, dispersion must be accounted for. Dispersion in the column results in peak broadening, which is modeled by decreasing the number of column segments (Wilson, 1986) . This can also be seen in . A direct comparison between the tanks in series model (Equation 2.5) and the MATLAB model shows very similar results (see Figures 2.3 and 2.4).

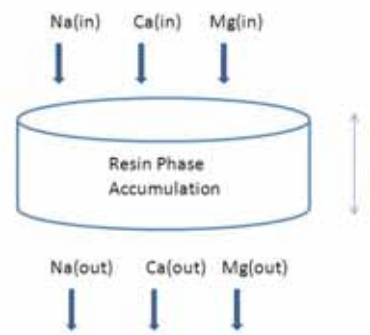

Figure 2.1. Model scheme.

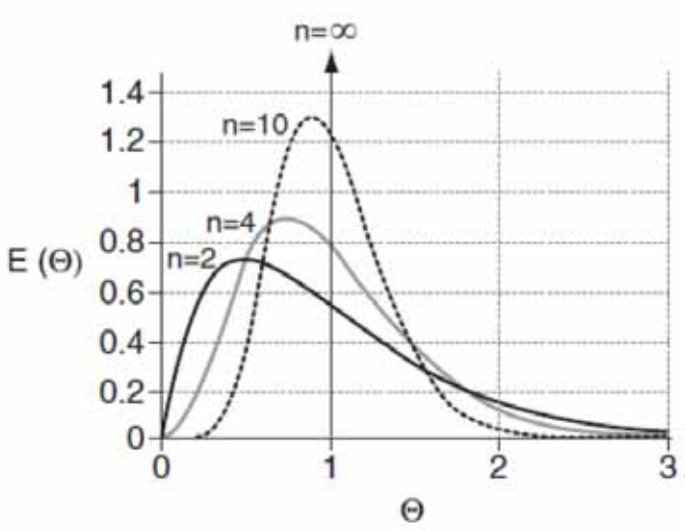

Figure 2.2. Response to pulse tracer input for tanks-in-series models using differing numbers of tanks (Fogler, 1999).

Equation 2.1: Vector Equation to Solve for Solution Phase Ion Equivalents, *C*

$$0 = \begin{bmatrix} q_T \\ q_T \\ q_T \end{bmatrix} \begin{bmatrix} \alpha_1 \\ \alpha_2 \\ \alpha_3 \end{bmatrix} \begin{bmatrix} C_1 \\ C_2 \\ C_3 \end{bmatrix} - \left(\begin{bmatrix} T \\ T \\ T \end{bmatrix} - \begin{bmatrix} C_1 \\ C_2 \\ C_3 \end{bmatrix} \right) \begin{bmatrix} \alpha_1 \\ \alpha_2 \\ \alpha_3 \end{bmatrix}$$

where q_T is resin capacity (meq, calculated by multiplying specific capacity by segment volume), α is separation factor, *C* is total solution phase ion equivalents (meq), and *T* is total ion equivalents in segment (meq, solution phase plus resin phase)

Equation 2.2: Vector Equation to Solve for Resin Phase Ion Equivalents

$$\begin{bmatrix} R_1 \\ R_2 \\ R_3 \end{bmatrix} = \begin{bmatrix} T \\ T \\ T \end{bmatrix} - \begin{bmatrix} C_1 \\ C_2 \\ C_3 \end{bmatrix}$$

where *R* is resin phase ion equivalents

Equation 2.3: Conversion of Solution and Resin Phase Ion Equivalents to Concentrations

$$\mathrm{C_{eq/L}} = \frac{C}{\mathrm{V_{seg}}} \text{ and } \mathrm{R_{eq/L}} = \frac{R}{\mathrm{V_{seg}}}$$

where V_{seg} is segment volume (L)

Equation 2.4: Equation for Segment Volume

$$\mathrm{V_{seg}} = \frac{q_T}{n}$$

where *n* is the user defined number of column segments

Equation 2.5. Cumulative time distribution (*F*) and relative time distribution (*E*) for the TIS model.

$$F(t) = \int_0^t E(t)dt \quad E(t) = \frac{t^{(n-1)}}{(n-1)!\tau^n} e^{\frac{-t}{\tau}}$$

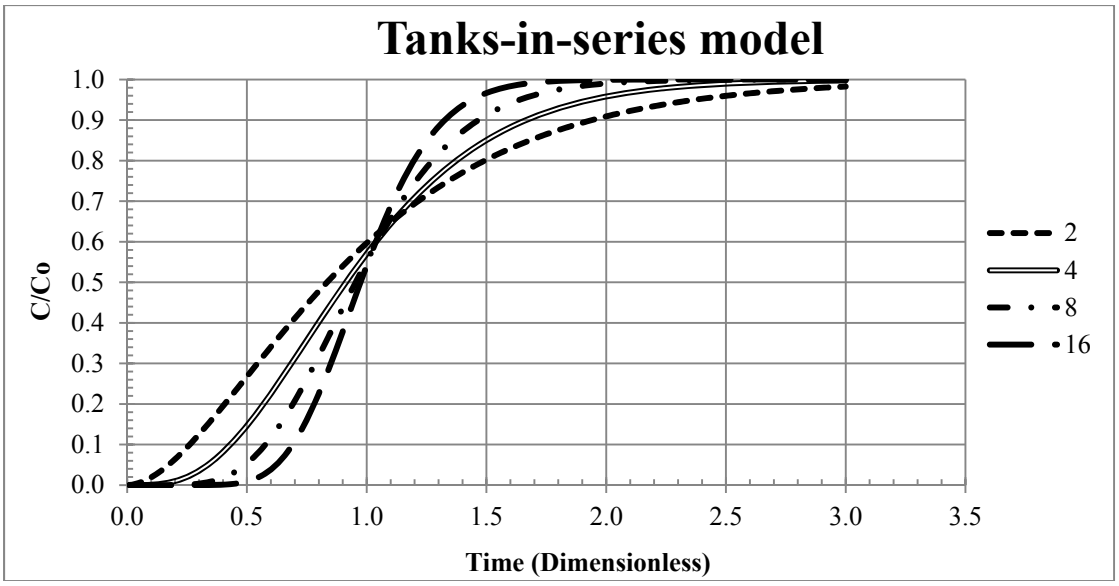

Figure 2.3. Effluent concentration curves from tanks-in-series models using different numbers of tanks.

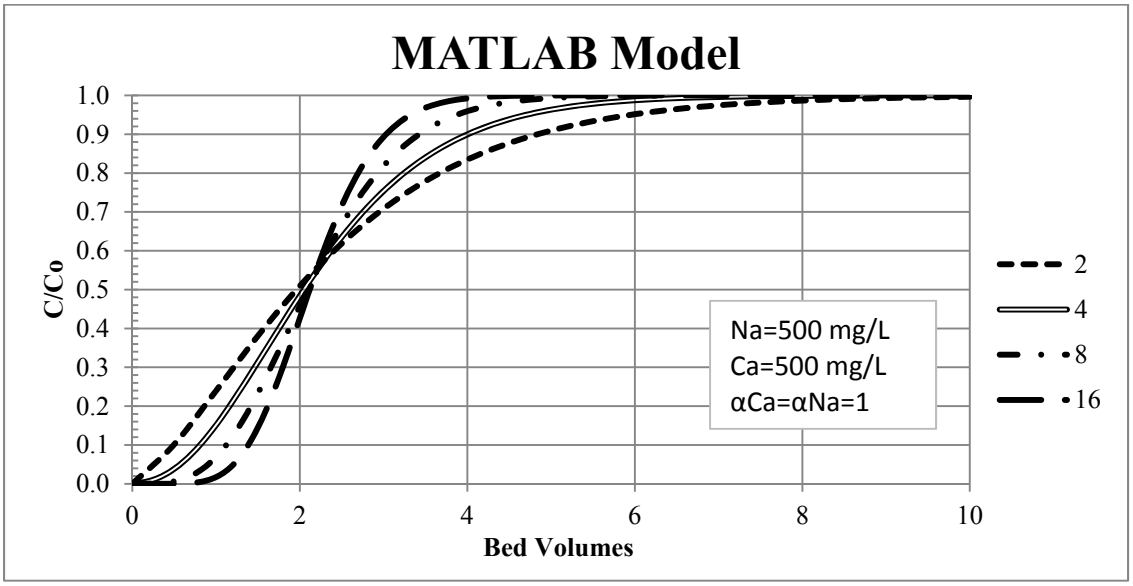

Figure 2.4. Effluent concentration curves from MATLAB models using different numbers of segments.

A graphical user interface (GUI) was developed to simplify data import and export. The input area on the GUI (see Figure 2.5) is on the left-hand side. Data inputs include the number of time steps, the number of column segments, the initial solution phase sodium concentration (mg/L), the column length (ft), the column diameter (in.), and the concentration of other ions in solution (mg/L). There is also a field for the concentration guess. This field feeds fsolve, the nonlinear solver, an initial guess for solution phase ion amounts (total meq). Because this number can vary greatly depending on the size of a particular element and the initial solution concentrations, this approach is better than hard coding a "one size fits all" guess into the function. It will not converge if the guess is too far from the actual value. The input guess is only used for the first time step in the first element. For all subsequent equations, the equilibrium concentration in the previous time step in the previous element is used as a guess.

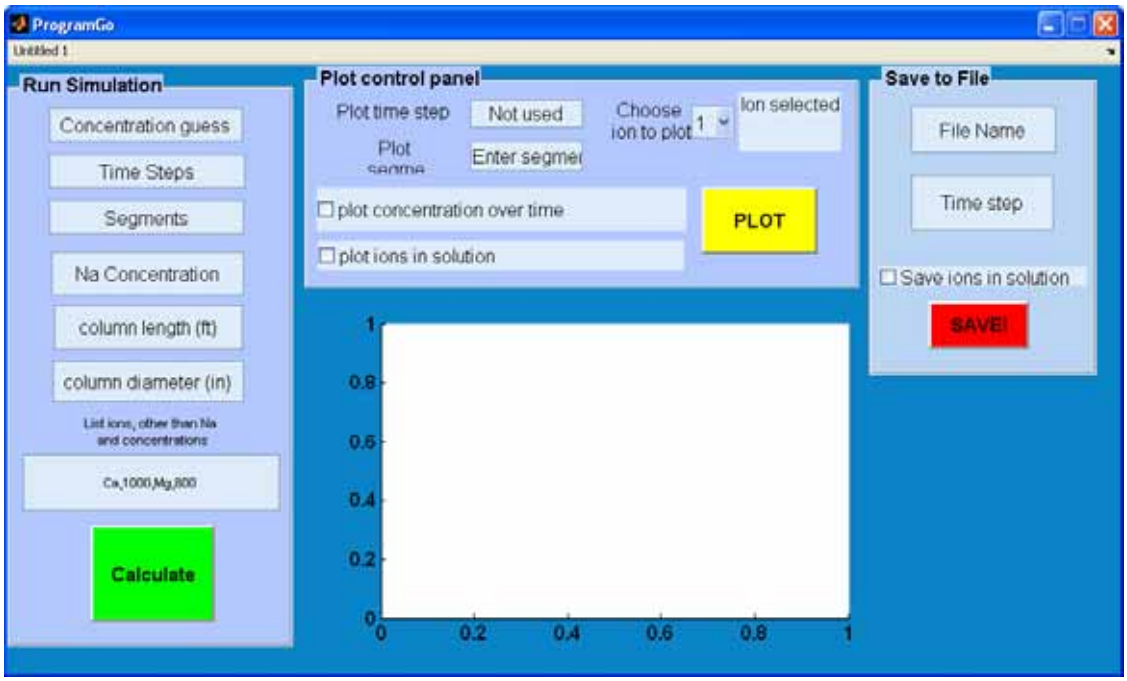

Figure 2.5. Graphical user interface for MATLAB model.

The GUI also allows graphing solution and resin phase ion equivalents over time and space. This feature was added to allow the user to confirm that the calculations were successful and to get a quick overview of the system. Users can export the solution or resin phase ion equivalents at a specific time for all segments as a text file that can be imported into any graphing program and can be plotted to show the distribution of ions within the column for any time (see Figure 2.6). The arrays can also be accessed directly from the MATLAB environment by using the functions employed by the GUI graphing feature. The function entitled get_segment_data allows the user to retrieve resin or solution phase ion equivalents for all segments at a specific time. The function is called by specifying an array (resin or solution), a segment, and an ion (Ca, Mg, other). The other useful function, get_time_data, returns the solution or resin phase ion equivalents at all times for a specific segment. It is called by specifying an array, a segment number, and an ion. Using this function, the user can generate solution phase ion equivalents at all times for the final segment, which is very similar to a breakthrough curve (see Figure 2.7). Any ion can be added to the model by inputting its molecular weight, charge, and separation factor into a straightforward and well commented file. The model code is available upon request.

The effect of increasing the number of segments while keeping the number of bed volumes treated and the selectivity of the resin constant can be in Figure 2.8. Although the equilibrium distribution of ions is constant, the sorption front becomes sharper as the number of segments increases. Sharper peaks also result in a longer time to breakthrough and a corresponding increase in column efficiency. The number of segments suitable for modeling a real reactor can be found by matching the observed dispersion of a nonreactive tracer with that modeled using a specific number of segments.

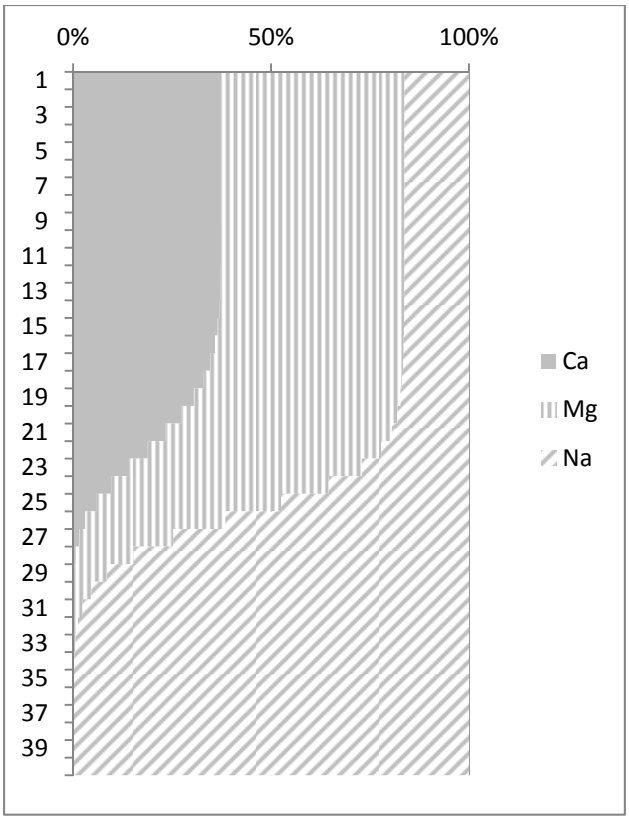

Figure 2.6. Example column snapshot from model.

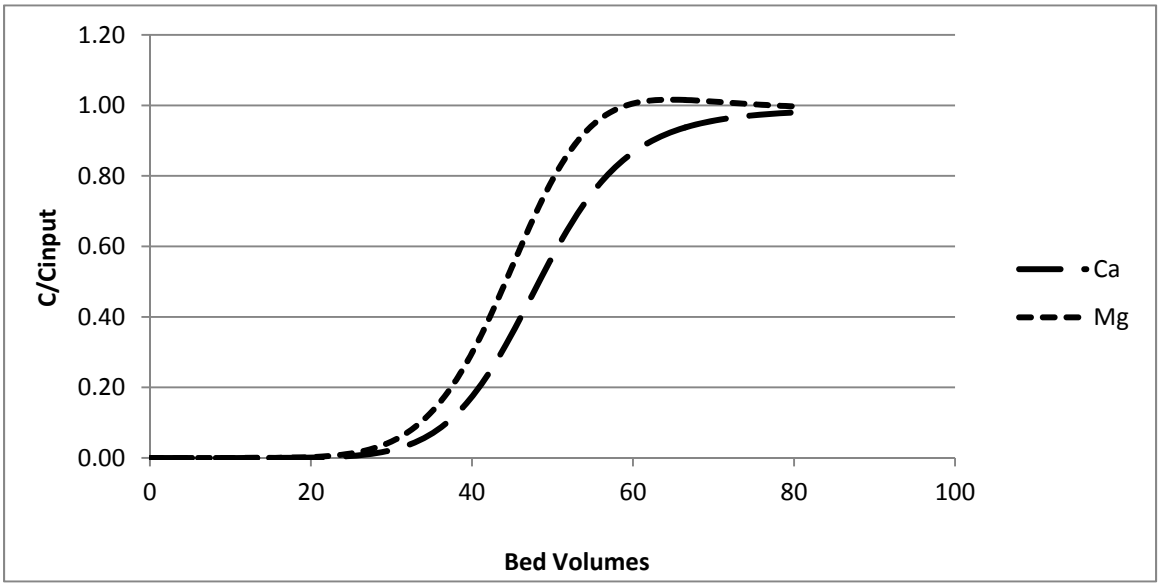

Figure 2.7. Example breakthrough curve from model.

Input Parameters	$\alpha_{Na}^{Ca}=2$ $\alpha_{Na}^{Mg}=1.5$	$C_{Ca}=C_{Mg}=C_{Na}=200$ mg/L

Segments 10

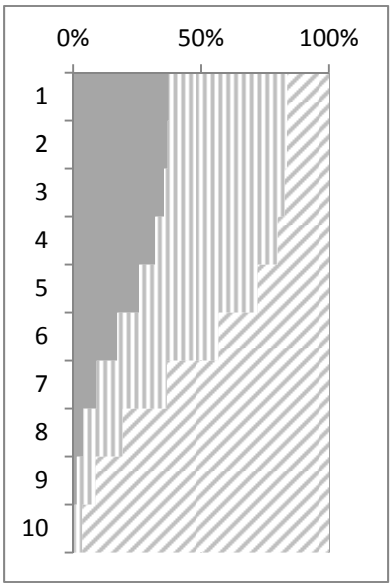

Segments 20

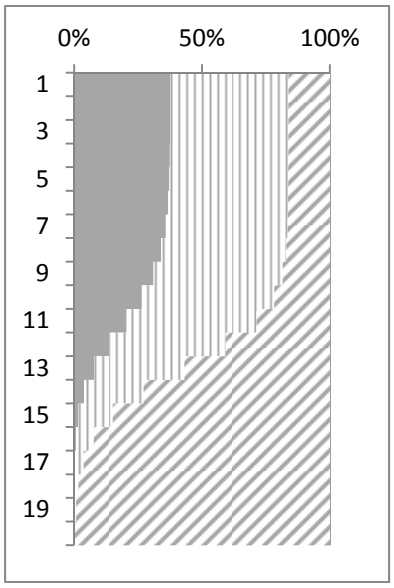

Segments 30

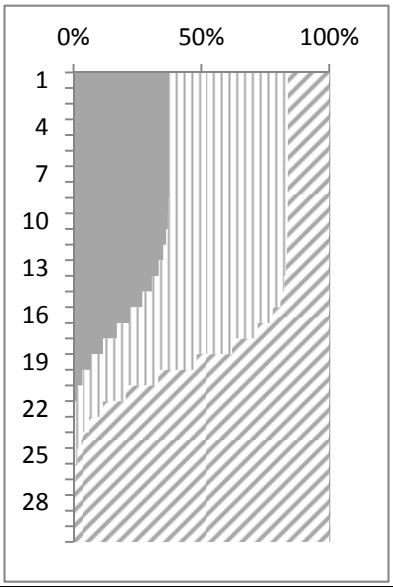

Segments 40

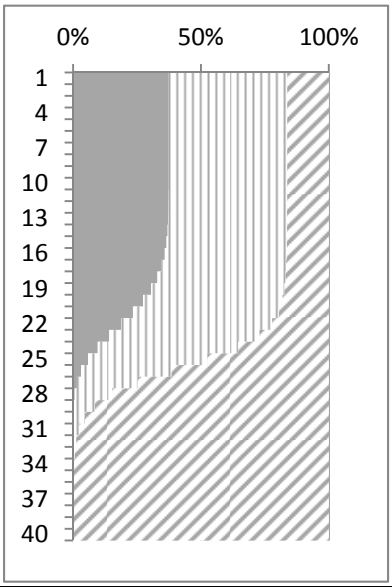

Input Parameters	$\alpha_{Na}^{Ca} = 2$ $\alpha_{Na}^{Mg} = 1.5$	$C_{Ca}=C_{Mg}=C_{Na}$=200 mg/L

Segments 100 200

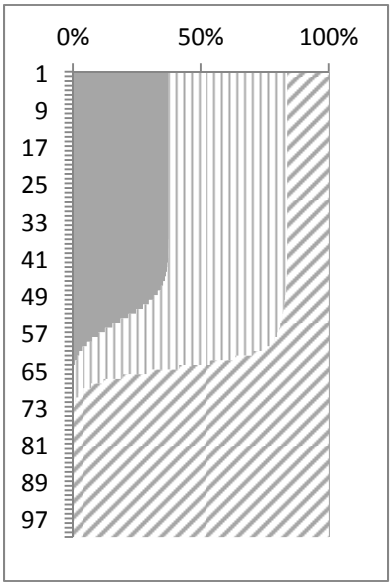

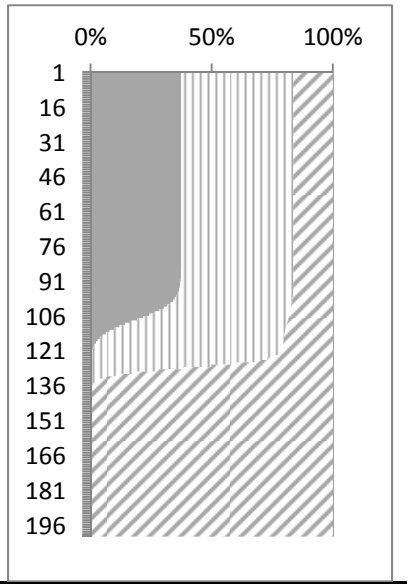

Figure 2.8. Comparison of column snapshots with different numbers of segments.

Chapter 3

Dependence of Resin Selectivity on Ionic Strength and Solution Composition

3.1 Chapter Objectives

This chapter describes the methods of and results from batch studies performed to determine the effect of changing ionic strength and ionic composition on the selectivity of cation and anion IX resins for common ions present in most RO concentrates, including calcium, magnesium, carbonate, bicarbonate, and sulfate. Ion selectivity directly relates to the feasibility of using these resins to treat RO concentrate.

3.2 Chapter Summary

The key results and conclusion from the batch isotherm experiments are as follows:

1. Selectivity for all divalent ions decreases with ionic strength.
2. Selectivity for all divalent ions decreases with solution phase equivalent fraction.
3. The best predictor of separation factors is a regression based on these two factors.
4. Cation and anion exchange resins have adequate selectivity for the major ions of interest in a broad range of solutions.

3.3 Methods

The objective of the first phase of the project was to determine how resin selectivity is affected by fundamental variables, including ionic strength and initial ion proportions. To achieve this objective, several IX isotherms were measured using anion and cation exchange resins donated by ResinTech and Purolite. Based on the manufacturer's specification from ResinTech, which detailed ranges of working conditions, selectivity, and exchange capacity, a SAC resin, CG-10, was selected for use (see Figure 2.1). Purolite A850, an SBA resin, was also selected. The solutions prepared for the isotherms were designed to test resin properties at a variety of ionic strengths and ion ratios, using ions common to brackish water sources and therefore likely to be in RO concentrate, including sodium, calcium, magnesium, chloride, sulfate, and carbonate. These ions are also components of several salts that may be recovered for beneficial reuse, such as calcium and magnesium carbonate or sulfate.

IX resins in the Na^+ or Cl^- form were rinsed and dried in a lab oven at 104 °C. Solutions were prepared by mixing together concentrated stock solutions of various salts. A sample of 50 mL of each solution was poured into a 50-mL vial. Using a Mettler Toledo AB104-S balance, 0.5 or 1 g of dried resin was weighed and added to each 50-mL vial.

Figure 3.1. Resin samples.

Vials were placed on a VWR DS2-500-1 laboratory shaker or a vertical rotating disk for a 24-h period. Metals were analyzed by flame atomic absorption spectroscopy (AAS) using a Varian SpectrAA 55BB atomic absorption (AA) spectrometer (see Figure 2.2). Specific ion lamps were newly purchased for this work, including those for calcium, magnesium, potassium, and barium. Sodium was measured using atomic emission spectrometry. Anions were determined by ion chromatography using a Dionex DX series ion chromatography system (IC) using a newly purchased AS-14 column. The equilibrated solution concentrations were compared with the initial concentrations of the solutions and the mass of ions exchanged was determined from the difference. In the final cation exchange isotherm, the equilibrated resin was washed with deionized (DI) water and then stripped with 2 N HCl. The resulting liquid was analyzed for calcium, magnesium, and sodium. These measurements were used to verify the measurements taken from initial and equilibrated solutions. The matrix of isotherm experiments is shown in Table 3.1 and results are presented in the next section.

Figure 3.2. Atomic absorption spectrometer (left) and ion chromatography system (right).

Table 3.1. Matrix of Isotherm Experiments (Ratios Are Based on Molarity)

Isotherm Type	Ions	Initial Ratio (Counter-ions:Na or Cl)	Ratio (Ca:Mg) or (SO_4/CO_3)	Ionic Strength (M)
Binary	Ca/Na	1:3, 1:1, 3:1	N/A	0.15, 0.5, 1.0, 1.5
Binary	Ca/Na	1:3, 3:1	N/A	0.10, 0.15, 0.20, 0.25
Binary	Mg/Na	1:3, 1:1, 3:1	N/A	0.15, 0.5, 1.0, 1.5
Binary	Mg/Na	1:3, 3:1	N/A	0.10, 0.15, 0.20, 0.25
Ternary	Ca/Mg/Na	1:3, 1:1, 3:1	4:1	0.15, 0.5, 1.0, 1.5
Ternary	Ca/Mg/Na	1:3, 3:1	1:3	0.10, 0.15, 0.20, 0.25
Ternary	Ca/Mg/Na	1:3, 1:1, 3:1	1:4	0.15, 0.5, 1.0, 1.5
Binary	SO_4/Cl	1:3, 3:1	N/A	0.10, 0.15, 0.20, 0.25
Binary	CO_3/Cl	1:3, 3:1	N/A	0.10, 0.15, 0.20, 0.25
Ternary	SO_4/ CO_3/Cl	1:3, 3:1	1:1	0.10, 0.15, 0.20, 0.25

Experiments in Phase 1 were designed to quantify changes in resin selectivity due to variations in ionic strength and solution equivalent fraction of exchanging ion. Initial ionic ratios were calculated by dividing the molar concentration of counter-ions by the molar concentration of sodium or chloride. The ratio of the initial concentration of competing counter-ions was also varied. In cationic ternary systems, for example, two different ionic ratios were quantified: the ratio of the sum of calcium and magnesium to sodium and the ratio of calcium to magnesium. It should be noted that ionic ratios change when solutions equilibrate with resins. Because it was not possible to predict ionic ratios for equilibrated solutions, solutions were designed to specific ionic ratios in their initial condition.

3.4 Results

The objective of this experimental phase was to determine the effect of changing ionic strength and ionic composition on the selectivity of IX resins for common ions found in RO concentrate. Preliminary batch isotherms were obtained at ionic strengths up to 1.5 M, but column tests demonstrated that the service cycle of a column process would be too short to be practical at that ionic strength, so later experiments were done at lower ionic strengths.

3.4.1 Cation Exchange Isotherms

Several cation exchange tests were performed in the course of the research. The different tests varied in terms of range of ion concentrations, number of points, and ions included. As lab experience increased, experimental procedures and data analysis improved. In particular, the concentration range of the exchanging ions decreased, and the number of points in the isotherm increased. This allowed more precise measurement of changes in selectivity over a smaller range of ionic strengths. Isotherm test parameters are listed in Table 3.2.

Table 3.2. Cation Exchange Isotherm Tests

Test #	Exchanging Ions	Experimental Notes	Initial Concentration Range (M)
1	Mg, Na	12 points	Mg: 0.020–0.526 Na: 0.013–0.719
2	Ca, Na	12 points	Ca: 0.018–0.413 Na: 0.009–0.687
3	Ca, Mg, Na	12 points	Ca: 0.015–0.323 Mg: 0.005–0.116 Na: 0.011–0.611
4	Ca, Mg, Na	24 points, stripped resin w/ HCl to measure resin phase concentrations	Ca: 0.003–0.077 Mg: 0.011–0.065 Na: 0.021–0.141

For the first three isotherm tests, exchanging ion concentrations were measured in the solution before and after equilibration with the resin. Equivalents of exchanged ions per gram of resin were calculated from these two values. For the last isotherm, concentrations of exchanging ions were measured in the initial solution and in the 2N HCl solution used to strip the equilibrated and washed resin. These two values were used to calculate the concentration of exchanging ions in the equilibrated solution. Ion concentrations were used to calculate separation factors and ionic strengths for each point on the isotherm. Equations 3.1–3.6 are used to calculate these values.

Equation 3.1: Resin Phase Ion Concentration (Tests 1-3)

$$q_i = \frac{\left([i]_{\text{init}} - [i]_{\text{final}}\right) * \text{V}}{M}$$

where q_i is the resin phase ion equivalent concentration, [i] is the solution phase ion equivalent concentration, V is the solution volume, and M is the resin mass

Equation 3.2: Resin Phase Ion Concentration (Test 4)

$$q_i = \frac{[i]_{\text{stripped solution}} \times \text{V}}{\text{M}}$$

Equation 3.3: Solution Phase Ion Concentration (Test 4)

$$C_i = \frac{\left([i]_{\text{init}} * \text{V} + \text{q}_i * \text{M}\right)}{\text{V}}$$

where C_i is the solution phase ion equivalent concentration

Equation 3.4: Solution Phase Equivalent Fraction

$$(X_1)_s = \frac{[1] z_1}{[1] z_1 + [2] z_2 + [3] z_3}$$

where $(X_1)_s$ is the equivalent fraction of ion 1 in solution and z_1 is the charge of ion 1

Equation 3.5: Separation Factor

$$\alpha_1^2 = \frac{(X_2)_r \times (X_1)_s}{(X_1)_r \times (X_2)_s}$$

where $(X_1)_r$ is the resin phase equivalent fraction of ion 2

Equation 3.6: Ionic Strength

$$IS = 0.5 * \sum \left(C_i z_i^2\right)$$

(Note: Co-ion concentration was estimated by sum of counter-ions.)

Separation factors for calcium and magnesium were calculated for all tests. Calcium separation factors are plotted against ionic strength and equivalent fraction in Figures 3.3 and 3.4. There was a general pattern of decreasing selectivity with both increasing equivalent fraction and ionic strength, but neither relationship was strong enough to be predictive. In both cases, the decrease appeared to be exponential, so a log-based regression was performed for separation factors with both variables, and a strong correlation was observed. The resulting equation and the associated regression statistics are shown in Table 3.3. The dotted line in the figure has a slope of 1. To illustrate this correlation, predicted separation factors are plotted against calculated separation factors in Figure 3.5.

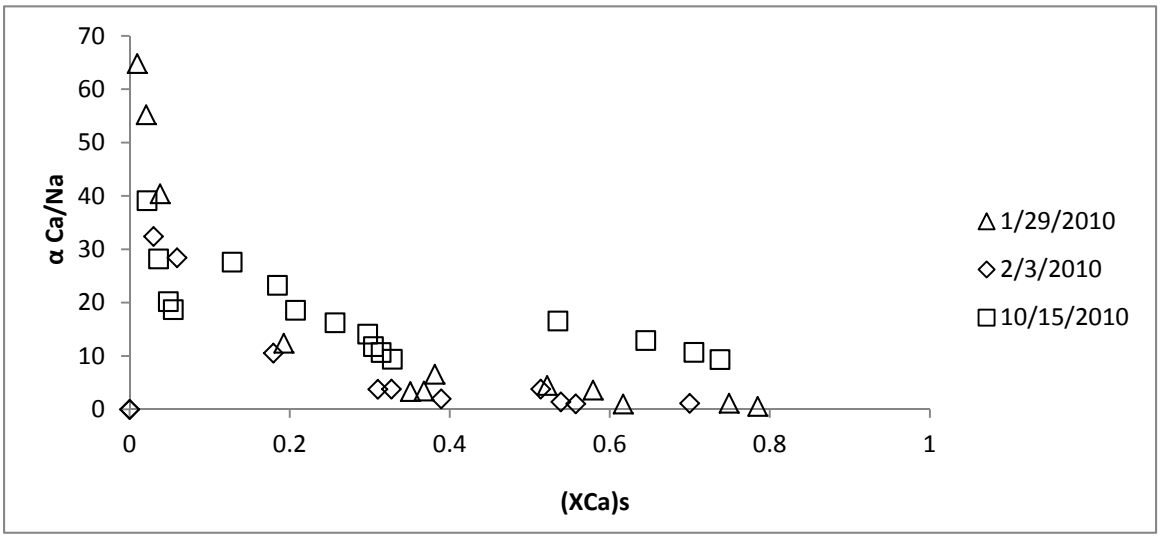

Figure 3.3. Calcium separation factors versus equivalent fraction of calcium.

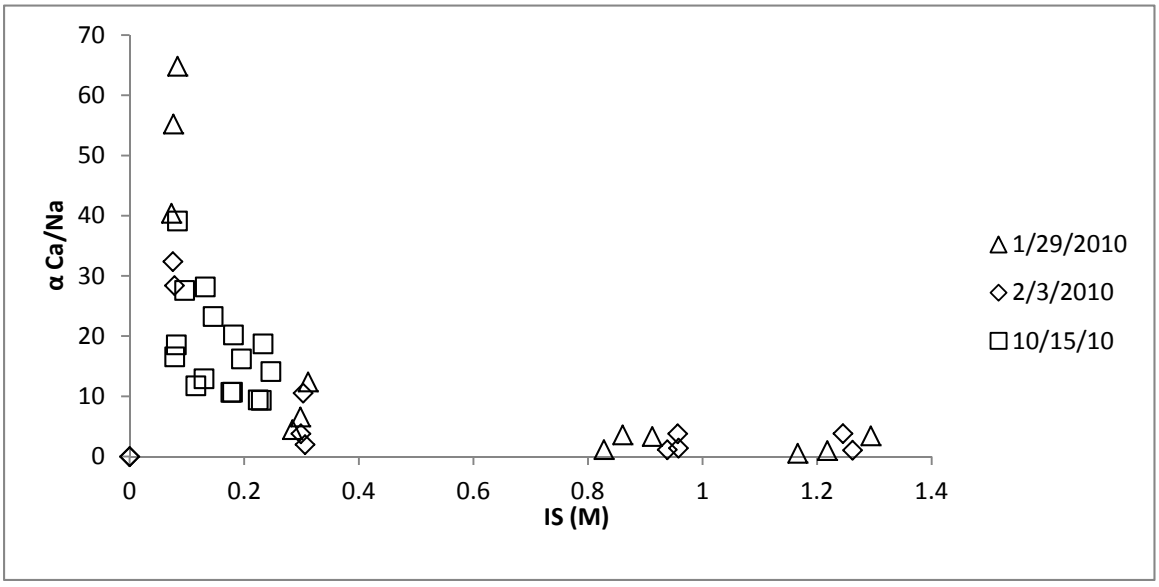

Figure 3.4. Calcium separation factors versus solution ionic strength.

Table 3.3. Regression Equation and Associated Statistics for Calcium Separation Factors

Regression Equation for Calcium Separation Factor:

$$\log(\alpha_{Na}^{Ca}) = -0.344 * \log((X_{Ca})_s - .885 * \log(\text{IS}) + 0.193$$

Regression Statistics	
Multiple *R*	0.96
R^2	0.92
Adjusted R^2	0.91
Standard error	0.15
Observations	28

Selectivity decreases with ionic strength because of the corresponding decrease in ion activity. It is also explained by the concept of Donnan potential, which is built up in response to the concentration gradients of co-ions between the solution and resin phases (Helfferich, 1962; Harland, 1994; Zagorodni, 2007). The gradient and the corresponding electrical potential generated at the resin–solution interface (Donnan potential) are highest when the resin is in contact with very dilute solutions. It excludes multivalent ions more efficiently than monovalent ions, and this effect becomes more pronounced as the solution becomes more dilute (Harland, 1994; Zagorodni, 2007).

Using the multiple regression equation, a matrix of predicted separation factors with changing ionic strength and solution phase equivalent fraction was created. Using the MATLAB model, the number of bed volumes to breakthrough was calculated. For the purposes of this investigation, breakthrough was defined as an effluent calcium concentration of C/C_0=0.1, which was equal to 5 mg/L. The parameters of the system used in the model are shown in Table 3.4. Breakthrough curves for four systems with separation factors ranging from 1.5 to 8 are shown in Figure 3.6.

Table 3.4. Parameters for Modeling the Bed Volumes to Breakthrough for Different Separation Factors

	mg/L	meq/L
Ca	500	0.02
Na	200	0.01
Eq Fraction Ca	0.74	
IS	0.04	

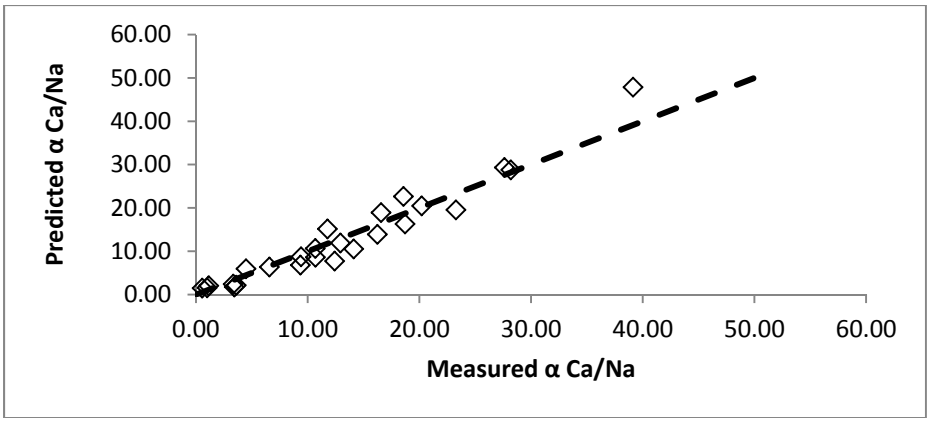

Figure 3.5. Predicted calcium separation factors versus measured calcium separation factors.

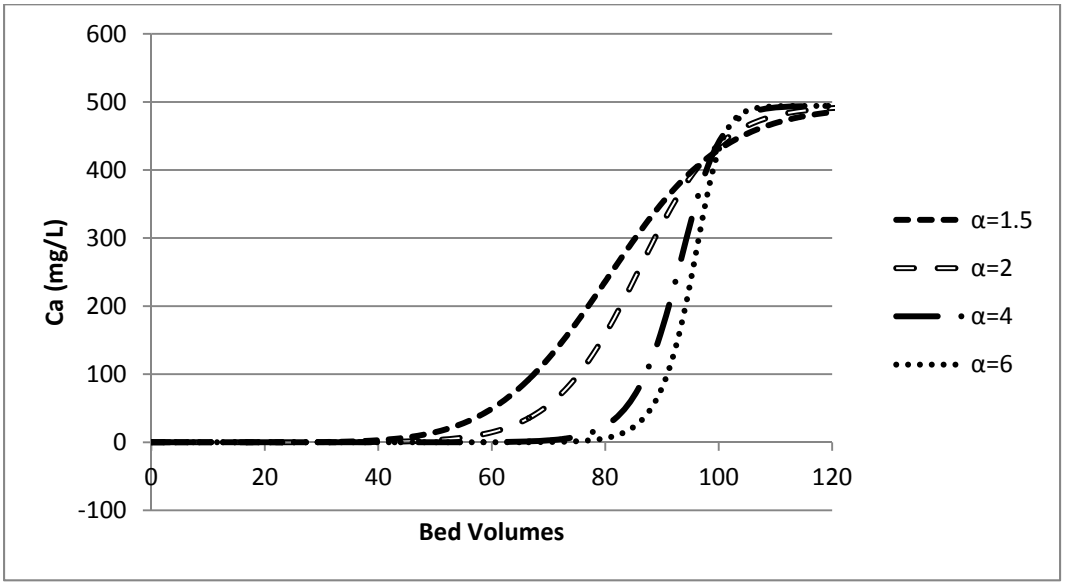

Figure 3.6. Modeled breakthrough curves for systems with separation factors ranging from 1.5 to 6.

Decrease in the separation factor results in a broader MTZ, which can be visualized as the difference in bed volumes between initial breakthrough and the point at which the influent calcium concentration is equal to the effluent concentration. As the MTZ becomes broader, more column capacity is unused at breakthrough. The length of the MTZ is also dependent on dispersion, but if dispersion is constant, a decrease in the separation factor will result in a decrease of column capacity. Figure 3.7 shows model predictions of the number of bed volumes to breakthrough as a function of the calcium separation factor using the number of column segments (20) that best fit the dispersion that existed in the laboratory columns discussed in the next section. The figure shows that the number of bed volumes to breakthrough decreases more quickly in response to changes in separation factor below four.

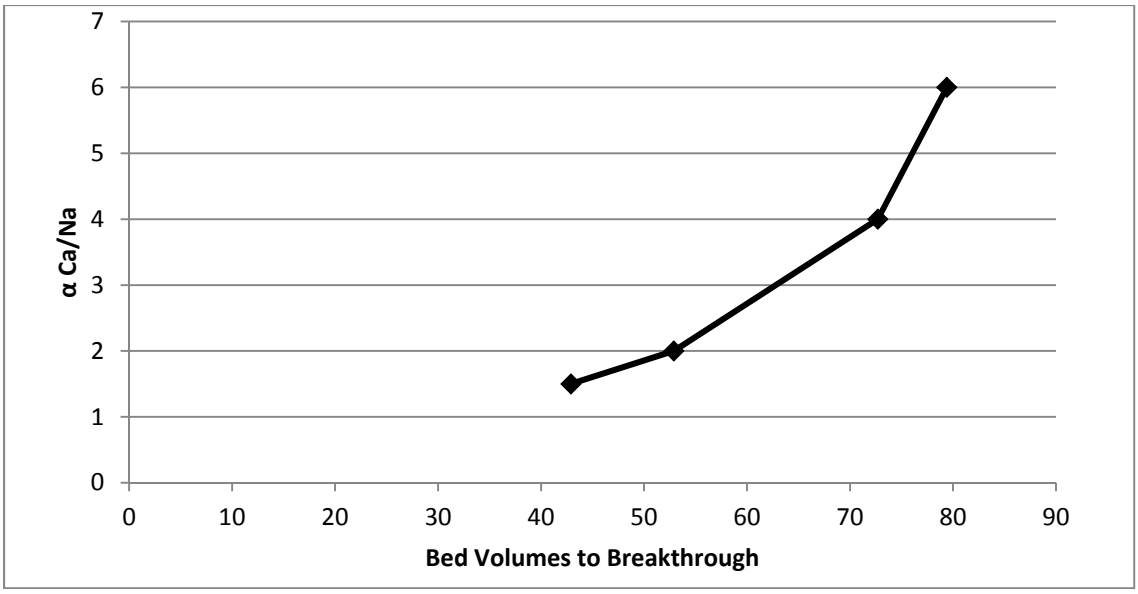

Figure 3.7. Bed volumes to breakthrough as a function of calcium separation factor.

When the regression is plotted as a surface (Figure 3.8), it is evident that the separation factor changes more quickly with ionic strength than with equivalent ionic fraction and that the most rapid changes with both variables occur in the lower ranges. At ionic strengths of 0.35 and below, separation factors are predicted to be above 4 even at very high equivalent fractions of calcium in solution. Resin selectivity is not a limiting factor for treatment of a wide range of RO concentrates.

The same analysis was done for magnesium isotherm measurements and similar results were found. Separation factor is plotted against equivalent fraction and ionic strength in Figures 3.9 and 3.10. There is a general trend of decreasing selectivity with both ionic strength and equivalent fraction. A multiple log regression of separation factor as a function of equivalent fraction and ionic strength showed a strong correlation between predicted and calculated separation factors. The regression equation and associated statistics are shown in Table 3.5, and Figure 3.11 shows the correlation between calculated and predicted separation factors.

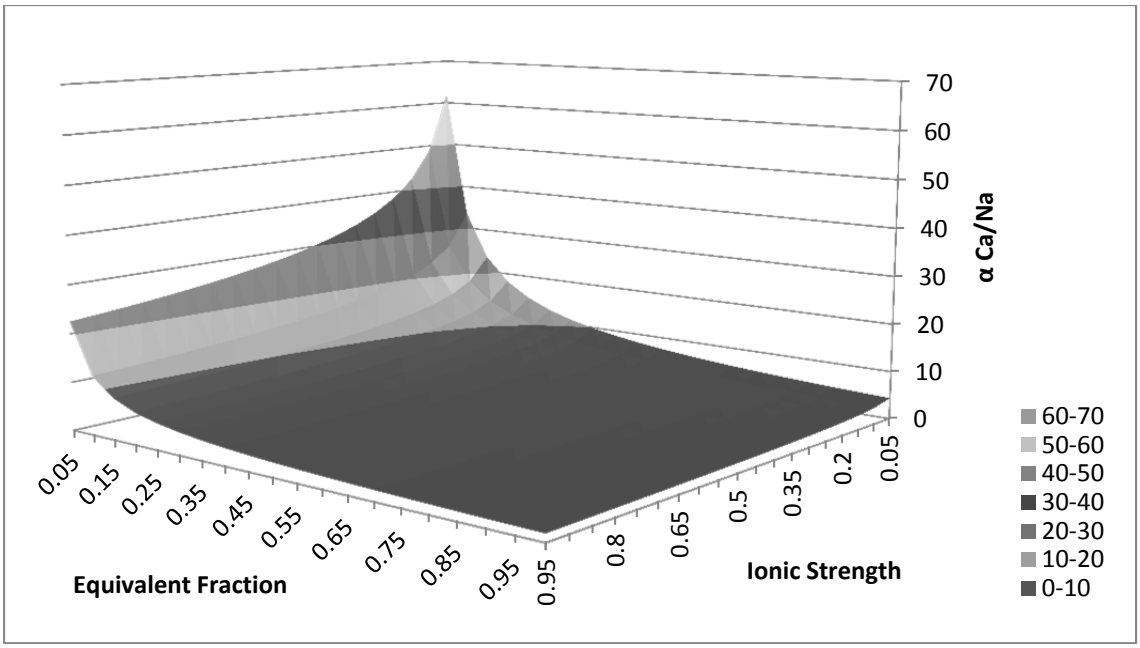

Figure 3.8. Separation factor as a function of ionic strength and equivalent ionic fraction of calcium.

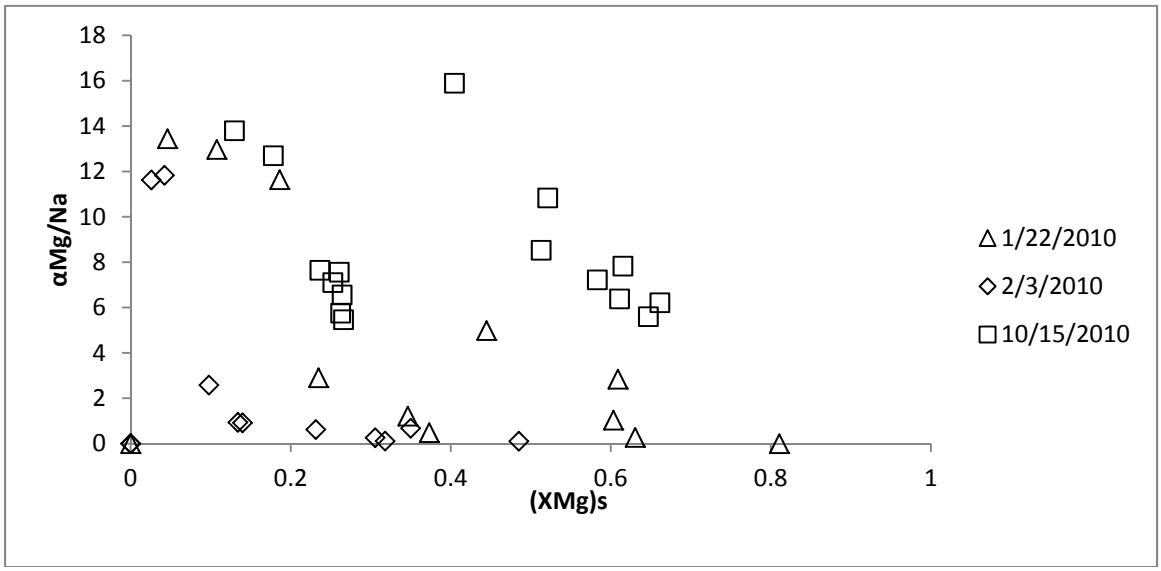

Figure 3.9. Magnesium separation factors versus equivalent fraction of magnesium.

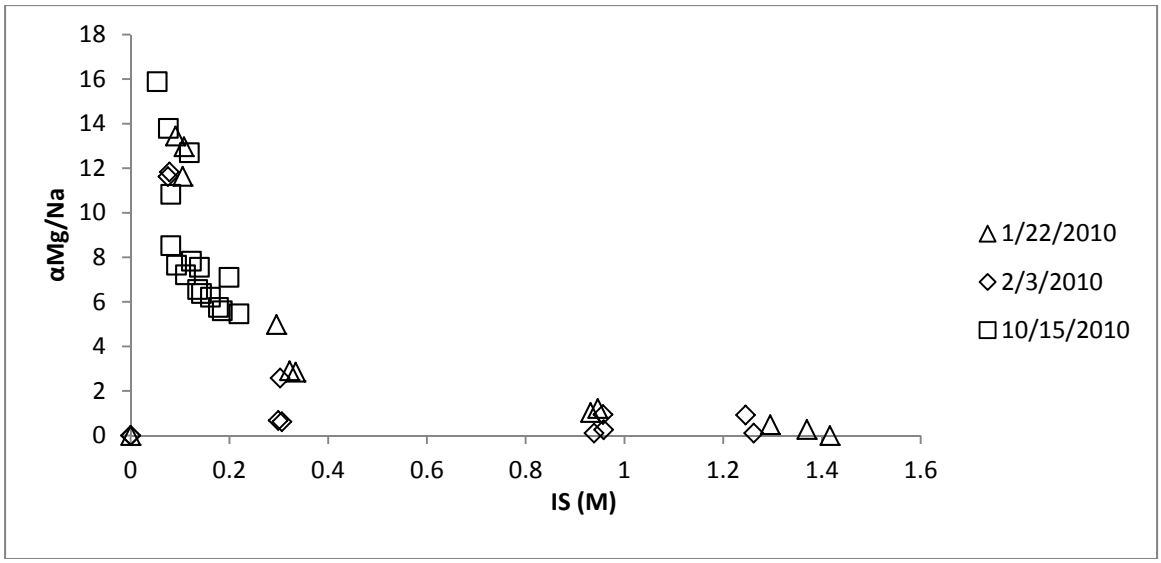

Figure 3.10. Magnesium separation factors versus ionic strength.

Table 3.5. Regression Equation and Associated Statistics for Magnesium Separation Factors

Regression Equation for Magnesium Separation Factor:

$$\log(\alpha_a^b) = -0.208 * \log((X_b)_s - 1.040 * \log(\text{IS}) - 0.139$$

Regression Statistics	
Multiple *R*	0.97
R^2	0.94
Adjusted R^2	0.94
Standard error	0.11
Observations	26

A surface was plotted to show how magnesium separation factors change as a function of ionic strength and equivalent fraction (see Figure 3.12). Magnesium separation factors react similarly to calcium separation factors as solution characteristics change. Both show a more rapid decrease in selectivity with increasing ionic strength than with increasing equivalent fraction in solution. Although the resin selectivity for the two ions responds similarly to changes in ionic strength and equivalent ratio, calcium selectivity is always greater than magnesium selectivity. This is a well-established selectivity sequence for SAC resins and was discussed previously.

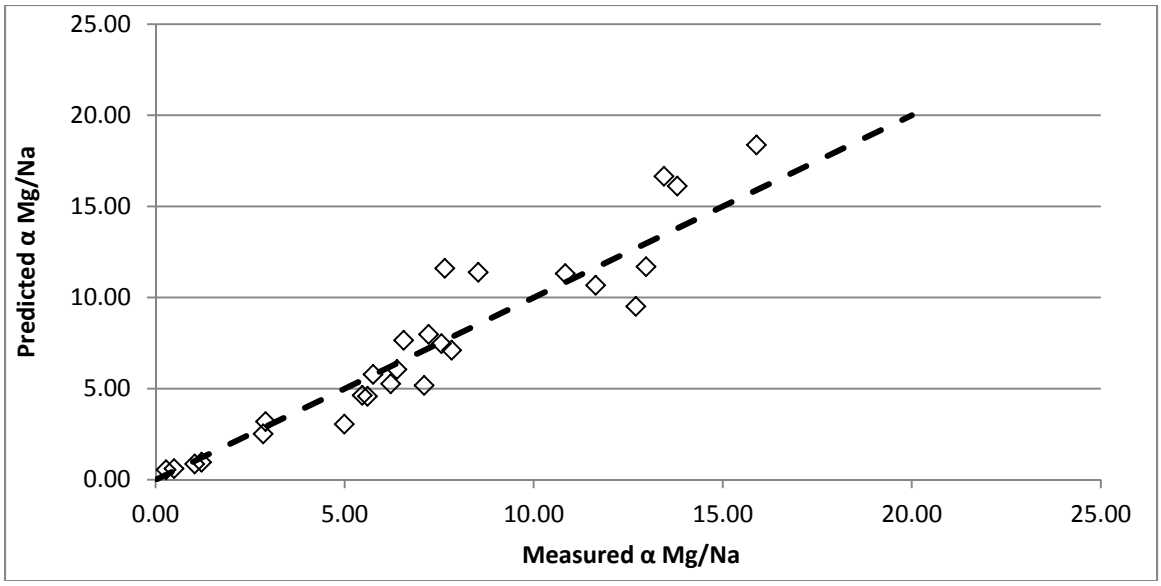

Figure 3.11. Predicted magnesium separation factors versus measured magnesium separation factors.

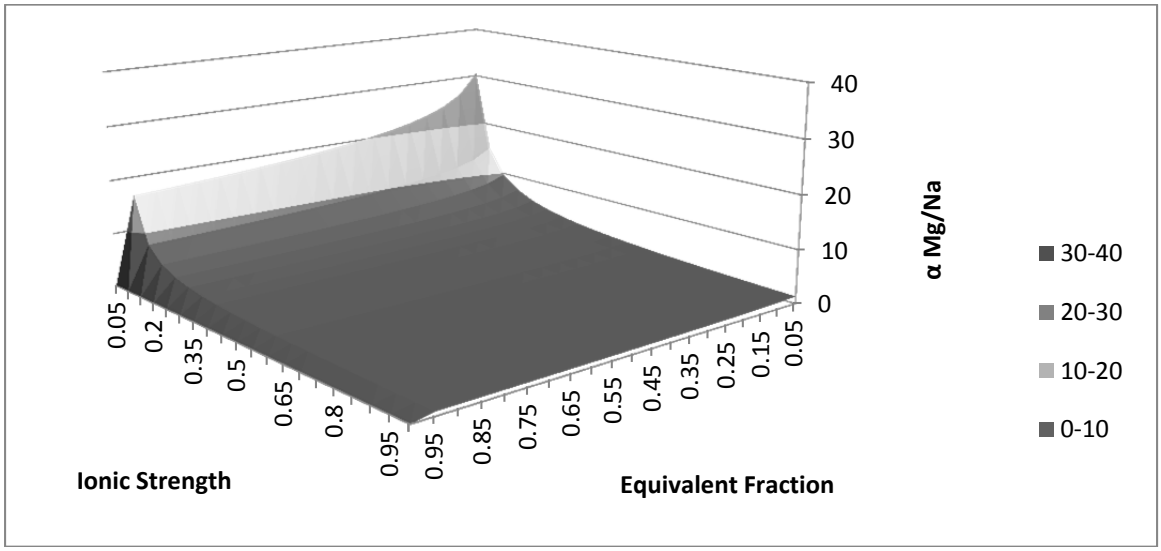

Figure 3.12. Surface plot showing changing separation factor with ionic strength and equivalent ionic fraction.

From cation exchange isotherm measurement, it was established that separation values for calcium and magnesium can be predicted by a log multiple regression on equivalent fraction in solution and ionic strength. For both ions, there is a more rapid decrease in selectivity with ionic strength than with equivalent fraction. Both regressions show a strong correlation. For both ions, selectivity values are adequate for efficient IX in solutions with ionic strengths above 0.25 M. To put this in perspective, an example feed water containing calcium, magnesium, potassium, sodium, sulfate, and chloride with an ionic strength of 0.27 has about 4500 mg/L of total dissolved solids (TDS). For solutions with high ionic strength, IX may still be feasible if the equivalent fraction of divalent ions in solution is low. However, selectivity is not the only factor to consider in the application of IX to RO concentrate. If resin loading is very high, the number of bed volumes to exhaustion may not be high enough to make the process efficient. This issue was addressed in Phase 2, in which lab scale column tests were conducted.

Table 3.6. Anion Exchange Isotherm Tests

Test #	Exchanging Ions	Experimental Notes	Initial Concentration Range (M)
1	SO_4, CO_3	18 points	SO_4: 0.017–0.192 $TOTCO_3$: 0.017–0.083

3.4.2 Anion Exchange Isotherms

An 18-point anion exchange batch isotherm was measured. Isotherm test numbers and parameters are listed in Table 3.6.

Separation factors for sulfate and carbonate were calculated for all tests. The concentration of bicarbonate in solution did not change significantly, so separation factors were not calculated for bicarbonate. Sulfate separation factors are plotted against ionic strength and equivalent fraction in Figures 3.13 and 3.14. Carbonate separation factors are plotted against ionic strength and equivalent fraction in Figures 3.15 and 3.16.

The sulfate separation factor is better correlated with ionic strength than with equivalent fraction, and a multiple regression on separation factor as a function of both variables did not produce a strong correlation. However, it was possible to fit a power function to the relationship between separation factor and ionic strength (see Figure 3.13). The same pattern of relationships was seen with carbonate separation factors (see Figures 3.15 and 3.16), but the correlation between ionic strength and separation factor was not as strong. This may be due to the fact that the dependence of carbonate speciation on pH made concentrations more difficult to measure. The predictive power of the relationship between sulfate separation and ionic strength is tested in the next section in which it is applied to column tests.

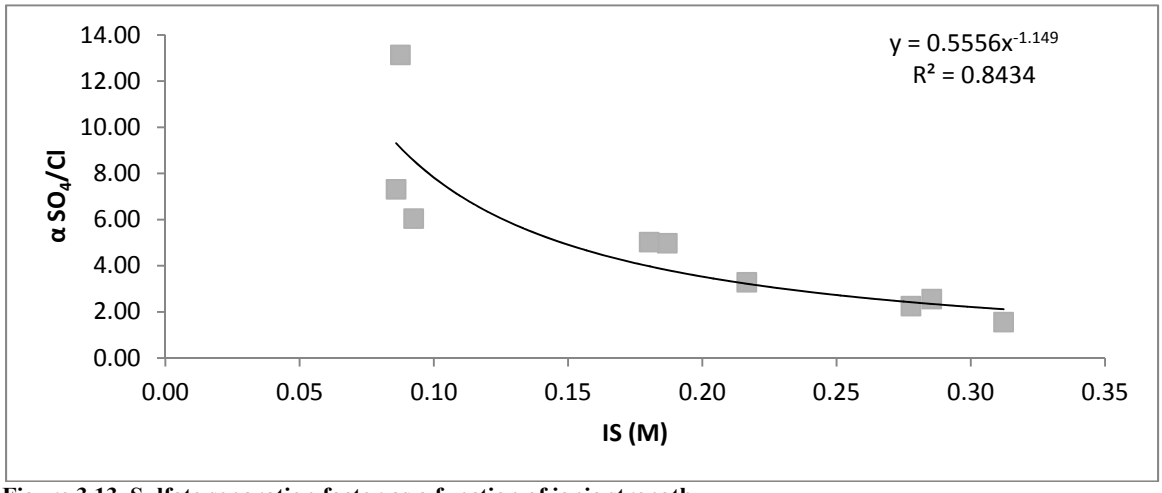

Figure 3.13. Sulfate separation factor as a function of ionic strength.

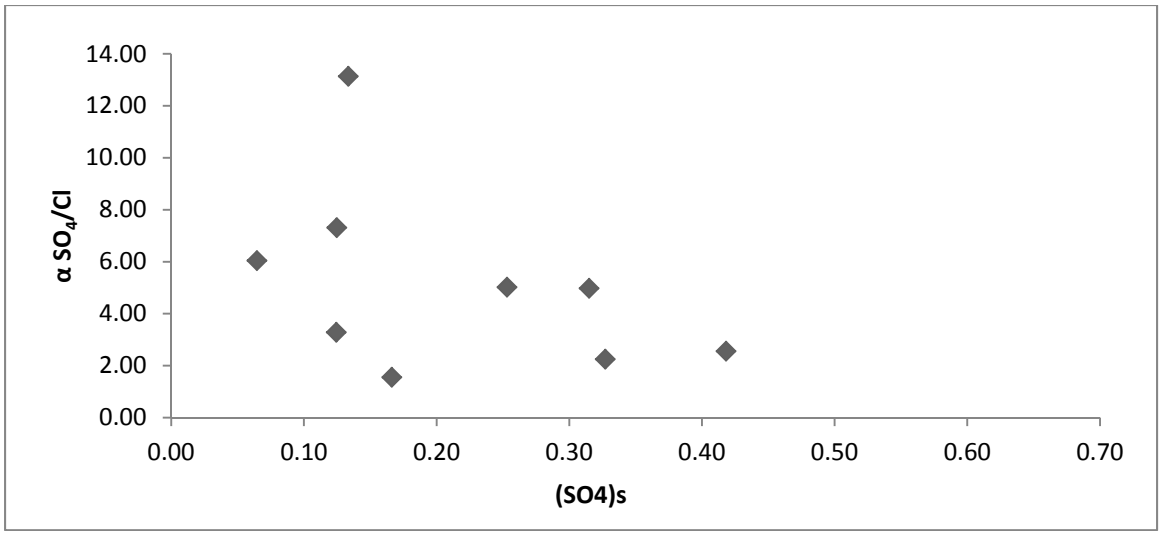

Figure 3.14. Sulfate separation factor as a function of ionic fraction.

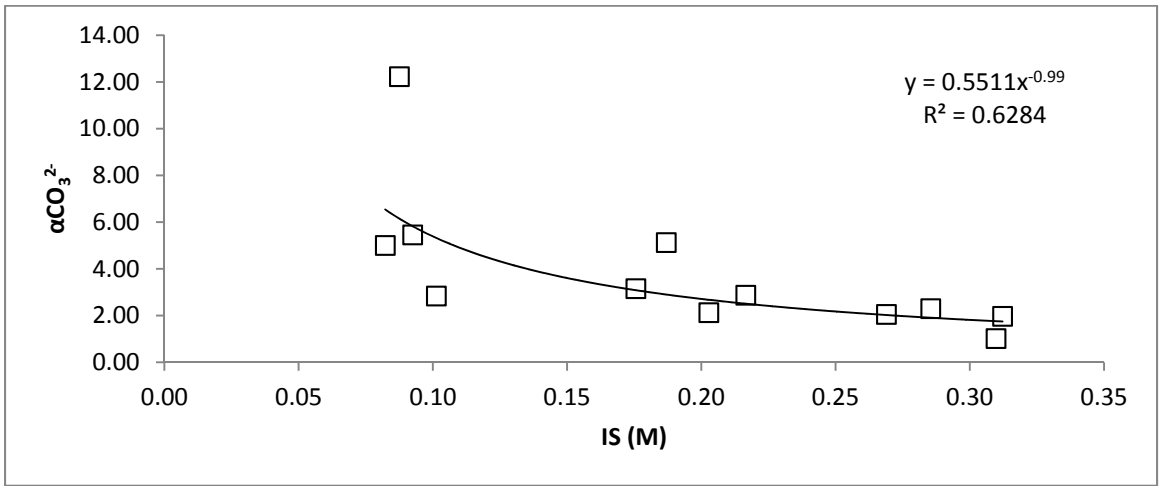

Figure 3.15. Carbonate separation factor as a function of ionic strength.

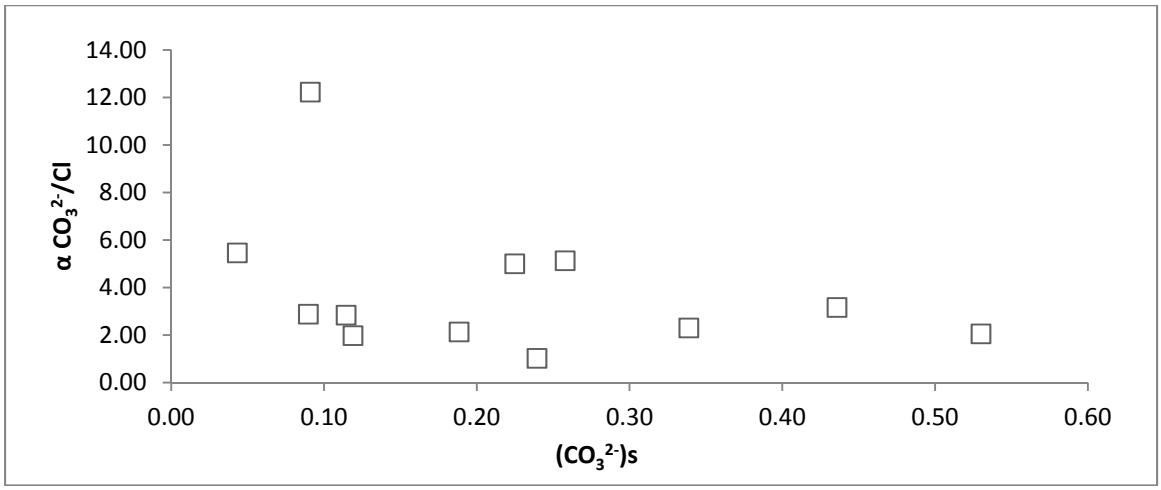

Figure 3.16. Carbonate separation factor as a function of equivalent fraction.

Chapter 4

Phase 2—Column Testing for Selectivity Verification and Ion Separation

4.1 Chapter Objectives

This section describes results from lab-scale column testing of IX resins with reference to three separate objectives:

1. To correlate column performance with selectivity values measured in batch isotherms for similar solutions.
2. To separate chromatographic peaks of ions during regeneration by varying regeneration flow rate, concentration, and direction.
3. To recover specific ions from a column by regeneration of a specific portion of a column. Resin phase concentrations of ions in a loaded column were measured using a specially designed column that allowed access to the resin along its longitudinal axis. Resin samples from along the column's length were analyzed to determine the concentrations of ions at each location.

4.2 Chapter Summary

The key results and conclusions from the lab scale column testing experiments are as follows:

1. Separation factors calculated in batch tests correlate well with separation factors estimated from column tests.
2. Elution curves show that chromatographic peaks for calcium and magnesium overlap when standard regeneration flow rates and sodium chloride concentrations are used.
3. Variation of regeneration flow rate, concentration, and direction did not result in sufficient separation of calcium and magnesium chromatographic peaks for separate ion capture.
4. Measurement of resin phase ion concentrations along the length of a loaded IX column showed that discreet ion layers do not form during loading. Instead equilibrium concentrations are propagated along the column, in the direction of flow.

4.3 Methods

A bench-scale IX system was constructed for Phase 2 experiments (see Figure 4.1). This system allowed the feed or regeneration solution to be pumped through two columns in series, in either direction. For example, fluid could move in a downward direction through Column 1 and then in an upward direction through Column 2. In addition, a third column could be regenerated while the other two columns were in use. Columns were held in place by reusable clamps, which allowed them to be moved or changed for other columns easily. This design also allowed changes to the flow pattern without adjustments to the tubing.

Figure 4.1. Phase 2 setup—front (left), back (right).

4.3.1 Observed Column Compared with Predictions

The first step in the experimental process was to verify that the separation factors determined during the batch tests in Phase 1 were applicable to column processes. Solutions similar to those that were used during Phase 1 were fed into an IX column until the column was exhausted. The regression relationship from Phase 1 was used to predict the separation factors, based upon the ionic strength of the feed solution and the solution-phase equivalent fraction of exchanging ions(s). Equation 4.1 shows the calculation of solution phase equivalent fraction. Predictions from the MATLAB model show a relationship between the size of the MTZ and the separation factor (see Table 4.1). This relationship is evident in the modeled breakthrough curves for a system with an influent solution containing 500 mg/L of calcium and 200 mg/L of sodium in Figure 4.2. The difference between the point of breakthrough and the point at which the effluent solution concentrations of calcium and magnesium are equal to the influent solution concentrations is the size of the MTZ in the column (see Figure 4.2).

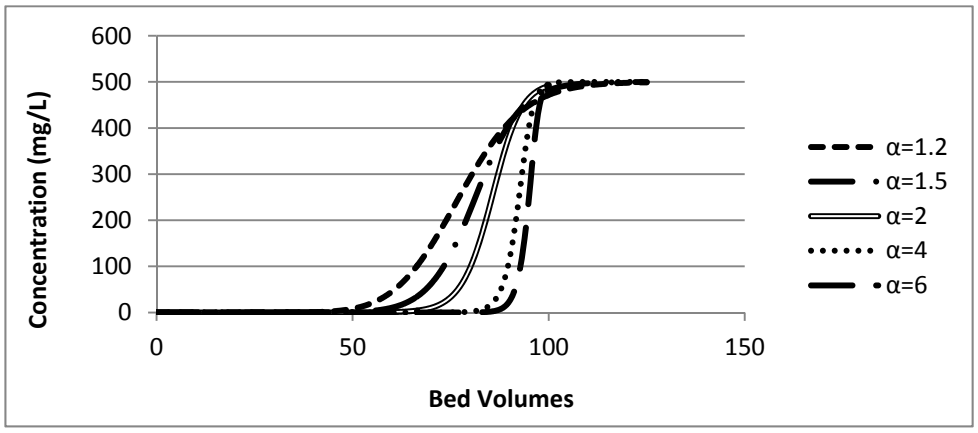

Figure 4.2. Modeled breakthrough curves for varied separation factors.

Equation 4.1: Calculation of Equivalent Fraction in Solution	$(X_i)_s = \frac{C_i}{C_i + C_{\text{Na or Cl}}}$ where $(X_i)_s$ is the solution phase ionic fraction of exchanging ion
Equation 4.2: Calculation of Column Efficiency	$\text{Efficiency}(\%) = \frac{\#\text{ of BV to Breakthrough}}{\#\text{ of BV to Exhaustion}} * 100$ where Exhaustion is defined as the point where effluent ion concentration is 75% of influent ion concentration and Breakthrough is defined at effluent ion concentration where C/C_0=0.10
Equation 4.3: Calculation of Predicted Resin Phase Ion Concentration	$q_{i\text{predicted}} = \text{efficiency} \times q_{i\text{equilibrium}}$
Equation 4.4: Calculation of Resin Phase Ion Equivalents of Exchanging Ions	$q_i = \frac{q_T C_i \alpha_k^i}{\sum_{k=1}^{n} \alpha_k^n C_n}$
Equation 4.5: Calculation of Bed Volumes to Breakthrough	$\text{BV}_{BT} = \frac{q_{i_{BT}}}{C_i}$ where q_{iBT} is the estimated concentration of exchanging ion on the resin at breakthrough

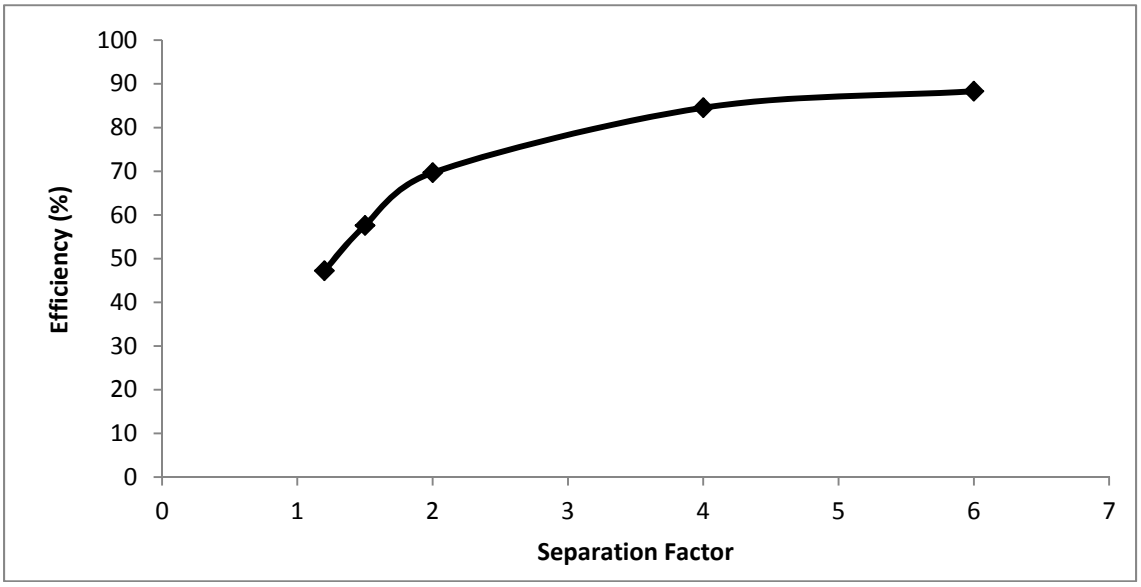

Figure 4.3. Relationship between separation factor and column efficiency.

Table 4.1. Size of Mass Transfer Zone and Efficiency of Column at Varied Separation Factors

α	BV to Breakthrough (A)	BV to C=0.95 C_{in} (B)	Mass Transfer Zone Size (BV) (B - A)	Efficiency
1.2	47.7	101	53.3	47.23
1.5	56.5	98.1	41.6	57.59
2	67.1	96.3	29.2	69.68
4	82	97	15	84.54
6	87	98.5	11.5	88.32

The column efficiency, as defined in this work, is the fraction of the column that is in equilibrium with the influent solution at breakthrough, and is calculated using Equation 4.2. The relationship between the column efficiency and the separation factor is shown in Figure 4.3. The amount (equivalents) of resin-phase-exchanging ion was predicted by multiplying the column efficiency by the amount of resin-phase-exchanging ion that would exist in the entire column at exhaustion (see Equation 4.3).The equilibrium amount of exchanging ion on the resin was calculated using Equation 4.4. The number of bed volumes to breakthrough was calculated using the predicted amount of resin phase exchanging ion at breakthrough and the influent concentration, using Equation 4.5.

For tests using more than one exchanging ion, the number of bed volumes to breakthrough of each ion was calculated. Determination of sulfate and carbonate separation factors from Phase 1 was unsuccessful, but a pattern was evident in plotting the measured separation factor as a function of ionic strength from Phase 1 (see Figure 4.4). A curve was fitted to the data and used to predict sulfate separation factors. These separation factors were correlated with column efficiency using the model, and the number of bed volumes to breakthrough was predicted (see Table 4.2). The flow rate for column tests in this section was 100 mL/min, and the column volume was 386 mL.

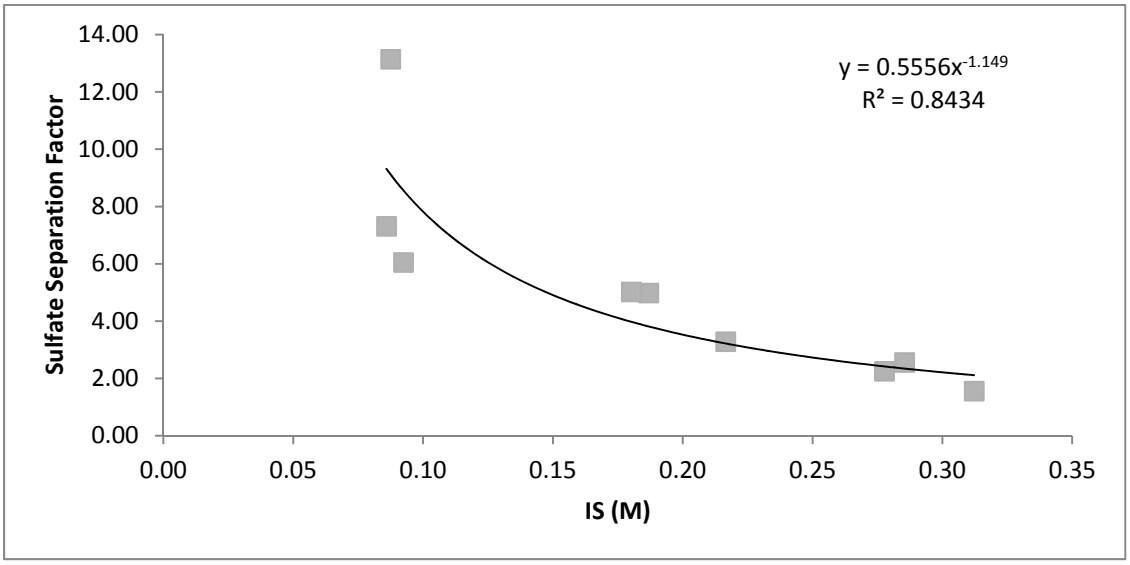

Figure 4.4. Sulfate separation factor as a function of ionic strength.

Table 4.2. Solution Ion Concentrations and Predicted Values for Selectivity Verification

Test #	[Ca]	[Na]	(XCa)s	IS (M)	Sep. Factor From Regression	Estimated Efficiency	Predicted qCa (eq/L)	BV_{BT}
1	0.045	0.015	0.86	0.15	8.81	0.89	0.99	26.99
2	0.150	0.050	0.86	0.50	3.04	0.77	0.80	6.99
3	0.225	0.075	0.86	0.75	2.12	0.70	0.70	3.89
4	0.090	0.030	0.86	0.30	4.77	0.85	0.92	12.79
5	0.083	0.250	0.40	0.50	3.95	0.84	0.55	10.18
6	0.125	0.375	0.40	0.75	2.76	0.75	0.42	5.48
7	0.050	0.150	0.40	0.30	6.20	0.89	0.70	20.08

Test #	[Mg]	[Na]	(XMg)s	IS (M)	Sep. Factor From Regression	Estimated Efficiency	Predicted qMg (eq/L)	BV_{BT}
8	0.150	0.050	0.86	0.50	1.54	0.58	0.67	5.81
9	0.225	0.075	0.86	0.75	1.01	0.40	0.46	2.67
10	0.090	0.030	0.86	0.30	2.62	0.73	0.85	12.18
11	0.083	0.250	0.40	0.50	1.81	0.63	0.73	11.36

Test #	[Mg]	[Ca]	[Na]	(XCa)s	(XMg)s	IS (M)	Ca Sep. Factor From Regression	Mg Sep. Factor From Regression
12	0.009	0.036	0.015	0.83	0.55	0.15	8.92	5.92
13	0.015	0.060	0.025	0.83	0.55	0.25	5.68	3.48
14	0.021	0.084	0.035	0.83	0.55	0.35	4.21	2.45
15	0.009	0.036	0.015	0.83	0.55	0.15	8.92	5.92

Test #	Estimated Efficiency (Mg)	Predicted qMg (eq/L)	Predicted qCa (eq/L)	BV_{BT}
12	0.88	0.14	0.86	20.50
13	0.80	0.13	0.83	10.32
14	0.72	0.11	0.78	6.27
15	0.88	.014	0.86	20.50

Test #	[SO4]	[Cl]	(XSO4)s	IS (M)	Predicted SO_4 Sep. Factor	Efficiency SO_4	Pred qSO_4 (eq)	BV_{BT}
17	0.045	0.030	0.750	0.30	1.9	0.69	0.21	5.47
18	0.045	0.030	0.750	0.30	1.76	0.63	0.17	4.85

Samples of column effluent were taken at short intervals to produce breakthrough and elution curves. These data were used to measure the actual number of bed volumes to breakthrough for each ion. These were compared with the predicted numbers of bed volumes to breakthrough in the next section.

4.3.2 Separation of Ions by Varying Regeneration Conditions

The second objective in this section was to separate chromatographic peaks of ions during regeneration by varying regeneration flow rate, concentration, and direction. This was only applied to the cation exchange column. Typical regeneration (25 mL/min and 12.5% sodium chloride solution) was performed on all exhausted columns from the selectivity verification experiments completed previously (Table 4.2 in the previous section). Effluent samples were taken during regeneration, and baseline elution curves were generated from these data. The process of regeneration is achieved by flooding the resin with a concentrated solution containing a low-selectivity ion such as sodium. For complete regeneration to occur, a selectivity sequence reversal must occur. The resin preference for higher-valence ions (electrostatic attraction) increases with greater solution dilution because of the increased Donnan potential (Harland, 1994). Contact with a highly concentrated solution reverses selectivity in favor of the lower-valence ion, and it exchanges with the higher-valence ion on the resin.

During regeneration, higher-selectivity ions should theoretically elute from the column later than lower-selectivity ions under normal conditions. Difference in selectivity is the basis for ion chromatography. However, in ion chromatography, columns are specifically designed for ion separation. Columns are packed and flow rates are optimized to limit the effects of dispersive and diffusive mixing within the column, so resin selectivity is the primary factor in the time that it takes each ion to exit the column. In standard IX, columns are designed for water treatment rather than ion separation, and dispersion can lead to mixing of ions during elution. It was postulated that reducing the strength of the regeneration solution would make it possible to elute lower-selectivity ions first and follow by eluting the higher-selectivity ions with a more concentrated regeneration solution. It is important to note that as the difference between selectivity factors of any two ions becomes smaller, it will be more difficult to separate them during elution. Dispersion may be reduced by reducing the velocity of the regeneration solution flowing through the column. For these reasons, regeneration solution concentration and flow rate were chosen as variables for this part of the experiment.

A mixed solution containing calcium, magnesium, barium, sodium, and chloride was used to load the resin in the column. Solutions of different ionic ratios and ionic strengths were used. Initially, the same solutions were used to load the columns as were used during selectivity verification, but later it made sense to use more concentrated solutions to accelerate the loading process even though it resulted in decrease of column efficiency. The concentration of the ions in the solutions used to load the columns prior to the regeneration experiments is shown in Table 4.3. The regeneration operating conditions that were varied to elute ions individually are shown in Table 4.4. Effluent samples were taken at short intervals to create elution curves (ion concentration plotted against bed volumes of regeneration solution). Results are presented in the next section.

Table 4.3. Ion Concentrations in Solutions Used to Load Column Prior to Regeneration Experiments

Test #	[Ca]	[Mg]	[Ba]	[Na]
1	0.036	0.009	—	0.015
2	0.237	0.059	0.005	0.099
3	0.237	0.059	0.005	0.099
4	0.237	0.059	0.005	0.099
5	0.237	0.059	0.005	0.099
6	0.473	0.118	0.009	0.197
7	0.473	0.118	0.009	0.197
8	0.237	0.059	0.005	0.099
9	0.237	0.059	0.005	0.099
10	0.237	0.059	0.005	0.099

Table 4.4. Regeneration Operating Conditions

Test #	Flow Rate mL/min	Concentration % NaCl	Flow Direction
1	25	12.5	co-current
2	25	0.5	co-current
3	25	0.25	co-current
4	6	0.5	co-current
5	6	0.5	co-current
6	6	12.5	co-current
7	6	12.5	co-current
8	10	12.5	countercurrent
9	10	12.5	countercurrent
10	10	12.5	countercurrent

4.3.3 Recovery of Specific Ions from a Loaded Column

The hypothesis that led to experimentation with regeneration parameters was that ions distribute in bands or zones in a column, based on selectivity, with more selective ions located near the feed. The third objective was to quantify the distribution of ions within an exhausted column. A column was constructed (see Figure 4.5) featuring 20 ports along its length, from which resin could be sampled or through which regeneration solution could be pumped. This allowed selected portions of the column to be regenerated separately.

Feed solution was passed through the column until it was loaded with calcium and magnesium, and resin samples were collected from the ports along the length and analyzed to determine ion distribution. The feed solution concentrations, the number for which solutions was treated, and the flow rate are shown in Table 4.5. Resin samples were thoroughly rinsed and then submerged in 2 N HCl to strip off all exchangeable ions. The HCl solution was analyzed by AAS to determine ion concentrations. Resin samples were separated from the HCl solution by filtration and then dried at 105 °C and weighed.

Filled Column	Open Resin Ports Close Up	Closed Resin Ports
		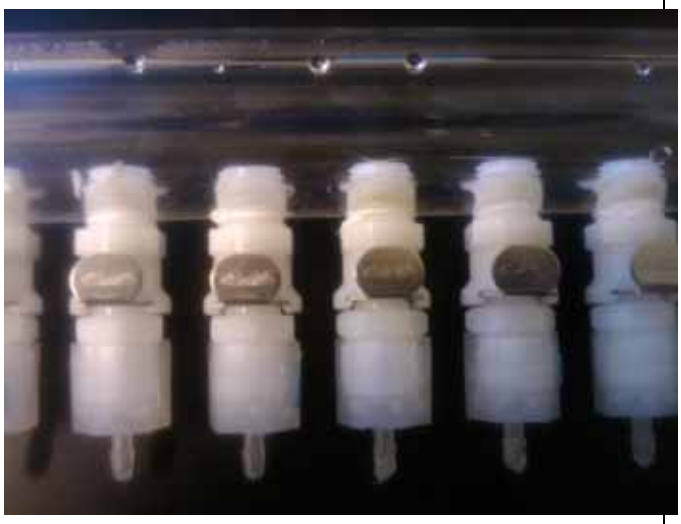

Full Column Schematic	Single Port Schematic
	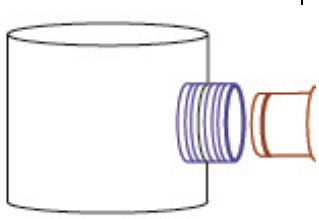

Figure 4.5. Specially designed research column with ports.

Table 4.5. Feed Solution Ion Concentrations and Number of Bed Volumes

[Ca]	[Mg]	[Na]	IS	BV	Flow Rate (mL/min)
0.06	0.02	0.10	0.35	12.26	100

4.4 Results

4.4.1 Column Performance Compared with Predictions

The first objective of this phase was to correlate column performance with separation factors measured in batch isotherms for similar solutions. Data from the two phases were compared using

a combination of modeling and regression of Phase 1 data. In Section 4.3.1, separation factors were predicted based on values of equivalent fraction of exchanging ion and ionic strength. Updated predictions of separation factors based on measured concentrations of ions in the mixed solution are shown in Table 4.6.

The number of bed volumes to breakthrough for each ion was predicted based upon the updated separation factors. Predicted number of bed volumes to breakthrough was compared with measured number of bed volumes to breakthrough to evaluate the applicability of separation factor regressions from batch isotherm test results to column processes. A measured breakthrough curve used to determine bed volumes to breakthrough is shown in Figure 4.6. Curves such as these were measured for each column test. Correlations between measured and calculated values for calcium and magnesium are shown in Figures 4.7 and 4.8, respectively. Values are listed in Table 4.7.

Table 4.6. Updated versus Original Separation Factor Predictions for Column Tests

Test #	Original Predicted αCa	Original Predicted αMg	Updated Predicted αCa	Updated Predicted αMg
1	8.81	N/A	8.25	N/A
2	3.04	N/A	4.04	N/A
3	2.12	N/A	1.93	N/A
4	4.77	N/A	4.50	N/A
5	3.95	N/A	3.74	N/A
6	2.76	N/A	2.63	N/A
7	6.20	N/A	5.91	N/A
8	N/A	1.54	N/A	1.84
9	N/A	1.01	N/A	0.97
10	N/A	2.62	N/A	2.60
11	N/A	1.81	N/A	1.97
12	8.92	5.92	8.99	6.06
13	5.68	3.48	5.60	3.43
14	4.21	2.45	4.41	2.56
15	8.92	5.92	8.37	5.50

Test #	Original Predicted αSO_4	Updated Predicted αSO_4
16	2.22	1.90
17	2.22	1.76

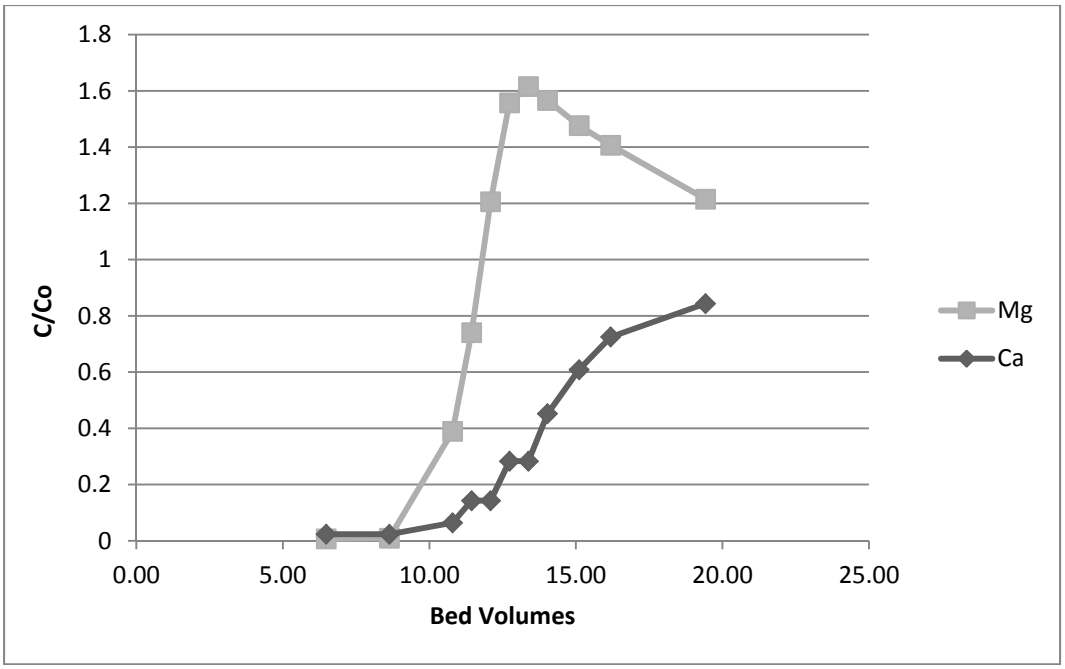

Figure 4.6. Breakthrough curve from Test #14.

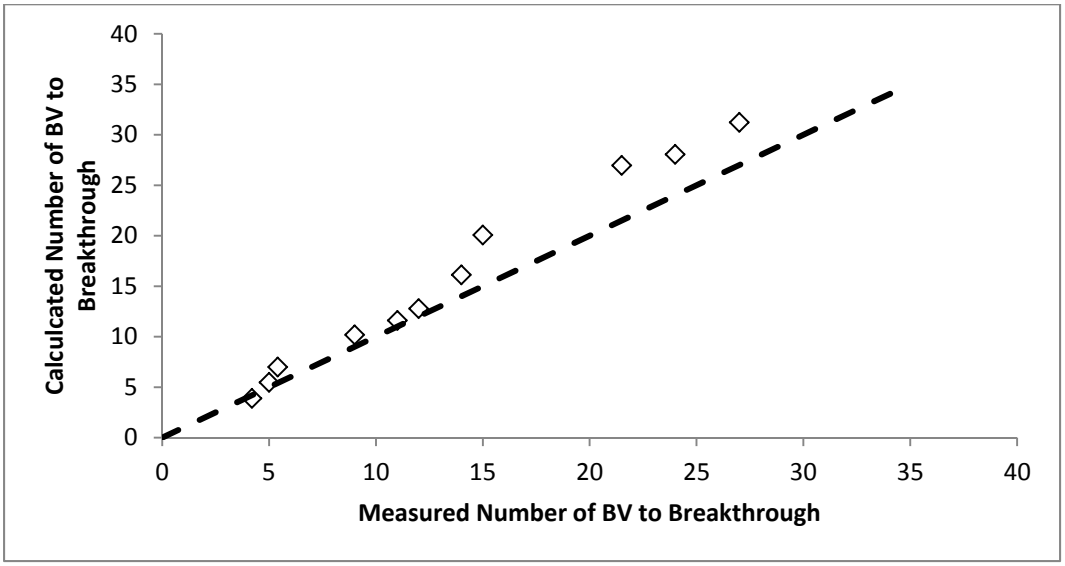

Figure 4.7. Correlation between calculated and measured numbers of bed volumes to calcium breakthrough.

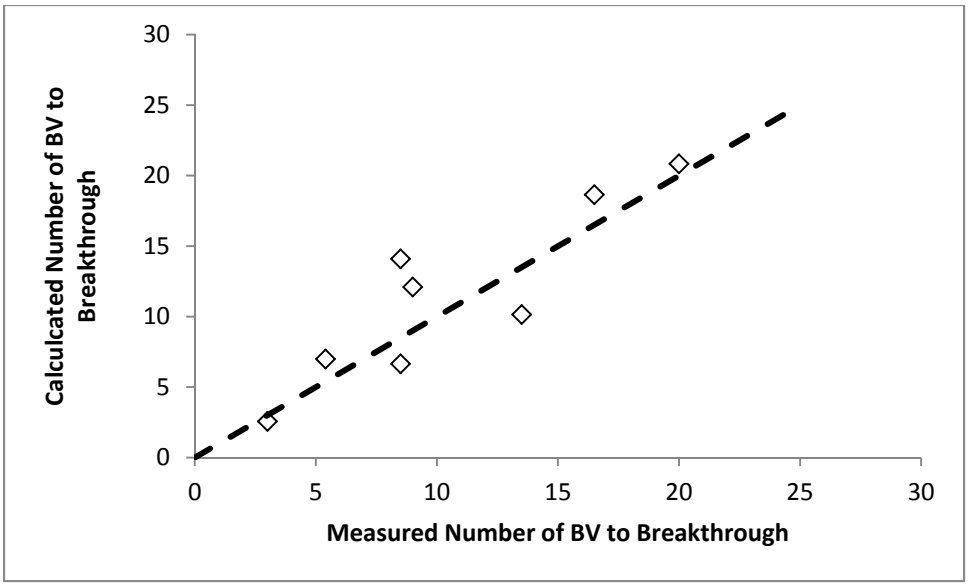

Figure 4.8. Correlation between calculated and measured numbers of bed volumes to magnesium breakthrough.

Table 4.7. Predicted versus Measured Number of Bed Volumes to Breakthrough for Column Tests

	Ca		Mg	
Test #	**Predicted BV_{BT}**	**Measured BV_{BT}**	**Predicted BV_{BT}**	**Measured BV_{BT}**
1	27.0	21.5	NA	NA
2	7.0	5.4	NA	NA
3	3.9	4.2	NA	NA
4	12.8	12	NA	NA
5	10.2	9	NA	NA
6	5.5	5	NA	NA
7	20.1	15	NA	NA
8	NA	NA	7.0	5.4
9	NA	NA	2.6	3
10	NA	NA	12.1	9
11	NA	NA	14.1	8.5
12	31.23	27	20.8	20
13	16.13	14	10.1	13.5
14	11.61	11	6.7	8.5
15	28.06	24	18.7	16.5

	SO_4	
Test #	**Predicted BV_{BT}**	**Measured BV_{BT}**
16	5.5	5
17	4.8	4.5

The correlation between measured and predicted number of bed volumes to breakthrough for the set based on calcium separation factors is very high. These results demonstrate that the regression relationship developed from batch isotherm data can predict separation accurately. The results also demonstrate that the correlation between column efficiency (size of the MTZ) and the separation factor predicted by the MATLAB model is useful in predicting the percentage of the column that is in equilibrium with the solution at the time of breakthrough. It is possible to predict the number of bed volumes to breakthrough for a column containing ResinTech CG-10 resin using the separation factor regression from Phase 1 and the model, even for solutions that have ionic strengths higher than usually treated with IX.

Correlations between measured and predicted numbers of bed volumes to breakthrough for magnesium are not as strong as those for calcium. Modeled column efficiency is a function of separation factor, not ion type, so the issue is either in the regression or in the measurement. The batch isotherm results for separation factor had more variability for magnesium than for calcium, indicating that the separation factors for magnesium may be more difficult to predict.

Only two anion exchange column tests were performed, so it is not possible to make a significant correlation, but the number of bed volumes predicted is very close to the measured value for both tests. More data are necessary to draw a definite conclusion, but it does appear that the sulfate separation factor can be predicted as a function of ionic strength.

Time to breakthrough for magnesium and calcium in column tests using solutions with ionic strengths up to 0.3 M is well predicted by combining regression of data from batch isotherm tests with column efficiency predicted by the MATLAB model. The measured time to breakthrough for sulfate agree well with that calculated by combining the relationship from Phase 1, in which sulfate separation factor is a function of ionic strength, with the column efficiency predicted by the MATLAB model. Accurate prediction of separation factors and consequent time to breakthrough in IX columns is very useful in design.

4.4.2 Separation of Ions by Varying Regeneration Conditions

The second objective of Phase 2 was to explore conditions that would allow ions to be eluted from the column separately during regeneration. Separation of ions during elution was investigated because it was hypothesized that this separation would facilitate the recovery of specific minerals from RO concentrate for beneficial reuse. The conditions that were investigated were the regeneration flow rate, concentration, and direction of flow. Testing for this objective was done only for cation exchange columns. Elution curves were measured during regeneration of column testing for Objective 1 to see how ions elute under standard conditions. Manufacturer specifications indicated that regeneration solution should contain 10–15% sodium chloride and that the flow rate should be 0.5–1.5 gpm per cubic foot. All column tests performed for this objective were regenerated with 12.5% sodium chloride solution at 0.5 gpm per cubic foot until all ions had been eluted. For the laboratory column, this corresponded to 25 mL/min. Figure 4.9 shows calcium elution curves measured during standard regeneration (25 mL/min, 12.5% NaCl). On the average, the peak calcium concentration occurred at approximately one bed volume, and the curves were asymmetrical. The calcium concentration increased quickly before the peak and declined more slowly afterward. As expected, because of its lower selectivity, peak magnesium concentrations occur slightly sooner, but the shape of the elution curves follow a similar pattern (see Figure 4.10).

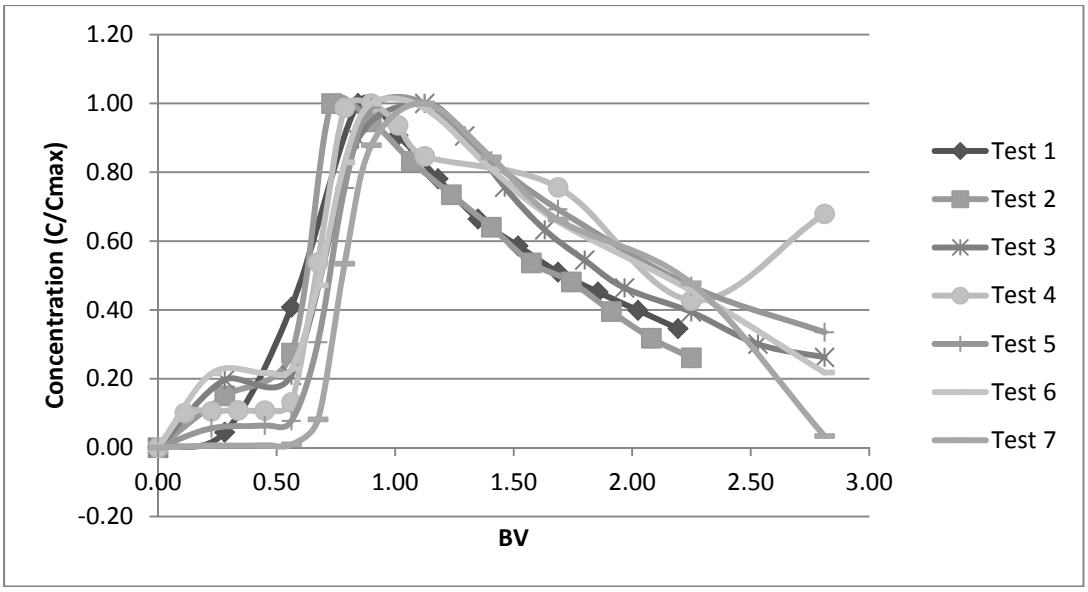

Figure 4.9. Calcium elution curves measured during standard regeneration.

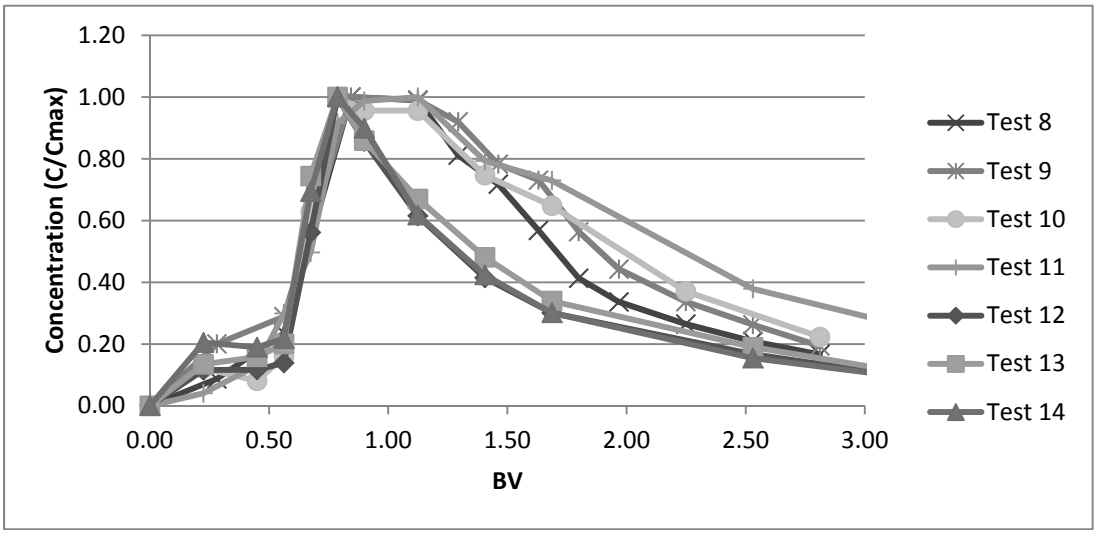

Figure 4.10. Magnesium elution curves measured during standard regeneration.

Based on the similarity of calcium and magnesium separation factors and the pronounced tailing of the elution curves, separating peaks enough to capture single cations would be difficult. In the next step, columns were loaded with solutions containing calcium, magnesium, barium, and sodium at the concentrations shown in Table 4.3. The columns were then regenerated with varying concentrations of sodium chloride solution, flow rates, and regeneration direction as shown in Table 4.4. Elution curves for the 10 regeneration variation tests are shown in Figure 4.11.

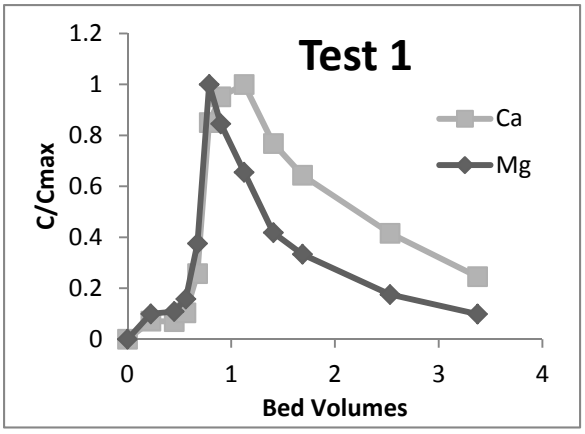
Test 1
C/Cmax
Bed Volumes
Ca
Mg

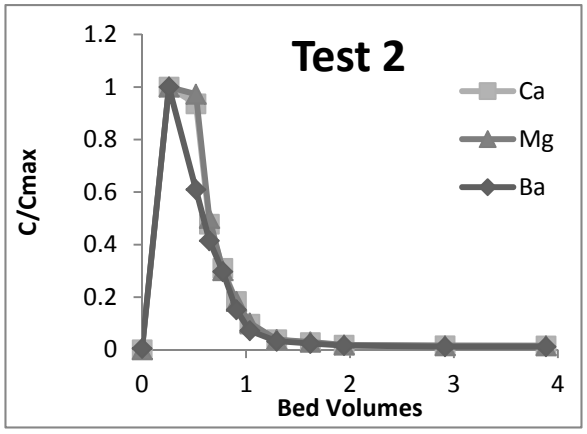
Test 2
C/Cmax
Bed Volumes
Ca
Mg
Ba

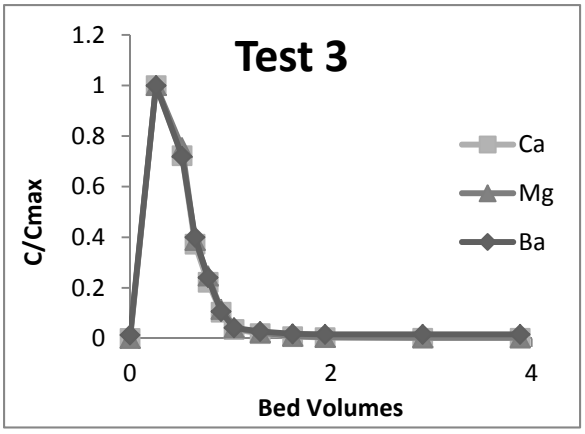
Test 3
C/Cmax
Bed Volumes
Ca
Mg
Ba

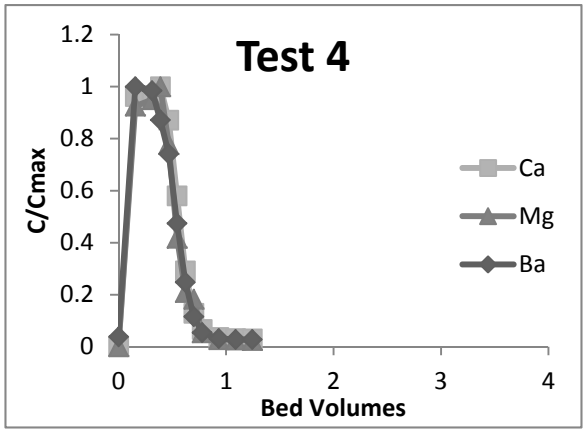
Test 4
C/Cmax
Bed Volumes
Ca
Mg
Ba

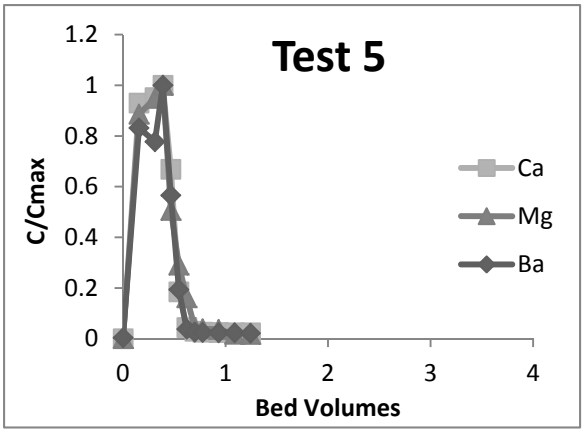
Test 5
C/Cmax
Bed Volumes
Ca
Mg
Ba

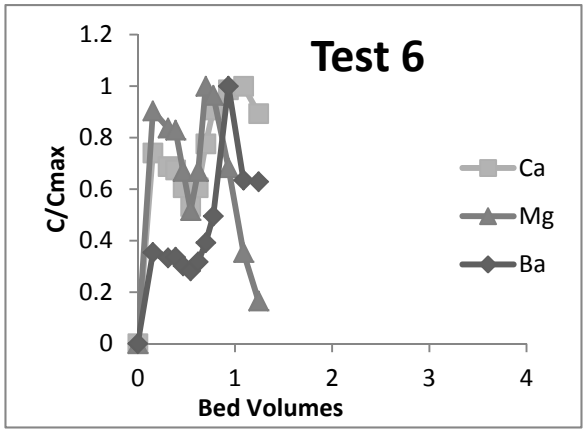
Test 6
C/Cmax
Bed Volumes
Ca
Mg
Ba

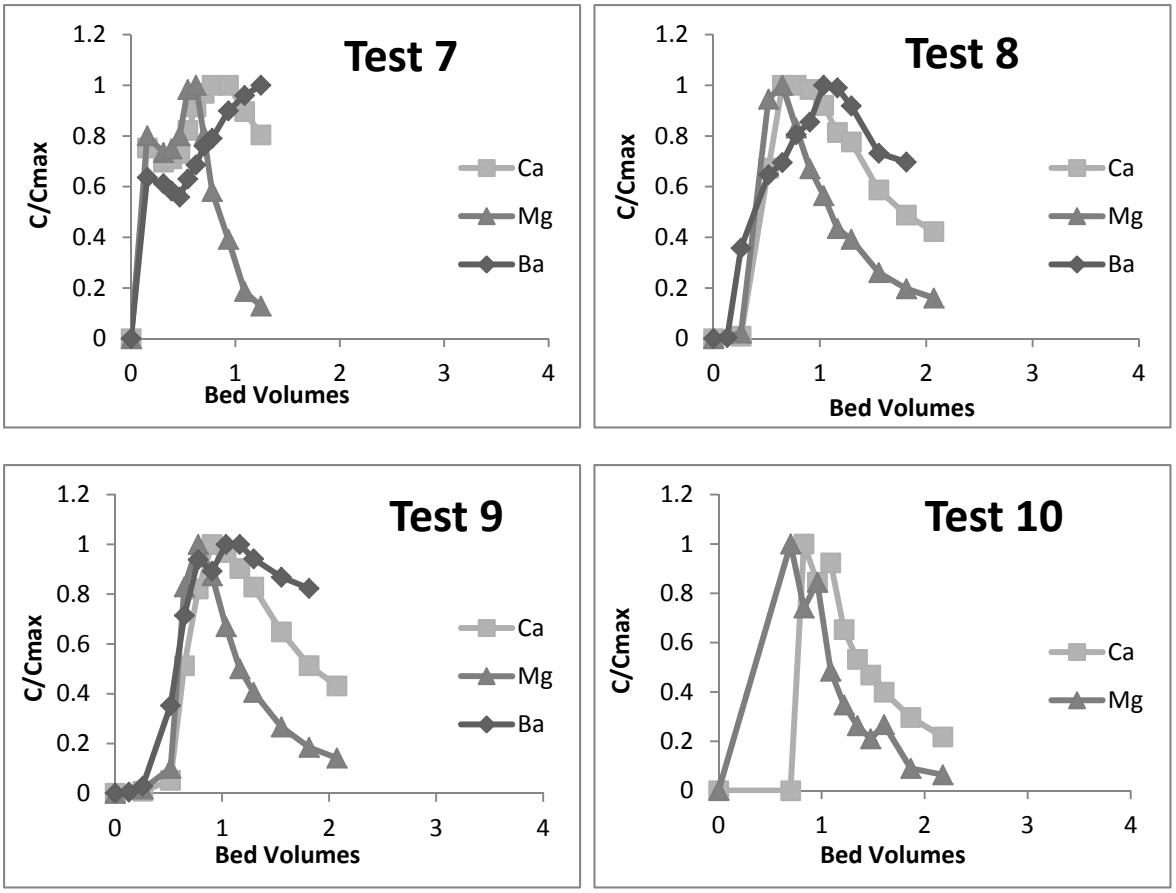

Figure 4.11. Elution curves for regeneration variation tests.

The most notable feature of all the tests is that despite changes in flow rate, direction of flow, and solution concentration, there is significant overlap in ion peaks. Ions were not able to be separated by varying regeneration characteristics or direction of flow. However, interesting patterns emerged from the data. In tests 2 through 5, sodium chloride concentration in the regeneration solution was less than 0.5%. Peak calcium concentrations occurred at 0.25 bed volumes, but they never exceeded the feed solution calcium concentration. It appears that the column was not actually being regenerated in these cases and that the peaks merely represent the solution phase ions in the pore space being flushed out by the regeneration solution. In tests 6 and 7, the flow rate was reduced to 6 mL/min. The conclusion from this set of tests is that although some changes in elution can be attributed to changing regeneration operation conditions, elution of these ions from the resin as separate peaks was not successful.

4.4.3 Recovery of Specific Ions from a Loaded Column

The third objective of Phase 2 was to quantify the resin phase ion concentrations along the length of a loaded IX column to evaluate whether it is possible to separate ions by regeneration of a specific portion of a column. Theory suggests that ions distribute in distinct layers in an IX column during loading, based on their selectivity properties.

The column containing ports along its length (described previously) was loaded by passing through a solution containing calcium, magnesium, and sodium, and resin was sampled from several points along the length of column. The resin samples were submerged in 2N HCl to

determine the resin phase ion concentrations at each location in the column. Table 4.8 lists the resin phase ion concentrations measured from the stripped resin that was taken from the various sampling ports along the longitudinal axis of the column. Gray shaded rows indicate that resin was not sampled from the port. Instead, concentrations from the ports above and below it were averaged. Separation factors were calculated (see Table 4.9) under the assumption that the resin from the topmost portion of the column was in equilibrium with the feed solution.

Chromatographic peaking of magnesium can be observed by comparing the equilibrium resin phase concentration of magnesium with the resin phase concentration along the column length. Whereas the calcium concentration decreases relative to the equilibrium concentration, the magnesium concentration increases (see Figure 4.12). Sample results indicate that ions were not present in distinct layers (Figure 4.13). Instead, there was a mix of ions in the resin phase at all locations along the column. A comparison of the column snapshot based upon the measured results with one generated by the model for a column treated with the same solution for the same number of bed volumes and using the same separation factors shows that the model is able to predict the resin phase concentrations well. Unfortunately, because the analysis did not reveal discreet ion banding or zoning, regeneration of the lower portion of the column was not an option for ion separation. Because ions were not able to be separated using column processes, the focus was moved to salt separation during precipitation, as described in the next section.

Table 4.8. Resin Phase Ion Concentrations Measured from Stripped Resin

Location	Ca	Mg	Na	Sum
	meq/g	meq/g	meq/g	
1	0.44	0.78	2.51	3.73
2	0.83	0.98	1.78	3.60
3	1.21	0.96	1.42	3.59
4	1.39	0.94	1.40	3.74
5	1.60	0.88	1.24	3.72
6	1.90	0.88	0.94	3.72
7	2.20	0.88	0.64	3.72
8	2.37	0.83	0.53	3.73
9	2.54	0.78	0.42	3.73
10	2.62	0.72	0.40	3.73
11	2.69	0.66	0.38	3.74
12	2.48	0.57	0.73	3.79
13	2.27	0.49	1.08	3.84
14	2.53	0.48	0.83	3.84
15	2.78	0.47	0.58	3.83
16	2.81	0.47	0.50	3.78
17	2.83	0.48	0.41	3.72
18	2.88	0.44	0.41	3.73
19	2.93	0.40	0.41	3.75

Table 4.9. Solution Concentrations and Calculated Separation Factors

Ion	Separation Factor, α	Solution Concentration (N)
Calcium	5.79	0.13
Magnesium	2.83	0.04
Sodium	1	0.10

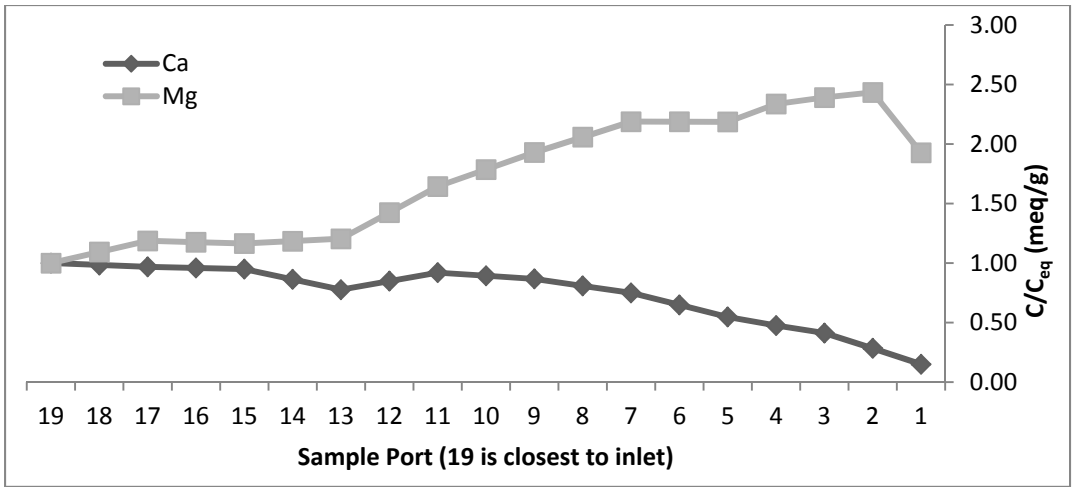

Figure 4.12. Resin phase concentration compared to equilibrium resin phase concentration.

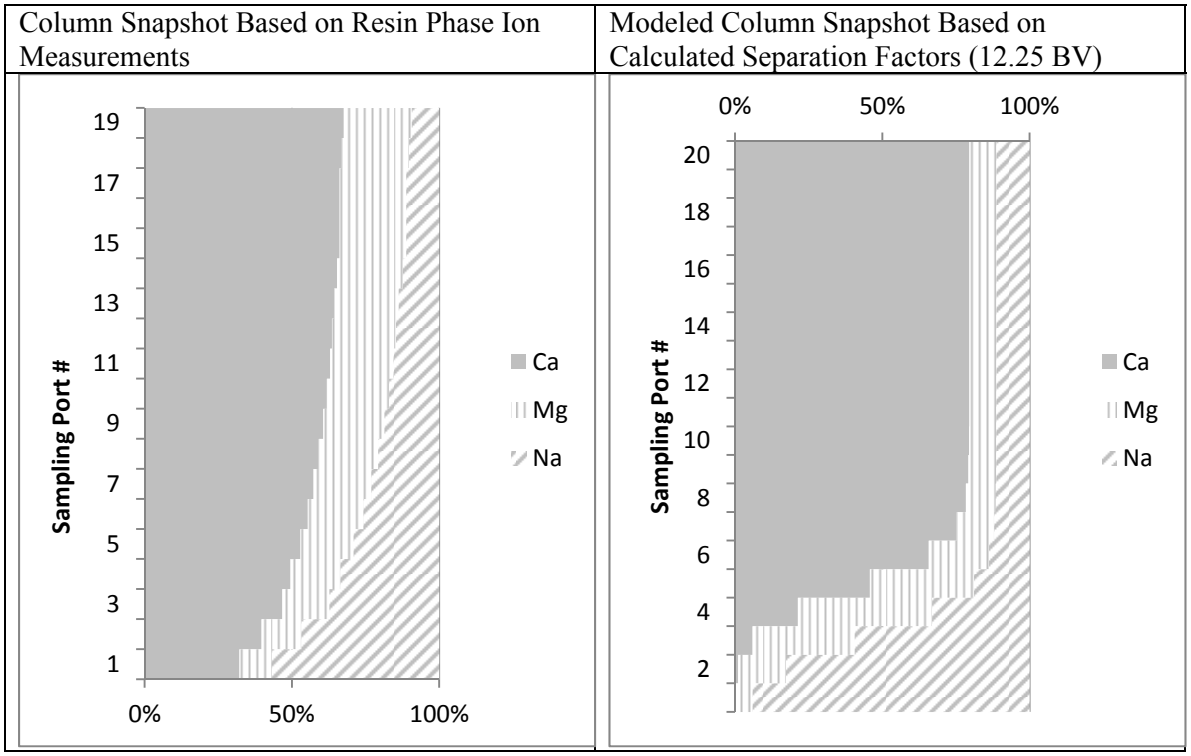

Figure 4.13. Distribution of ions in the resin phase axially through a column.

Chapter 5

Phase 3—Salt Precipitation

5.1 Chapter Objectives

This section describes experiments in which laboratory-simulated cation and anion regeneration solutions were mixed under different pH conditions to form precipitates. The goal of varying the pH during mixing was to precipitate carbonate and sulfate salts separately. Precipitates were analyzed by SEM, EDS, and XRD to determine their characteristics and mineralogy.

5.2 Chapter Summary

The key results and conclusions from precipitation-testing experiments were as follows:

1. Equilibrium modeling using Visual MINTEQ showed that several salts are supersaturated in a mixture of cation and anion regeneration solutions.
2. Visual MINTEQ modeling also showed that adjusting pH can control the precipitation of carbonate salts.
3. A precipitate containing a heterogeneous mix of phases including halite, bassanite, bassirite, bischofite, and calcium carbonate ($CaCO_3$) is formed when cation and anion regeneration solutions are mixed without pH adjustment.
4. Calcium sulfate precipitated in mixtures in which the pH of the anion regeneration solution was reduced below 5 prior to mixing with cation regeneration solution.
5. A precipitate containing calcium, magnesium, and carbonate was obtained from the supernatant of the solution, which had previously precipitated calcium sulfate when its pH was increased above 9.5.

5.3 Methods

Chemical modeling in Visual MINTEQ showed that pH was an important variable in controlling the precipitation of specific salts from the mixture. Figure 5.1 shows the calcite and gypsum saturation indices as functions of pH as predicted by Visual MINTEQ. Input calcium and carbonate concentrations were each 1 M and the activity corrections were made using the specific ion interaction theory model. For this model, solids are allowed to be supersaturated rather than precipitating. SIs greater than zero indicate that the solution is supersaturated. The figure shows that calcite precipitation is predicted to occur when pH is equal to 4.4. Gypsum precipitation is predicted to occur regardless of pH (between 2 and 7). By adjusting the pH of a mixed solution containing calcium, carbonate, and sulfate to between 2 and 4.4, gypsum precipitation should occur while carbonate stays in solution. If sufficient calcium is left after calcium sulfate precipitate comes to equilibrium with the solution, the pH can be increased and the calcium should precipitate as a carbonate salt. This was the basis of experiments with simulated regeneration solutions.

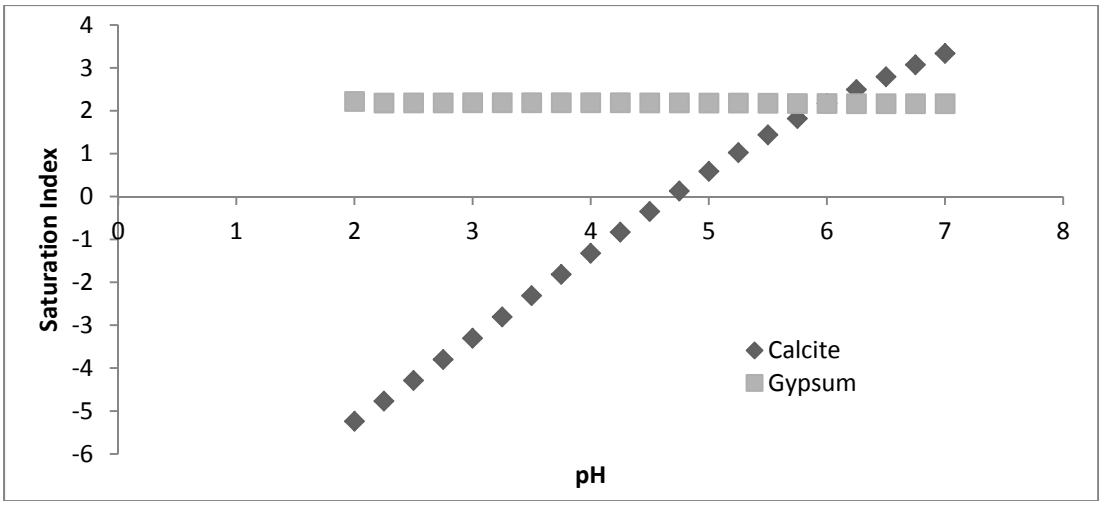

Figure 5.1. Calcite saturation index as a function of pH.

The procedure for these experiments was as follows. Synthetic cation and anion regeneration solutions were created in the laboratory. They were made to represent the regeneration solutions that would be recovered from anion and cation exchange columns that had treated RO concentrate with a 3:1 ratio of divalent cations to sodium with an ionic strength of 0.25. Regeneration solution ionic concentrations are listed in Table 5.1. Regeneration solutions were mixed (volumes are listed in Table 5.2) and solids were allowed to precipitate. Tables 5.2, 5.3, and 5.3 list the parameters and notes for experiments in Phase 3.

Table 5.1. Anion and Cation Regeneration Solution Concentrations

	g/L	M
Cation regeneration solution for experiments 2A, 3		
Mg	4.49	0.1849
Ca	14.82	0.3698
Ba	0.51	0.0037
K	1.45	0.0370
Na	39.46	1.7164
Cl	101.76	2.8701
Anion regenerant solution for experiments 2A, 3		
SO_4	26.43	0.2752
CO_3	16.51	0.2752
NO_3	4.27	0.0688
F	0.05	0.0028
Na	66.29	2.8833
Cl	60.80	1.7151
Cation regenerant solution for experiments 4–7		
Mg	6.20	0.2549
Ca	20.44	0.5099
Ba	0.07	0.0005
K	5.98	0.1530
Na	40.51	1.7621
Cl	120.36	3.3948
Anion regenerant solution for experiments 4–7		
SO_4	26.43	0.2752
CO_3	16.51	0.2752
NO_3	4.27	0.0688
F	0.05	0.0028
Na	66.29	2.8833
Cl	60.80	1.7151

Table 5.2. Experimental Matrix for Phase 3

Experiment Number	V_{Cation}	V_{Anion}	pH
2A	100	100	Not adjusted
3	100	100	2.43, 9.84, 11.07
4	100	100	Not adjusted
5	50	70	2.99, 7.5, 10.19
6	100	100	4.5,10.04
7	100	100	5.06,10.03

Notes: V_{Cation}—volume (mL) cation solution; V_{Anion}—volume (mL) anion solution

Table 5.3. Samples Collected from Phase 3 Experiments

Experiment Number	Samples Taken From Each Experiment
2A	Liquid: Initial solutions, supernatant Solid: Final precipitate
3	Liquid: Initial solutions, at pH 2.43, at pH 9.84, at pH 11.07, after heat Solid: At pH 2.43, at pH 9.84, after heat
4	Liquid: Initial solutions, supernatant Solid: Final precipitate
5	Liquid: Initial solutions, at pH 2.99, at pH 7.5, at pH 10.19 Solid: At pH 2.43, at pH 7.5, at pH 10.19
6	Liquid: Initial solutions, at pH 4.5, at pH 10.04 Solid: At pH 4.5, at pH 10.04
7	Liquid: None Solid: At pH 5.06, at pH 10.03

Table 5.4. Notes for Phase 3 Experiments

Experiment Number	Notes
2A	Used same concentration factor for cation and anion solutions, added cation solution to anion solution
3	Reduced pH of anion solution to 2.43, added cation solution, raised pH to 9.84, then to 11.07
4	Used greater concentration factor for cation than anion solutions because of different exchange capacities
5	Lowered pH of anion solution to 2.99, mixed in cation solution, settled precipitate, increased pH to 7.5 by adding 20mL of anion solution, filtered solution, increased pH to 10.19, centrifuged to separate precipitate
6	Lowered pH of anion solution to 4.26, mixed in cation solution, settled precipitate after 10 min, increased pH 10.04, centrifuged to separate precipitate
7	Repeat of Experiment #6, except solids were rinsed prior to drying

At the end of each experiment, solids were separated from the supernatant by filtration using a vacuum flask and a cellulose fiber pad (Gelman Sciences 47-mm pure cellulose fiber filter pads #66025) or centrifuged to separate liquid and solid materials. Both liquid and solid samples were analyzed to determine the characteristics of the salt precipitate from each experiment. Concentrations of ions in liquid samples were measured by AAS and IC. Solid samples were dried and then examined using SEM and XRD. One challenge of working with SEM and XRD is that samples must be dried prior to examination. The most common form of calcium sulfate is gypsum ($CaSO_4 \cdot 2H_2O$), but it can be converted to anhydrite ($CaSO_4$) by heating to a temperature above 200 °C. The common forms of calcium carbonate are all anhydrous. Limited mineralogical changes are expected to occur at 104 °C, the temperature at which solid samples were dried in the laboratory oven. The SEM was also equipped with EDS, which can identify the elemental composition of a sample and provide a semiquantitative analysis. Through a combination of these analyses, it was possible to speculate about the character of the precipitate from completed Phase 3 experiments.

5.4 Results

Salts were precipitated from a mixture of anion and cation regeneration solutions under three different conditions. In the first, no pH adjustments were made. This occurred in experiments 2A and 4. SEM images and EDS spectra were taken for precipitates from both experiments, and an XRD spectrum was taken for precipitate from experiment 2. As can be seen in SEM images in Figure 5.2, these precipitates are similar. The images show a heterogeneous collection of solids of different sizes and shapes. The difference in brightness between particles indicates differences in atomic weight. Lighter shades indicate heavier elements. EDS spectra from different portions of each image (Figure 5.2) indicate that most of the precipitate from both experiments consists of calcium, oxygen, carbon, sodium, and chloride, although small amounts of magnesium, sulfur, and barium were also detected. The presence of sodium and chloride is most likely due to the fact that precipitates were not rinsed before drying in the oven. For this reason, ions that were still in solution at the end of the experiment may have precipitated during the drying process. It is likely that any sodium or chloride salts present in the samples precipitated in this fashion, because they are generally soluble. In later precipitation experiments (#7 from this phase and Phase 4), all precipitates were rinsed thoroughly before drying. Figure 5.3 shows the XRD spectrum of precipitate from experiment 2, which shows the presence of several different salts including sodium chloride (NaCl), bassanite ($Ca(SO_4)(H2O)_{0.5}$), bassirite ($Ca(SO_4)(H_2O)_{0.8}$), bischofite ($MgCl_2(H_2O)_6$), and calcium carbonate ($CaCO_3$).

Experiment 2A

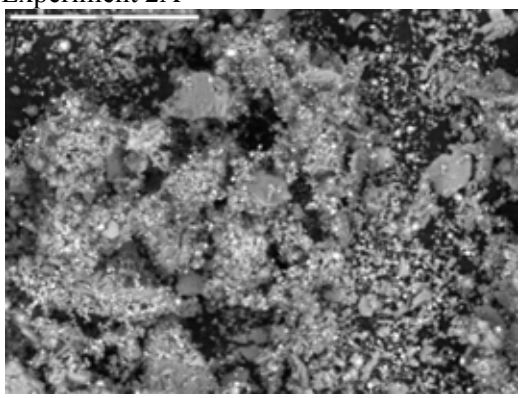

Experiment 4

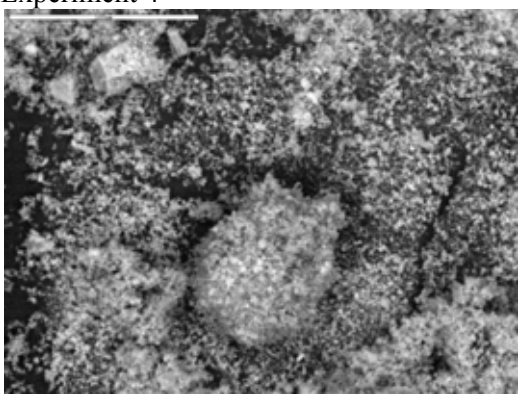

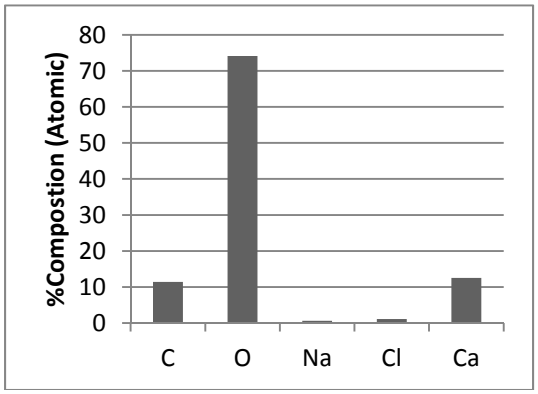

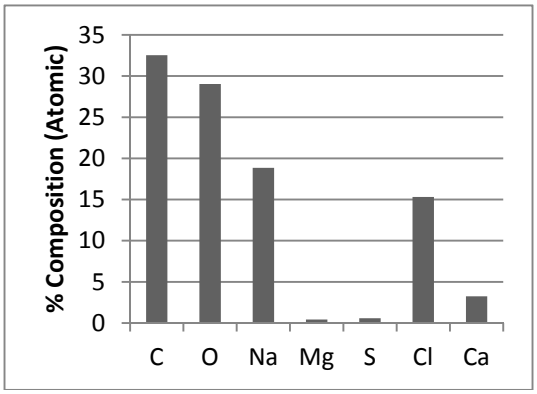

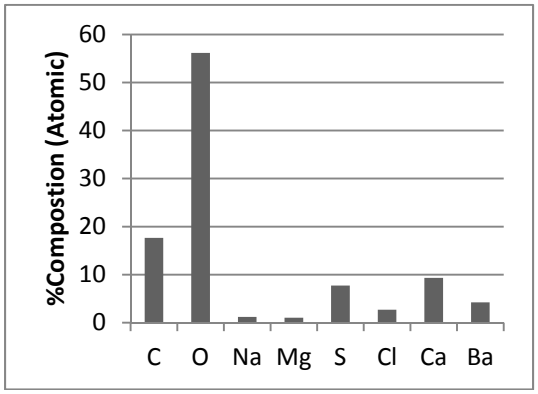

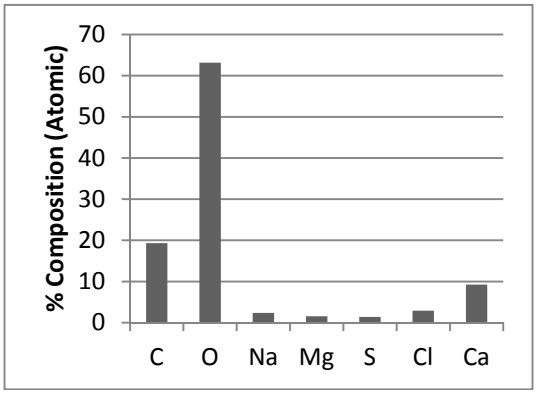

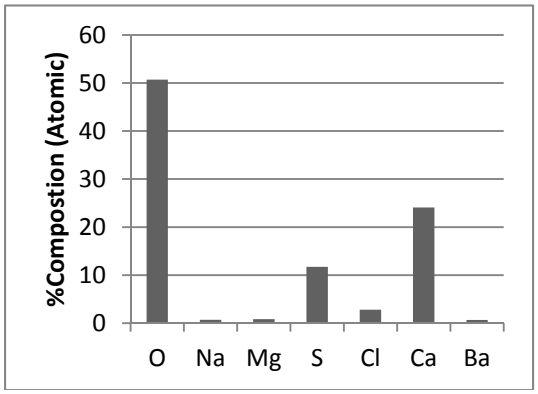

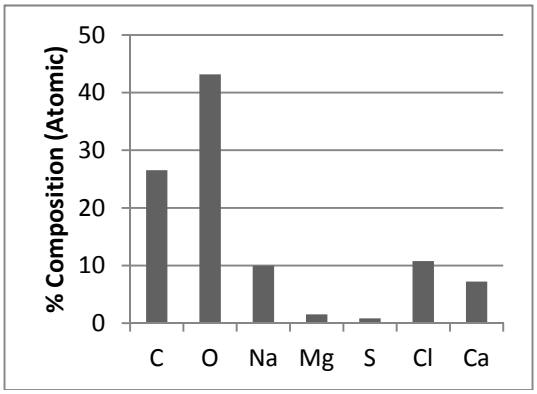

Figure 5.2. SEM image (top 2 graphs) and EDS data (bottom 4 graphs) from Experiments 2A and 4.

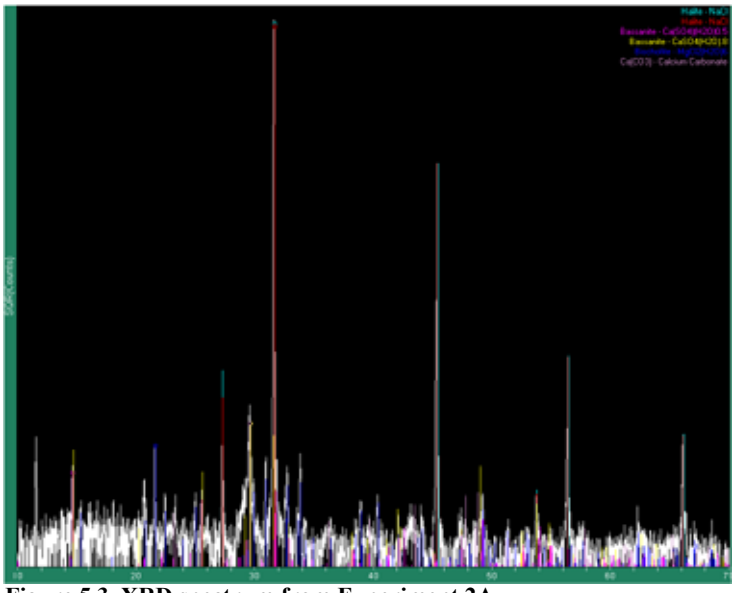

Figure 5.3. XRD spectrum from Experiment 2A.

It must be noted that the EDS data do not include nitrogen in their analysis. EDS in general is not a good method for measuring nitrogen, because *K*α X-rays are strongly absorbed by carbon-bearing materials, of which the detector window is made. It may be possible to analyze the samples using a wavelength-dispersive spectrometer at a later time.

An analysis of the ion concentrations in the supernatant compared with those in the regeneration solutions was also conducted to determine the extent of precipitation for each ion. The liquid analysis shows that all the cations and anions except sodium and chloride have left the solution in significant amounts (see Figure 5.4). From these data, it can be concluded that mixing the solutions without any pH adjustment results in a mixed precipitate. Mixing cation and anion regeneration solutions results in significant salt precipitation; however, it is unclear whether the recovered mixed salts have sufficient purity to have any beneficial uses.

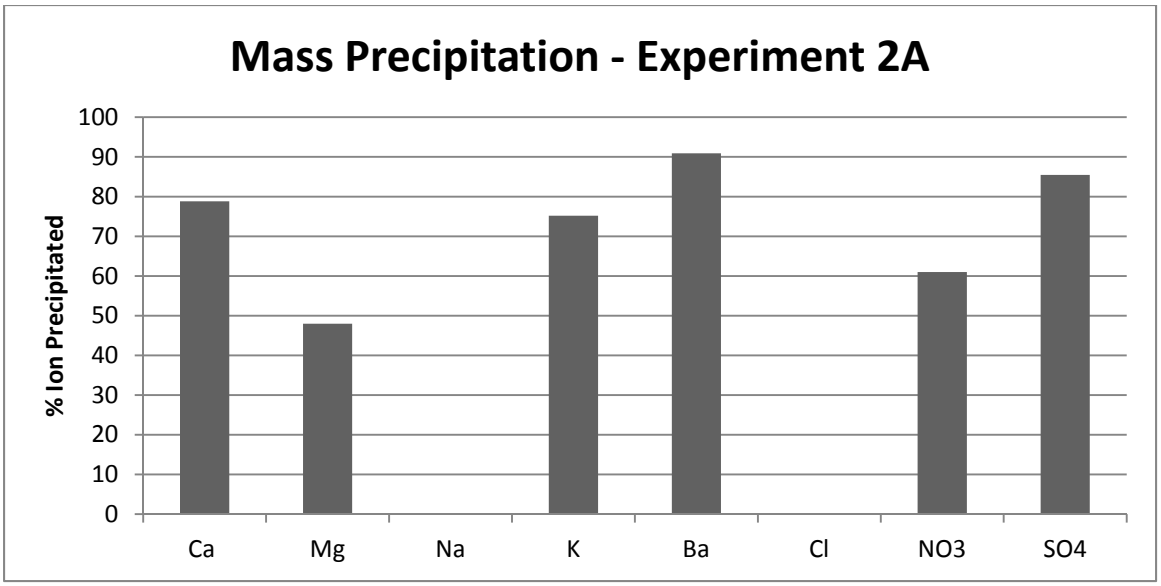

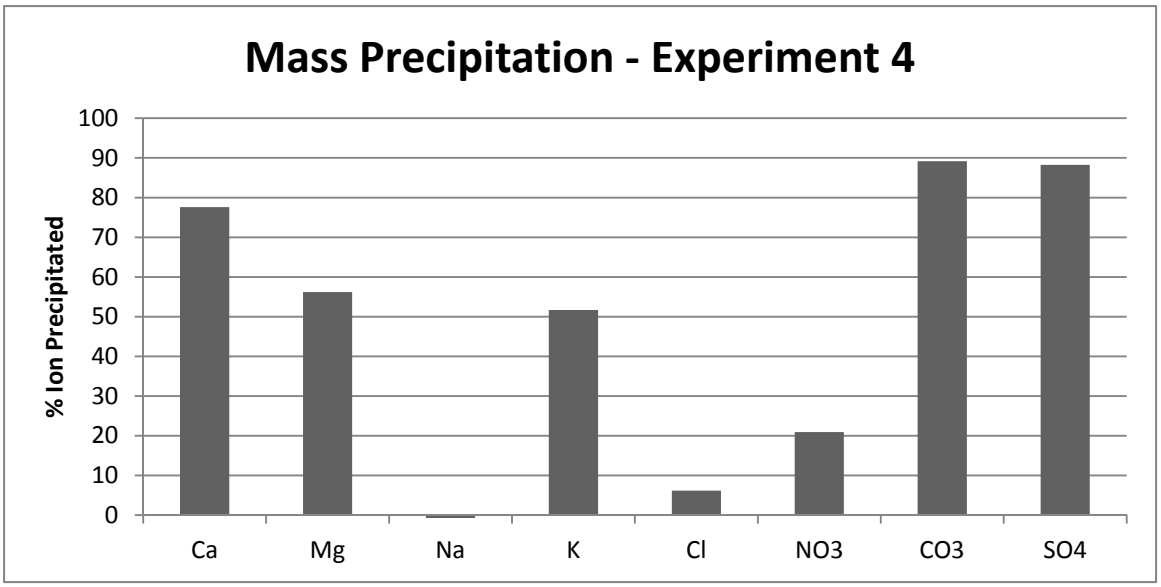

Figure 5.4. Results from liquid analysis of Experiments 2A and 4.

The next two types of precipitate result from experiments in which the pH was adjusted. This occurred in experiments 3 through 7. The sequence in these experiments was as follows: (1) reduce the pH of the anion regeneration solution using HCl and mix the solutions together, (2) separate the precipitate from the supernatant, and (3) increase the pH of the supernatant and capture additional precipitate. In this way, two types of precipitate were formed during each experiment. SEM images of precipitates from low- and high-pH conditions are shown in Figure 5.5. In all of these images, a clear difference in morphology can be seen between the two corresponding images for each test. In most of the images of precipitates formed at high pH, the most abundant shapes are small spheres, which are a common shape for calcium carbonate. The images of precipitates formed at low pH of precipitate are more homogenous and contain either hexagonal needles or flat flakes, which are associated with calcium sulfate phases such as selenite and gypsum.

Test #	Low pH	High pH
3	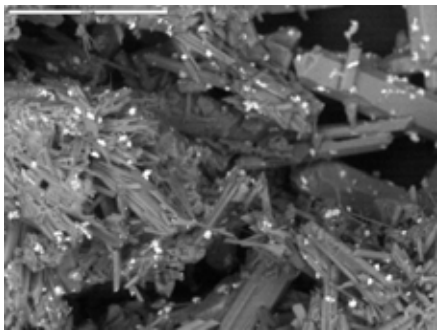	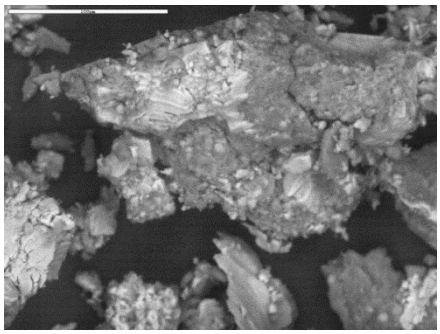
5	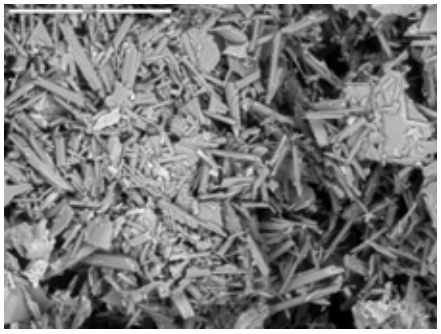	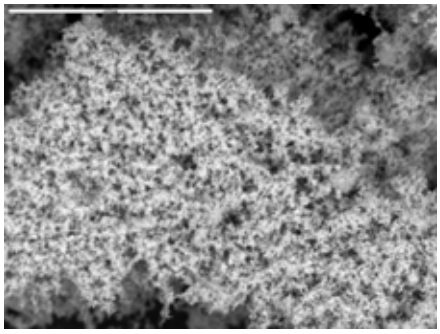
6	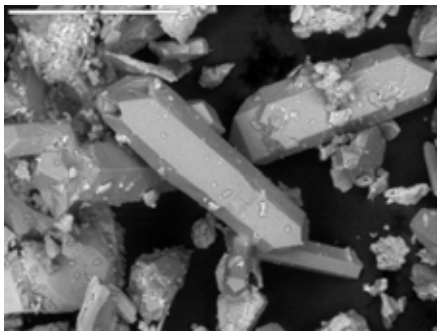	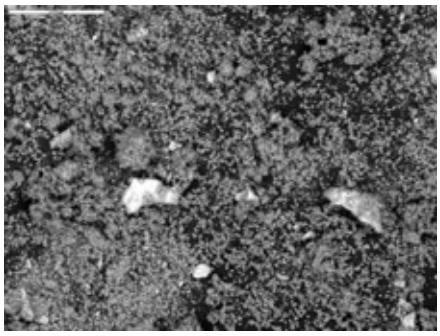
7		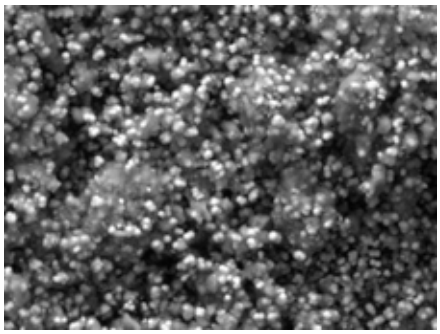

Figure 5.5. SEM images from Experiments 3 and 5–7.

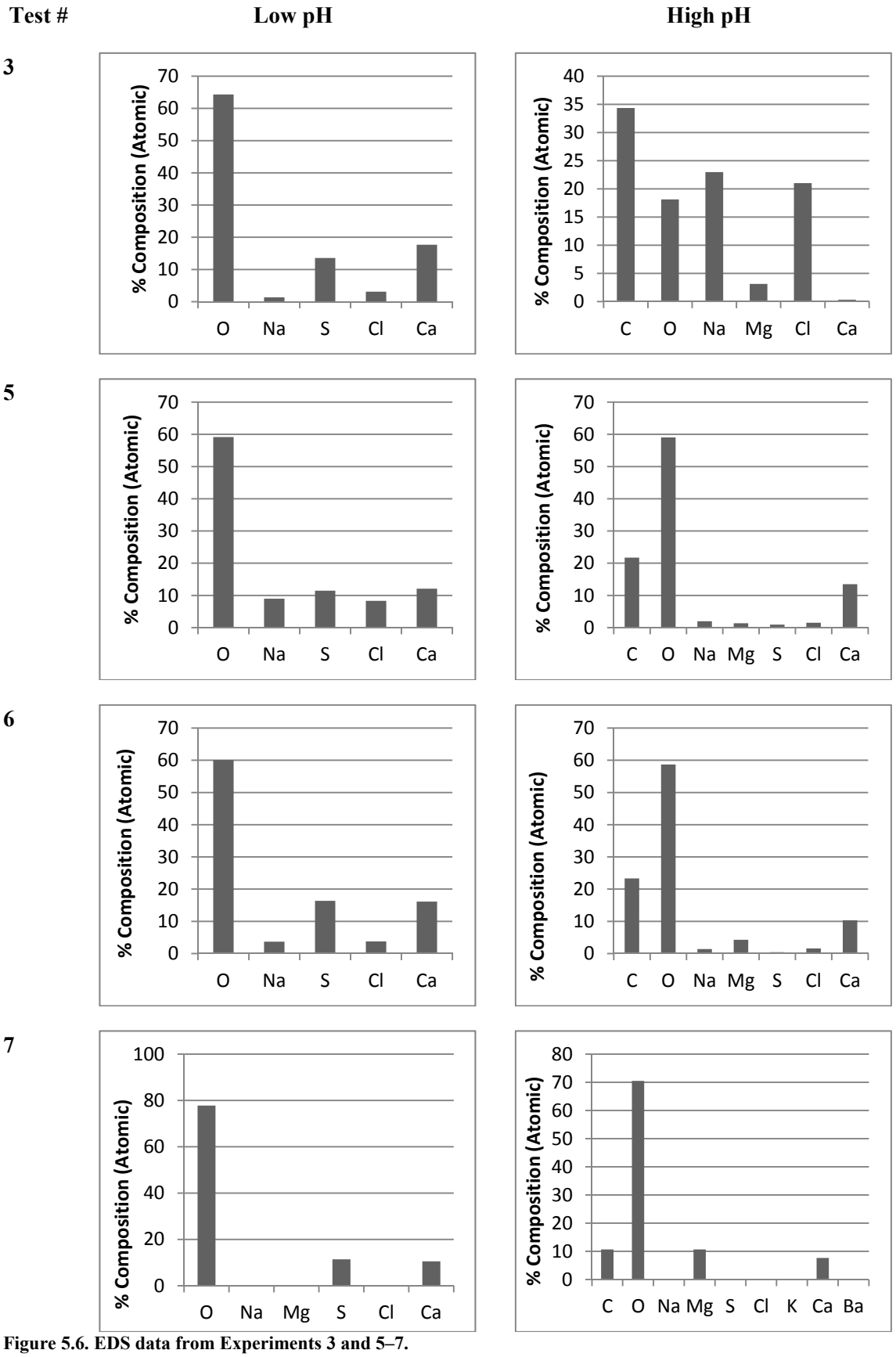

Figure 5.6. EDS data from Experiments 3 and 5–7.

EDS data show that the precipitate formed at low pH consisted mostly of calcium, sulfate, oxygen, sodium, and chloride (see Figure 5.6). In test 7, in which the precipitate was rinsed with DI water before drying, no sodium or chloride was detected by EDS. This indicates that their presence in the other low-pH precipitates was probably due to the evaporation of the supernatant in the oven. The atomic ratio of these elements matches that of calcium sulfate. The EDS spectra of precipitates formed at high pH show the presence of calcium, sodium, magnesium, oxygen, carbon, and chloride. Just as in the low-pH test, sodium and calcium were not detected in precipitate from experiment 7. Based on the combination of elements detected by EDS, these precipitates are mostly likely a mixture of calcium and magnesium carbonate.

XRD analysis was performed on precipitate from high- and low-pH conditions from tests 5, 6, and 7 (see Figure 5.7). The only crystal phases identified in precipitate formed at low pH were gypsum and halite. Precipitates formed at high pH contained calcite, halite, brucite, magnesite, and magnesium carbonate. Analysis of ion concentrations in solution before and after precipitation under high- and low-pH conditions was done for tests 3, 5, and 6. Results show that a large fraction of the sulfate and nitrate precipitation occurred under low-pH conditions and that they precipitated with calcium and magnesium (see Figure 5.8). These results also show that some sodium and chloride precipitated prior to drying in the oven, although some error is built into sodium and chloride measurements because of the very high dilution required to make them. Low-pH precipitation is limited by the amounts of sulfate and nitrate in these solutions and by the solubility of sulfate and nitrate phases. When these ions are consumed, the remaining calcium and magnesium stay in solution. When the pH increases, most of the remaining calcium and magnesium precipitates with carbonate.

Results from Phase 3 experiments showed that it is possible to recover calcium sulfate from a mixed solution of cations and anions if the pH is reduced below 4.4. Depending on the purity of this salt, it may be suitable for commercial use. The carbonate salt that is produced during the high-pH precipitation contains both calcium and magnesium. The ionic strength of the concentrate does not significantly inhibit precipitation of supersaturated salts. The recovery of other salts will require further concentration of the ions in solution, which may be economically feasible, depending on the value of the salts and their particular properties in terms of solubility.

Test #	Low pH	High pH
5	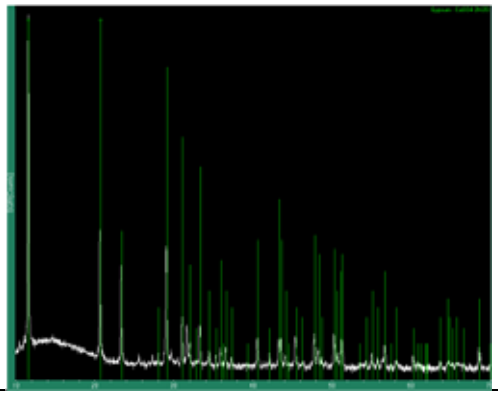	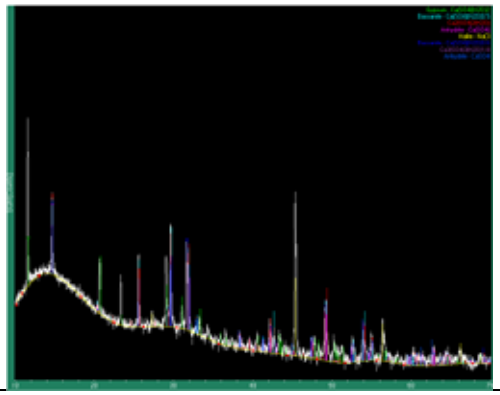
6	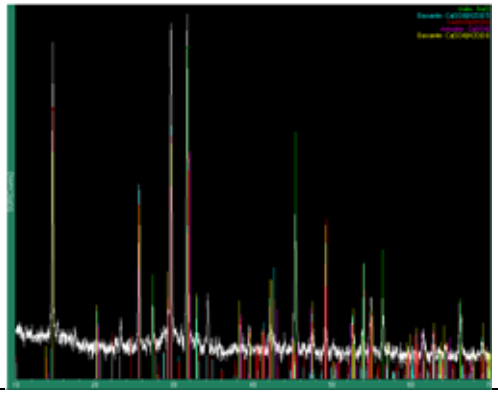	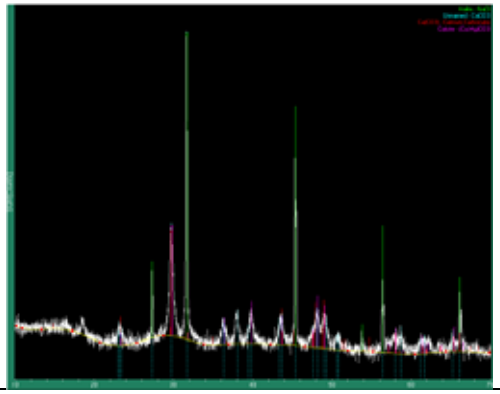
7	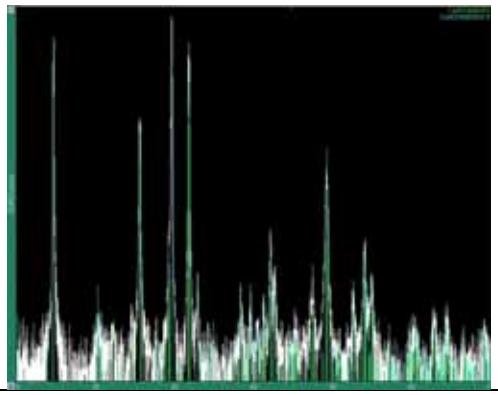	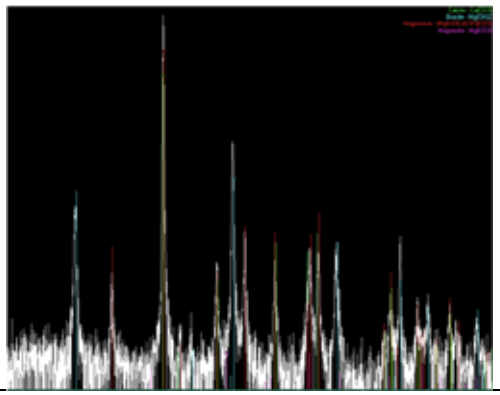

Figure 5.7. XRD spectra from Experiments 3 and 5–7.

Test #	
3	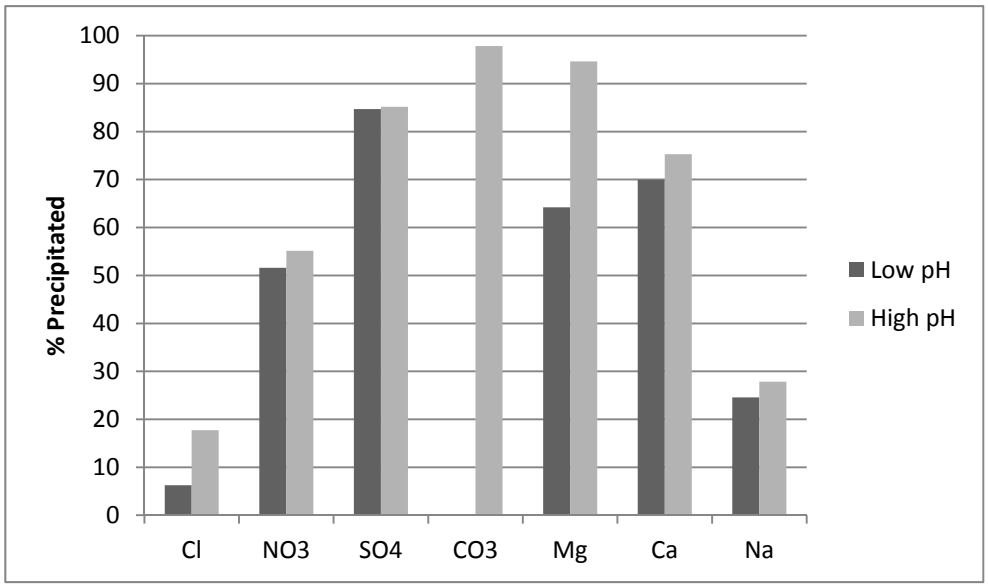 100 90 80 70 60 50 40 30 20 10 0 % Precipitated Cl NO3 SO4 CO3 Mg Ca Na Low pH High pH
5	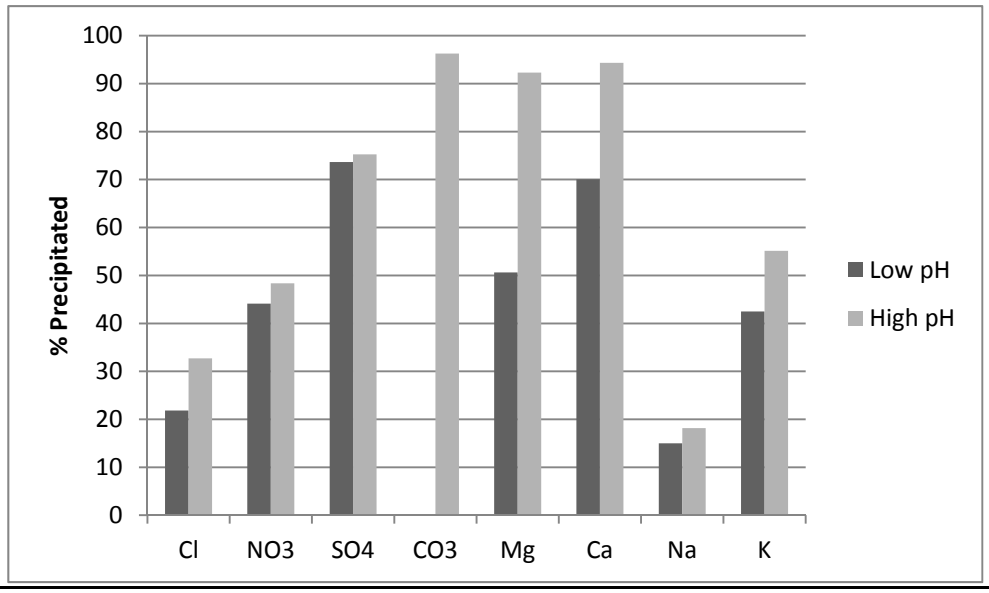 100 90 80 70 60 50 40 30 20 10 0 % Precipitated Cl NO3 SO4 CO3 Mg Ca Na K Low pH High pH

Test #

6

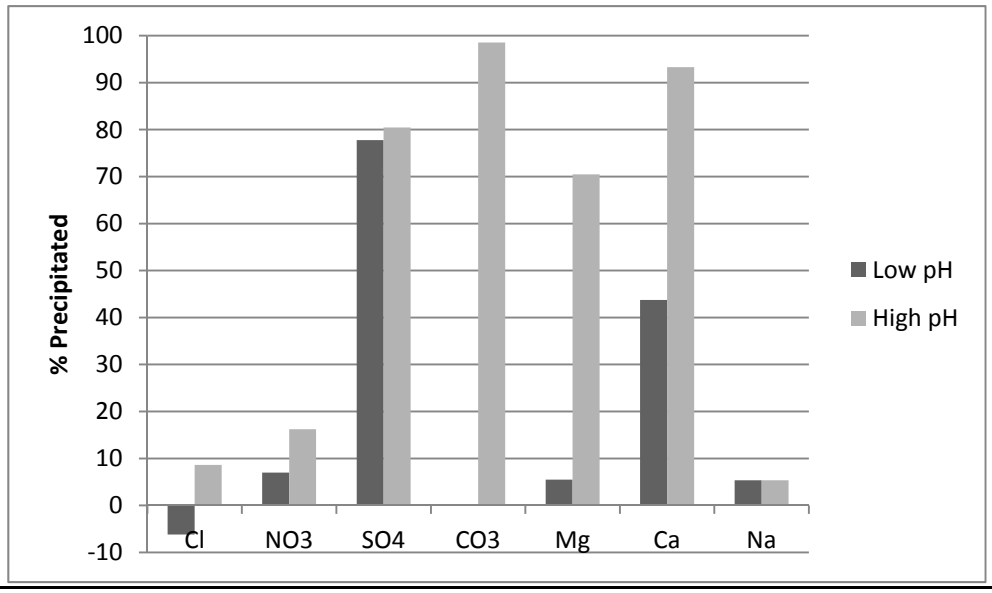

Figure 5.8. Estimated salt precipitation for Tests 3, 5, and 6 based on ion concentrations.

Chapter 6

Phase 4—Pilot-Scale Process Testing in Brighton, CO

The pilot study was conducted in conjunction with CDM at the East Cherry Creek Valley Water and Sanitation District's Brine Minimization Pilot, located in Brighton, CO. The pilot study was intended to test the efficiency of the treatment process designed to recover salts from RO concentrate using interstage sequential IX columns. The following were the major objectives of the pilot study:

- Determine the consistency of the mass and purity of the recovered salt products.
    - Anion and cation regenerant fluids were mixed under high- and low-pH conditions to spontaneously precipitate supersaturated salts. Laboratory results have shown that gypsum and mixed carbonate salts can be recovered.
- Determine the best fraction of the regenerant solution to use for salt recovery.
    - For example, if the first and last quarter of the regeneration process yield low ion concentrations, it may be more useful to collect only the fluid from the middle portion of the process in order to increase the solubility index and precipitate a greater quantity of salt.
- Determine the effect of antiscalant addition on the resin capacity.
    - An anionic antiscalant may foul the anion exchange column and result in a capacity decrease. A fouling-resistant anion resin has been selected to decrease this likelihood.
- Optimize the operation cycle length to maximize ion concentrations in regeneration solutions and minimize unused cation exchange capacity.
    - The cation exchange resin has a higher exchange capacity than the anion exchange resins, so normal operation cycles are limited by the anion exchange capacity. This leaves some unused cation exchange capacity. A breakthrough curve was measured during Week 3, and the operation cycle was extended during Weeks 5 and 6.
- Determine if pilot effluent recycling affects the performance of the second-stage RO system.
    - Pressure, temperature, and permeate flow were measured during the second-stage RO system operation.

6.1 Pilot Design and Experimental Methods

The pilot system featured two IX columns in series, the first containing Purolite SST65, a SAC resin, and the second containing Purolite A850, a SBA resin. The pilot design only allowed the use of one cation exchange resin and one anion exchange resin. Purolite resins were selected over ResinTech resins because Purolite also manufactures a resin that can be regenerated using a brine with a lower sodium concentration, which may be more suitable in the long run. Purolite is currently exploring integrating IX with RO and was interested in collaborating on the pilot.

Table 6.1. Pilot Feed Water Ion Concentrations

	mg/L	M
Ca	460	
Mg	190	
K	20	
Na	570	
Cl	610	
SO_4	690	
TDS	4450	
CO_3		0.0274

The feed water was the concentrate from a pilot-scale RO unit operated by CDM. Feed water chemistry is listed in Table 6.1. The system was designed with solenoid valves and a timer for automatic operation and regeneration.

The normal service cycle of the IX process was 2 h at 0.44 gpm. Effluent from the pilot was sent to a single-stage RO unit until enough concentrate was produced for daily regeneration requirements. Sodium chloride was added to the RO concentrate until the target concentration (10%) was reached. The rest of the pilot effluent was saved for column rinsing or wasted. The normal countercurrent regeneration cycle lasted 52.5 min at 0.0870 gpm. For the first 23 min of the regeneration cycle , 10% NaCl solution was pumped through the columns. This was followed by 30 min of rinsing with pilot effluent. Regeneration and rinse fluids from each column were collected during selected regeneration cycles. The fluids from the SAC and SBA columns were mixed to precipitate supersaturated salts. The total normal cycle time including operation, regeneration, and rinse was 2.875 h. The pilot was located on the I-76 Frontage Rd directly south of the E 160th St exit. The pilot system design is shown in Figure 6.1 and the legend and operations information are shown in Table 6.2.

Pictures of the pilot equipment are presented in Figures 6.2–6.6.

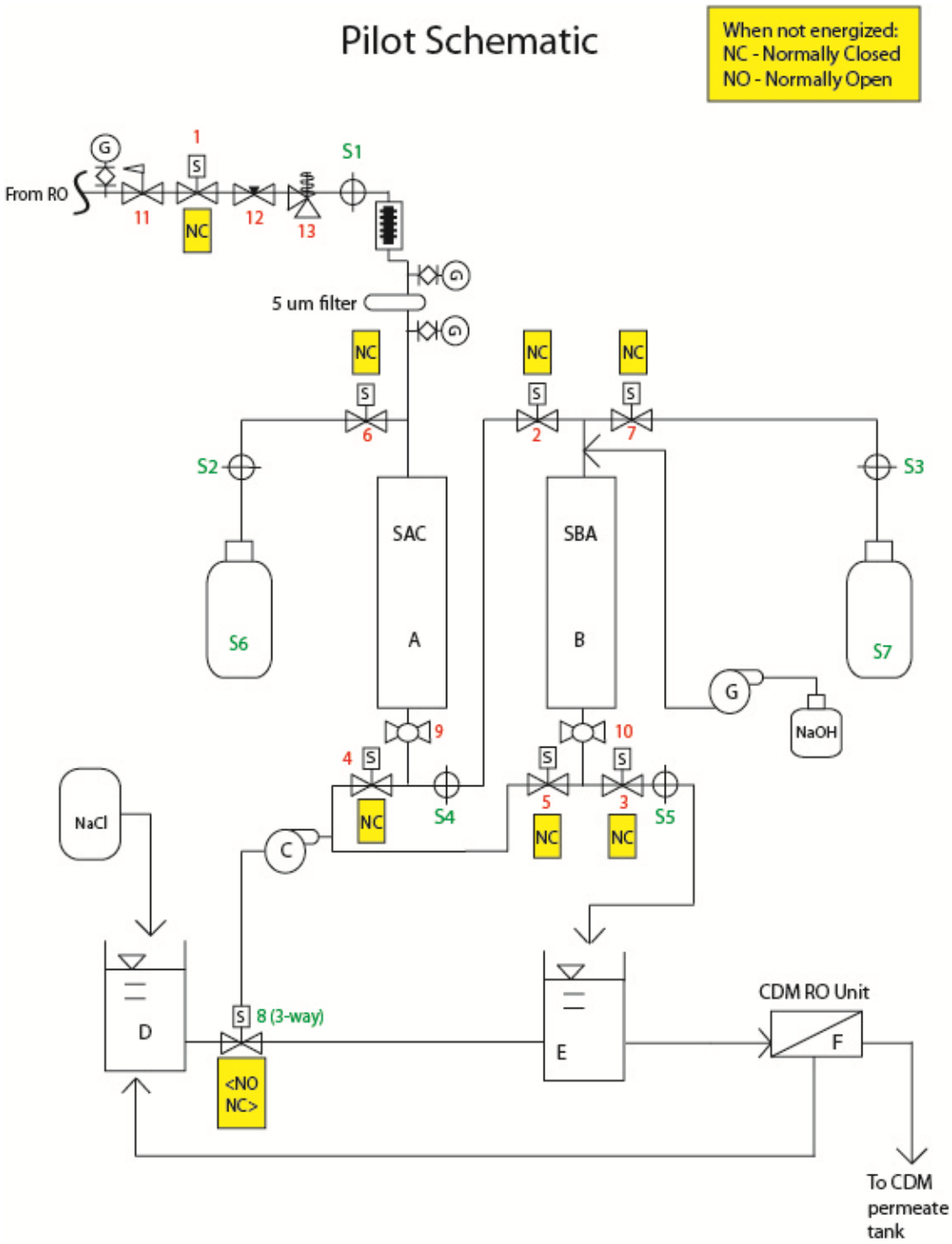

Figure 6.1. Pilot schematic.

Table 6.2. Legend for Schematic Diagram

A	Strong acid cation exchange column
B	Strong base anion exchange column
C	Strong acid cation regeneration pump
D	IX regenerant/brine
E	Tank IX effluent/stage 2 RO feed tank
F	Stage 2 RO unit
G	NaOH metering pump
S=Sample Port	
S1	Feed
S2	Cation regeneration fluid
S3	Anion regeneration fluid
S4	Cation effluent/regenerant feed
S5	Anion effluent/regenerant feed
S7	Mixed cation regeneration fluid
	Mixed anion regeneration fluid
Valves	
1-7	
8	2-way solenoid valves
9-10	3-way solenoid valves
	Manual, ball
11	Pressure reducing valve
12	Needle valve (for throttling)
13	Pressure relief valve

	Valve Operation (x=energized)		
Valve	Service	Regen	Rinse
1-3, circuit 1	x		
4-7, circuit 2		x	
8, circuit 3			x
Time (min)	120 (regular), 165 (optimized)	23	30

Control sequence		Time (min)
1	Energize circuit	120 or 165
2	Energize circuit 2, pump C	52.5
3	Energize circuit 3	22.5
4	Start over	0

Column Dimensions (Anion and Cation Exchange)	**English**	**Unit**	**Metric**	**Unit**
Column diameter	4	in.	10.16	cm
Resin depth	4	ft	1.22	m
Column area	0.0873	ft^2	81.1	cm^2
Resin volume	0.35	ft^3	9.88	L

Service parameters	English		Metric	
		Unit		Unit
Service rate	10	BV/hr		
Service cycle	20	BV		
Operating time	2	h		
Flow rate	0.44	gpm	1.65	L/min
Velocity	4.99	gpm/ft^2	12.19	m/h

Regeneration parameters	English		Metric	
		Unit		Unit
Regen salt	NaCl			
Regen mode	Countercurrent			
NaCl concentration	10	%	10	%
Regen volume	0.75	BV	0.75	BV
Regen rate	2	BV/h	2	BV/h
Regen time	0.375	h		
Flow rate	0.0870	gpm	0.33	L/min
Velocity	0.997	gpm/ft^2	2.4	m/h
Regen sol'n density	66.8		1.07	kg/L
NaCl conc in regen solution	6.68	lb/ft^3	0.107	kg/L
NaCl mass	1.75	lb	0.793	kg
NaCl dose	5.0	lb/ft^3	0.080	kg/L

Rinse parameters	English		Metric	
		Unit		Unit
Rinse volume	1	BV	1	BV
Rinse rate	2	BV/h	2	BV/h
Rinse time	0.5	h		
Flow rate	0.0870	gpm	0.33	L/min
Velocity	0.997	gpm/ft^2	2.4	m/h

Summary		
SAC resin	Purolite SST65	
SBA resin	Purolite A850	
Total cycle time	2.875	h
Cycles/day	8.35	
Volume treated/day	436.0	gal
SAC regen/day	16.3	gal
SBA regen/day	16.3	gal
SAC rinse/day	21.8	gal
SBA rinse/day	21.8	gal
Total regen/rinse	76.3	gal
Net IX recovery	82.5	%
Total salt/day	29.2	lb

Figure 6.2. Pilot equipment on site.

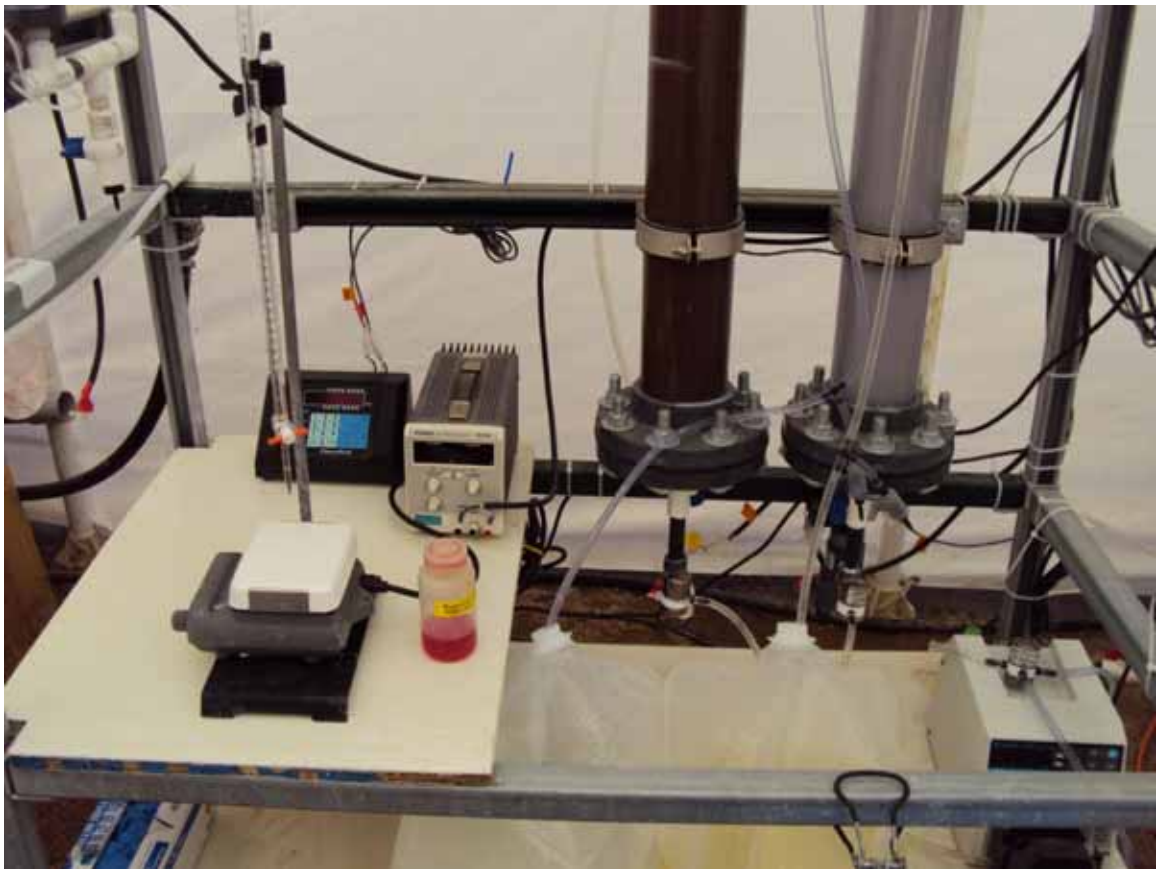

Figure 6.3. Pilot equipment including timer (far left), power supply (middle), titration setup (front), and regeneration pump (far right).

Figure 6.4. Solenoid valves at tops of columns.

Figure 6.5. Solenoid valves at bottoms of columns.

Figure 6.6. Control sequence at pilot input including pressure reducer, solenoid valve, pressure gauge, needle valve, and pressure relief valve.

6.1.1 Daily Operations

The following tasks were performed on a daily basis to maintain the pilot system and verify system operation. These tasks are also listed on the Parameter Checklist Form, located in Appendix D. The pilot project schedule is shown in Figure 6.7.

- Parameter checklist
- Flow—verify feed flow (on flow meter) twice per day (morning and evening)
- pH—verify feed pH twice per day (morning and evening)
- Conductivity—verify feed conductivity twice per day (morning and evening)
- Pressure—record pressure from each of three pressure gauges twice per day (morning and evening)
- Make regeneration brine (once per day)
- Approximately 40 gal of regeneration brine is required per day
- The amount of pilot effluent necessary to feed the second-stage RO system will depend on the recovery
- Pilot effluent was directed to holding tank (Tank E)
- When enough pilot effluent is collected, the second-stage RO system is run (as daily batch) to generate concentrate effluent
- Two regeneration fluid tanks were used, so system operations did not have to be stopped to generate regeneration fluid
- Pilot effluent was directed to Tank E and used as rinse water
- When 40 gal concentrate were generated, sodium chloride was added (amount determined based on the correlation between conductivity and % solution) until 10% solution was achieved

6.1.2 Week 1

Pilot was assembled and set up for automatic operation and regeneration. Flow meter was calibrated for RO concentrate, which is denser than water. Sample taps were installed, and all working parameters were verified. Data were collected for Objective 1, and high- and low-pH salt precipitation commenced.

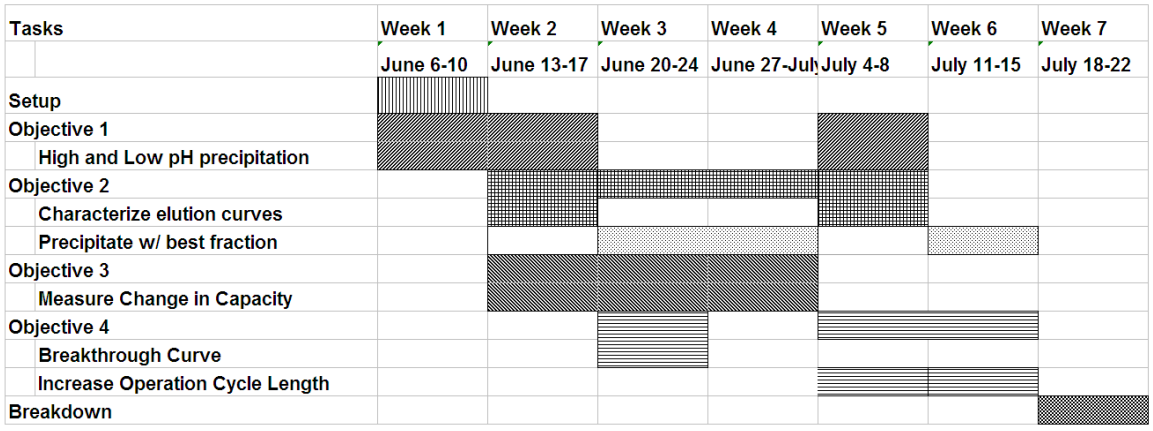

Figure 6.7. Pilot project schedule.

6.1.3 Week 2

Data collection and precipitation for Objective 1 continued. In addition, samples were taken to create elution curves to be used for Objective 2. Resin samples were also taken at the end of service cycles to measure exchange capacity for Objective 3.

6.1.4 Weeks 3 and 4

Resin samples continued to be taken at the end of service cycles to measure exchange capacity for Objective 3. For Objective 2, salts were precipitated using the same procedure described for Objective 1, using the most concentrated fractions of regeneration fluids determined from measurements taken during Week 2. Measurement of the column breakthrough curve was done during Week 3 to determine the optimum length for the operation cycle to be implemented during Week 5.

6.1.5 Week 5

The length of the operation cycle was increased based on data from a breakthrough curve measured during Week 3. Samples were also taken to generate elution curves for Objective 2 and salts were precipitated under high- and low-pH conditions for Objective 1.

6.1.6 Week 6

Salts were precipitated under high- and low-pH conditions using the best fractions of regeneration fluids determined from measurements taken during Week 5 for Objective 2.

6.1.7 Week 7

The pilot was disassembled and transported back to UNM.

At the end of each week during the pilot testing program, samples were transported to UNM for analysis.

6.1.8 Detailed Data Collection and Analysis Procedures

Objective 1: Quantify the consistency of the recovered salt products in terms of mass and purity.

The purity of the recovered salts was measured. Data were collected to satisfy this objective during Weeks 1, 2, and 5. During Weeks 1 and 2, a 20-bed-volume operation cycle was implemented. During Week 5, the operation cycle increased to 28 bed volumes. Salts were precipitated and analyzed for two cycles in Week 1, three cycles in Week 2, and three cycles in Week 5. A total of eight cycles were analyzed, three of which occurred during Week 5 with the extended operation cycle (see Table 6.3).

Objective 2: Determine the most concentrated fraction of the regeneration solution to use for salt recovery.

The objective of the process was to maximize the quality and quantity of salt products that can be recovered by mixing cation and anion regeneration fluids. The regeneration process includes 0.75 bed volumes of 10% NaCl regeneration solution followed by 1.0 bed volumes of rinse water (effluent from pilot). Thus, each column generates 1.75 bed volumes of regeneration fluid per

cycle. Earlier research showed that the maximum concentration of calcium and sulfate during regeneration occurs at approximately 1 bed volume into the regeneration process. By capturing the most concentrated effluent, it may be possible to generate a greater quality and quantity of salt product. To evaluate this hypothesis, elution curves were constructed from samples taken at different times during the regeneration process. Based on these curves, the most concentrated fraction of the regeneration fluid was captured for salt precipitation. Data showed that the maximum cation and anion concentrations occurred at the same points in the regeneration cycle, so the same fractions were captured during cation and anion regeneration cycles. The collected fractions were mixed and allowed to precipitate using the procedure described previously for salt precipitation.

Data to create the elution curves were collected during Weeks 2 and 5 and analyzed during the following weekends so that salts could be precipitated using the optimum fraction of the regeneration solutions during Weeks 3 and 6 (see Table 6.4).

Procedure (analysis of salt products for objectives 1 and 2):

1. Collect feed water from sample tap S1 at the beginning of the service cycle.
    a. Measure pH, conductivity, temperature, and total carbonate (on site).
    b. Fill a 250-mL Nalgene bottle and store for analysis of cations and anions at UNM during the following weekend.
    c. At UNM, analyze for calcium, magnesium, sodium, and potassium concentrations using the AA spectrometer.
    d. At UNM, analyze for chloride, nitrate, fluoride, and sulfate using the ion chromatograph.

2. Collect SAC regeneration waste from regeneration in a 5-gal cubitainer. During Weeks 1, 2, and 5, the entire regeneration waste was collected. During Weeks 3, 4, and 6, a predetermined fraction of the regeneration cycle was collected (determined by elution experiments during Week 2).
    a. After ensuring that contents of the cubitainer are well mixed, measure pH, conductivity, temperature, and total carbonate (on site).
    b. Label cubitainer and store for analysis of ions and precipitation at UNM during the following weekend (ion analysis is identical to Steps 1.b to 1.d).

3. Collect SBA regeneration waste in a 5-gal cubitainer. Procedure is identical to Step 2 for SAC regeneration waste.

4. Precipitation at ambient pH (at UNM):
    a. Mix 100 mL of SAC regeneration solution with 100 mL of SBA regeneration solution in a tared Erlenmeyer flask.
    b. Allow precipitates to form and settle for 36 h.
    c. Collect a sample of supernatant and conduct all analyses for feed water in Step 1.
    d. Transfer to four 50-mL centrifuge vials and centrifuge to separate liquid and solid.
    e. Decant approximately three-fourths of the liquid from each vial and combine the remaining mixture from the four vials into one vial. Centrifuge again.

f. Decant three-fourths of the liquid again and replace with DI water. Centrifuge again. Repeat the process three times.
g. Decant most of the DI water and return the remaining mixture to the tared Erlenmeyer flask.
h. Dry in the lab oven at 104 °C for 24 h.
i. Remove flasks from oven, allow them to equilibrate to room temperature, and weigh them.
j. The difference between the tared mass and the mass after drying is assumed to be the total precipitated mass, although it is possible that a small amount of precipitate redissolved upon contact with DI water.
k. Analyze precipitated solid by SEM, EDS, XRD, and XRF.

5. Precipitation at low pH:
    a. Collect 100 mL of SBA regeneration solution and reduce pH to 4.5 using hydrochloric acid.
    b. Mix the pH-adjusted SBA regeneration waste with 100 mL of SAC regeneration solution in a tared Erlenmeyer flask. Continue all analyses listed in Step 4.

Procedure (development of elution curve—Weeks 2 and 5 only):

1. Collect approximately 250 mL of regeneration fluid from sample taps S2 and S3 in clean Nalgene bottles at 15, 20, 25, 30, 35, 40, and 45 min into the regeneration process.
    a. Measure pH, conductivity, temperature, and total carbonate (on site).
    b. Store the Nalgene bottle for analysis of cations and anions at UNM during the following weekend.
    c. At UNM, analyze for calcium, magnesium, sodium, and potassium concentrations using the AA spectrometer.
    d. At UNM, analyze for chloride, nitrate, fluoride, and sulfate using the ion chromatograph.

2. Generate elution curves based on the data analyzed at UNM, and select the times at which the most concentrated fractions of the regeneration process were obtained for use during precipitation experiments.

Table 6.3. Sampling and Analysis Plan (Objective 1)

Sample Location	Sample Type	Frequency	Analyses
S1	Feed water	2 cycles—Week 1 3 cycles—Week 2	Calcium, magnesium, sodium, potassium, carbonate, bicarbonate, chloride, nitrate, fluoride, sulfate, and pH
S6, S7	Regeneration fluids	2 cycles—Week 1 3 cycles—Week 2	Calcium, magnesium, sodium, potassium, carbonate, bicarbonate, chloride, nitrate, fluoride, sulfate, and pH
Precipitation bucket after precipitation—no pH adjustment	Supernatant	2 cycles—Week 1 3 cycles—Week 2	Calcium, magnesium, sodium, potassium, carbonate, bicarbonate, chloride, nitrate, fluoride, sulfate, and pH
Precipitation bucket after precipitation—no pH adjustment	Solid	2 cycles—Week 1 3 cycles—Week 2	SEM, EDS (relative elemental composition), XRD (presence of known crystal phases), mass
Precipitation bucket after precipitation—low-pH condition	Supernatant	2 cycles—Week 1 3 cycles—Week 2	Calcium, magnesium, sodium, potassium, carbonate, bicarbonate, chloride, nitrate, fluoride, sulfate, and pH
Precipitation bucket after precipitation—low-pH condition	Solid	2 cycles—Week 1 3 cycles—Week 2	SEM, EDS (relative elemental composition), XRD (presence of known crystal phases), mass
Precipitation bucket after precipitation—high-pH condition	Supernatant	2 cycles—Week 1 3 cycles—Week 2	Calcium, magnesium, sodium, potassium, carbonate, bicarbonate, chloride, nitrate, fluoride, sulfate, and pH
Precipitation bucket after precipitation—high- pH condition	Solid	2 cycles—Week 1 3 cycles—Week 2	SEM, EDS (relative elemental composition), XRD (presence of known crystal phases), mass

Table 6.4. Sampling and Analysis Plan (Objective 2)

Sample Location	Sample Type	Frequency	Analyses
S2, S3	Regeneration fluids	At 15, 20, 25, 30, 35, 40 and 45 into the regen cycle 2 cycles—Week 2 2 cycles—Week 5	Calcium, magnesium, sodium, potassium, carbonate, bicarbonate, chloride, nitrate, fluoride, sulfate, and pH
S6, S7	Regeneration Fluids	3 cycles—Week 3 3 cycles—Week 6	Calcium, magnesium, sodium, potassium, carbonate, bicarbonate, chloride, nitrate, fluoride, sulfate, and pH
Precipitation bucket after precipitation—no pH adjustment	Supernatant	3 cycles—Week 3 3 cycles—Week 6	
Precipitation bucket after precipitation—no pH adjustment	Solid	3 cycles—Week 3 3 cycles—Week 6	SEM, EDS (relative elemental composition), XRD (presence of known crystal phases), mass
Precipitation bucket after precipitation—low-pH condition	Supernatant	3 cycles—Week 3 3 cycles—Week 6	Calcium, magnesium, sodium, potassium, carbonate, bicarbonate, chloride, nitrate, fluoride, sulfate, and pH
Precipitation bucket after precipitation—low-pH condition	Solid	3 cycles—Week 3 3 cycles—Week 6	SEM, EDS (relative elemental composition), XRD (presence of known crystal phases), mass
Precipitation bucket after precipitation—high-pH condition	Supernatant	3 cycles—Week 3 3 cycles—Week 6	Calcium, magnesium, sodium, potassium, carbonate, bicarbonate, chloride, nitrate, fluoride, sulfate, and pH
Precipitation bucket after precipitation—high-pH condition	Solid	3 cycles—Week 3 3 cycles—Week 6	SEM, EDS (relative elemental composition), XRD (presence of known crystal phases), mass

Objective 3: Determine antiscalant effect on resin capacity.

Anionic antiscalants can potentially foul anion exchange resins, lowering their exchange capacity. Purolite A850 was designed to reduce organic fouling, so it is particularly suited for treating water containing organic antiscalants. However, it is important to quantify any capacity reduction and determine the extent of organic fouling due to antiscalant addition. SBA resin capacity was determined by analysis of a resin sample taken from a column at the end of the service cycle (see Table 6.5). Resin samples were submerged in 2 N sodium hydroxide and the ions in the resulting liquid were analyzed for carbonate, bicarbonate, chloride, nitrate, fluoride, and sulfate using IC and titration. Fouling was indicated by the presence or absence of organic carbon in the liquid sample, which was measured using the TOC analyzer.

Procedure

1. At the end of the service cycle, pilot operation was halted and a resin sample of approximately 5 g was removed from the top of the SBA column and stored in a sealed container.
2. During the following weekend, the resin sample was rinsed with DI water until all nonadsorbed ions are removed.
3. The resin sample was divided into three 1-g amounts (for triplicate analysis) using an analytical balance and placed into 50 mL of 2 N NaOH to strip off the adsorbed ions and the TOC (if any).
4. Liquid samples were analyzed by IC, titration, and the TOC analyzer to measure carbonate, bicarbonate, chloride, nitrate, fluoride, sulfate, and TOC.
5. Data from each cycle were compared to determine if capacity decreased and if it can be correlated with the amount of organic carbon present on the resin.

Objective 4: Optimize the operation cycle to increase run length before regeneration is necessary.

One measure of process efficiency is the ratio of the operation cycle volume to the regeneration cycle volume. A conservative estimate was used to determine the operation cycle for the first four weeks of the experiment, but it is important to determine the limits of efficiency. A breakthrough curve was measured during the third week (see Table 6.6) to determine the capacity of the IX columns with respect to the major ions of interest: calcium, magnesium, and sulfate. Based on these data, an extended cycle was implemented. The cation column has a higher capacity than the anion column because the cation resin has approximately three times more capacity than the anion resin. In a full-scale system, it might have been possible to equalize the anion and cation removal capacity by having different cation and anion resin volumes, but constraints on the current system did not allow it for this project. Equal resin volumes were simulated by running the cation column to its full capacity even though the capacity of the anion column was exceeded. When the anion exchange capacity was reached, the effluent was diverted from the feed tank so that it would not be treated by the second-stage RO unit. In this way, both columns could be run to capacity. Regeneration solutions from the extended cycle were mixed to precipitate salts, and during Week 6 only the most concentrated fractions of the regeneration solutions were used.

Table 6.5. Sampling and Analysis Plan (Objective 3)

Sample Location	Sample Type	Frequency	Analyses
Resin from top of the SBA column	Resin sample	2 cycles – Week 2 2 cycles – Week 3 2 cycles – Week 4	Strip with NaOH, then measure carbonate, bicarbonate using titration, measure chloride, nitrate, fluoride, sulfate using the IC, and measure organic carbon using the TOC analyzer

Table 6.6. Sampling and Analysis Plan (Breakthrough Curve for Week 3)

Objective	Sample Location	Sample Type	Frequency	Analyses
1	S4 at 120, 132, 144, 156, 168, 180, 192. 204, 216, and 228 min after normal cycle	Regeneration fluids	1 cycles—Week 3	Calcium, magnesium, sodium, potassium, and conductivity
2	S5 at 120, 132, 144, 156, 168, 180, 192. 204, 216, and 228 min after normal cycle	Regeneration fluids	1 cycles—Week 3	Carbonate, bicarbonate, chloride, nitrate, fluoride, sulfate, and conductivity

Objective 5: Determine if pilot effluent affects the performance of the second-stage RO system.

If ion leakage occurs during pilot operations, it is possible that membrane fouling could occur in the second-stage RO system. To determine if this occurred, several parameters related to RO operations were recorded on a daily basis including feed pressure, concentrate pressure, feed temperature, and permeate flow (see Table 6.7). These values were entered into RODataxls, a spreadsheet provided by Hydranautics, which calculated normalized permeate flow. Pressure and flow was read directly from gauges and meters located on the RO unit operations panel. Temperature was measured using a handheld meter. A form for recording data from the RO unit is located in Appendix C.

Sampling forms for each week, for daily operations, and for RO unit data (Table 6.8) are saved as PDF files and can be found in Appendix C.

Table 6.7. Sampling and Analysis Plan for Objective 5

Sample Location	Frequency	Data to Be Measured/Read
2nd stage RO unit	Daily, during RO operation	Feed pressure, concentrate pressure, feed temperature, and permeate flow

Table 6.8. Data Forms and File Names Located in Appendix D

File Type	Filename
Data Form—Week 1	Week 1 Form.pdf
Data Form—Week 2	Week 2 Form.pdf
Data Form—Week 3	Week 3 Form.pdf
Data Form—Week 4	Week 4 Form.pdf
Data Form—Week 5	Week 5 Form.pdf
Data Form—Week 6	Week 6 Form.pdf
Daily Operations Form	DailyOps.pdf
RO Data Form	ROData.pdf

6.2 Pilot Results

6.2.1 Mass Analysis

The first objective of the pilot project was to measure the mass and purity of recovered salts. The composition of precipitated salts was examined using three methods. Fist, precipitated salts were viewed using SEM. They were then analyzed by EDS to determine elemental composition and XRD to identify mineral phases. The solutions relevant to the mass analysis were the anion and cation regeneration solutions and the supernatants from the high- and ambient-pH precipitation tests. Solutions were analyzed using AA and IC to measure the concentrations of common ions including calcium, magnesium, potassium, sodium, chloride, and sulfate. Acid titrations to measure total carbonate were also performed on anion and cation regeneration solutions. Results from the liquid analysis of the cation and anion regenerant solutions are shown in Tables 6.9 and 6.10 (—indicates that no data are available). Samples from three different regeneration cycles were taken every week, and the average ion concentration is an average of ion concentration measurements from those three samples.

Operation cycles in Weeks 1 through 4 were 20 bed volumes, and the volume of the regeneration and rinse cycle was 1.75 bed volumes. If all ions that entered the column during the operation cycle were exchanged onto the resin, and if they were removed from the resin during regeneration, the ion concentration factor (ratio of ion concentration in the regeneration solution to ion concentration in the feed solution) would be equal to the ratio of the number of bed volumes of operation to the number of bed volumes of regeneration. For Weeks 1 through 4, this ratio was equal to 11.43. In Weeks 5 and 6, when the operation cycle was increased to 28 bed volumes, the ratio became 16.00. Table 6.11 shows the actual concentration factors for ions in each cycle for each week. Week 1 was excluded because only one cycle was taken that week, and the pilot was still experiencing some startup problems. With an operation cycle of 20 bed volumes, no divalent cation should break through, so their concentration factors should be equal to the ratio of the number of bed volumes of operation to the number of bed volumes of regeneration. Potassium may break through the column before the operation cycle is complete and therefore have a lower concentration factor. The same is true for divalent and monovalent ions in the anion column. Sulfate should have the highest possible concentration factor, whereas bicarbonate, the dominant form of dissolved CO_2 at moderate pH values, may break through before the operation cycle is complete. In Week 2, concentration factors follow expected patterns. In Week 5, when the operation cycle was extended, calcium and magnesium appear to break through before the end of the cycle.

Table 6.9. Average Ion Concentrations in the Cation Regeneration Solution

	Ca	Mg	K	Na	Cl	SO_4	CO_3
Week	mg/L	mg/L	mg/L	mg/L	mg/L	mg/L	M
1	5,154	1306	2	6,132	24,188	460	—
2	5,096	1919	—	8,064	27,510	394	0.03
3	11,855	5600	206	10,411	51,871	255	0.04
4	13,679	5824	180	6,221	49,765	175	0.04
5	5,798	1708	83	3,702	21,297	460	0.03
6	12,546	3703	163	6,663	46,180	301	0.05

Table 6.10. Average Ion Concentrations in the Anion Regeneration Solution

Week	Ca mg/L	Mg mg/L	K mg/L	Na mg/L	Cl mg/L	SO_4 mg/L	CO_3 M
1	62	28	2	13,604	12,992	8,224	—
2	—	—	—	—	13,042	10,236	0.20
3	—	—	80	25,662	26,324	17,012	0.20
4	38	31	—	22,989	16,292	26,998	0.22
5	179	122	44	10,178	5,021	17,673	0.13
6	129	133	103	10,389	5,266	48,167	0.25

Table 6.11. Concentration Factors for Each Ion for Weeks in Which the Entire Regeneration Cycle Was Captured

	Cycle	Ca	Mg	K	SO_4	$TOTCO_3$
Week 2	1	9.8	10.3	10.1	11.8	7.2
	2	11.2	10.2	—	11.6	7.7
	3	10.4	7.9	—	10.2	6.3
	2a	10.1	12.7	—	11.9	7.7
Week 5	1	13.5	8.9	5.4	18.2	—
	2	13.5	8.1	5.3	17.9	4.5
	3	13.2	8.7	5.0	17.4	5.0

Using concentrations listed in Tables 6.9 and 6.10, it was possible to calculate the total mass of each ion present when equal volumes of the solutions were mixed. In cases where the pH of the anion regeneration solution was reduced, the additional chloride mass from the added HCl was calculated using a combined mass and charge balance and was added to the total chloride mass present in the mixed solution. The calculation of additional HCl was done according the following technique. The charge of the anion regenerant solution was calculated based only upon the pH and the resulting carbonate speciation (the total carbonate was known). Then the charge of the pH adjusted solution was calculated based upon the new pH, the new carbonate speciation, and a variable amount of chloride. Using Goal Seek in Excel, the change of the pH adjusted solution was matched to the original solution by changing the concentration of chloride. Each solution (50 mL) required about 3 mL of HCl to reduce the pH to the desired amount, but acid concentrations varied. The additional mass of chloride was calculated by multiplying the molar concentration of chloride obtained in the equation by the volume of the solution (50 mL + 3 mL) and then multiplying by the molar mass. Chloride could not be adjusted for Week 1, cycle 1 because carbonate measurements were not made.

Inspection of precipitates from each week and pH condition was performed with an SEM, and it was possible to develop a preliminary identification of the salts based on characteristic shape. These identifications were corroborated by EDS and XRD analyses. SEM images of precipitate from each week and pH condition are shown in Figures 6.8 and 6.9. The most commonly observed shapes in these images are smooth spheres, textured spheres, and needles.

EDS spectra were taken on several instances of each of these shapes to identify them in terms of elemental composition. According to the semiquantitative integration of the EDS spectra, smooth and textured spheres consist mainly of calcium carbonate. Figure 6.10 shows the elemental composition (in percent) of several examples of these spheres from different samples compared with the atomic composition of pure calcium carbonate, shown at the top of the figure. Each

example displays the signature 20% calcium and carbon and the 60% oxygen characteristic of calcium carbonate. All of the samples that precipitated under ambient pH conditions contain these spheres. Figure 6.11 shows several examples of the needlelike structures that occurred in several samples with associated semiquantitative atomic composition, with the atomic percent composition for reference. These samples were analyzed under a low-pressure vacuum, which can make carbon measurement difficult because of interference from carbon molecules in the air. What is notable in this analysis is that calcium and sulfur occur in the characteristic 1 to 1 ratio. When carbon measurements are deleted from the analysis, the percent compositions match up very well with those of pure calcium sulfate.

Week 1

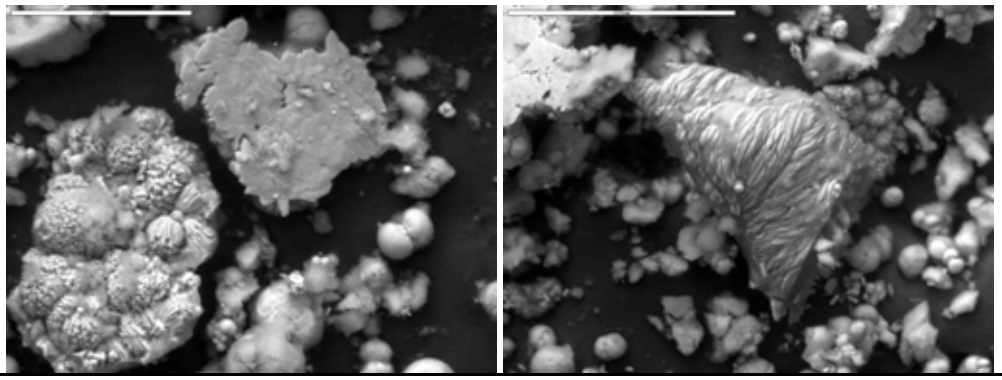

Week 2

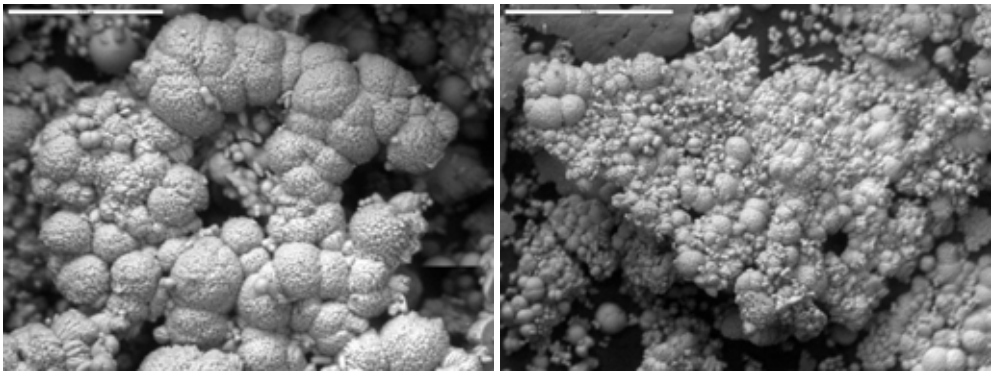

Week 3

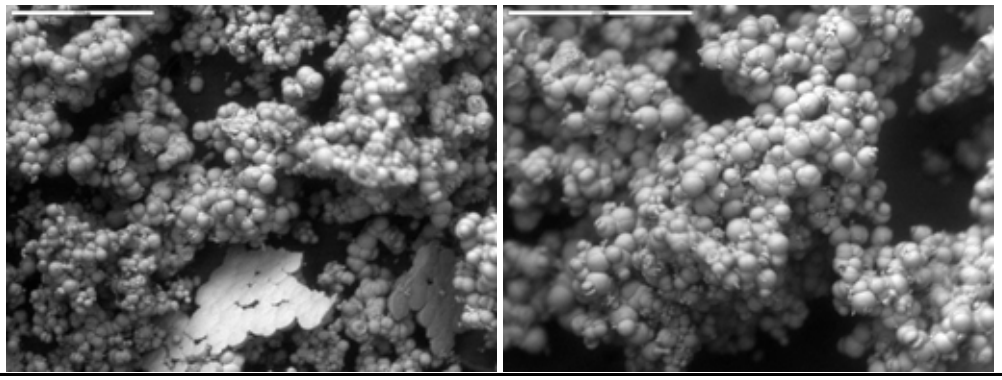

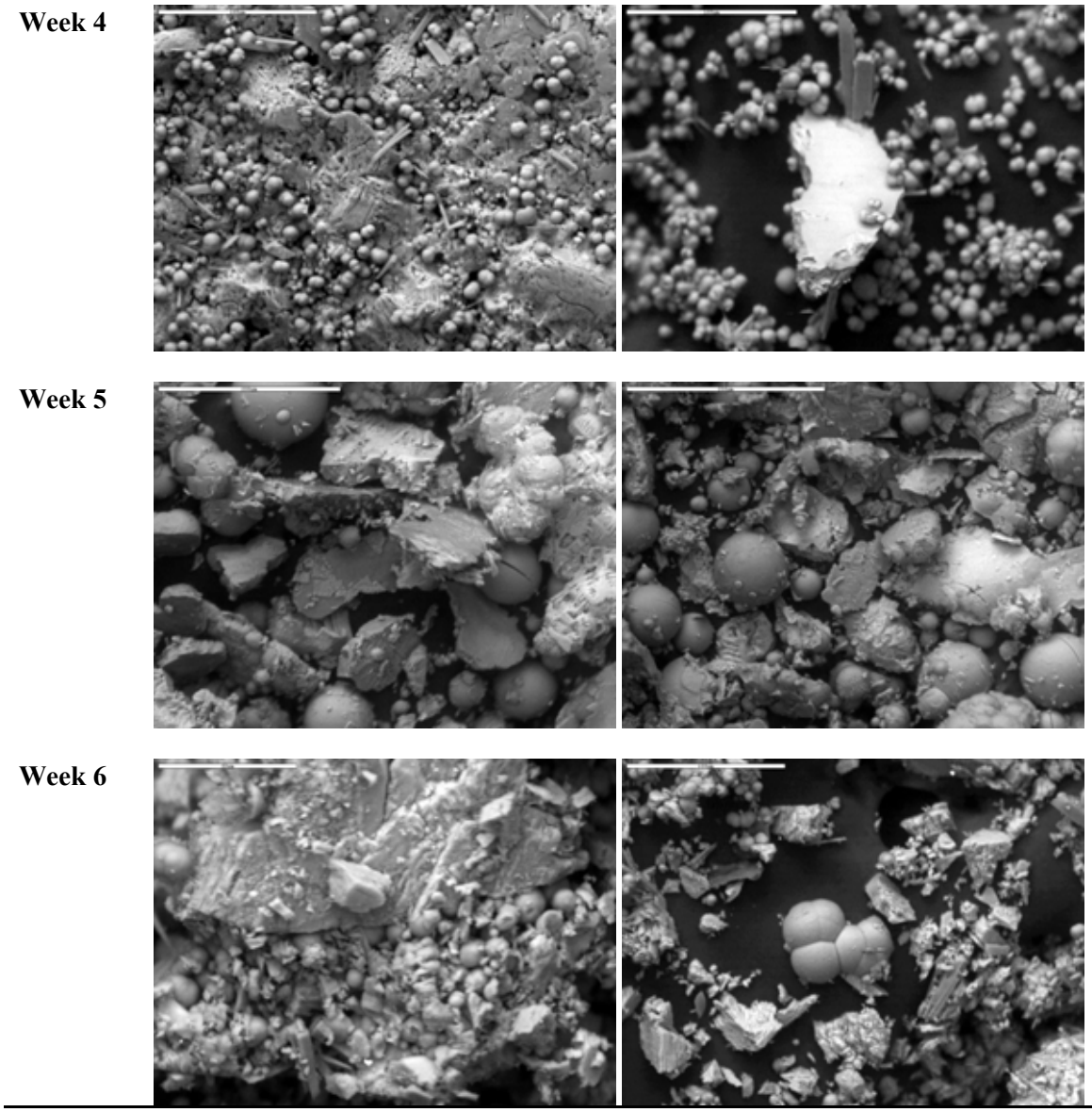

Figure 6.8. SEM images of precipitate under ambient-pH conditions.

Week 1	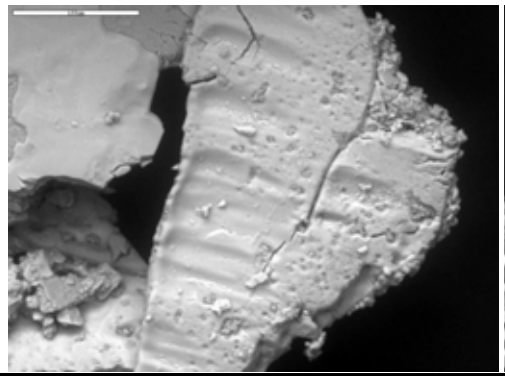	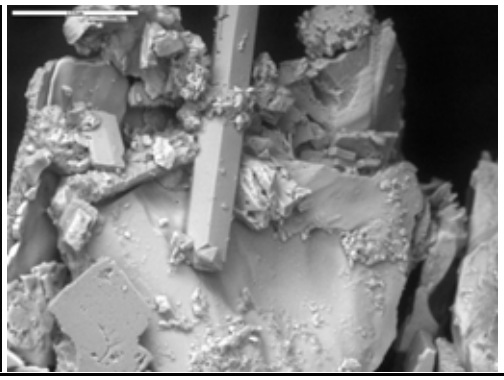
Week 2	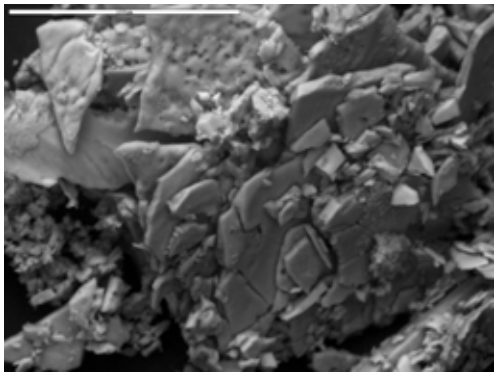	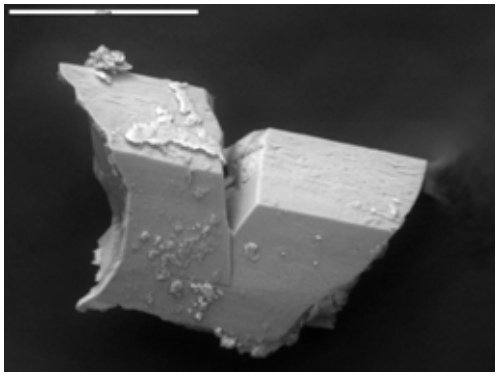
Week 3	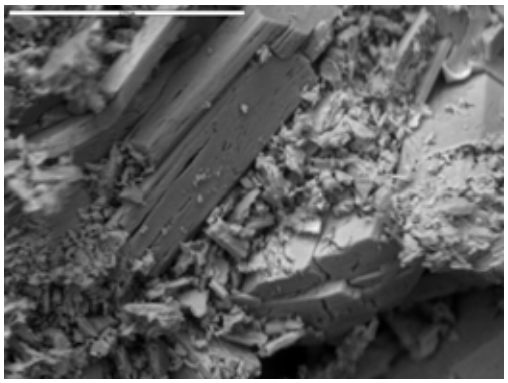	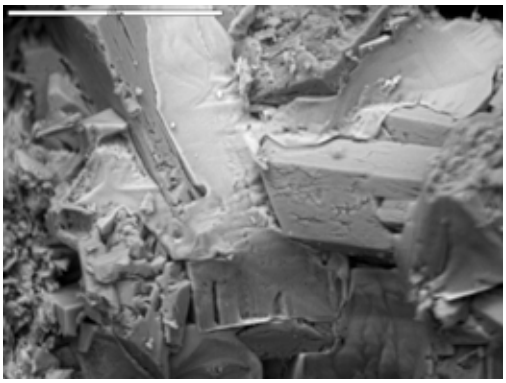
Week 4	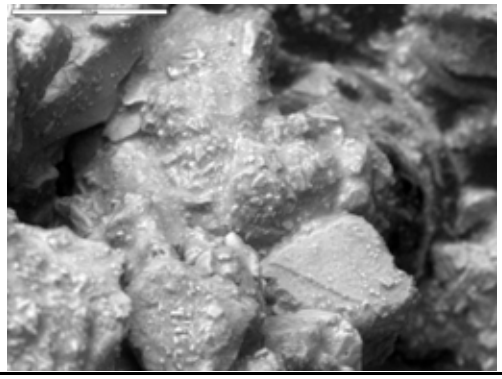	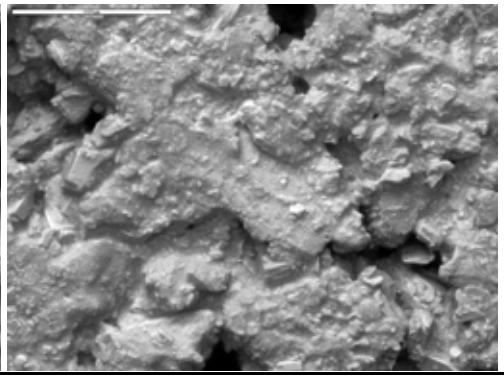

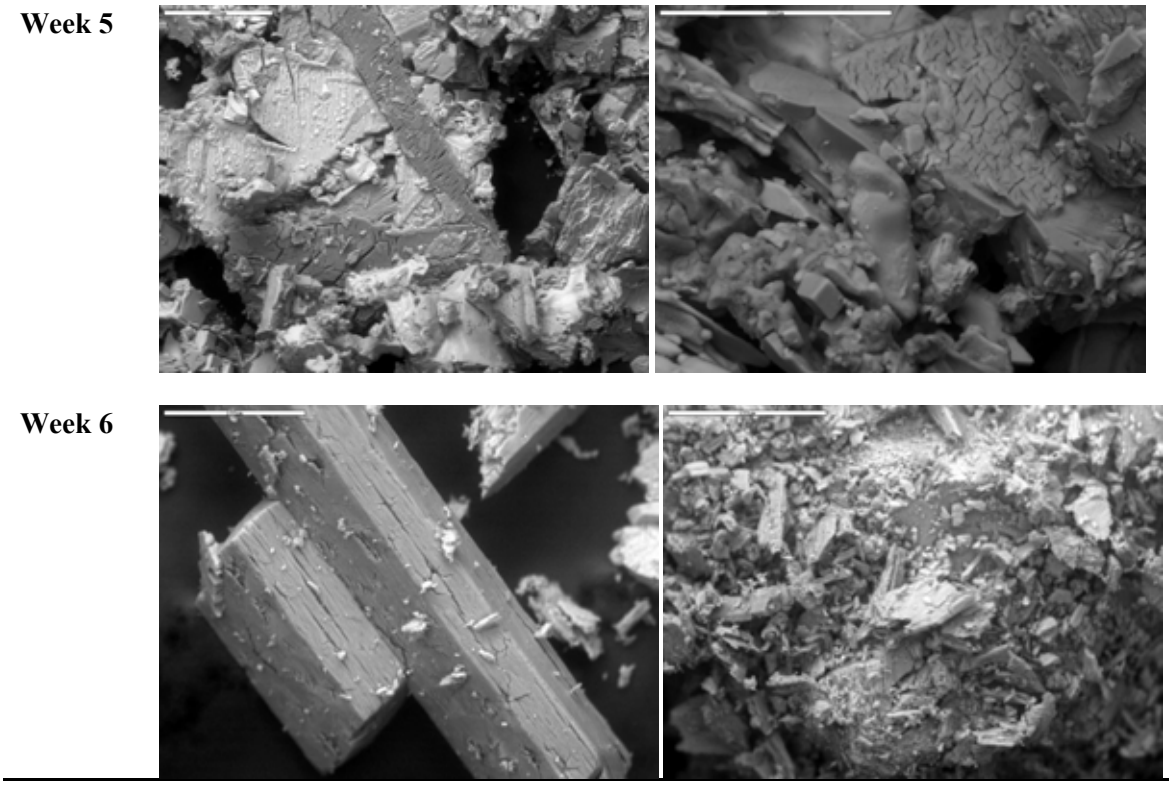

Figure 6.9. SEM images of precipitate under low-pH conditions.

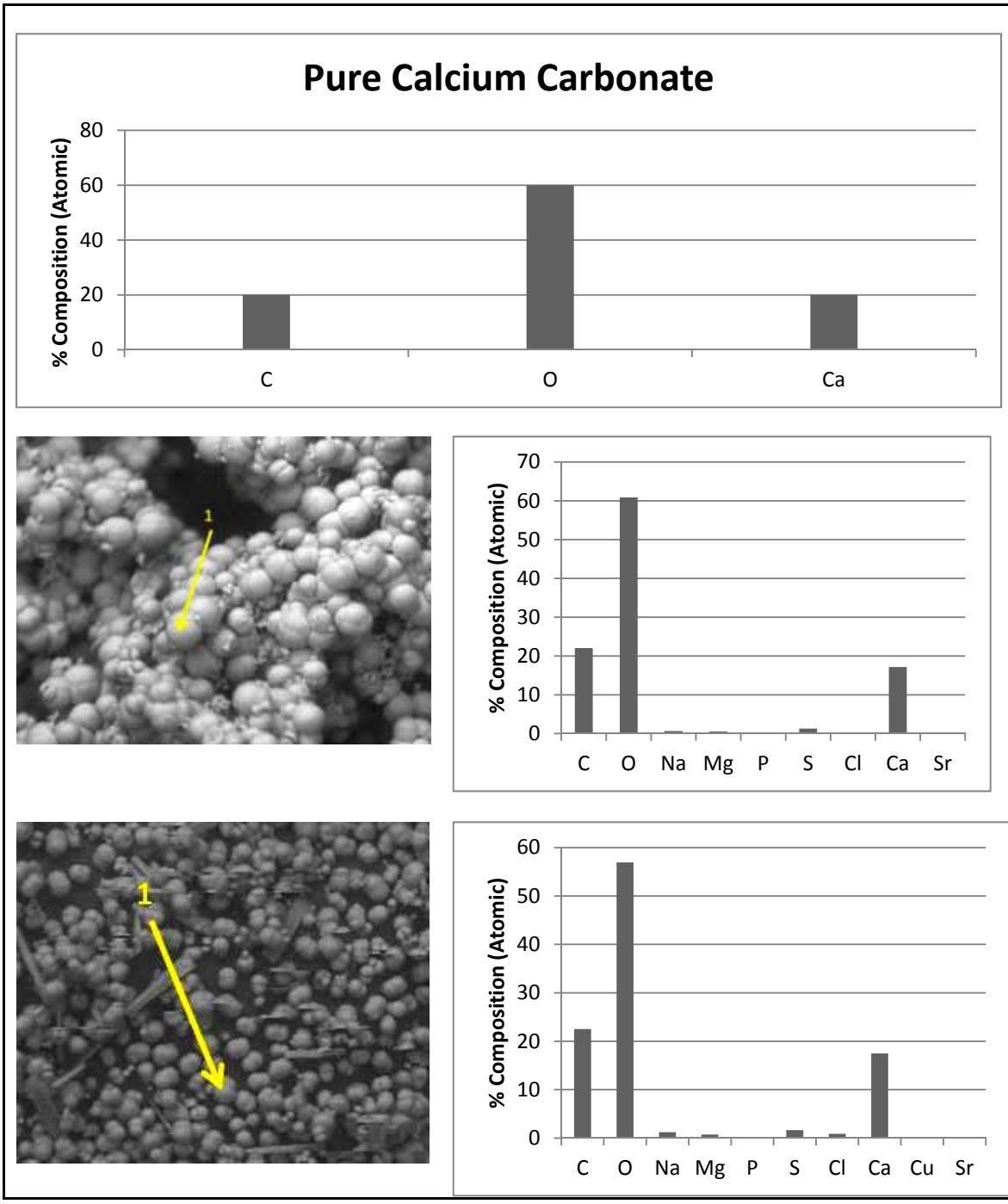
Pure Calcium Carbonate
% Composition (Atomic)
80
60
40
20
0
C
O
Ca
1
% Composition (Atomic)
70
60
50
40
30
20
10
0
C O Na Mg P S Cl Ca Sr
1
% Composition (Atomic)
60
50
40
30
20
10
0
C O Na Mg P S Cl Ca Cu Sr

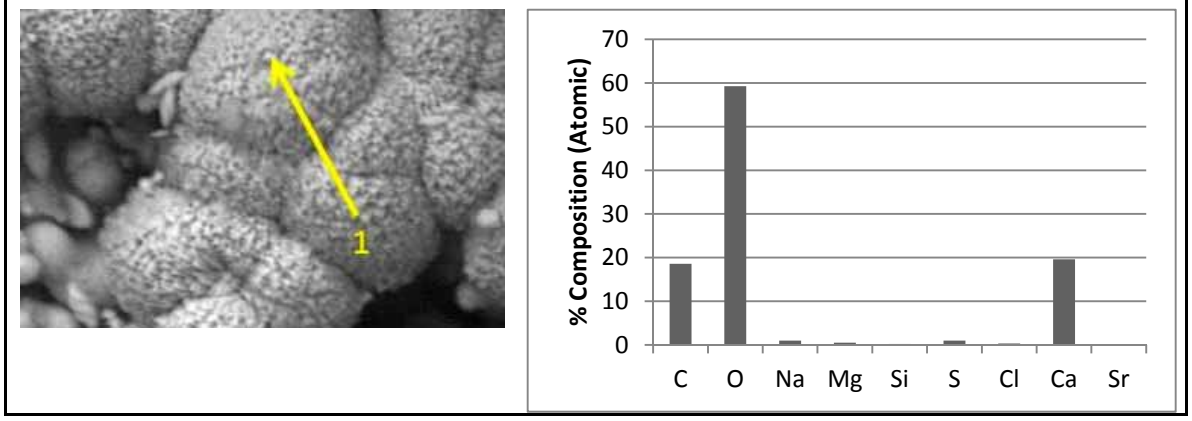

Figure 6.10. Semiquantification of EDS spectra showing % composition of spheres identified by SEM.

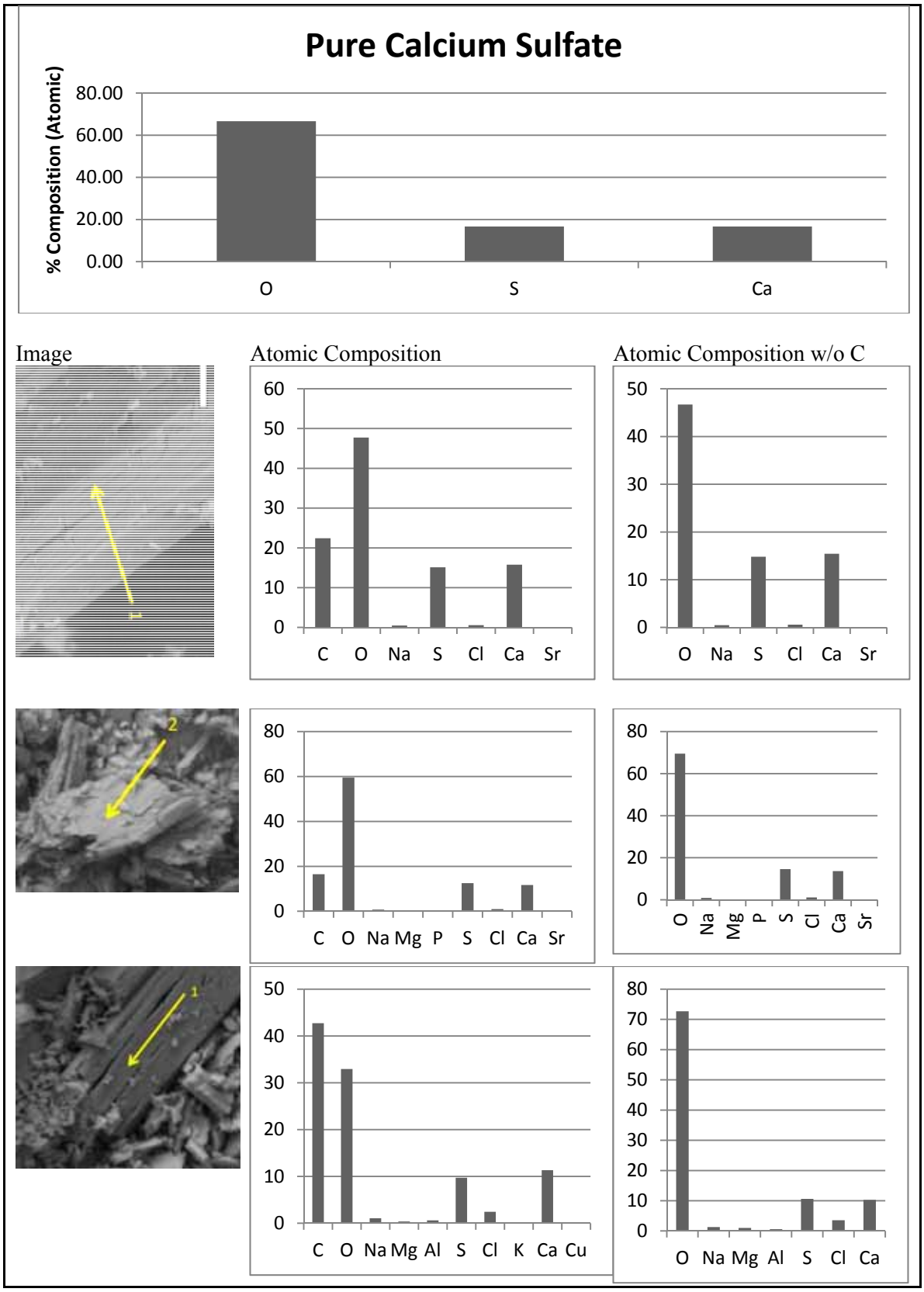

Figure 6.11. Semiquantification of EDS spectra showing % composition of needles identified by SEM.

XRD was used to characterize the precipitates from each week. XRD will only detect phases that have regular crystalline structures. Amorphous phases do not produce a diffraction pattern. Based on visual inspection by SEM, it can be seen that the vast majority of the precipitate is in crystalline form. However, there is one image taken from a precipitate formed under ambient pH conditions in Week 1 that appears to contain some amorphous material (see Figure 6.12), but this may be an instrument focus issue, because this was not seen in any other images from this sample, nor was it seen in images from any other sample. The XRD equipment available for use required more than 0.5 g of mass to obtain a spectrum, so samples obtained from mixing conditions that did not produce at least this amount of mass were not included in the analysis. Sufficient mass was produced under ambient-pH mixing conditions for Weeks 2, 3, 4, and 6 and under low-pH mixing conditions for Weeks 3, 4, and 6. XRD results are shown in Figure 6.13.

Jade 9.1 (Materials Data Incorporated) was used to analyze the XRD spectra. Results from the XRD analysis show that the major constituent of the precipitate that formed at ambient pH conditions in all weeks but Week 6 is calcium carbonate. Calcium carbonate was identified as calcite or generic calcium carbonate, but the spectra are very similar for all calcium carbonate crystals, so it is difficult to pinpoint the crystal phase. XRD spectra show that the bulk constituent of the precipitate that formed under low-pH mixing conditions for Weeks 3 and 6 was calcium sulfate. Several crystal phases were identified in the XRD crystal library, including bassanite, anhydrite, and generic calcium sulfate displaying a few different levels of hydration.

Using Jade 9.1, it is possible to overlay spectra to determine their similarities. This produces as a qualitative measure of spectra similarities. Two overlays were created to compare spectra. Those identified as mainly calcium carbonate were overlaid, and the similarity index between them was calculated to be 90%. The spectra identified mainly as calcium sulfate were also overlaid, and the software calculated a similarity index of 91%. These overlays are shown in Figure 6.14.

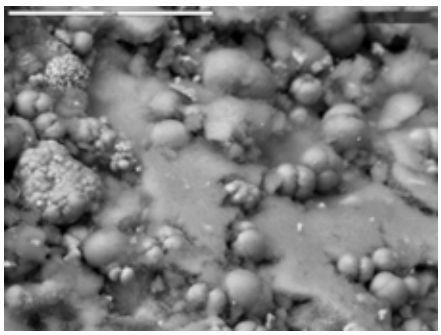

Figure 6.12. SEM image showing possible amorphous material.

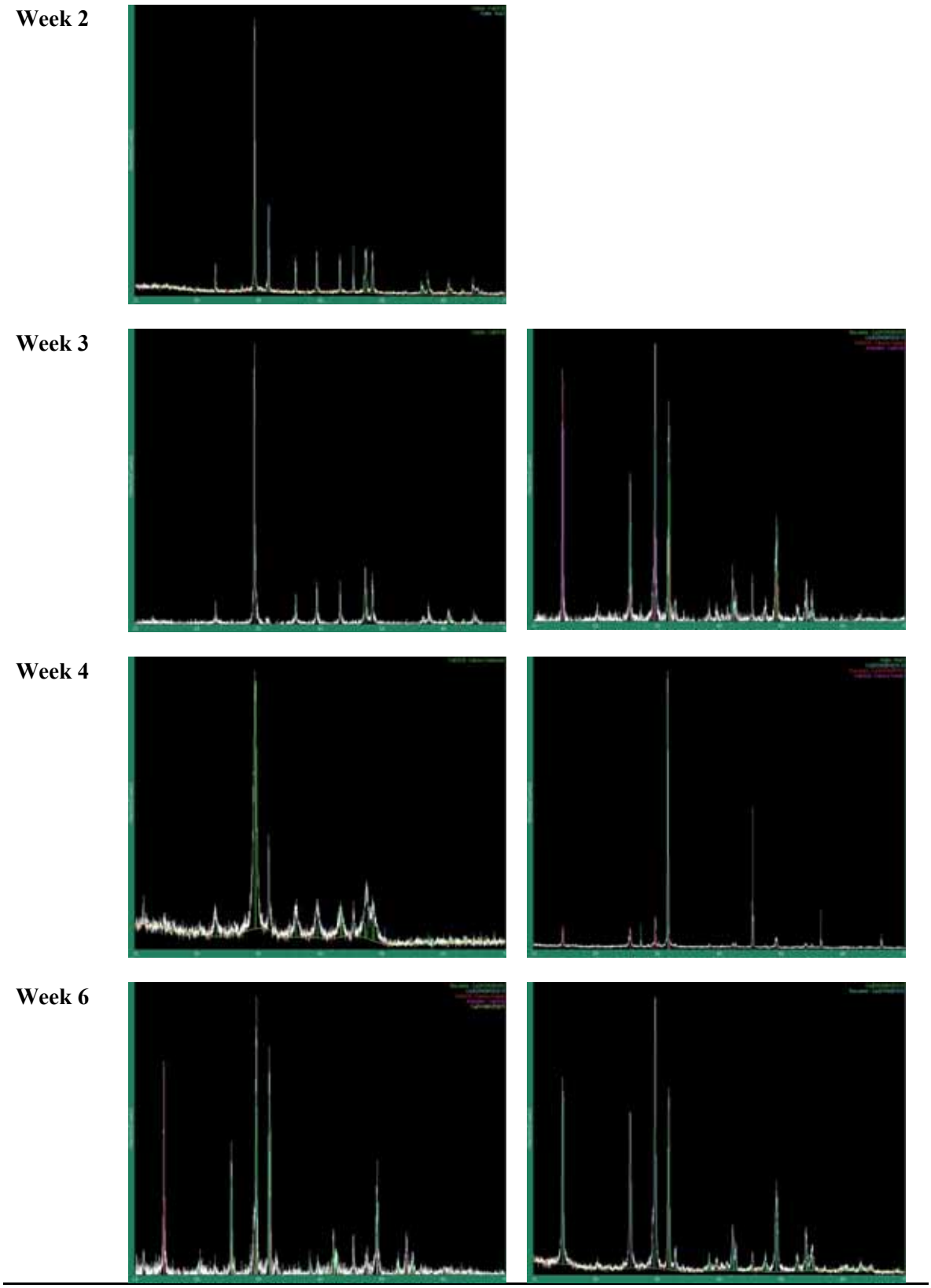

Figure 6.13. XRD spectra of precipitate samples.

Spectra ID'd as Calcium Carbonate	Spectra ID'd as Calcium Sulfate

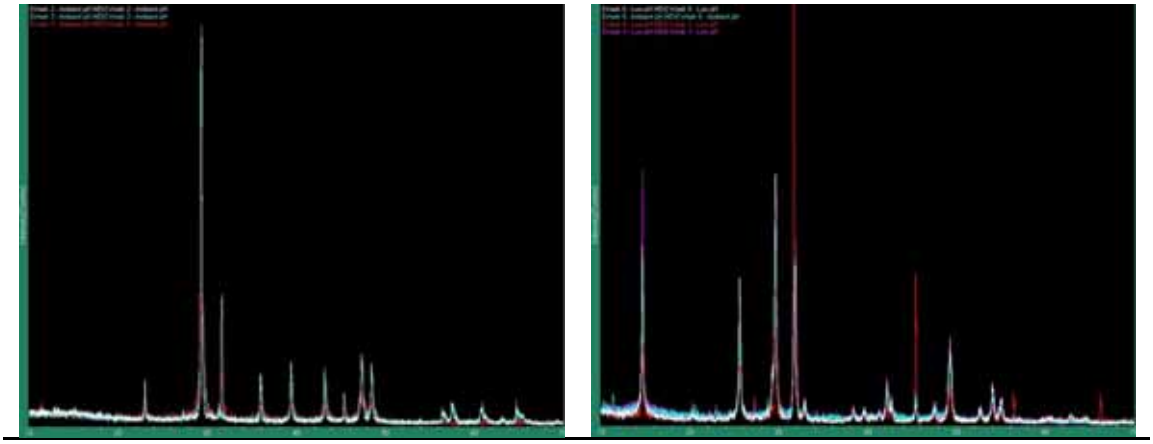

Figure 6.14. Overlaid spectra from XRD analysis.

Precipitate mass was quantified according the procedure outlined in the previous section. One cycle was chosen from each week for mass analysis.. Results from this analysis are reported in Table 6.12.

Table 6.12. Precipitate Mass from Each Week for Ambient- and Low-pH Techniques

Week	Cycle	pH Condition	Initial pH of Anion Regen Solution	Final pH of Anion Regen Solution	Precipitate Mass (g)
1	1	Ambient	N/A	N/A	0.4565
2	2	Ambient	N/A	N/A	0.6403
3	2	Ambient	N/A	N/A	2.1022
4	2	Ambient	N/A	N/A	1.2904
5	2	Ambient	N/A	N/A	0.1998
6	2	Ambient	N/A	N/A	2.3512
1	1	Low	8.33	2.17	0.1443
2	2	Low	8.39	2.52	-0.0408
3	2	Low	8.34	2.57	1.8152
4	2	Low	8.67	3.15	1.0366
5	2	Low	8.45	2.59	0.1592
6	2	Low	8.64	2.86	2.4508

During Weeks 3, 4, and 6 of the pilot test, regeneration solution was only collected between minutes 15 and 35 of the 53 min regeneration cycle in order to obtain the most concentrated fraction and to increase the mass of the spontaneous precipitate. During these weeks a total of 13.2 L of regeneration solution (cation plus anion) was collected per cycle, as opposed to the 34.98 L obtained when the entire cycle was collected during Weeks 1, 2, and 5. For Weeks 1 through 4, using a 20-bed-volume operation cycle, there were 8.35 regeneration cycles per day, so the flow rate for collected regeneration solution during Weeks 1 and 2 was 292.08 L/day, as opposed to 110.22 L/day during Weeks 3 and 4. For Weeks 5 and 6, using a 28-bed-volume operation cycle, there were 8.00 regeneration cycles per day, so the flow rate for collected regeneration solution during Week 5 was 231.22 L/day, as opposed to 87.25 L/day during Week 6. The amount of precipitate that could be produced per cubic meter of RO concentrate for each week and pH condition was calculated and is shown in Figures 6.15 and 6.16.

According to the pilot design, regeneration solution was only collected from the most concentrated portion of the regeneration cycle during Weeks 3, 4, and 6. The entire cycle was collected during Weeks 1, 2, and 5. During Weeks 5 and 6, the operation cycle was extended by 8 bed volumes. These changes to the pilot operation and collection methods caused changes in the salt production rate and the salt character.

In Weeks 1 and 2, ambient-pH conditions produced a much greater amount of salt precipitation than low-pH conditions. This was most likely the result of increased solubility of calcium carbonate at the low pH. Under ambient-pH mixing conditions, calcium carbonate precipitated immediately, consuming the available calcium that would otherwise have been able to precipitate with sulfate. However, sulfate concentrations were low in these solutions, so even under low-pH conditions, only a small amount of calcium sulfate precipitated.

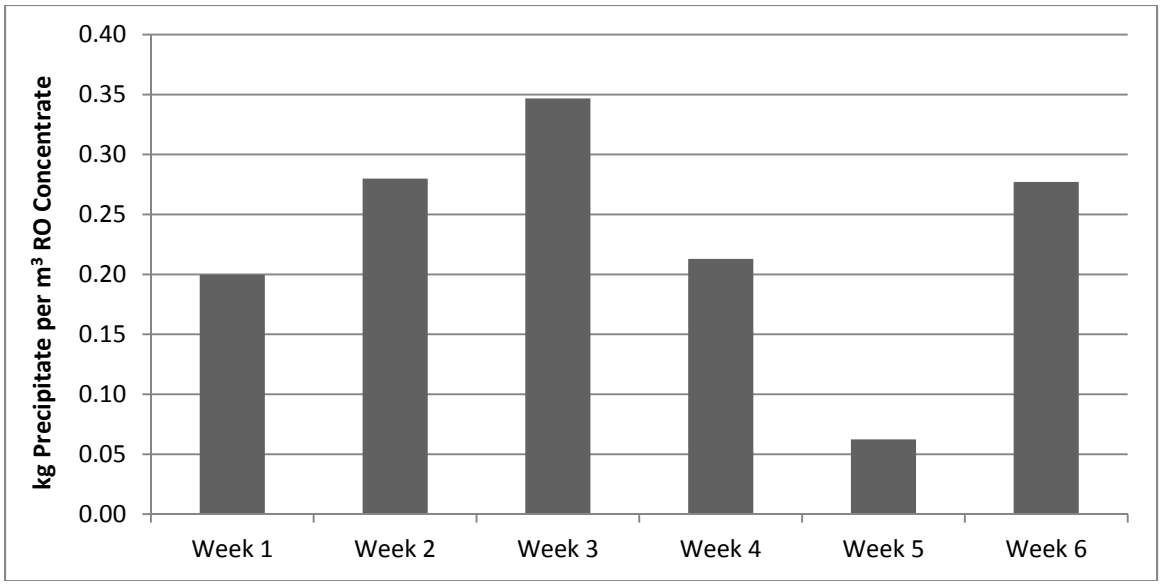

Figure 6.15. Calculated salt yield per cubic meter of reverse osmosis concentrate for each week at ambient pH.

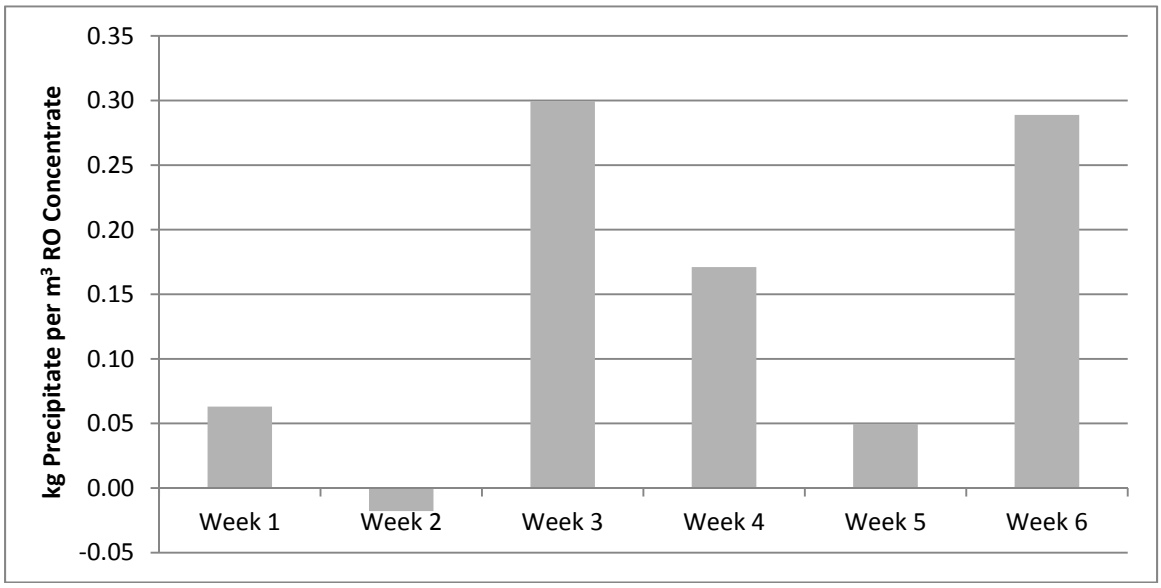

Figure 6.16. Calculated salt yield per cubic meter of RO concentrate for each week at low pH.

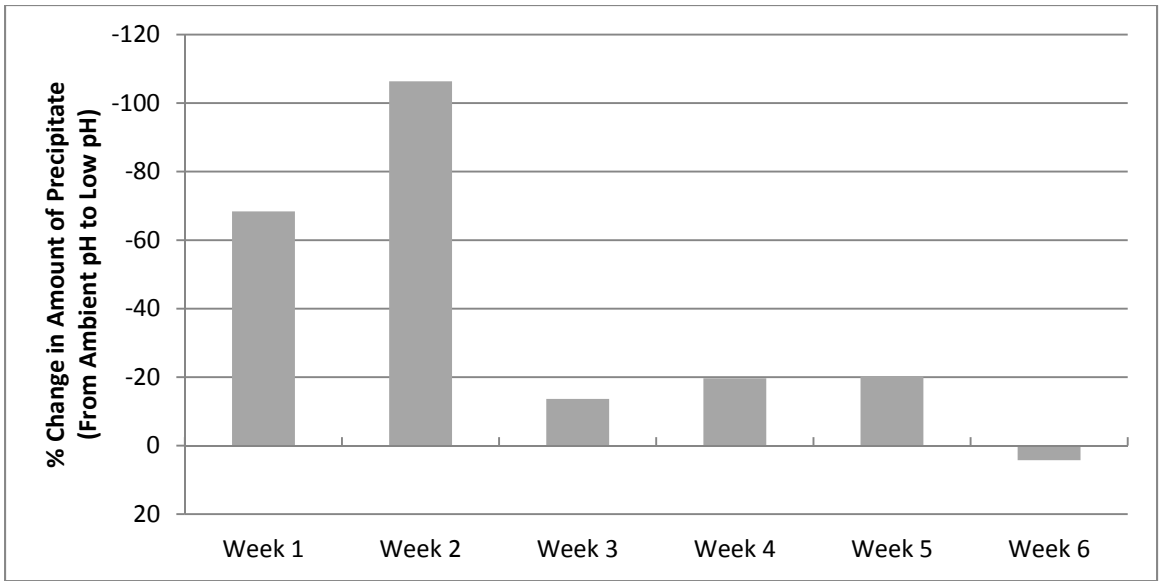

Figure 6.17. Difference in yield between precipitation under ambient- and low-pH conditions.

During Week 5, in which the operation cycle was extended, sulfate concentrations increased relative to carbonate concentrations, and there was also a small increase in calcium concentrations. In ambient pH conditions, less precipitate formed compared to the same test from Weeks 1 and 2. This was likely due to the decrease in carbonate concentration. Because of the increase in sulfate concentration, more precipitate formed under low-pH conditions in Week 5 than in Weeks 1 and 2. This can also be seen from the difference in mass precipitation under ambient- and low-pH conditions between Weeks 1 and 2 and Week 5 (see Figure 6.17).

During the weeks in which the most concentrated portion of the regeneration cycle was collected, precipitation tests yielded increased mass compared to tests for which the full regeneration cycle was collected. Sulfate concentrations during these weeks were 2 to 3 times higher than during weeks in which full regeneration cycles were collected. This resulted in calcium sulfate precipitation regardless of pH mixing conditions.

Regeneration solution in Week 6 was higher in sulfate concentration than that in Weeks 3 and 4, because of increased operational cycles. Precipitate produced under ambient-pH mixing conditions in Weeks 3 and 4 was mainly calcium carbonate, although a very small amount of calcium sulfate also precipitated in Week 4. Mixing regeneration solutions at low pH during Weeks 3 and 4 produced calcium sulfate precipitate at a lower salt yield than that which occurred under ambient-pH mixing conditions.

In Week 6, sulfate concentrations were higher than in any other week because of the combination of increased operational cycles and collection of the most concentrated portion of the regeneration cycle. Sulfate was so abundant that it consumed all the available calcium to form calcium sulfate under both ambient- and low-pH conditions at the same yield. No calcium carbonate was detected in these samples.

6.2.2 Conclusions from Investigation of Precipitate

A few general conclusions can be drawn from the combination of data from SEM, EDS, and XRD. First, calcium sulfate and calcium carbonate can be precipitated separately by controlling the pH when mixing cation and anion regeneration solutions. For all weeks except Week 6,

mixing under ambient-pH conditions resulted in a calcium carbonate precipitate. The carbonate consumed the available calcium, and only negligible amounts of calcium sulfate precipitated. Analyses of cations in solution, which were somewhat unreliable, showed that some magnesium precipitated as well. If that happened, it would most likely be in the form of a calcium magnesium carbonate such as dolomite, but this was neither observed under the SEM nor identified by XRD. EDS did indicate a very low percentage (less than 1.5% in all cases) of magnesium precipitation, but that is close to the detection limit of the instrument. In Week 6, the precipitate from both ambient- and low-pH mixing conditions was mainly calcium sulfate, although a small amount of calcium carbonate was identified visually in the SEM images from that sample. XRD identified both samples as calcium sulfate. All samples that precipitated under low-pH conditions consisted mostly of calcium sulfate. This was observed visually through the SEM and was confirmed by EDS and XRD. The data show that calcium carbonate precipitation can be controlled by reducing the pH to less than 4 during mixing. If sufficient sulfate exists to consume the available calcium, pH adjustment is not needed to suppress calcium carbonate precipitation.

One of the concerns that arose in relation to precipitation of salts by mixing cation and anion regeneration solutions was the high ionic strength of the mixture and the presence of phosphonate-based antiscalants. Phosphonates are highly water-soluble salts and esters of phosphonic acid, $HPO(OH_2)$. The inhibition action of phosphonates is significantly better toward calcium carbonate, magnesium hydroxide, and barium sulfate than toward calcium sulfate precipitation (Antony et al. 2011). They are able to suppress precipitation of both calcium sulfate and calcium carbonate at high levels of supersaturation (S. Jasbir, 1999). The effect of phosphonate-based antiscalant on precipitation in simulated RO concentrate from the a brackish water system was studied by Greenlee et al. (2010). It was found that solution pH is a major factor in antiscalant effectiveness. Significant calcite precipitation occurred at pH 10.5 in the presence of antiscalant (as opposed to pH 8 in solutions without antiscalant). PreTreat Plus 100 is only weakly attracted to the anion resin and easily eluted during regeneration, according to King Lee, the manufacturer. For this reason, it will not be concentrated by the anion exchange process. The antiscalant is not likely to significantly suppress precipitation at low concentrations, but it may have some effect on the size and morphology of precipitated crystals (Greenlee et al., 2010).

In addition to the high concentrations of divalent ions, there are also high concentrations of sodium and chloride, because the columns are regenerated with a 10% sodium chloride solution. The ionic strength of the cation and anion regeneration solutions, calculated only from the measured ions, ranged from 0.6 to 2.5 M. Although the decreased activity of divalent ions may decrease the salt yield, salts precipitated spontaneously when the regeneration solutions were mixed. The feed flow rate to the RO system producing concentrate for the pilot was approximately 1.75 gpm. From the mass quantification section, it was estimated that during Week 6, it was possible to precipitate about 12 kg of salt per cubic meter of regeneration solution. If the RO system was treating 5 million gallons per day (MGD) of RO concentrate, the salt yield would be approximately 6 tons/day. Using this process, it is possible to recover approximately 45% of the calcium and approximately 28% of the sulfate from the mixed regeneration solution. That is equal to an overall recovery of approximately 15% of the total gypsum in the RO concentrate.

6.2.3 Determination of Most Concentrated Regeneration Solution Fraction

The second objective of this phase of the project was to determine which portion of the regeneration cycle yielded the highest concentrations of ions and to compare precipitation using only that fraction with precipitation using the regeneration solution from an entire regeneration cycle. Comparison of salt yields from concentrated fractions versus standard cycles was discussed previously, so this section will focus only on the determination of the most concentrated fraction.

Elution curves were taken in Week 2 and Week 5 to capture any changes due to extension of the operation cycle. Figures 6.18–6.21 show the concentration of ions eluting from the column, the total carbonate of the solutions, and the conductivity of the solutions, throughout the cycle.

Electrical conductivity was measured in the field, whereas calcium concentration was measured in the laboratory. Time constraints during pilot operation prevented the measurement of calcium concentration at the time the elution curves were taken. The calcium concentration appears on the elution curves, although it was measured later and did not impact the determination of the most concentrated portion of the cycle. Conductivity and total carbonate both peaked about 1 bed volume into the regeneration cycle, so the most concentrated portion of the cycle was determined to occur between 0.67 and 1.17 bed volumes or between 15 and 35 min into the regeneration cycle. As is evident from the elution curves, calcium concentration peaked slightly earlier in the regeneration cycle than conductivity and carbonate concentration. In retrospect, it might have been more useful to collect the fraction between about 0.60 and 1.10 bed volumes instead. The concentrations of ions in the regeneration solutions are shown in Tables 6.9 and 6.10.

One factor that should not be overlooked when these data are considered is that there may have been variations in the sodium chloride regeneration solution concentration that affected the elution curve. Regeneration solution was prepared using a conductivity meter, salt pellets used for home water softening, and a scale with a 0.02 lb precision. The amount of salt that needed to be added was calculated by taking a conductivity reading from a tank containing approximately 40 gal of secondary RO concentrate, referring to a chart that related conductivity to concentration in lb/gal, subtracting the current concentration of salt from 0.89 lb/gal (10% solution), and multiplying by 40. The desired amount was weighed on the scale, poured into the tank, and mixed until it was dissolved as much as possible. Complete dissolution of the salt pellets was difficult to achieve. This method was fairly crude and likely resulted in a range of solution concentrations. Given that consideration, the elution curves from the two different weeks are quite similar. The main difference between the two is that the calcium curve is broader and peaks a bit later in the elution from Week 5. The conductivity of the cation regeneration solution is higher in Week 2, which may account for the earlier calcium peak.

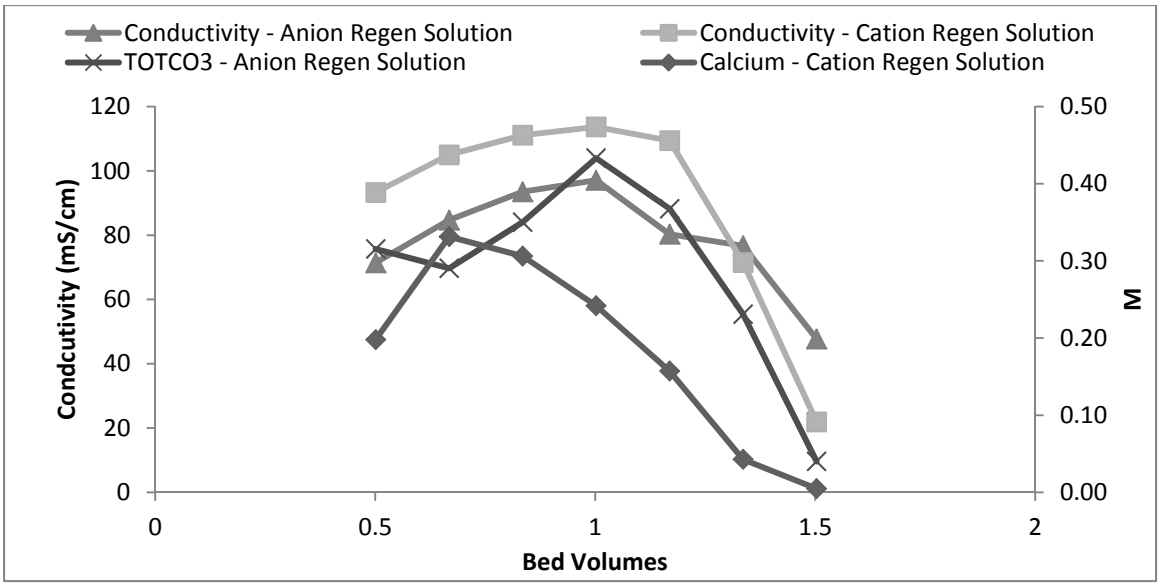

Figure 6.18. Elution curve for Week 2.

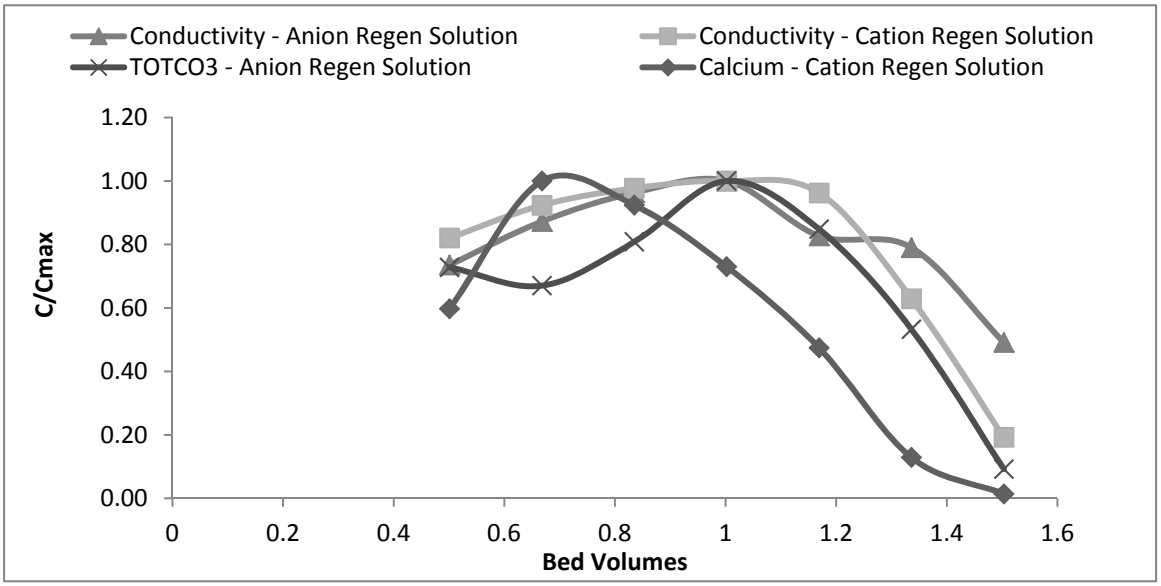

Figure 6.19. Normalized elution curve for Week 2.

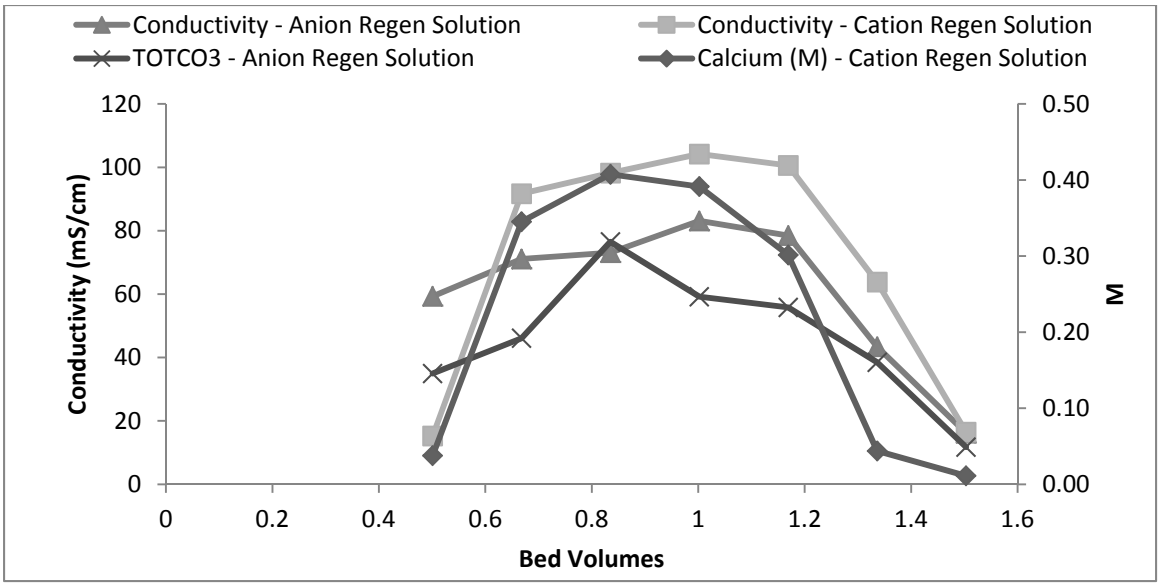

Figure 6.20. Elution curve for Week 5.

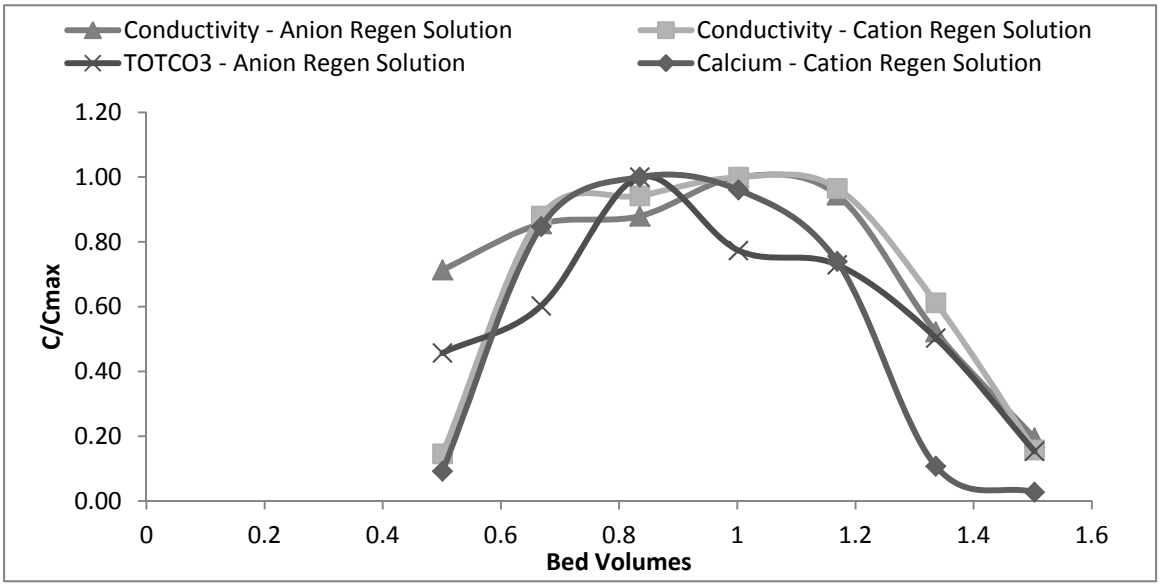

Figure 6.21. Normalized elution curve for Week 5.

During pilot design, it was difficult to predict the number of bed volumes necessary to regenerate the columns completely, but elution curves show that the majority of ions were displaced from the column during the1.75-bed-volume regeneration cycle. In standard practice, the number of bed volumes used for regeneration and rinsing is much larger. In this application, however, it makes sense to use the smallest volume of regeneration solution possible in order to maintain the highest possible concentration of ions. The elution curves show that the majority of ions are removed from the column before 1.75 bed volumes and that it may be possible to reduce the rinsing time by a few minutes without compromising column efficiency.

6.3 Effect of Antiscalant on Resin Capacity

Fouling of the anion exchange resin by organic antiscalant was a potential problem identified at the beginning of the study. The feed water to the primary RO system was treated with King Lee Pretreat Plus 100, which is a phosphonate-based antiscalant that works as a chelating agent to complex the metals and prevent precipitation.

According to chemists at King Lee, phosphonate is weakly attracted to the anion resin and easily eluted during regeneration. To confirm that the resin was not fouled over time, regardless of the cause, resin samples were taken from the top of the anion exchange column at the end of the operation cycles during Weeks 2, 3, and 4. Resin samples were washed, dried, weighed, and then stripped using 1N NaOH and allowed to equilibrate. Liquids were then analyzed for sulfate, chloride, nitrate, and total organic carbon (TOC). Based on results of the liquid analysis, the total number of equivalents of ions on the resin per gram was calculated. The amount of TOC (in parts per million [ppm] C) per resin gram was also calculated, but the ratio between ppm C and equivalents is unknown, so it could not be added to the sum of equivalents from the ions. Specification sheets from Purolite list 1.25 eq/L as the minimum capacity of A850 resin. Laboratory measurements of dry resin show that it has a density of 0.73238 g/mL, indicating that dried resin should have a minimum capacity of 1.7 eq/g. A total of 18 samples were analyzed. Two resin samples were collected per week, and each was separated into three 1 g masses for analysis. Mass concentrations of ions were measured, converted to milliequivalents, multiplied by the solution volume, and then divided by the exact mass measurement (close to 1 g) to find the amount of meq/g on the resin for each ion. Results from this analysis are shown in Figure 6.22 and Table 6.13.

Carbonate titrations were not done for these samples because of the extremely high pH of the solution used to strip the resins. However, there is no reason to expect that the ratio of ions on the resin would change over time, so even if the total capacity including the carbonate is a little higher, the trend of total capacity of time should still be valid. The total concentration of ions on the resin displays a slight decrease in Week 4 compared to Weeks 2 and 3, but this is not necessarily due to fouling by the antiscalant. There are several factors that could potentially lead to a decrease in anion exchange capacity. Other organic compounds in the feed water could foul the resin, or the decrease in exchange capacity could be due to the buildup of higher capacity ions that were not measured in the laboratory. Although the cause of the decrease in capacity is unknown, the effect of it on the overall operation of the pilot was very minor. The anion exchange column operated without a problem throughout the duration of the pilot and there was no measured decrease in sulfate exchange.

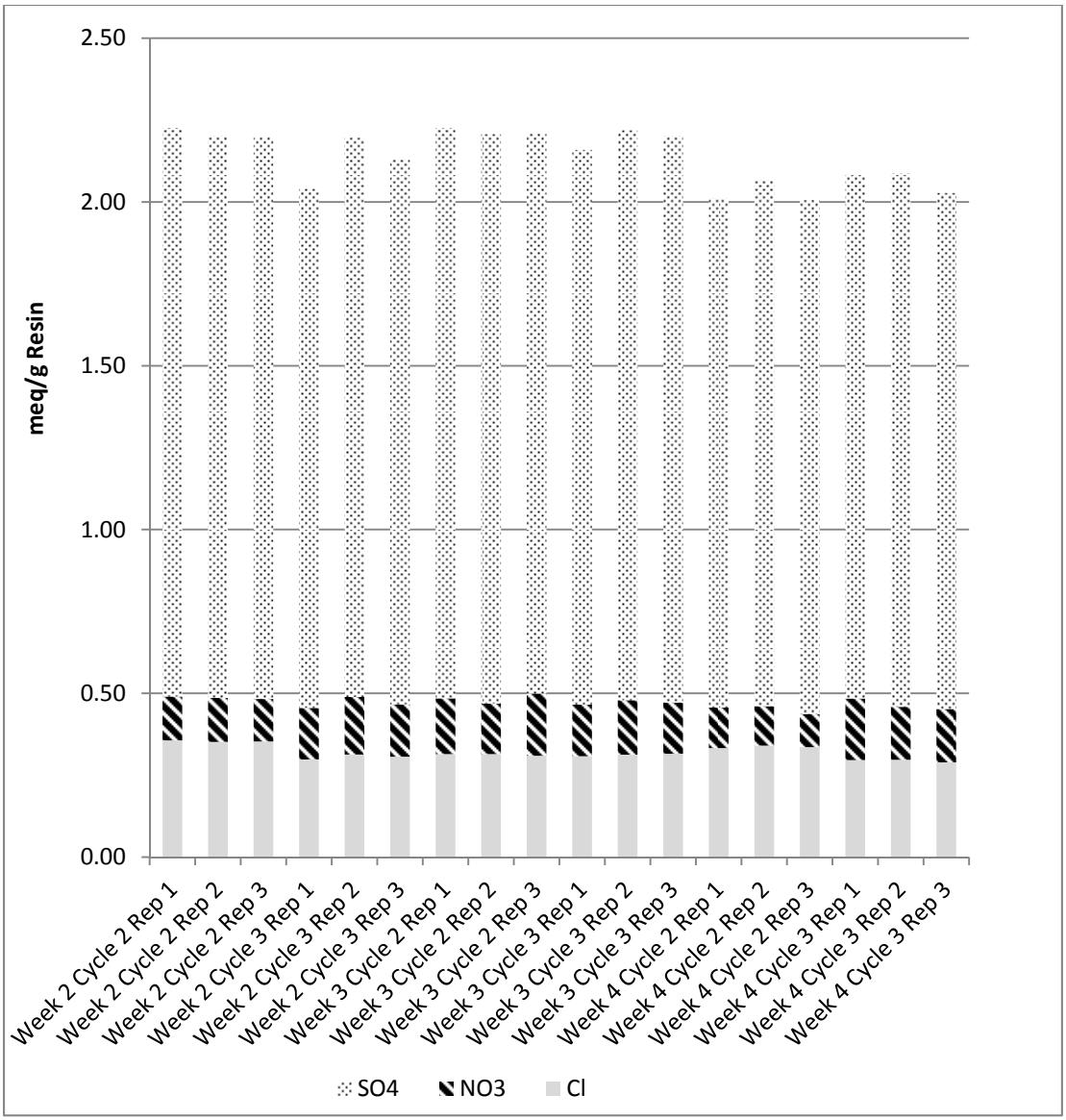

Figure 6.22. Concentration of Cl, NO_3, and SO_4 on resin stripped (meq/g).

Table 6.13. Amounts of Cl, NO_3, and SO_4 on Resin Stripped with NaOH (meq/g)

	Resin	Cl	NO_3	SO_4	Total
	g	meq/g	meq/g	meq/g	meq/g
Week 2 Cycle 2 Rep 1	1.0003	0.36	0.13	1.74	2.23
Week 2 Cycle 2 Rep 2	1.0004	0.36	0.13	1.71	2.20
Week 2 Cycle 2 Rep 3	1.0008	0.36	0.13	1.72	2.20
Week 2 Cycle 3 Rep 1	1.0005	0.30	0.16	1.58	2.04
Week 2 Cycle 3 Rep 2	1.0001	0.32	0.18	1.71	2.20
Week 2 Cycle 3 Rep 3	1.0001	0.31	0.16	1.67	2.14
Week 3 Cycle 2 Rep 1	1.0002	0.32	0.17	1.74	2.23
Week 3 Cycle 2 Rep 2	0.9994	0.32	0.15	1.74	2.21
Week 3 Cycle 2 Rep 3	0.9998	0.31	0.19	1.71	2.21
Week 3 Cycle 3 Rep 1	1.0003	0.31	0.16	1.69	2.16
Week 3 Cycle 3 Rep 2	1.0003	0.32	0.17	1.74	2.22
Week 3 Cycle 3 Rep 3	0.9996	0.32	0.16	1.73	2.20
Week 4 Cycle 2 Rep 1	1.0001	0.34	0.12	1.55	2.01
Week 4 Cycle 2 Rep 2	1.0002	0.35	0.12	1.61	2.07
Week 4 Cycle 2 Rep 3	1.0005	0.34	0.10	1.57	2.01
Week 4 Cycle 3 Rep 1	1.0000	0.30	0.19	1.60	2.09
Week 4 Cycle 3 Rep 2	1.0000	0.30	0.16	1.63	2.09
Week 4 Cycle 3 Rep 3	0.9997	0.29	0.16	1.58	2.03

Solutions containing the constituents stripped from the resin were also analyzed for TOC. The TOC concentration on the resin ranged from 11.16 ppm C/g to 8.45 ppm C/g. TOC concentrations are compared to total concentration (meq/g) of ions in Figure 6.23 There does not appear to any correlation between these, besides a general decrease in both values over time. The same values, normalized to the maximum concentrations of each, are shown in Figure 6.24. In each constituent, the decrease is slight compared to the maximum value and did not impact column performance. To verify trends and understand long-term impacts, it would be necessary to obtain performance for a series of months.

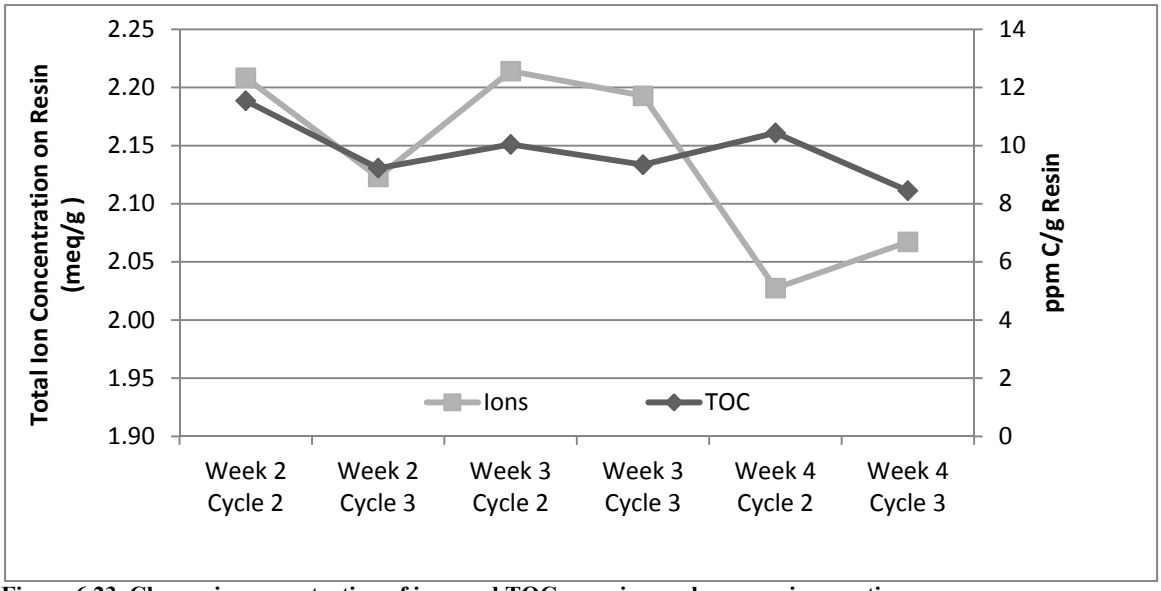

Figure 6.23. Change in concentration of ions and TOC on anion exchange resin over time.

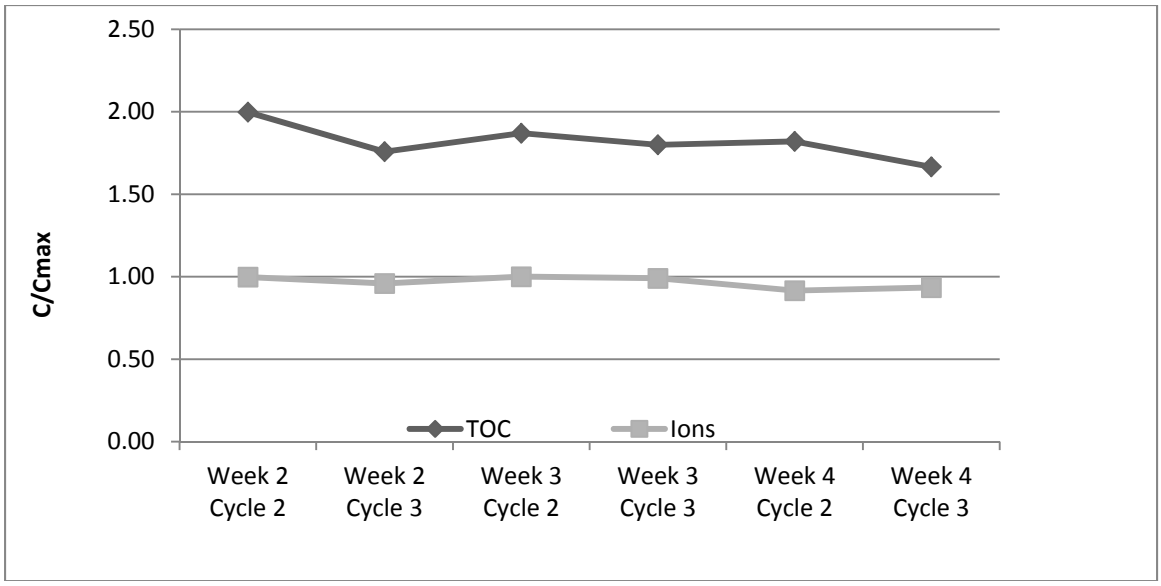

Figure 6.24. Change in normalized concentration of ions and TOC on anion exchange resin over time.

6.4 Optimization of Operation Cycle Length

One of the difficulties in performing sequential cation and anion exchange is that most cation resins have higher exchange capacities than anion resins. For the purposes of this pilot, identical columns were used for both resins to simplify the hydraulics, but this resulted in wasted exchange capacity in the cation exchange column. The design operation cycle length was based on the estimated anion exchange capacity, but the actual capacities of both columns were unknown. To optimize the length of the operation cycle, it was necessary to generate a breakthrough curve to map the concentration of cations and anions in the effluent. During Week 3, an operation cycle was extended by 108 min (18.44 bed volumes), and samples were taken every 12 min. The samples were analyzed by AA, IC, and acid titration to measure calcium, magnesium, sulfate, and total carbonate. The resulting breakthrough curves are shown in Figure 6.25.

The figure shows that effluent carbonate concentration had already reached the influent concentration at the end of the standard operation cycle, indicating that it was present in the effluent that was stored and treated by a secondary RO system to produce regeneration solution. The regeneration solution, therefore, contained even more carbonate, and this could potentially cause problems if any cations leaked into the effluent or if carbonate concentrations became high enough to cause precipitation in the cation exchange column. Precipitation can occur in the cation column during regeneration if sulfate and carbonate are present in sufficient quantities.

The breakthrough curves show that the sulfate begins to break through the anion exchange column at about 22 bed volumes, so the operational cycle based on this column was already close to being fully optimized with regard to sulfate. At 20 bed volumes, the entire resin capacity for carbonate appears to be exhausted, and the fact that the effluent concentration is greater than the influent concentration indicates that it is being displaced from the resin by higher-selectivity ions, such as sulfate (i.e., chromatographic peaking). That phenomenon explains why sulfate concentrations in the anion regeneration solution were so much higher in Week 6 than in Weeks 3 and 4.

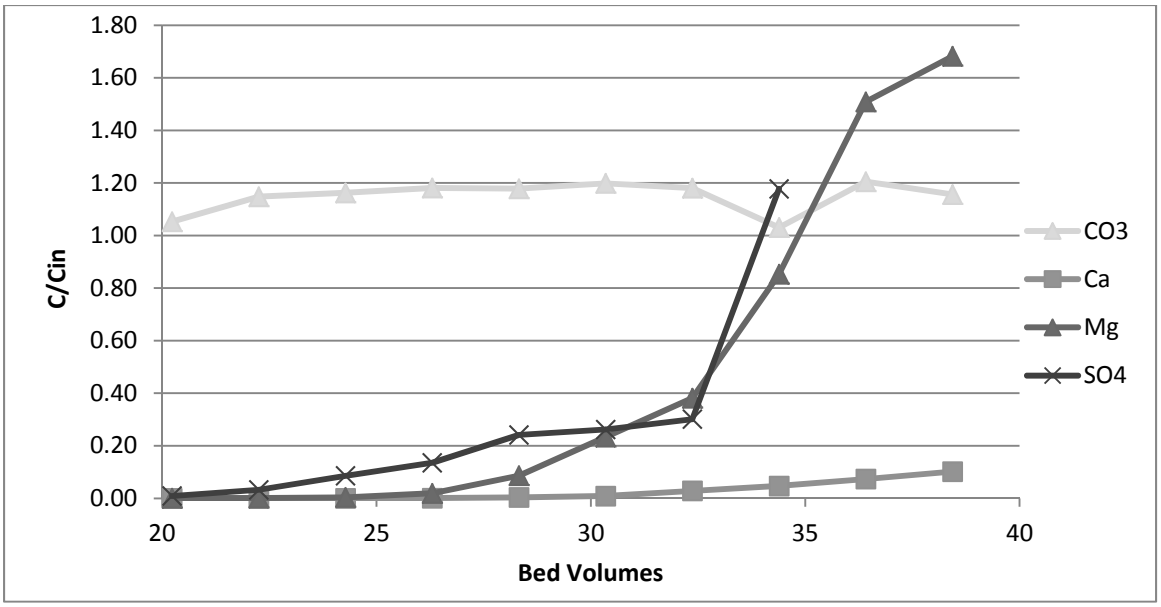

Figure 6.25. Breakthrough curve from extended operation cycle in Week 3.

Breakthrough of calcium began at about 32 bed volumes, but magnesium appeared in the effluent at about 28 bed volumes. Magnesium exceeded the influent concentration at 34 bed volumes, at the same time that the calcium concentration began to increase. This represents the displacement of magnesium from the resin by calcium, which has a higher selectivity. If samples had been taken beyond 38 bed volumes, the magnesium concentration would eventually have approached the influent concentration as the resin in the column equilibrated to the influent concentrations. Some displacement of magnesium by calcium occurred during the 8-bed-volume extension of the operation cycle, and this can be seen in the comparison of the average calcium-to-magnesium ratios in the cation regenerant solution between the normal and extended cycles (see Table 6.14). When the operation cycle was extended, the ratio of calcium to magnesium on the resin increased. This phenomenon could be optimized to increase calcium concentrations in the regeneration by increasing the size of the anion exchange column relative to the cation exchange column.

To avoid possible precipitation of magnesium salts, the operation cycle was extended to 28 bed volumes. The last 8 bed volumes of effluent were diverted from the second-stage RO system to prevent sulfate precipitation from occurring on the membrane or having it build up in the secondary concentrate being used to regenerate the columns. Extending the operation cycle also greatly increased the sulfate concentration on the anion exchange resin. By extending the operation cycle and capturing the most concentrated fraction of the regeneration solution, it was possible to precipitate calcium sulfate without adjusting the pH during mixing, because of the high concentration of sulfates in the anion regeneration solution. In a full-scale system, this could represent a large saving in terms of process simplification, safety, and costs related to acid.

Table 6.14. Average Concentrations Ratio (eq) between Calcium and Magnesium

	Ca:Mg (eq)	Std Dev
Normal cycle (2–4)	1.44	0.164
Extended cycle (5–6)	2.06	0.003

6.5 Reverse Osmosis System Performance in Treating Pilot Effluent

For the duration of pilot testing, effluent from the sequential IX process was stored and treated by a single-element RO system to produce more water and to produce concentrate to use as the IX regeneration solution. Several parameters were recorded on a regular basis to keep track of system performance over time. These parameters included feed pressure, concentrate pressure, concentrate flow, permeate flow, feed temperature, feed conductivity, feed pH, concentrate temperature, concentrate conductivity, and concentrate pH. The RO system was not run continuously because only a small amount of secondary concentrate was needed to regenerate the columns on a daily basis. On most days, the system was only run for a few hours, and occasionally enough secondary concentrate was produced so that the system did not have to be run at all on certain days. In particular, extra concentrate was produced on Fridays to avoid having to run the RO system over the weekend. Effluent that was not treated by secondary RO was stored and used for rinsing at the end of the regeneration cycle.

Although data were recorded on a regular basis (see Table 6.15) when the RO system was in use, frequent system shutdowns make them difficult to interpret. There were significant changes in ambient temperature during system operation, which often occurred between 7:30 a.m. and 11:00 a.m. One incident that may have damaged the membrane occurred during the first weekend (June 10–11) when the back pressure in the feed line prevented the feed valve from closing during the regeneration cycle. As a result, the columns were unable to regenerate, and effluent full of divalent ions was sent to the effluent storage tank and subsequently to the secondary RO system before the problem was realized. Within an hour, the RO system was shut down, and a short autoflushing sequence was run. However, some scaling may have occurred at that time. During Week 3 (June 19–25), an algal growth problem developed in the effluent storage tank that fed the RO system. Although it was realized during Week 4, further inspection of the cartridge filters on the pilot system and the RO system revealed it had been occurring unnoticed before that time. The tank was emptied and washed with chlorine bleach. The membrane was removed from the RO system and a chlorine flush was performed. System performance deteriorated at the end of June, and the membrane was replaced was on June 29. It is unclear which of the issues that occurred caused the decline in performance. The fouled membrane was retained and remains in cold storage, and a membrane autopsy may be performed as part of an adjoining study.

Hydranautics ESPA-2 membranes were used in the RO system. See the datasheet in Appendix D for further information. Recorded data were entered into the ROData spreadsheet provided by Hydranautics, which contains the specific membrane information needed to normalize the data. Figure 6.26, showing normalized permeate flow, was generated by the ROData spreadsheet. As can be seen on this chart, membrane performance declined steadily over time between June 16 and June 28 (Weeks 3 and 4), and then improved upon membrane replacement on June 29. It is unclear whether the decline was due to the scaling from treating the pilot effluent or fouling from algal growth.

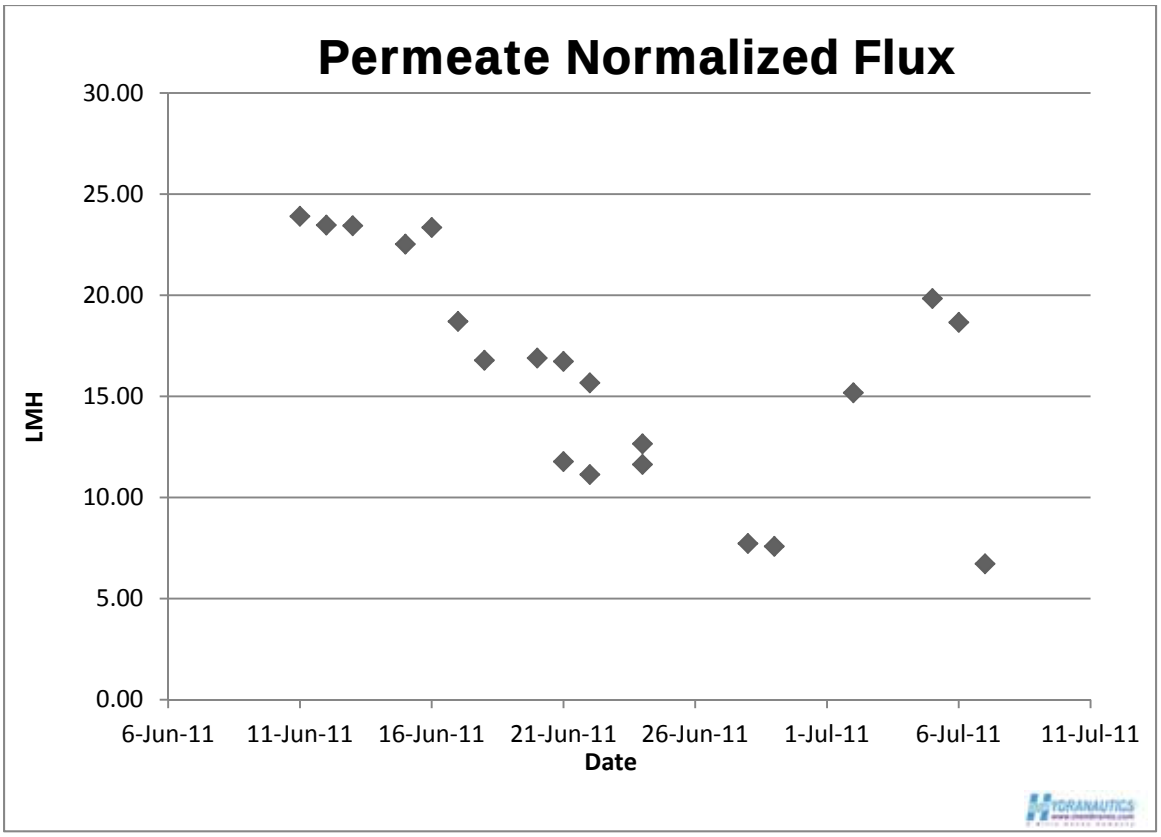

Figure 6.26. Normalized permeate flux (from Hydranautics spreadsheet).

Table 6.15. RO Data Recorded during System Operation

Date/Time	Feed Pressure	Concentrate Pressure	Concentrate Flow	Permeate Flow	Permeate Flow	Feed Temp
	psi	psi	gpm	gpm	m^3/d	°C
6/10/11 8:05 AM	260	245	0.2	0.65	3.54	15.8
6/11/11 7:30 AM	258	245	0.175	0.7	3.82	17.7
6/12/11 9:00 AM	261	255	0.175	0.75	4.09	20.1
6/13/11 7:30 PM	265	255	0.15	0.8	4.36	22.8
6/14/11 7:59 AM	270	260	0.18	0.85	4.63	19.1
6/15/11 1:26 PM	260	252	0.2	0.75	4.09	23.9
6/16/11 8:41 AM	265	255	0.2	0.7	3.82	19.5
6/17/11 8:40 AM	265	255	0.2	0.6	3.27	20.7
6/18/01 9:20 AM	265	259	0.15	0.5	2.73	19
6/20/11 8:24 AM	265	255	0.15	0.48	2.62	17.5
6/21/11 8:42 AM	265	260	0.2	0.5	2.73	17.4
6/21/11 11:26 AM	262	255	0.2	0.4	2.18	21.2
6/22/11 7:55 AM	270	260	0.2	0.5	2.73	18.8
6/22/11 10:13 AM	260	255	0.2	0.38	2.07	21.8
6/24/11 7:43 AM	270	265	0.2	0.45	2.45	21.7
6/24/11 9:58 AM	260	252	0.2	0.4	2.18	22.6
6/28/11 9:05 AM	262	253	0.2	0.27	1.47	20.6
6/29/11 10:01 AM	261	252	0.18	0.3	1.64	25.8
7/2/11 6:00 PM	265	260	0.18	0.55	3.00	
7/5/11 4:34 PM	258	249	0.2	0.69	3.76	25.1
7/6/11 9:37 AM	250	235	0.2	0.6	3.27	24
7/7/11 11:09 AM	261	252	0.2	0.25	1.36	22.5

Date/Time	Feed Conductivity	Feed pH	Concentrate Temp	Concentrate Conductivity	Concentrate pH
	mS/cm		°C	mS/cm	
6/10/11 8:05 AM			22.8		
6/11/11 7:30 AM	6.1		23	24	7.7
6/12/11 9:00 AM	6.05				
6/13/11 7:30 PM	6		26.9	26.4	7.7
6/14/11 7:59 AM			25.1	24.3	7.68
6/15/11 1:26 PM	6.99		30.7	25.2	7.75
6/16/11 8:41 AM	7.13	7.42	26.3	24.7	7.73
6/17/11 8:40 AM	7.01	7.53	28.1	24.1	7.83
6/18/01 9:20 AM	7.26	7.73	26.4	22.4	7.74
6/20/11 8:24 AM	7.22	7.6	25.5	20.9	7.83
6/21/11 8:42 AM	7.14	7.5	25.6	17.81	7.76
6/21/11 11:26 AM	7.01	7.62	29.9	18.03	7.81
6/22/11 7:55 AM	7	7.54	25.8	15.44	7.74
6/22/11 10:13 AM	7.22	7.43	31.7	19.14	7.77
6/24/11 7:43 AM	7.07	7.44	26.7	16.47	7.65
6/24/11 9:58 AM	7.24	7.44	32.2	18.6	7.69
6/28/11 9:05 AM	6.78	7.34	33.3	15.1	7.61
6/29/11 10:01 AM	6.87	7.41	36.9	15.8	7.62
7/2/11 6:00 PM	7.21	7	34	26.7	7.64
7/5/11 4:34 PM	6.87	7.75	31.4	24.5	7.38
7/6/11 9:37 AM	6.88	7.69	29.9	19.92	7.6
7/7/11 11:09 AM	6.68	7.6	34.1	14.01	7.51

Chapter 7

Discussion and Conclusions

7.1 Conclusions

7.1.1 Ions of Interest Can Be Recovered from Higher-Ionic-Strength Solutions Using Ion Exchange

IX is traditionally used to treat low-ionic-strength solutions, and resin selectivity toward multivalent ions is known to decrease with increasing ionic strength. The prediction of selectivity becomes more difficult with increasing solution concentration because of the formation of complexes, decreased ion activity, specific ion interactions, and incomplete hydration (Harland 1994). Results from this research indicate that the decrease in calcium and sulfate selectivity occurring with higher ionic strength up to 0.3 M is not prohibitive to the salt recovery process. Feed solution to the pilot system had an ionic strength of 0.27 M, and a substantial mass of salt was recovered by mixing cation and anion regeneration solutions. As seen from the regression relationship between calcium selectivity, ionic strength, and ionic fraction, calcium selectivity decreases more rapidly with ionic strength than with ionic fraction. Solutions with high ionic fractions of calcium can be treated, provided that the ionic strength remains below 0.35 M (see Figure 7.1). For sulfate, selectivity is correlated with ionic strength by a power relationship. No data were measured for solutions with ionic strength higher than 0.35, so it is difficult to speculate about their effect on sulfate selectivity. However, for solutions with ionic strength less than or equal to 0.35 M, selectivity is sufficient for sulfate recovery and salt precipitation.

		Equivalent Fraction of Calcium																			
		0.05	0.1	0.15	0.2	0.25	0.3	0.35	0.4	0.45	0.5	0.55	0.6	0.65	0.7	0.75	0.8	0.85	0.9	0.95
Ionic Strength	0.05	61.94	48.80	42.45	38.45	35.61	33.44	31.71	30.29	29.09	28.05	27.15	26.35	25.63	24.99	24.40	23.86	23.37	22.92	22.49
	0.1	33.54	26.42	22.98	20.82	19.28	18.11	17.17	16.40	15.75	15.19	14.70	14.27	13.88	13.53	13.21	12.92	12.66	12.41	12.18
	0.15	23.43	18.46	16.05	14.54	13.47	12.65	11.99	11.46	11.00	10.61	10.27	9.96	9.69	9.45	9.23	9.03	8.84	8.67	8.51
	0.2	18.16	14.31	12.45	11.27	10.44	9.81	9.30	8.88	8.53	8.23	7.96	7.73	7.52	7.33	7.15	7.00	6.85	6.72	6.60
	0.25	14.91	11.74	10.22	9.25	8.57	8.05	7.63	7.29	7.00	6.75	6.53	6.34	6.17	6.01	5.87	5.74	5.62	5.52	5.41
	0.3	12.69	9.99	8.69	7.87	7.29	6.85	6.50	6.20	5.96	5.75	5.56	5.40	5.25	5.12	5.00	4.89	4.79	4.69	4.61
	0.35	11.07	8.72	7.58	6.87	6.36	5.98	5.67	5.41	5.20	5.01	4.85	4.71	4.58	4.46	4.36	4.26	4.18	4.09	4.02
	0.4	9.83	7.75	6.74	6.10	5.65	5.31	5.04	4.81	4.62	4.45	4.31	4.18	4.07	3.97	3.87	3.79	3.71	3.64	3.57
	0.45	8.86	6.98	6.07	5.50	5.09	4.78	4.54	4.33	4.16	4.01	3.88	3.77	3.67	3.57	3.49	3.41	3.34	3.28	3.22
	0.5	8.07	6.36	5.53	5.01	4.64	4.36	4.13	3.95	3.79	3.66	3.54	3.43	3.34	3.26	3.18	3.11	3.05	2.99	2.93
	0.55	7.42	5.84	5.08	4.60	4.26	4.01	3.80	3.63	3.48	3.36	3.25	3.16	3.07	2.99	2.92	2.86	2.80	2.74	2.69
	0.6	6.87	5.41	4.71	4.26	3.95	3.71	3.52	3.36	3.23	3.11	3.01	2.92	2.84	2.77	2.71	2.65	2.59	2.54	2.49
	0.65	6.40	5.04	4.39	3.97	3.68	3.45	3.28	3.13	3.01	2.90	2.80	2.72	2.65	2.58	2.52	2.47	2.41	2.37	2.32
	0.7	5.99	4.72	4.11	3.72	3.45	3.24	3.07	2.93	2.81	2.71	2.63	2.55	2.48	2.42	2.36	2.31	2.26	2.22	2.18
	0.75	5.64	4.44	3.86	3.50	3.24	3.04	2.89	2.76	2.65	2.55	2.47	2.40	2.33	2.27	2.22	2.17	2.13	2.09	2.05
	0.8	5.33	4.20	3.65	3.31	3.06	2.87	2.73	2.60	2.50	2.41	2.33	2.27	2.20	2.15	2.10	2.05	2.01	1.97	1.93
	0.85	5.05	3.98	3.46	3.13	2.90	2.72	2.58	2.47	2.37	2.29	2.21	2.15	2.09	2.04	1.99	1.94	1.90	1.87	1.83
	0.9	4.80	3.78	3.29	2.98	2.76	2.59	2.46	2.35	2.25	2.17	2.10	2.04	1.99	1.94	1.89	1.85	1.81	1.78	1.74
	0.95	4.57	3.60	3.13	2.84	2.63	2.47	2.34	2.24	2.15	2.07	2.00	1.95	1.89	1.85	1.80	1.76	1.73	1.69	1.66
	1	4.37	3.44	3.00	2.71	2.51	2.36	2.24	2.14	2.05	1.98	1.92	1.86	1.81	1.76	1.72	1.68	1.65	1.62	1.59

Figure 7.1. Regression relationship of calcium selectivity with ionic fraction and ionic strength.

7.1.2 Breakthrough Curves Can Be Predicted Using Separation Factor Regression Relationships and Modeling

The IX column model was an equilibrium model that worked by discretizing the column into a number of equal volume segments in which resin- and solution-phase ion concentrations were calculated using user-entered separation factors. The numerical dispersion that occurred, based on the number of segments into which the column was divided, was used to model physical dispersion of ions in the column. Because dispersion is modeled by varying the number of column segments, the number of segments used in the model must be empirically calibrated to the behavior of a specific column. Separation factors were generated using the regressions discussed previously. Column efficiency was defined as the fraction of the column that was in equilibrium with the influent solution at breakthrough, and a correlation was found between modeled column efficiency and separation factor. Time to breakthrough was calculated using the model based upon the correlations between influent solution ion concentrations, separation factors, and column efficiency. Calculated results were verified by column tests in the lab. The tools that were developed (MATLAB model and regression relationships) can be used in the future to predict breakthrough curves and resin-phase concentration for any solution falling within the parameters used to create the regressions.

7.1.3 Calcium and Magnesium Selectivity Are Too Similar for Ion Separation by Regeneration

In theory, ions exit the column in the order of reverse selectivity during regeneration, with the least selective ion exiting the column first. Measurements of ion concentrations taken during regeneration of the laboratory scale columns showed that although the peak concentration of magnesium occurred prior to the peak concentration of calcium, the concentration curves overlapped almost entirely (see Figure 7.2). Overlapping peaks are caused by mixing within the column and by the fact that calcium and magnesium have similar separation factors with respect to sodium. All tests in which regeneration conditions were altered by changing flow rate, flow direction, and sodium chloride concentration showed little change in peak characteristics.

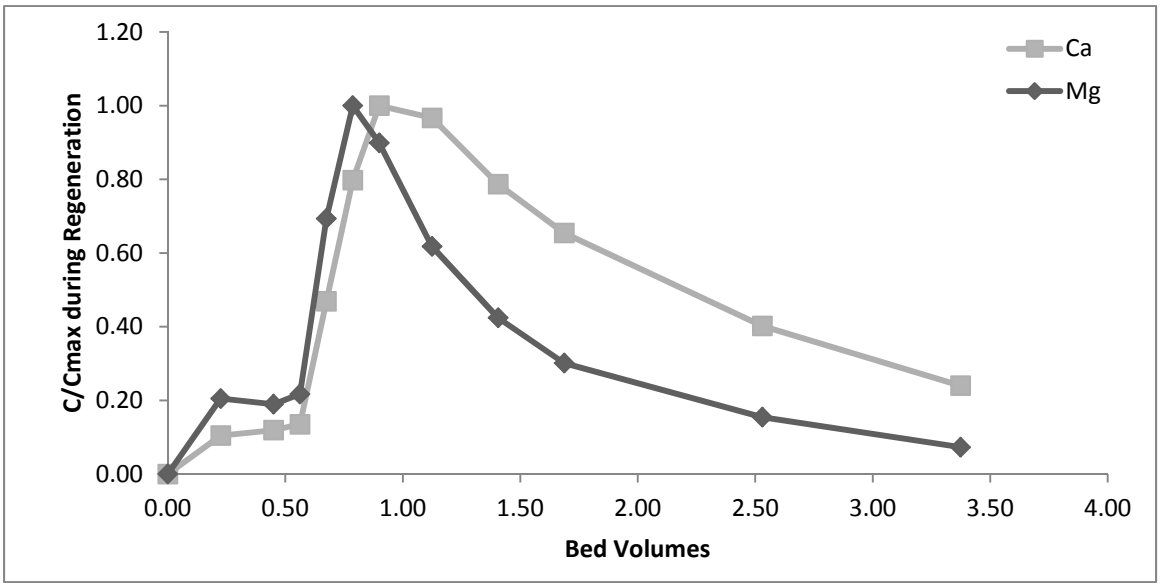

Figure 7.2. Overlapping concentration curves of calcium and magnesium during regeneration.

During loading, ions are thought to distribute within the column in ion-rich zones, with lower-selectivity ions near the bottom of the column and higher-selectivity ions near the inlet. This occurs because when the feed solution initially contacts the resin, there are many open active sites available, and even lower-selectivity ions will exchange. As more high-selectivity ions arrive in the fresh solution, they displace the lower-selectivity ions. Over the length of column, a series of ion-rich zones develop based on selectivity. In theory, it may be possible to elute these accumulation zones separately by isolating them in a partially loaded column. Resin-phase ion concentrations were measured by taking resin samples from a column with ports along its length. It was found that the calcium and magnesium zones overlapped to such a degree that the two could not be separated efficiently. A resin-phase accumulation of magnesium was seen, but it was not very large. When the bottom of the column was regenerated separately, a marked decrease in the ratio of calcium to magnesium was observed, but this technique was not successful in recovering a solution with only one cation.

7.1.4 Gypsum Can Be Recovered from a Mixture of Cation and Anion Regeneration Solutions

Results from mixing both simulated and pilot-generated cation and anion regeneration solutions showed that by controlling the pH at the time of mixing, carbonate salt precipitation can be suppressed. This allows gypsum to be precipitated separately. During the pilot testing, the columns were run to breakthrough of sulfate and near to breakthrough of calcium (Week 6) to maximize the amounts of calcium and sulfate on the resin. The resulting regeneration solution contained more calcium and sulfate than those from the previous weeks. When the most concentrated 30% of the regeneration solutions were mixed under ambient-pH conditions, only gypsum precipitated, because of the increased amount of sulfate present in solution. Maximizing calcium and sulfate concentrations can be accomplished by equalizing the cation and anion exchange capacities. This can be achieved by increasing the volume of the anion exchange column relative to that of the cation exchange column. Results from mixing the most concentrated pilot-generated cation and anion regeneration solutions show that it is possible to recover 0.29 kg of gypsum per cubic meter of treated RO concentrate.

7.2 Discussion

A novel method of concentrate reduction has been proposed and tested. The impacts of improving the management and treatment of RO concentrate could be very powerful. They include driving down the total cost of water production, allowing desalination to be utilized in areas where concentrate management is the limiting factor, increasing total water recovery, and saving energy. The scope of these impacts is wide because water-scarce inland regions can be found across the United States and around the world.

The efficiency of sequential IX for reduction of RO concentrate increases with the ratio of the length of the operation cycle to the length of the regeneration cycle. This research has shown that most exchanging ions can be eluted from a column using 0.75 bed volumes of regeneration solution and 1.00 bed volumes of rinse water. The length of the operation cycle is limited by the influent ion solution concentrations, the dispersion, and the separation factor of the exchanging ion. The efficiency of a specific system can be modeled using the MATLAB equilibrium model and the separation factor regression relationships.

Salt recovery is optimized by increasing column efficiency in terms of the length of the MTZ and the reduction of unused column capacity. Because anion and cation exchange resins generally have different capacities, the system should be optimized to use the full capacity of each column.

In the pilot test, this was done by extending the operation cycle past sulfate breakthrough and diverting the extra effluent to waste. It can also be achieved by increasing the volume of the anion exchange column relative to that of the cation exchange column until the total capacities are equal.

Modeling breakthrough curves is useful in deciding whether the IX process is applicable to a particular solution. The highest possible concentration factor of the regeneration solution relative to the feed solution is the number of bed volumes of operation divided by the number of bed volumes required for regeneration. The concentration factor for a particular ion decreases as the concentration of that ion in the feed solution increases. It will also decrease with increased dispersion and with decreasing separation factor. Modeling will indicate the extent of ion recovery if the separation factors and the amount of dispersion are known. The resin capacity of most common SAC exchange resins is approximately 2.5 eq/L. To maintain a concentration factor greater than 10, the RO concentrate to be treated cannot contain more than 0.25 eq/L of exchanging ion. That corresponds to about 5000 mg/L of calcium. In reality, separation factors are reduced because of high ionic strength and by other ions that are also exchanging with the resin, so the upper limit is slightly lower. If the RO system recovery were at 75%, the raw water could not contain more than 1250 mg/L of calcium. This falls within the range of calcium concentrations for most brackish water sources.

Although it may seem counterintuitive, overall recovery of a system including RO and sequential IX may increase if the RO recovery is reduced to maintain a suitable concentrate for the IX system. If the recovery were reduced to 65%, the raw water could contain up to 1750 mg/L of calcium. A comparison between a RO system at high recovery and a RO system at lower recovery with interstage sequential IX is shown in Figure 7.3. Lower-recovery RO systems also require less energy and less antiscalant. In addition to increased water recovery, there is the added benefit of salt production.

Gypsum and carbonate salts can be spontaneously precipitated from regeneration solutions from a sequential IX system. When the process is optimized, pH adjustment is not necessary for spontaneous precipitation of gypsum. Pilot tests showed that approximately 45% of the calcium and 28% of the sulfate was recovered.

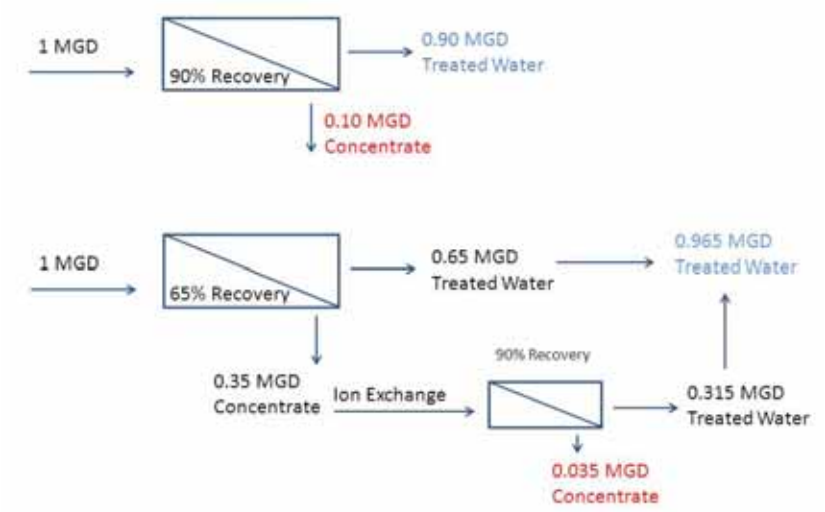

Figure 7.3. Comparison between reverse osmosis system at high recovery and reverse osmosis at lower recovery combined with ion exchange.

References

Ahmed, M.; Arakel, A.; Hoey, D.; Thumarukudy, M. R.;Goosen, M. F. A.; Al-Haddabi, M.; Al-Belushi, A. Feasibility of Salt Production from Inland RO Desalination Plant Reject Brine: A Case Study. *Desalination* **2003,** *158* (1–3), 109–117.

Amara, M. and H. Kerdjoudj Modification of the Cation Exchange Resin Properties by Impregnation in Polyethyleneimine Solutions: Application to the Separation of Metallic Ions. *Talanta* **2003,** *60* (5), 991–1001.

Antony, A.; Low, J. H.; Gray, S.; Childress, A. E.; Le-Clech, P.; Leslie, G. Scale Formation and Control in High Pressure Membrane Water Treatment Systems: A Review. *J. Membr. Sci.* **2011,** *383* (1–2), 1–16.

Benjamin, M. M. *Water Chemistry;* McGraw-Hill: Boston, 2002.

Borba, C. E.; Silva, E. A.; Spohr, S.; Santos, G. H. F.; Guirardello, R. (2011). Application of the Mass Action Law to Describe Ion Exchange Equilibrium in a Fixed-Bed Column. *Chem. Eng. J.* **2011,** *172* (1), 312–320.

Bromley, L. A. (1973). Thermodynamic Properties of Strong Electrolytes in Aqueous Solutions. *AIChE J.* **1973,** *19* (2), 313–320.

Christensen, S. G.; Thomsen, K. Experimental Measurement and Modeling of the Distribution of Solvent and Ions between an Aqueous Phase and an Ion Exchange Resin. *Fluid Phase Equilib.* **2005,** *228–229:* 247–260.

Committee on Advancing Desalination Technology, National Research Council of the National Academies. *Desalination: A National Perspective;* National Academies Press: Washington, DC, 2008.

Crittenden, J. and Montgomery Watson Harza. *Water Treatment Principles and Design;* Wiley: Hoboken, NJ, 2005.

Fogler, H. S. (1999). *Elements of Chemical Reaction Engineering,* 3rd ed.; Prentice-Hall: Upper Saddle River, NJ, 1999.

Gabelich, C. J.; Williams, M. D.; Rahardianto, A.; Franklin, J. C.; Cohen, Y. High-Recovery Reverse Osmosis Desalination Using Intermediate Chemical Demineralization. *J. Membr. Sci.* **2007,** *301* (1–2), 131–141.

Greenlee, L. F.; Testa, F.; Lawler, D. F.; Freeman, B. D.; Moulin, P. The Effect of Antiscalant Addition on Calcium Carbonate Precipitation for a Simplified Synthetic Brackish Water Reverse Osmosis Concentrate. *Water Res.* **2010,** *44* (9), 2957–2969.

Harland, C. E.. *Ion Exchange: Theory and Practice,* 2nd ed.; Royal Society of Chemistry: London, 1994.

Heijman, S. G. J.; Guo, H.; Li, S.; van Dijk, J. C.; Wessels, L. P. (2009). Zero Liquid Discharge: Heading for 99% Recovery in Nanofiltration and Reverse Osmosis. *Desalination* **2009,** *236* (1–3), 357–362.

Helfferich, F. G. *Ion Exchange;* McGraw-Hill: New York, 1962.

Hendricks, D. W. *Water Treatment Unit Processes: Physical and Chemical;* CRC Press: Boca Raton, FL, 2006.

Howe, K. Class notes, University of New Mexico.Unpublished.

Jasbir S, G. A Novel Inhibitor for Scale Control in Water Desalination. *Desalination* **1999,** *124* (1–3): 43–50.

Jordahl, J. *Beneficial and Nontraditional Uses of Concentrate*; WateReuse Foundation: Alexandria, VA, 2006.

Letterman, R. D.; American Water Works Association. *Water Quality and Treatment: A Handbook of Community Water Supplies*; McGraw-Hill: New York, 1999.

Levenspiel, O. *Chemical Reaction Engineering; An Introduction to the Design of Chemical Reactors*; Wiley: New York, 1962.

Marina, M. L.; Rodriguez, A. R.; San Andres, M. P.; Poitrenaud, C. (1992). Ion Exchange in Concentrated Media. Correlations for Variation of Selectivity Coefficients with Medium. *React. Polym.* **1988,** *16* (3): 271–286.

Marton, A.; Inczédy, J. Application of the Concentrated Electrolyte Solution Model in the evaluation of Ion Exchange Equilibria. *React. Polym. Ion Exch. Sorbents* **1988** *7* (2–3): 101–109.

Matsusaki, K.; Hashimoto, N.; Kuroki, N.; Sata, T. Selectivity of Anion Exchange Resin Modified with Anionic Polyelectrolyte. *Anal. Sci.* **1997,** *13* (3), 345–350.

Mehablia, M. A.; Shallcross, D. C.; Stevens, G. W. Prediction of Multicomponent Ion Exchange Equilibria. *Chem. Eng. Sci.* **1994,** *49* (14), 2277–2286.

Melis, S.; Markos, J.; Cao, G.; Morbidelli, M. Multicomponent Equilibria on Ion-Exchange Resins. *Fluid Phase Equilib.* **1996** *117* (1–2), 281–288.

Muraviev, D.; Noguerol, J.; and M. Valiente, M. Separation and Concentration of Calcium and Magnesium from Sea Water by Carboxylic Resins with Temperature-Induced Selectivity. *React. Funct. Polym.* **1996,** *28* (2), 111–126.

Nakamura, K.; Saitoh, T.; Shiga, Y.; Nittami, T.; Matsumoto, K. A Prediction Method for the Breakthrough Curve in the Column Packed with H, Na, NH_4 from Ion Exchange Resins. *J. Chem. Eng. Jpn.* **2010,** *43* (6), 494–501.

Ostroski, I. C.; Borba, C. E.; Silva, E. D.; Arroyo, P. A.; Guirardello, R.; Barros, M. A. S. D. Mass Transfer Mechanism of Ion Exchange in Fixed Bed Columns. *J. Chem. Eng. Data* **2011,** *56* (3), 375–382.

Rahardianto, A.; Gao, J.; Gabelich, C. J.; Williams, M. D.; Cohen, Y. High Recovery Membrane Desalting of Low-Salinity Brackish Water: Integration of Accelerated Precipitation Softening with Membrane RO. *J. Membr. Sci.* **2007,** *289* (1–2), 123–137.

Vo, B. S.; Shallcross, D. C. Multi-Component Ion Exchange Equilibria Prediction. *Chem. Eng. Res. Des.* **2003**, *81* (10), 1311–1322.

Wang, L. K. *Membrane and Desalination Technologies*; Humana Press: New York, 2011.

Wilson, D. J. Modeling of Ion-Exchange Column Operation. I. Equilibrium Model for Univalent-Divalent Exchange. *Sep. Sci. Technol.* **1986,** *21,* 767–787.

Wilson, G. M. Vapor–Liquid Equilibrium. XI. A New Expression for the Excess Free Energy of Mixing. *J. Am. Chem. Soc.* **1964,** *86* (2), 127–130.

Zagorodni, A. A. *Ion Exchange Materials: Properties and Applications,* 1st ed.; Elsevier: Amsterdam, 2007.

Appendix A

Utility Survey

This survey was administered to facilities that currently operate or were planning to operate RO systems. Only nine responses were received. Because the sample size was so small, data analysis was not possible. Completed surveys are available upon request.

1. Operating an RO facility?

CDM and the University of New Mexico are researching methods to selectively recover salts and minerals from the waste stream from desalination facilities. The research is sponsored by the WateReuse Foundation. Separation of salts from the waste stream would also increase water recovery. As part of this project, we are interested in finding out the level of interest in salt recovery by utilities, what benefits might accrue, and what problems would need to be overcome. This survey should only take about 15-20 minutes.

In appreciation for completing this survey, the WateReuse Foundation has agreed to provide respondents with an electronic copy of our final report (due in 2011).

1. Does your utility currently operate a treatment facility using any form of reverse osmosis (reverse osmosis, nanofiltration, membrane softening, etc)?

- ○ Yes
- ○ No

2. Background (operating facilities)

1. What is the name of your utility?

2. What is the name and location of your treatment facility?

3. What membrane process is being used?

- ○ Reverse Osmosis
- ○ Nanofiltration

4. What is source water?

- ○ Seawater
- ○ Brackish Surface Water
- ○ Brackish Ground Water
- ○ Hard Groundwater
- ○ Other (please specify)

5. What is the plant capacity (mgd)?

6. What is the source water TDS (mg/L)?

3. Concentrate management (operating facilities)

1. What is your concentrate flowrate?

2. What is your concentrate TDS (in mg/L)? (Whole number between 0 and 100000)

3. How does your facility dispose of concentrate?

- ☐ Discharge to surface water
- ☐ Discharge to ocean
- ☐ Discharge to sewer/WWTP
- ☐ Deep well injection
- ☐ Evaporation pond
- ☐ Other (please specify)

4. Was your current disposal method the only option considered during design?

- ○ Yes
- ○ No

6. Why was the chosen concentrate disposal option selected?

7. Does your concentrate quality vary – seasonally or on any cycle?

- Yes
- No

If yes, please describe briefly.

8. What is the total capital cost of your facility? (estimate total worth in today's dollars)

9. What percentage of capital costs were dedicated to concentrate management and disposal facilities? (Enter a whole number percentage)

10. What percentage of operating costs are dedicated to concentrate management and disposal issues? (Enter a whole number percentage)

11. What percentage of operator time is dedicated to concentrate management and disposal issues? (Enter a whole number percentage)

4. Planning or designing an RO facility?

1. Is your utility currently planning or designing a treatment facility using any form of reverse osmosis (reverse osmosis, nanofiltration, membrane softening, etc)?

- Yes
- No

5. Background (planning/design)

1. What is the name of your utility?

2. What is the name and location of the treatment facility?

3. What membrane process(es) is being planned? (Check all that apply)

- [ ] Reverse Osmosis
- [ ] Nanofiltration
- [ ] Softening
- [ ] Other (please specify)

4. What is source water?

- ( ) Seawater
- ( ) Brackish Goundwater
- ( ) Brackish Surface Water
- ( ) Hard Groundwater
- ( ) Other (please specify)

5. What is the source water TDS (in mg/L)?

6. What is the projected plant capacity (mgd)?

7. What is the projected capital cost of your facility?

6. Concentrate management (planning/design)

1. What concentrate management and disposal options are being considered (check all that apply)?

- [ ] Discharge to surface water
- [ ] Discharge to ocean
- [ ] Discharge to sewer/WWTP
- [ ] Deep well injection
- [ ] Evaporation pond
- [ ] Other (please specify)

2. Why was the chosen concentrate management option selected?

3. What is your concentrate flowrate?

4. What is your concentrate TDS (in mg/L)? (Enter a whole number between 0 and 100000)

7. Selective recovery and beneficial use

1. Rank the following factors in order of importance with regard to concentrate management and disposal:

	Very important	Important	Slightly important	Not important at all
Capital Cost	○	○	○	○
Operating Cost	○	○	○	○
Minimizing Volume	○	○	○	○
Minimizing Land Use	○	○	○	○
Minimizing Chemical Use	○	○	○	○
Regulatory Restrictions	○	○	○	○
Environmental Concerns	○	○	○	○
Ease of Permitting	○	○	○	○
Sustainability/longevity of Method	○	○	○	○

2. What other factors are important with regard to concentrate management and disposal?

3. If technology was available to recovery salts from the concentrate stream that could be sold (and simultaneously recover more water), how much would you be willing to spend on this technology as a percentage of your total facility cost?

- ○ None
- ○ < 5%
- ○ 5-15%
- ○ 15-25%
- ○ 25-50%
- ○ > 50%

Additional Comments

Appendix B

Salt Market Analysis

FINAL

University of New Mexico

RO Salt Market Analysis Report

University of New Mexico

October 2011

CDM

Contents

Section 1 Desalination Concentrate Market Analysis 133

1.1 Introduction 133

Section 2 Concentrate Disposal and Management 135

2.1 Current Options for Concentrate Disposal 135

2.1.1 Concentrate Disposal Costs 136

2.1.2 Zero Liquid Discharge and Near Zero Liquid Discharge 136

2.2 Characteristics of RO Concentrate 137

2.3 Water Quality from Representative Aquifers 138

2.4 Salt Solubility 140

2.5 Concentrate Products Uses 142

2.5.1 Calcium Carbonate 142

2.5.2 Calcium Sulfate 143

2.5.3 Sodium Sulfate 144

2.5.4 Sodium Carbonate 144

2.5.5 Sodium Chloride 145

2.5.6 Calcium Chloride 146

Section 3 Market Trends and Analysis 147

3.1 Market Descriptions and Trends 147

3.1.1 Calcium Carbonate 147

3.1.2 Calcium Sulfate (Gypsum) 148

3.1.3 Sodium Sulfate 148

3.1.4 Sodium Carbonate (Soda Ash) 149

3.1.5 Sodium Chloride 149

3.1.6 Calcium Chloride 150

3.2 Purity Requirements and Obstacles for Use 151

3.2.1 Calcium Carbonate 151

3.2.2 Calcium Sulfate 152

3.2.3 Sodium Sulfate 152

3.2.4 Sodium Carbonate (Soda Ash) 153

3.2.5 Sodium Chloride 154

3.2.6 Calcium Chloride 155

3.3 Regional Use of Concentrate Products 155

3.4 Regional Markets 156

3.5 Synthetic Salt Production 157

3.6 Market Analysis 158

3.7 Case Studies 160
3.7.1 Case Study 1—Sandoval County, NM 5-MGD Desalination Treatment Facility 161
3.7.2 Case Study 2 - East Cherry Creek Valley Water and Sanitation District Zero Liquid Discharge (ZLD) Pilot Study 162

Section 4 Conclusions and Recommendations 163

References 165

Tables

Table 1 Existing Concentrate/Disposal Minimization Methods 135
Table 2 Evaporation Pond/Deep Well Injection Cost Comparison 136
Table 3 Typical RO Feedwater and Concentrate TDS 137
Table 4 Water Quality Comparison - Ocean Water and Ten Brackish Groundwater Sources in the United States 139
Table 5 Major Cations and Anions in Brackish Groundwater 140
Table 6 General Salt Precipitation Sequence 141
Table 7 Solubility of Candidate Salts for Removal and Recovery 142
Table 8 Calcium Carbonate Pricing 2005 147
Table 9 Domestic Calcium Sulfate Production and Pricing 1999-2009 148
Table 10 Domestic Sodium Sulfate Production and Pricing 1999-2009 148
Table 11 Domestic Sodium Carbonate Production and Use 1999-2009 149
Table 12 Domestic Sodium Chloride Production and Use 1999-2009 150
Table 13 Calcium Chloride Pricing 2005 150
Table 14 Soda Ash Quality 153
Table 15 Regional Brine Market Matrix 157
Table 16 Synthetic Salt Production Summary 158
Table 17 Domestic Production of Selected Salts 2009 159
Table 18 Potential Annual Revenue from the Sale of Recoverable Salts 160

Section 1

Desalination Concentrate Market Analysis

1.1 Introduction

Desalination technologies have been the focus of significant research and treatment evaluations in the United States and worldwide in recent years due to the increasing scarcity of water as an essential resource. Reverse osmosis (RO) membrane, ion exchange, and electrodialysis technologies have been the preferred technical option to create potable water from brackish and saline water sources which contain more than 1,000 milligrams per liter (mg/L) total dissolved solids (TDS). RO, ion exchange, and electrodialysis desalination processes generate significant quantities of concentrate in the range of 10 to 30% of total water treated. The concentrate contains high concentrations of TDS, which are almost exclusively inorganic salts and metals. Concentrate disposal is becoming problematic especially in the desert southwest where the TDS associated with the concentrate stream can have a significant impact on the limited surface water supplies as well as groundwater supplies. The limited capacity of existing surface and alluvial groundwater supplies to handle RO concentrate disposal has resulted in many desalination plants not being built due to a lack of a cost-effective concentrate disposal solution (Mickley, 2006).

Concentrate disposal is also becoming an increasing concern for the planning, management, and operation of water resources due to the increasing cost for permitting and disposal. Consequently, the beneficial use of concentrate is being considered as a possible option to offset some of these economic factors. Access to existing and future salt markets may provide operators of desalination facilities with revenue sources that might compensate for the high operating, transportation, and market access costs.

The purpose of this market analysis is to

1. Identify the primary salts generated from brackish water supplies using RO processes.
2. Evaluate the market potential of these salts in select industries that currently use salt products in the production of other goods.
3. Provide a guide for possible uses of recoverable salts to a utility operating a desalination plant that could offset the cost of RO concentrate disposal.

Section 2

Concentrate Disposal and Management

Currently, typical brackish water RO membranes achieve greater than 98% rejection of all ions, so the concentrate contains a mixture of all the available salts. Using a variety of existing and new technologies, it is technically feasible that RO concentrate brine could potentially be segregated into different types of salts and as either a liquid or a dried product. Previous studies have shown that a range of salts could be obtained from RO concentrate brine (Ahuja and Howe, 2007) depending on the composition of the brackish water supply. Use of these salts would depend largely on the presence of a local or regional market for salt products and meeting the purity requirements for the potential end users.

Currently there are no brackish water RO systems that separate one or several specific salts for beneficial use, and in all cases the composite concentrate is disposed of as a waste product. The selection of a disposal method involves selecting the most economical means of brine disposal. A number of methods currently used for brine and salt disposal are discussed in the following section.

2.1 Current Options for Concentrate Disposal

One of the most significant challenges in both the design and operation of desalination plants is disposing of the brine discharge or salt concentrate waste that is generated in the treatment process. Table 1 presents current methods of concentrate disposal and minimization.

Table 1. Existing Concentrate Disposal/Minimization Methods

Surface Water Discharge
Sewer Discharge
Deep Well Injection
Evaporation Ponds
Wetlands Developments
Thermal Mechanical Evaporation Near Zero Liquid Discharge
Spray Dryers and Crystallizers Zero Liquid Discharge

Selection of the most feasible and cost-effective method of disposal is site-specific, as there are a number of factors that must be considered, such as

- Flow and water quality in potential receiving water
- Local restrictions on discharges to a wastewater treatment plant (WWTP)
- Suitable geology for deep well injection
- Cost of land
- Climatic limitations (solar ponds and evaporation ponds)
- Concentrations of constituents in concentrate (land application)

Most of the existing large municipal brackish water RO plants are located in Florida and California and the most common methods of disposal in these locations are sanitary sewers, surface water discharge, and deep well injection (Jordahl, 2006). Common disposal methods for inland desalination plants are deep well injection, evaporation ponds, sanitary sewers, and land application.

2.1.1 Concentrate Disposal Costs

Recent trends in concentrate disposal showed more plants discharging to sanitary sewers and deep well injection than to surface water or evaporation ponds (Jordahl, 2006). In the case of inland brackish water treatment plants where disposal to a surface water body is not possible, deep well injection and evaporation ponds are the two most common disposal options. Deep well injection, where possible, is a lower-cost alternative than evaporation ponds, which are more expensive due to their large land requirements and high distribution piping costs. However, deep well injection is not viable in all instances, as many areas of the country do not have suitable geologic conditions. Deep well injection is generally applicable for disposal of larger volumes of concentrate where economies of scale make this option more affordable (Mickley, 2004).

A comparison of the disposal costs associated with evaporation ponds and deep well injection for the Kay Bailey Hutchinson Desalination Plant in El Paso (CDM, 2006) is presented in Table 2.

Table 2. Evaporation Pond/Deep Well Injection Cost Comparison[1]

Option	Cost[2]
Evaporation Pond	$41,000,000
Deep Well Injection[3]	$6,500,000

[1] 18 MGD Treatment Plant, 3.2 MGD concentrate production
[2] In 2005 dollars
[3] Three Class I wells drilled to 4300 feet

2.1.2 Zero Liquid Discharge and Near-Zero Liquid Discharge

Zero liquid discharge (ZLD) and near-zero liquid discharge processes are high-recovery processes that reduce RO concentrate to slurry (near-zero liquid discharge) or a solid (zero liquid discharge) for disposal in a landfill. These processes consist of thermal evaporators, crystallizers, and spray dryers. The capital operations and maintenance costs of these processes are significantly influenced by the energy required to operate the process, and typically the capital cost is increased to add heat exchangers and multiple effects to reduce the amount of energy required. ZLD processes have mainly been used in industrial applications and generally have not been used at the scale of a municipal water treatment

plant (CDM, 2009). The primary purpose of ZLD has been to reduce the volume of concentrate and increase water recovery. Although it is possible to extract some commercially usable salts from ZLD processes, a much more complicated ZLD process is required to eliminate the impurities that affect the marketability of the salts (CDM, 2009).

A ZLD processing scheme developed by Geo-Processors USA, Inc. has been successfully pilot-tested outside the United States to recover commercial grade salts from many different waters. This technology involves a series of volume reduction steps followed by a salt recovery step. The results of the testing are proprietary, and commercial viability has not been demonstrated in the United States (Mickley, 2008).

ZLD processes, as well as other processes (RO, nanofiltration, and ion exchange) that concentrate waste solutions and isolate salts, are important for selective salt recovery. Treatment steps such as pH adjustment, chemical addition, thickening, and washing may also be required. A selective salt recovery process would involve a series of concentration and treatment steps to obtain an individual salt in its desired form. If multiple salts were recovered, the process might involve a series of concentration and treatment steps that would recover the salts sequentially from the lowest to the highest solubility. However, a discussion of the composition of RO concentrate, the major ions found in brackish groundwater, and the solubility of the recoverable salts is essential to understand the process and limitations of obtaining usable salts from RO concentrate.

2.2 Characteristics of RO Concentrate

RO concentrate has constituents similar to those of the raw feed water, except that much of the water has been removed. Thus the concentrations of the constituents in concentrate from a typical RO process are four to six times greater than in the feed water. In seawater desalination, sodium chloride is the primary salt, and in brackish water desalination, a mixture of calcium, magnesium, sulfates, and carbonates is concentrated along with sodium chloride and trace elements.

Typical TDS concentrations in RO feed water and in concentrate are presented in Table 3.

Table 3. Typical RO Feedwater and Concentrate TDS[1]

Process	Feedwater TDS (mg/L)	Concentrate TDS (mg/L)	Concentration Factor
Seawater RO	32,000–45,000	50,000–80,000	1.7–2.5
Brackish Water RO	1,000–10,000	3,000–40,000	2.9–6.7

1. Adapted from Jordahl, 2006

The amount of concentrate generated by an RO plant can vary throughout the year. Concentrate production generally peaks in the summertime, when water demand and production are high, and is much less in the winter, when water demands are lower. The seasonal fluctuations in concentrate production are a significant factor in the marketability of recoverable salts.

2.3 Water Quality from Representative Aquifers

Ahuja and Howe (2007) compared water quality data from ten representative aquifers located around the United States with that of ocean water. This comparison is presented in Table 4.

Table 4. Water Quality Comparison—Ocean Water and Ten Brackish Groundwater Sources in the United States[1]

State		Alabama	Arizona	California	Colorado	Florida	New Mexico	New York	Ohio	Texas	Wyoming
County		Montgomery	Maricopa	Orange	Mesa	Palm Beach	Tularosa Basin	Niagara	Tuscarawas	Bexar	Carbon
Source	**Ocean Water**	Single Well	Median	Median	Median	Median	Single Well	Single Well	n/a	Median	Single Well
Parameter (mg/L)											
Sodium	10,500	230	210	717	935.5	1,010	125	1,010	12.4	455	1,260
Potassium	380	2.0	5.6	5.19	10.65	36	85	30.9	11	26.9	2.26
Calcium	400	520	340	282	285.5	124	650	643	374	543	40.3
Magnesium	1,350	4.4	90	116	272	131	120	192	201	195	27.4
Strontium	8	n/a	2.7	2.09	n/a	13.6	n/a	n/a	3	n/a	0.94
Barium	0.03	0.03	0.1	0.045	0.016	n/a	0.13	n/a	n/a	6	0.006
Chloride	19,000	110	650	349	473	1,760	180	1,470	2.6	874.5	118
Sulfate	2,700	1,100	380	1,180	2,830	350	1,350	2,180	2,210	1,710	2,580
Carbonate	140	430	390	1,130	507.5	152	350	506	60.5	283.5	134
Fluoride	1.3	0.7	0.4	0.4	0.85	0.8	1.53	n/a	0.2	2.7	0.18
Nitrate	1.8	0.1	13	0.05	n/a	n/a	0	n/a	0.05	n/a	0.004
Silica	3	26	63.1	23.5	19.25	14	15	n/a	13.2	18.8	9.32
Alkalinity	n/a	350	320	929	416	152	350	506	60.5	240	134
TDS	33,484	2,400	2,138	3,805	5,334	3,591	2,877	6,032	2,887	4,115	4,172

[1] Ahuja and Howe (2007)
n/a = data not available

As shown in Table 4, the predominant cation in ocean water is sodium and the predominant anion is chloride, so that 85% of the salinity of ocean water is made up of sodium chloride. Brackish groundwater contains other major and minor cations and anions in addition to sodium chloride, which are listed in Table 5.

Table 5. Major Cations and Anions in Brackish Groundwater

Cations	Anions
Sodium	Sulfate
Calcium	Chloride
Magnesium	Carbonate

It is important to note that of these major anions, carbonate can be present as bicarbonate or carbonate. However, bicarbonate is the main carbonate species in virtually all natural waters. Sulfate can be more common in groundwater than chloride (Ahuja and Howe, 2007).

There are also minor cations in brackish groundwater, such as ferrous iron and manganese, and minor anions, such as fluoride, phosphate, and nitrate. These ions account for less than one% of the ions in water and are of minimal interest, because the focus of this study is the recovery of commercial quantities of salts that may have significant value.

2.4 Salt Solubility

The solubility of salts associated with the major and minor cations is an important consideration in the beneficial use of RO concentrate. Solubility is a measure of how difficult it is to recover a specific salt. Generally a salt with a low solubility is easier to recover than a salt with a high solubility using a fractioning process. This may not be the case using a membrane separation process, since the selectivity of the membrane controls the fractionization process. Ahuja and Howe (2007) evaluated the solubility of major cation and anion salts and found that chloride salts and sodium salts are highly soluble and calcium and magnesium salts that do not contain chloride are considerably less soluble. The same study also noted that the solubility of carbonate and hydroxide species is pH-dependent. Solubility increases as pH decreases, and calcium carbonate and magnesium hydroxide precipitate at high pH.

The solubility of the salts produced in the RO process is important, as salts precipitate in the sequence of their solubility. The RO process is affected by the precipitation of sparingly soluble salts. Thermal brine concentrators, which can be used to process concentrate, are affected by moderately soluble salts such as sodium carbonate and sodium sulfate. Crystallizers precipitate sodium carbonate, sodium sulfate, and sodium chloride, but have a waste stream for highly soluble salts such as calcium chloride and magnesium chloride (Mickley, 2008). A general sequence of salt precipitation in the RO process is presented in Table 6.

Table 6. General Salt Precipitation Sequence

Solubility Level	Salt
Low soluble salts	Calcium carbonate, calcium sulfate
Moderately soluble salts	Sodium carbonate, sodium sulfate
Soluble salts	Sodium chloride
Highly soluble salts	Calcium chloride, magnesium chloride

Ahuja and Howe (2007) identified four candidate salts for removal and recovery for beneficial use based on their solubility. Two additional salts from that study, calcium chloride and sodium carbonate, have been added to this report as potentially marketable salts. These salts and their solubilities and factors regarding their recovery are presented in Table 7.

Table 7. Solubility of Candidate Salts for Removal and Recovery

Salt	Solubility (mg/L)	Factors Regarding Recovery
Calcium carbonate	6.6	Sparingly soluble. Removal could be controlled by raising the pH, which increases the carbonate concentration in RO concentrate.
Calcium sulfate	2,050	Sparingly insoluble. Solubility not dependent on pH. May be possible to control separation of calcium sulfate from other carbonate and hydroxide compounds if separation occurred at low pH.
Sodium sulfate	281,000 (28% solution)	Moderately soluble. In some waters the amount of calcium is insufficient to remove the sulfate. Sodium sulfate would need to be removed in these waters to adequately remove sulfate present in the concentrate.
Sodium carbonate	307,000 (30% solution)	Moderately soluble. May be difficult to precipitate sodium carbonate as a dry salt.
Sodium chloride	360,000 (36% solution)	Very soluble. May be difficult to concentrate RO concentrate to precipitate sodium chloride as a dry salt. If substantial amounts of sulfate and carbonate are removed with calcium, then chloride will remain for pairing with sodium.
Calcium chloride	813,000 (81% solution)	Extremely soluble. May be difficult to concentrate RO concentrate to precipitate calcium chloride as a dry salt.

Ahuja and Howe (2007) suggest that by focusing on these calcium and sodium salts, 85 to 95% of the mass of dissolved solids in the concentrate could potentially be separated and marketed. The uses of these recoverable salts are presented in the following section.

2.5 Concentrate Products Uses

2.5.1 Calcium Carbonate

Calcium carbonate exists in three polymorphic crystalline forms: calcite, aragonite, and vaterite. Calcite is by far the most abundant of these forms and is one of the most abundant minerals on earth, making up about 4% of the earth's crust. It is also the most stable form of calcium carbonate. The main source of calcium carbonate is the mining of limestone, which is currently mined in all regions of the United States.

Calcium carbonate is commercially available as ground calcium carbonate (GCC) or as precipitated calcium carbonate (PCC). GCC is processed natural calcium carbonate and has impurities that result in a lower brightness. PCC is a white powder that is typically 99% pure and is produced using mechanical segregating processes to remove impurities, followed by one of three chemical processes: the Solvay process, a byproduct of caustic soda production, and through the recarbonizing process. Out of the 15 million tons of calcium carbonate

produced in 2005, almost 75% was GCC and the remaining 25% was PCC (Ahuja and Howe, 2007). In 2006, almost 90% of the PCC produced was used by the paper industry.

Significant end-uses and industrial applications for calcium carbonate include

- Pulp and paper
- Building construction (marble floors, roof materials, and roads)
- Glass (improves chemical durability)
- Rubber (mainly PCC)
- Paint (extend resin and polymers and control texture)
- Plastic (PVC pipe, mainly GCC)
- Dietary supplement (antacids)
- Water treatment (pH control, softening)

2.5.2 Calcium Sulfate

Calcium sulfate can exist in three crystalline forms: $CaSO_4$ (anhydrite), $CaSO_4$-$1/2H_2O$ (hemihydrite or basanite), and $CaSO_4$-$2H_2O$ (dihydrite or gypsum). Calcium sulfate is obtained through the mining of gypsum. Gypsum is mined in 29, states with 77% of the production taking place in 8 states: Oklahoma, Arkansas, Iowa, California, Nevada, Texas, Indiana, and Michigan (Kostick, 2008).

Gypsum is processed (calcined or uncalcined) depending on its final use. Most gypsum that is produced (about 75%) is calcined before use and the remaining 25% remains uncalcined. The calcination process involves grinding gypsum to no less than 100 mesh and then heating it to drive off excess water. Calcination produces the hemihydrite form of calcium sulfate, which is then mixed with other ingredients to make wallboard and plaster. Uncalcined gypsum is used in cement and in agriculture.

In 2009, 95% of the gypsum consumed in the United States was used for wallboard plaster products and cement. The remaining 5% was used for agricultural uses, and a small amount of high purity gypsum was used for industrial processes (glass making and smelting). Gypsum waste generated by wallboard manufacturing, installation, and building demolition can be recycled for use in agriculture and to manufacture new wallboard. Other potential markets for recycled wallboard include athletic field marking, cement production as a stucco additive, grease adsorption, sludge drying, and water treatment (Crangle, 2010).

Synthetic calcium sulfate is also manufactured from a process called flue gas desulfurization, which removes sulfur dioxide from power plant emissions to prevent acid rain. Flue gas

desulfurization is a wet scrubbing process that produces calcium sulfite. A subsequent oxidation process converts calcium sulfite into calcium sulfate (synthetic gypsum), which can then be sold to wallboard manufacturing facilities.

2.5.3 Sodium Sulfate

Sodium sulfate has two common crystalline forms, anhydrous sodium sulfate (Na_2SO_4) and sodium sulfate decahydrate ($Na_2SO_4 \cdot 12H_2O$). It can also be produced from natural deposits or synthetically manufactured. Natural sodium sulfate is produced in the United States by two production facilities, one in California and one in Texas. Natural sodium sulfate is mined from deposits of dry lake beds or directly from brine lakes. Synthetic sodium sulfate is produced by using waste products from other chemical manufacturing processes, such as battery reclamation and cellulose production (Kostick, 2010).

According to Kostick (2010), the primary use of sodium sulfate is powdered detergents, with 35% of the sodium sulfate produced in 2009 being used for this purpose. The remaining uses are

- Glass (18%)
- Pulp and paper (15%)
- Textiles (4%)
- Carpet freshener (4%)
- Miscellaneous (24%)

2.5.4 Sodium Carbonate

Sodium carbonate, or "soda ash," either is produced by mining or is synthesized similarly to calcium chloride as another product in the Solvay process. Over 85% of soda ash comes from Wyoming, with the remaining 15% coming from the Searles Valley, California.

According to Kostick (2010), the main uses of soda ash are

- Glass production (48%)
- Chemicals (29%)
- Soap and detergents (10%)
- Pulp and paper (2%)
- Water treatment (2%)
- Flue gas desulfurization (2%)

2.5.5 Sodium Chloride

Sodium chloride is one of the most widely used inorganic feedstocks in chemical manufacturing and has many uses. Sodium chloride in all of its chemical permutations has over 14,000 applications. The major uses of sodium chloride in 2009 information provided by Kostick (2010) are

- Roadway deicing (43%)
- Chemical industry (35%)
- Distributors (8%)
- Agriculture and food (3% each)
- Water treatment (3%)

It should be noted that salt in brine form represented 90% of the salt used for feedstock in the chemical industry (Kostick, 2010).

Sodium chloride is produced by four methods:

1. Surface or underground mining of rock salt
2. Solar evaporation of seawater or brines
3. Mechanical evaporation of purified brine feedstock
4. Production of salt brine by solution mining of underground halite deposits

Sodium chloride is available in a dry form (rock salt or flake salt) and in brine form. Salt obtained from underground mining, solar evaporation, and mechanical evaporation produces a dry salt. Salt produced by solution mining is used in a brine form and is not evaporated to form a dry salt. Brine obtained from solution mining is used in the chlor-alkali industry, which produces chlorine and sodium hydroxide. Domestic sources of rock salt and salt from brine are located in the northeast, western, and southern gulf states.

An average of 40% of sodium chloride used in the United States is used for road deicing. Approximately 18 million tons of rock salt and brine is used annually by municipalities to prepare roads for motor traffic. The demand is heavily driven by weather conditions and has also recently been affected by the reduced financial resources of many cities and towns. Geographically, most of the demand is generated in the northeast and midwest United States, the Great Lakes area, and the state of Alaska. However, it is also used in the colder climates and higher elevations of the western United States, where snow and winter road conditions are common.

2.5.6 Calcium Chloride

Calcium chloride is a white crystalline salt and is very soluble in water. It is produced by refining naturally occurring brine, by neutralizing hydrochloric acid with limestone, and as a by–product of the Solvay process used to produce synthetic sodium carbonate (soda ash). Extremely pure calcium chloride products can be produced using the limestone–hydrochloric acid process if the hydrochloric acid purity is sufficient. In the United States, production of calcium chloride is carried out by concentrating and purifying brines from salt lakes. Calcium chloride produced from natural brine lakes is not as pure as calcium chloride produced from the Solvay process or from the limestone–hydrochloric acid process. Calcium chloride produced as a by-product of the Solvay process is a 10 to 15% solution that contains a percentage of sodium chloride. This stream is then purified using the methods used for natural brines.

Commercial products are supplied in dry form as powders, flakes, and pellets and in liquid form as a 30 to 45% solution. The main uses of calcium chloride are

- Deicing/road stabilization
- Dust control
- Oil extraction and completion fluids
- Accelerator in concrete
- Industrial processing
- Plastics manufacturing

Section 3

Market Trends and Analysis

This section presents a description of the existing markets for the concentrate salts discussed in Section 2. This section also presents purity requirements for use, a matrix of regional markets, and an analysis of the marketability of the salts.

3.1 Market Descriptions and Trends

This section presents a market analysis for each of the six salts discussed in Section 2. The market analysis contains production information, pricing, uses, and a discussion of the market trends and issues associated with each of the salts.

3.1.1 Calcium Carbonate

Information on the domestic production and consumption and the average price of calcium carbonate in five-year increments for the period 1999 to 2009 was not available from USGS Mineral Commodity Summaries. Extensive research into price trends and production and consumption trends indicated that prices and production of calcium carbonate are proprietary and cannot be obtained without subscribing to a reporting service. However, pricing information from 2005 was available from a WateReuse Foundation study (Jordahl, 2006) and is presented in Table 8.

Table 8. Calcium Carbonate Pricing 2005

Type	Price ($/Ton)
Ground, Dry Coarse	$60–$65
Ground, Dry Medium	$95–$100
Ground, Dry Fine	$230–$280
Precipitated	$264–$350

3.1.2 Calcium Sulfate (Gypsum)

Domestic calcium sulfate (gypsum) production and demand and price history in five year increments for the period 1999 to 2009 are presented in Table 9.

Table 9. Domestic Calcium Sulfate Production and Pricing 1999 to 2009[1]

	1999	2004	2009
Production (thousand tons)			
Crude	21,400	19,800	10,400
Synthetic	3,600	12,100	8,500
Calcined	22,700	28,100	15,400
Consumption (thousand tons)	35,000	43,000	23,100
Average Price (per ton)			
Crude	$6.92	$6.90	$7.71
Calcined	$17.02	$20.00	$36.29

[1]Crangle, 2000, 2005, 2010

***Market trends*—**Demand for gypsum depends on the strength of the construction industry since almost 95% of the gypsum consumed is for construction products such as wallboard, plasters, and cement. Wallboard plants that use synthetic gypsum will reduce the use of natural gypsum. The US has adequate domestic resources but they are unevenly distributed, resulting in imports from Canada and Mexico. Synthetic gypsum generated by industrial processes is an important substitute for mined gypsum and in 2009 synthetic gypsum made up 57% of the total domestic supply (Crangle, 2010).

3.1.3 Sodium Sulfate

Domestic sodium sulfate production and demand and price history in five-year increments for the period 1999 to 2009 is presented in Table 10.

Table 10. Domestic Sodium Sulfate Production and Pricing 1999 to 2009[1]

	1999	2004	2009
Production (thousand tons)	650	470	330
Consumption (thousand tons)	580	360	310
Average Price (per ton)	$114	$114	$127

[1]Kostick, 2000, 2005, 2010

Market trends—The primary market for sodium sulfate is powdered detergents, where it serves as a low-cost inert white filler. However, the market is increasing toward liquid laundry detergents that do not contain sodium sulfate. The major market for powdered detergents containing sodium sulfate is in Asia and Latin America. Sodium sulfate use in the textile industry has also been decreasing due to imports of less expensive textile products.

Sodium sulfate resources are adequate to last hundreds of years at the rate of current consumption. Sodium sulfate can also be obtained as a by-product of battery recycling and the production of chemicals such as boric acid, chromium chemicals, rayon, and cellulose. Sodium hydroxide and emulsified sulfur can be substituted for sodium sulfate in the pulp and paper industry (Kostick, 2010).

3.1.4 Sodium Carbonate (Soda Ash)

Domestic sodium carbonate (soda ash) production and demand and price history in five-year increments for the period 1999 to 2009 is presented in Table 11.

Table 11. Domestic Sodium Carbonate Production and Use 1999 to 2009[1]

	1999	2004	2009
Production (thousand tons)	11,100	11,900	12,000
Consumption (thousand tons)	7,300	6,900	6,700
Average Price (per ton)	$117.50	$117.50	$272.50

[1]Kostick, 2000, 2005, 2010

Market Trends—The soda ash industry suffered in 2009 because of the recession. The two main suppliers in the United States reduced outputs for most of the year, mostly due to increased competition from China. However, overall worldwide demand is expected to grow 1.5 to 2% per year over the next several years.

There appears to be adequate reserves of soda ash in the Green River and Searles Lake mines to last for many years. There are also many other sources in the world that have yet to be quantified. It is possible to manufacturer synthetic soda ash from salt and limestone but it is more costly to produce and creates hazardous wastes (Kostick, 2010).

3.1.5 Sodium Chloride

Domestic sodium chloride production and demand in five-year increments for the period 1999 to 2009 are presented in Table 12.

Table 12. Domestic Sodium Chloride Production and Use 1999 to 2009[1]

	1999	2004	2009
Production (thousand tons)	45,600	49,700	50,700
Consumption (thousand tons)	53,900	59,400	62,700
Average Price Dry salt, bulk, $/ton			
Vacuum	$110	$122	$165
Solar	$40	$55	$67
Rock	$19	$24	$35
Brine	$6	$7	$8

[1]Kostick, 2000, 2005, 2010

Market Trends—Table 12 indicates that more salt is consumed than is produced. The balance is made up from imports, which make up 19% of the salt consumed. The market for road salt has been impacted by state and local budget constraints due to the recession. This may affect the availability and consumption of rock salt for deicing in 2010.

World salt resources are practically unlimited and salt from the oceans is inexhaustible. Sources of rock salt and salt from brine are in the Northeast, Central Western, and Gulf Coast states and saline lakes and solar evaporation facilities are located near populated regions in the western United States. There are no economic substitutes for sodium chloride. Calcium chloride, calcium magnesium acetate, and potassium chloride can be used for deicing and in other processes, but at a higher cost (Kostick, 2010).

3.1.6 Calcium Chloride

Information on the domestic production and consumption and the average price of calcium chloride in five-year increments for the period 1999 to 2009 was not available from USGS Mineral Commodity Summaries. Extensive research into price trends and production and consumption trends indicated that prices and production of calcium chloride are proprietary and cannot be obtained without subscribing to a reporting service. However, pricing information from 2005 was available from (Jordahl, 2006) and is presented in Table 13.

Table 13. Calcium Chloride Pricing 2005

Type	Price ($/Ton)
Conc. Reg 77–80%	$200
Conc. Reg 77–80% flake	$250–$280
Anhydrous 94–97% bulk	$275
Anhydrous 94–97% 50 lb	$346–$354
Liquid 35% basis	$135–$153
Liquid 45% basis	$160–$175

3.2 Purity Requirements and Obstacles to Use

3.2.1 Calcium Carbonate

Purity Requirements

Purity requirements for the uses of calcium carbonate vary depending on the use and whether it is GCC or PCC. Purity requirements for GCC and PCC used for industrial applications are listed here:

GCC [11]

- Purity as $CaCO_3$—Minimum 96%
- Calcium carbonate content—96%
- Silica as SiO_2—Maximum 0.3% by weight
- Magnesium oxide (MgO)—Maximum 0.5% by weight
- Sulfate—Maximum 0.3% by weight
- Chloride—Maximum 0.1% by weight
- Iron, Aluminum, Phosphate—Maximum 0.5% by weight
- Sodium oxide (Na_2O)—Maximum 0.2% by weight

PCC [1]

- Purity as $CaCO_3$—Minimum 96%
- Calcium carbonate content—96%
- Silica as SiO_2—Maximum 0.3% by weight
- MgO—Maximum 0.5% by weight
- Sulfate—Maximum 0.3% by weight
- Chloride—Maximum 0.1% by weight
- Iron, Aluminum, Phosphate—Maximum 0.1% by weight
- Na_2O—Maximum 0.2% by weight

Obstacles to Use

Calcium carbonate is mined and used in the dry state. Opportunities for direct use of calcium carbonate brine appear to be limited, and brine solutions are not expected to have widespread marketability. However, calcium carbonate is very insoluble and can be precipitated from RO concentrate by increasing the pH. It may be possible to precipitate calcium carbonate from the concentrate for use as a dry material. Precipitated calcium carbonate (PCC) from RO concentrate would have to meet the purity requirements for PCC that is currently obtained through the Solvay process.

[1]Adapted from http://www.famousminerals.net)

3.2.2 Calcium Sulfate

Purity Requirements

- The ASTM standard for gypsum (ASTM C-22) requires that gypsum shall not contain less than 70% by weight of $CaSO_4 \cdot 2H_2O$. Silica and sodium chloride should not be more than 6% and 0.01% by weight, and it should also be free from clayey material.
- Gypsum with a purity of 75 to 85% is used in cement manufacturing, but a minimum of 82% is preferred.
- Gypsum used for plaster of Paris requires purity ranging from 80 to 97%.
- Gypsum of 75% purity and below is used as manure or sweet lime.
- Gypsum used in wallboard is negatively affected by certain salts. The maximum content of Na_2O, K_2O, and Mg_2O in wallboard is 0.3% by weight and the maximum concentration of chloride in gypsum in 100 ppm (Ahuja & Howe, 2007).

Obstacles to Use

Calcium sulfate is mined and used in the dry state, and opportunities for use of sodium sulfate brine appear to be limited. Calcium sulfate obtained by precipitation from a brine solution would have to meet the purity requirements for wallboard, which limit the amounts of other salts, chlorides, and silica that can be present in the gypsum precipitate. In addition, the direct use of brine in the production of concrete would be severely limited by the presence of other ions in the brine. Chlorides in the brine may not be desirable and excess gypsum added to the cement could make the setting time excessively long.

A potential direct use of the brine would be direct irrigation to improve the quality of soil. Salt-affected (sodic) soils in the southwest United States have very low infiltration rates and surface crusting and do not support agriculture. This results in water loss to the local area, as rainwater does not enter groundwater pathways (Jordahl, 2006). Gypsum is currently used for remediation of sodic soils, which suggests that calcium sulfate brine applied to the soil could be used to improve the quality of the soil. However, direct irrigation using RO concentrate presents a series of challenges, as the volume of concentrate produced may exceed the available land and the cost to haul the concentrate to the application area may be high. Also, irrigation with RO concentrate would be subject to regulatory requirements and concerns about potential groundwater impacts.

3.2.3 Sodium Sulfate

Purity Requirements

The main use of sodium sulfate is in powdered laundry detergent. Purity requirements for sodium sulfate used for detergent and dye chemicals have the following specifications[2]:

- Sodium sulfate > 99% by weight
- Calcium, magnesium < 0.15% by weight
- Iron < 0.002%

[2] http://made-in-china.com/showroom/shengongchem/product

- Moisture < 0.2%
- Water insoluble < 0.05%
- Whiteness > 85%

Purity requirements for other uses were not available.

Obstacles to Use

Sodium sulfate is highly soluble and is commonly used in a dry form. The major market for sodium sulfate for detergents is in Asia and Latin America, which limits the potential domestic use of sodium sulfate produced from RO concentrate. In the pulp and paper industry, the use of sodium-emulsified sulfur and caustic soda can replace sodium sulfate.

The market analysis presented in Section 3.1 indicated that there are more than adequate reserves of naturally occurring sodium sulfate that are expected to last for many years. Sodium sulfate can also be obtained by recycling car batteries and as a byproduct of other industrial products. Isolating and recovering sodium sulfate from RO concentrate may be difficult and costly, and with plentiful supplies of lower-cost sodium sulfate available, and a limited domestic marketplace, there does not appear to be a market for sodium sulfate produced from RO concentrate.

3.2.4 Sodium Carbonate (Soda Ash)

Purity Requirements

Soda ash is usually supplied in Grades A and B, which are more than 99% pure. Soda ash with a bulk density greater than 0.8% is called dense soda ash. The purity requirements for Grades A and B natural soda ash produced in the United States are presented in Table 14.

Table 14. Soda Ash Quality[1]

Composition	Grade A	Grade B
Na_2CO_3	99%	99.80%
$NaHCO_3$	-	-
NaCl	0.03%	0.02%
Na_2SO_4	0.07%	0.02%
Fe_2O_3	0.0006%	0.0005%
NaF	0	0
H_2O Insol	0	0

[1]http://www.ndctz.com/sodaash.html

The main use of sodium carbonate is glass production. Glass production requires a dense pure soda ash that is free of chloride and iron impurities. Dense soda ash is also used in water treatment applications because of its handling characteristics. It has little dust and good flow characteristics. It is typically used to increase the pH in water treatment processes.

Obstacles to Use

Sodium carbonate is more soluble than sodium sulfate and may be more difficult to obtain from RO concentrate than other salts because of the necessity to raise the pH to precipitate it. It is commonly used in the dry form, which means that direct use of the brine is not possible. Extraction of sodium carbonate from concentrate is likely to be difficult and expensive and may not prove to be economical.

3.2.5 Sodium Chloride

Purity Requirements

Brine is used in the chlor-alkali industry to produce chlorine and sodium hydroxide. Most salt brine is produced by the same companies that use it. However, some chlor-alkali producers purchase brine from independent supply companies, and in some cases brine is produced by a chemical company that uses some of it and sells the rest to a neighboring chemical company (Kostick, January 2010).

The production processes used to generate chlorine and sodium hydroxide require brine free of sulfate, calcium, magnesium, barium, and metals that would affect the electrolytic process. Many of the processes used to generate chlorine and sodium hydroxide have a brine pretreatment process to remove impurities before the electrolytic process. Brines used in these processes typically have low concentrations of calcium and magnesium, which allow the use of an ion exchange pretreatment process. Brackish water used for municipal water supplies typically has high concentrations of calcium and magnesium, which would require softening the concentrate before it could be sent to a chlor-alkali plant.

Rock salt is used in on-site sodium hypochlorite generating systems. Rock salt used in this process must meet the following purity requirements[3]:

- Sodium chloride—96%
- Calcium sulfate—0.3% maximum
- Magnesium chloride—0.06%
- Calcium chloride—0.1%
- Magnesium sulfate—0.02% maximum
- Insolubles—0.1% maximum
- Metals (lead, copper, iron)—0.007% maximum
- Fluoride—0.002% maximum

ASTM D632 specifies a minimum sodium chloride content of 95% for sodium chloride used for road salt but does not specifically discuss impurities.

Obstacles to Use

Sodium chloride has many uses and offers possibilities for extraction and/or use of the RO concentrate. On the other hand, it is extremely soluble, which increases the difficulty of concentrating the RO concentrate to precipitate sodium chloride as a dry salt. Dry salt is commonly extracted from brine

[3]Severn Trent Services, 2010

through solar evaporation and mechanical evaporation of purified brine feedstock. These processes suggest that it is possible to obtain dry salts from RO concentrate/brine.

As previously discussed, brine is used directly in the production of chlorine and sodium hydroxide. However, both of these processes require brine with low concentrations of impurities, primarily other chlorides that prevent direct use of RO concentrate in these processes. In addition, nearly half of the brine used by chemical manufacturers is produced from brine wells owned by the manufacturer and is not purchased on the open market (Ahuja and Howe, 2007). This may limit the opportunities for RO concentrate use as a source of supply for a chemical manufacturer.

3.2.6 Calcium Chloride

Purity Requirements

ASTM Standard D98 provides purity requirements for both dry and liquid calcium chloride. Purity requirements limit the amount of impurities, primarily other chlorides such as alkali chlorides and magnesium chlorides. Other limits on impurities are specific to the purchaser and the end use and are generally proprietary.

Dry calcium chloride is classified by grade, which is related to the minimum calcium chloride concentration. Grade 1 requires a minimum 77% concentration, Grade 2 requires a minimum 90% concentration, and Grade 3 requires a minimum 94% concentration. Liquid calcium chloride is typically provided to a purchaser in concentrations of 28 to 42%.

Obstacles to Use

Calcium chloride is extremely soluble and may be more difficult to obtain from RO concentrate than other salts. Calcium chloride obtained from RO concentrate would also have to meet the purity requirements of the potential end user, which could require additional refining steps to remove impurities. For example, calcium chloride used for dust control is hygroscopic, that is, it adsorbs moisture from the atmosphere. Brines high in sodium chloride do not have this quality and would be of limited value for dust control.

Another issue is that some states do not allow the use of concentrates for dust control and deicing. Colorado prohibits the use of concentrates for dust control and deicing and California requires new products to undergo extensive health and environmental testing before they can be placed in use (Jordahl, 2006).

3.3 Regional Use of Concentrate Products

Many of the salts found in RO concentrate have regional uses that may help with determining the potential marketability of the salt. For example, dry sodium chloride (rock salt) and calcium chloride are used extensively in cold climates for deicing and are not used in warmer climates, such as southern states and the desert southwest. Industrial uses of salts such as calcium carbonate in the paper and plastic industry and gypsum (calcium sulfate) may also have regional uses.

In an effort to correlate potential markets with locations of existing and future desalination plants, the following marketing regions were established and are described in the following.

Hot Arid Region

The Hot Arid Region includes New Mexico, west Texas, Arizona, inland California, and Nevada. Based on data from Jordahl (2006), there were a total of 62 desalination plants in this region, with the majority located in California and Texas.

This area is experiencing significant population growth and high water demand as well as scarce water resources. This region features high evaporation rates, low precipitation, and high annual average temperatures. The likelihood of inland desalination plants being constructed in this region is high due to limited supplies of potable water, frequent drought, and population growth. In addition, common concentrate disposal options such as deep well injection and evaporation ponds may be limited because of regulatory factors, geology, and cost and availability of land.

Cold Arid Region

The Cold Arid Region includes the states of Colorado, Wyoming, Montana, Idaho, and Utah and also parts of North and South Dakota, western Nebraska, and Kansas. On the basis of data from Jordahl (2006), there were a total of 14 desalination plants in this region.

This region is defined by areas at higher latitudes that receive low annual rainfall and have higher evaporation rates than humid areas. The state of Colorado, in particular, is experiencing high population growth and water demands, so that inland desalination plants are becoming a likely source of potable water. Concentrate disposal options in this region may also be limited due to low evaporation rates and restrictions on disposing to sanitary sewers. Geology may also limit deep well injection.

Warm and Humid Region

The Warm and Humid Region includes the Gulf Coast states, east Texas, Florida, Georgia, and North and South Carolina. This region has the largest concentration of existing desalination plants, with the vast majority being located in Florida. However, communities in coastal Georgia and South Carolina, where saltwater intrusion from the Atlantic Ocean is contaminating groundwater sources, are also considering or have in place desalination plants for treatment of brackish water. This region receives a significant amount of rain during the year and has relatively low annual evaporation rates. This region has rapidly growing population centers, which have resulted in the expansion of urban areas into rural areas that were sources of water for coastal communities.

Other U.S. Regions

The remaining areas of the United States include the Pacific Northwest, Appalachian states, and the Northeast/ New England states. These regions generally obtain water from surface sources or groundwater sources that are seen as plentiful. However, these areas have also experienced tremendous population growth in recent years, which has stressed existing water supplies.

3.4 Regional Markets

Marketing RO concentrate products will require an evaluation of potential markets in proximity to the existing and/or future RO treatment facility to determine if any current or planned industries would have a need for salt products. To facilitate this evaluation, a matrix of potential uses of RO concentrate salts and the regions where they may be used is presented in Table 15.

Table 15. Regional Brine Market Matrix

	Hot Arid Region	Cold Arid Region	Warm Humid Region	Other U.S. Regions
Calcium carbonate	Paper Glass Building materials	Paper Glass Building materials	Paper Glass Building materials	Paper Glass Building materials
Calcium sulfate (gypsum)	Wallboard Building materials Cement production	Wallboard Building materials Cement production	Wallboard Building materials Cement production	Wallboard Building materials Cement production
Sodium sulfate	Glass Detergents	Glass Detergents	Glass Detergents Textiles	Glass Detergents
Sodium carbonate (soda ash)	Glass Chemicals	Glass Chemicals	Glass Chemicals	Glass Chemicals
Sodium chloride	Chlor-alkali industry	Road salt Chlor-alkali industry	Chlor-alkali industry	Chlor-alkali industry
Calcium chloride	Dust control	Road salt Dust control	Dust control	Dust control

3.5 Synthetic Salt Production

All of the salts evaluated in this study can be mined in a brine form, produced synthetically by precipitation, or produced from the waste stream of another industrial process. The production of these chemicals from brine or waste streams is summarized in Table 16.

Table 16. Synthetic Salt Production Summary

Salt	Synthetic production by precipitation from brine and/or waste
Calcium carbonate	PCC made up 25% of the total U.S. market in 2009. PCC is made by the milk of lime process, which involves calcining limestone ($CaCO_3$) to make lime (CaO), dissolving the lime in water to form $Ca(OH)_2$, and then adding CO_2, which precipitates $CaCO_3$. Processes to remove impurities occur at several steps along the way. If the PCC is to be used in a paper mill or shipped to a latex paint plant, the slurry may be used directly. If it is to be used as a solid, the slurry is dewatered, dried, milled, and packaged.
Calcium sulfate	Synthetic calcium sulfate made up 25% of the total U.S. market in 2009[1]. Synthetic calcium sulfate is made as a waste product from flue gas desulfurization, in which the flue gas from a power plant is contacted with lime slurry in a wet scrubbing operation. The reaction between SO_2 gas in the flue gas and the lime produces a calcium sulfite ($CaSO_3$) precipitate. A subsequent forced oxidation process can convert the calcium sulfite to calcium sulfate.
Sodium sulfate	Synthetic sodium sulfate made up 50% of the U.S. market in 2009. It can be produced as a by-product of battery recycling and the production of chemicals such as hydrochloric acid, boric acid, rayon, and cellulose. Natural sodium sulfate can be produced directly from brine lakes.
Sodium carbonate (soda ash)	Whereas sodium carbonate is produced from trona in the United States, synthetic sodium carbonate (soda ash) is produced using the Solvay process in large quantities in Europe and other countries. The Solvay process combines sodium chloride (NaCl) and limestone ($CaCO_3$) to form sodium carbonate and calcium chloride according to the following overall reaction: $2\ NaCl + CaCO_3 \rightarrow Na_2CO_3 + CaCl_2$. The actual process is more complex and includes several intermediate steps and a significant amount of energy. Ammonia is required, but most of the ammonia is recycled through the process so that the actual addition of ammonia can be relatively small if losses are controlled.
Sodium chloride	Forty% of sodium chloride was produced by solution mining in the U.S. in 2008[2], and most of this is used in brine form by the industrial chemical industry. In addition, sodium chloride is precipitated from seawater or natural saline brines using solar evaporation and vacuum pan evaporation.
Calcium chloride	Produced synthetically by the Solvay process as noted previously.

[1]Kostick, 2010

[2]Kostick, January 2010

Synthetic salt production is very similar to the process of recovering salts from RO concentrate. As noted in Table 16, many of the salts in this study are produced from brine or waste streams from other processes. RO concentrate is a waste stream from a water treatment process that contains many of the salts used in other applications. This suggests that existing brine treatment and production processes in the chlor-alkali industry and other industries may be applicable to treatment of RO concentrate.

3.6 Market Analysis

The 2009 domestic production of the six recoverable RO concentrate salts evaluated in this study is presented in Table 17.

Table 17. Domestic Production of Selected Salts 2009

Salt	Volume Produced (tons/year)[1]
Calcium carbonate[2]	1,223,220,000
Calcium sulfate	34,272,200
Sodium sulfate	330,600
Sodium carbonate	12,011,800
Sodium chloride	50,692,000
Calcium chloride[3]	1,700,000
TOTAL	**1,332,226,600**

[1]Volume converted from metric tons to short tons
[2] As limestone
[3] 2004 production data. More recent data were not available.

As shown in Table 17, the salt industry produced over a billion tons of potentially recoverable salts in 2009. Although this quantity is partially skewed by the volume of calcium carbonate produced as limestone, the total quantity produced is still large. To put this quantity in perspective with the volume of salt produced by an RO plant, a 10 MGD RO plant using zero discharge technology (i.e., 100% recovery) treating water with a TDS of 5000 mg/L would generate approximately 80,000 tons per year of salt. This is less than one-tenth of 1% of the total volume of the salts listed in Table 17.

The comparatively small amount of salt produced in a year from a single treatment plant suggests that it would have a minimal impact if it was sold on the open market, because there are plentiful supplies of these salts produced each year. It may be possible to find a local user of the salt, such as a municipality that uses road salt or calcium chloride for deicing, or a chemical plant that could use the brine in a chlor-alkali process.

A potential problem associated with a RO plant as a salt supplier is that the plant may produce more salt than a municipality or industry can use. For instance, Colorado uses approximately 35,000 tons per year for deicing (CDM, 2009). This is less than half the salt produced by the 10-MGD plant discussed previously using a ZLD process. If the same plant was operating at 80% recovery, it would still generate more salt than the state could use in a year.

It should be noted that the types and concentrations of salts found in RO concentrate are dependent upon the concentrations of the constituents in the raw water stream and the treatment characteristics of the RO system and the ZLD system, if one is being used. It should also be noted that the ability to sell the salts at market price depends upon achieving the required purity in the recovery process.

Assuming a potential market or customer could be found for a recoverable salt, the potential revenue generated could offset disposal costs or be less costly than commonly used disposal methods such as evaporation ponds or deep well injection. Table 18 presents an estimate of the potential revenue that could be generated by recovering salts from the desalination plant described in the preceding paragraph, assuming a market could be obtained for the salt. The assumed percentages of each salt in the concentrate are

- Calcium carbonate—10%
- Calcium sulfate—20%
- Sodium sulfate—20%
- Sodium carbonate—10%
- Sodium chloride—30%
- Calcium chloride—10%

Table 18. Potential Annual Revenue from the Sale of Recoverable Salts[1]

Salt[2]	Annual Revenue[3]
Calcium carbonate	$494,650
Calcium sulfate	$129,370
Sodium sulfate	$1,932,940
Sodium carbonate	$2,073,725
Sodium chloride	$799,050
Calcium chloride	$1,522,000

[1]Assumptions: 10 MGD Plant, 100% recovery(ZLD process), 5000 mg/L TDS feed water.
[2]Dry form.
[3]Based on costs from 2009.

As shown in Table 18, the recoverable salts with the greatest potential revenue in the dry form are sodium carbonate (soda ash), calcium chloride, and sodium sulfate. It should be noted that sodium chloride brine has a very low market price of $8 per ton, which will reduce the potential revenue, as the value of dry sodium chloride is greater than that of the brine. However, sodium chloride brine should be easier to produce than dry salt and potentially easier to market, because it is used in the chlor-alkali industry and it is not uncommon for chlor-alkali producers to purchase brine from other sources for use.

A 10 MGD plant with a raw water TDS concentration of 5000 mg/L generates approximately 80,000 tons of solids per year. Assuming a landfill disposal cost of $50.00 per ton, the annual cost of disposing of these solids in a landfill would be $4,000,000. Thus, if the utility was able to give the RO concentrate to an industrial partner at no cost, the avoided cost of landfill disposal would result in significant savings.

3.7 Case Studies

Two case studies of future RO plants in which selective salt recovery was considered in the design of the facility are presented in the following two sections. Although neither plant has been constructed, the purpose of presenting the case studies is to illustrate the approaches to selective salt recovery that were considered for these future facilities. It is important to note that selective salt recovery was not the primary focus of these studies. However, data were obtained that can be used to give a utility an idea of the issues associated with planning a future plant with selective salt recovery.

In the case of Sandoval County, selective salt recovery using nanofiltation to recover sodium chloride brine was considered to offset the cost of operating the proposed 5-MGD treatment plant. The East

Cherry Creek project evaluated two ZLD technologies that could recover a large portion of the concentrate from a brackish water RO treatment system. The ZLD processes generate a dry salt that can be landfilled or possibly marketed. It is important to note that the purpose of the study was not to determine budget costs for a standard ZLD project. The effectiveness of ZLD processes is site-specific, as the quality of the brackish water has a profound effect on the operating conditions of the membrane processes.

3.7.1 Case Study 1—Sandoval County, NM 5-MGD Desalination Treatment Facility

In 2009, a pilot test was conducted on a brackish groundwater aquifer in Sandoval County, NM for potential use as a source of potable water. The county planned to design and eventually construct a 5-MGD treatment plant to meet future water demands in the area. The brackish water aquifer was 4000 ft below ground, was under artesian pressure, and had a temperature of 150 °F. The brackish groundwater contained high concentrations of dissolved solids (12,000 mg/L), hardness, arsenic, and radionuclides, as well as dissolved carbon dioxide and hydrogen sulfide gases. Although the primary objective of pilot testing was to identify the treatment processes required for producing potable water, a secondary objective was to identify treatment processes such that salts could be selectively recovered from the concentrate to facilitate disposal and allow beneficial reuse.

The results of pilot testing recommended pretreatment with aeration for gas removal, combined coagulation/sedimentation for arsenic reduction, and warm lime softening. Granular media filtration would follow the softening step, and a weak-acid-cation ion exchange process would serve as a polishing step before final treatment with RO. The numerous pretreatment processes before RO were necessary to remove arsenic and radionuclides as well as hardness and to prevent scaling of the RO membranes. The pretreatment processes also allowed potential beneficial reuse of the RO concentrate by removing many of the contaminants that would restrict potential use.

Pilot test data on the RO concentrate were evaluated to identify the composition of the waste stream and the potential beneficial reuse of recoverable salts. The RO brine concentrate consisted primarily of blended sodium chloride and sodium sulfate. A nanofiltration process was evaluated to determine if the sodium chloride could be recovered at a reasonable purity. Computer projections using Dow NF270 membranes indicated that 98% pure sodium chloride brine could be produced from a 5-MGD plant operating at 90% recovery. The sodium chloride brine would then be sent to a thermal brine concentrator and a crystallizer and possibly used in the treatment plant's sodium hypochlorite disinfection process, or possibly sold as road salt. The sodium sulfate waste stream was not evaluated to determine if a marketable product could be recovered from the waste brine stream.

The study concluded that the revenue generated by recovering and selling the sodium chloride and deep-well injection of the sodium sulfate brine would be more economical than the annual cost of RO concentrate disposal by deep well injection (UAM and CDM, 2009).

3.7.2 Case Study 2—East Cherry Creek Valley Water and Sanitation District Zero Liquid Discharge (ZLD) Pilot Study

In 2008, CDM conducted a pilot study on the concentrate stream from the town of Lochbuie, CO low-pressure reverse osmosis (LPRO) facility. Raw water being treated at the facility had a TDS concentration of 900 mg/L and the concentrate TDS was 3500 mg/L. The primary purpose of the pilot study was to evaluate the effectiveness of two ZLD treatment processes to increase water recovery:

high-recovery RO and vibratory shear enhanced process (VSEP). A secondary objective of the pilot test was to generate representative dry solids from concentrated brine wastes to determine their composition and ability to be landfilled or marketed as a usable product. Concentrate from the LPRO treatment plant was considered to be representative of many brackish RO projects with typical concentrations of calcium, magnesium, and sulfate and elevated levels of sodium, chloride, and silica.

Results of the pilot testing showed that the high-recovery RO system consistently achieved 94 to 95% recovery. The VSEP process was capable of achieving recoveries of 94 to 97%, but the process required continual permeate flushing and/or frequent chemical cleaning. The concentrated brine from both processes was sent to an evaporation basin. After the water was evaporated, the dried mixed salts from each process were analyzed to determine the mineral composition. The mineral composition of the salts generated from each ZLD process is

- High-recovery RO—Primarily sodium carbonates, but when fully dried, converted to halite (sodium chloride) and thenardite (sodium sulfate).
- VSEP—The concentrate from this process was saturated with calcium sulfate (gypsum) and halite (NaCl).

It should be noted that the composition of the dry salts will vary, based on the pretreatment process selected for the concentrate from an RO system.

It was concluded that the dried mixed salts had little commercial value because of the high percentage of sodium chloride in the mixture and the presence of many trace minerals. More complicated evaporation processes would possibly yield commercially valuable minerals; however, it is not likely that the cost of the additional processes would be offset by the value of the minerals recovered.

Section 4

Conclusions and Recommendations

The six recoverable salts discussed in this report are marketable, as there are many uses, as well as demand. Recovering dry salts and or/brine also has an economic benefit to the utility, as it would reduce the costs of disposal. However, there are numerous challenges to overcome in marketing the salts. These challenges are

- Existence and size of the local market
- Meeting purity requirements
- The volume of concentrate and/or salt produced at a RO plant may exceed market demand
- Plentiful natural sources of salts that reduce the market for salts obtained from RO concentrate
- Treatment costs associated with producing and marketing salts from RO concentrate
- The salts with the greatest market value (calcium chloride and sodium carbonate) and the salt with the largest market for use (sodium chloride) are among the most soluble of the salts and will be the most difficult and costly to recover
- Potential conflict between producing water as a utility and producing salt and/or brine as a price variable commodity

Another challenge facing a utility that is considering recovering and selling salts from RO concentrate is the lack of an existing market. Most successful marketing ventures are based on creating a product that meets a need. In the case of an RO plant marketing concentrate, the product (concentrate) already exists, and it is the market that needs creating. Also, many industries that use the salts are used to entering into long-term contracts with suppliers. Potential industries/users may not be inclined to change their source of supply, as there may be concerns with the form and purity of the salt and/or brine. A solution to the lack of an existing large-scale market is to look for a local, site specific market close to the RO plant that may have a use for one or more of the salts or the brine.

Meeting purity requirements is also a significant challenge. Most existing RO plants have established methods of disposing of concentrate (sanitary sewers, deep well injection, evaporation ponds) and would need to be modified to treat the concentrate to make it marketable. Although this is certainly possible using a series of ZLD processes, the capital cost of modifying the existing treatment plant would outweigh the benefit of recovering the salts. Also, ZLD processes have not been proven on the scale of a municipal water-treatment plant, although it is anticipated that these processes will become more economical as demand for higher recovery increases.

The possibility of incorporating ZLD technology and salt/brine recovery could be considered in the planning for a new RO plant similarly to the case studies discussed at the end of Section 3. The possibility of recovering concentrate salts and/or brine could be evaluated to offset the operations and maintenance cost of operating the plant or as a by-product of a ZLD process incorporated into the design to recover as much water as possible from the plant. It is

important to note that the feasibility of selective salt recovery is site-specific, as water quality varies from site to site, and a suitable market may not be available in the vicinity of the proposed treatment plant.

Although there are a number of challenges to selective salt recovery in the short term, in the long term selective salt recovery will become more viable. With an increasing demand for potable water, more seawater and inland brackish water desalination plants will be required and the issue of concentrate disposal will have to be addressed. As ZLD technologies become more cost-effective, the cost of processing the concentrate will also decrease, thus making selective salt recovery more viable. Selective salt recovery and maximizing water recovery are also a sustainable solution for concentrate disposal, which is an issue facing every RO treatment plant.

References

Abbazasadegan, Morteza; Peter Fox; Mostafa Kabiri Badir; et al. 2009. Inland Membrane Concentrate Treatment Strategies for Water Reclamation Systems. Water Research Foundation. Denver, Colorado.

Ahuja, Nishant and Dr. Kerry J. Howe, P.E. 2007. Controlled Precipitation and Beneficial Use of Concentrate to Increase Recovery of Inland Reverse Osmosis Systems. Department of Civil Engineering, University of New Mexico.

Camp, Dresser and Mc Kee (CDM). February 27 2009. East Cherry Creek Valley Water and Sanitation District Zero Liquid Discharge (ZLD) Pilot Study Draft Report.

Crangle, Robert D. Jr. 2010 US Geological Survey Mineral Commodity Statistics and Information: Gypsum. United States Department of the Interior.

Greeley, Alexandra. A Pinch of Controversy Shakes Up Dietary Salt. FDA Consumer Magazine. United States Food and Drug Administration.

Jordahl, Jim (Principal Investigator). 2006. Beneficial and Nontraditional Uses of Concentrate. WateReuse Foundation. Alexandria, Virginia.

Kostick, Dennis S. January 2010. US Geological Survey Minerals Yearbook: Salt[{Advance Release]. United States Department of the Interior.

Kostick, Dennis S. 2010. US Geological Survey Mineral Commodity Statistics and Information: Salt. United States Department of the Interior.

Kostick, Dennis S. 2010. US Geological Survey Mineral Commodity Statistics and Information: Sodium Sulfate. United States Department of the Interior.

Kostick, Dennis S. 2010. US Geological Survey Mineral Commodity Statistics and Information: Salt. United States Department of the Interior.

Kostick, Dennis S. 2010. US Geological Survey Mineral Commodity Statistics and Information: Soda Ash. United States Department of the Interior.

Maliva, Robert. 2006. Deep Well Injection for Concentrate Disposal. RO Roundtable Meeting. Camp Dresser and McKee (CDM).

Mickley, Michael. 2004. Review of Concentrate Management Options.

Mickley, Michael. 2008. Survey of High Recovery and Zero Liquid Discharge Technologies for Water Utilities. WateReuse Foundation. Alexandria, Virginia.

Severn Trent Services. March 2010. Chlor-Tec On-site Sodium Hypochlorite Generation System Engineering Design Considerations. Section I, Page 7.

Universal Asset Management and Camp, Dresser and McKee (CDM). December 15, 2009 Sandoval County Wholesale Water Supply Utility Desalination Treatment Facility DRAFT Preliminary Engineering Report.

Producer Websites:

- http://www.cargill.com/salt/
- http://www.compassminerals.com/products-services/salt-other-minerals.html
- http://www.k-plus-s.com/en/geschaeftsbereiche/gb-salz.html
- http:// www.famousminerals.net/calcium carbonate-calcit-powder.html
- http://www.jostchemical.com/chemicals/2745.html
- http://www.tetrachemicalseurope/Calcuim_Chloride_Process.aqf
- http://www.oxy.com/Our_Business/chemicals/Pages/chem_products_basic_Calcium chloride.aspx
- https://www.sriconsulting.com/CEH/Public/Reports/724.6000

Appendix C

Pilot Data Collection Forms

Daily Operations

	Morning	Evening	Morning	Evening	Morning	Evening	Morning	Evening
Date								
Time								
Feed Flow								
Feed pH								
Feed Conductivity								
Pressure Gauge 1								
Pressure Gauge 2								
Pressure Gauge 3								
Concencentrate 2B								
Effluent pH								
Effluent Conductivity								
Initials								

	Morning	Evening	Morning	Evening	Morning	Evening	Morning	Evening
Date								
Time								
Feed Flow								
Feed pH								
Feed Conductivity								
Pressure Gauge 1								
Pressure Gauge 2								
Pressure Gauge 3								
Concencentrate 2B								
Effluent pH								
Effluent Conductivity								
Initials								

Week 1

	Date	Time Start
Cycle 1		

Sample Location	Sample Type	Time	pH	Constituents to measured at UNM	Initials
S1	Feed Water			calcium, magnesium, sodium, potassium, carbonate, bicarbonate, chloride, nitrate, fluoride, sulfate	
S6	Regeneration Fluids			calcium, magnesium, sodium, potassium, carbonate, bicarbonate, chloride, nitrate, fluoride, sulfate	
S7	Regeneration Fluids			calcium, magnesium, sodium, potassium, carbonate, bicarbonate, chloride, nitrate, fluoride, sulfate	
Precipitation bucket after precipitation– no pH adjustment	Supernatant			calcium, magnesium, sodium, potassium, carbonate, bicarbonate, chloride, nitrate, fluoride, sulfate	
Precipitation bucket after precipitation– no pH adjustment	Solid			SEM, EDS (relative elemental composition), XRD (presence of known crystal phases), mass	
Precipitation bucket after precipitation – low pH condition	Supernatant			calcium, magnesium, sodium, potassium, carbonate, bicarbonate, chloride, nitrate, fluoride, sulfate	
Precipitation bucket after precipitation – low pH condition	Solid			SEM, EDS (relative elemental composition), XRD (presence of known crystal phases), mass	
Precipitation bucket after precipitation – high pH condition	Supernatant			calcium, magnesium, sodium, potassium, carbonate, bicarbonate, chloride, nitrate, fluoride, sulfate	
Precipitation bucket after precipitation – high pH condition	Solid			SEM, EDS (relative elemental composition), XRD (presence of known crystal phases), mass	

Week 1

	Date	Time Start
Cycle 2		

Sample Location	Sample Type	Time	pH	Constituents to measured at UNM	Initials
S1	Feed Water			calcium, magnesium, sodium, potassium, carbonate, bicarbonate, chloride, nitrate, fluoride, sulfate	
S6	Regeneration Fluids			calcium, magnesium, sodium, potassium, carbonate, bicarbonate, chloride, nitrate, fluoride, sulfate	
S7	Regeneration Fluids			calcium, magnesium, sodium, potassium, carbonate, bicarbonate, chloride, nitrate, fluoride, sulfate	
Precipitation bucket after precipitation– no pH adjustment	Supernatant			calcium, magnesium, sodium, potassium, carbonate, bicarbonate, chloride, nitrate, fluoride, sulfate	
Precipitation bucket after precipitation– no pH adjustment	Solid			SEM, EDS (relative elemental composition), XRD (presence of known crystal phases), mass	
Precipitation bucket after precipitation – low pH condition	Supernatant			calcium, magnesium, sodium, potassium, carbonate, bicarbonate, chloride, nitrate, fluoride, sulfate	
Precipitation bucket after precipitation – low pH condition	Solid			SEM, EDS (relative elemental composition), XRD (presence of known crystal phases), mass	
Precipitation bucket after precipitation – high pH condition	Supernatant			calcium, magnesium, sodium, potassium, carbonate, bicarbonate, chloride, nitrate, fluoride, sulfate	
Precipitation bucket after precipitation – high pH condition	Solid			SEM, EDS (relative elemental composition), XRD (presence of known crystal phases), mass	

Week 2

	Date	Time Start	Time - End of Op Cycle	Time - Regen Start
Cycle 1				

Sample Location	**Sample Type**	**Time**	**Time into cycle**	**pH**	**Constituents to measured at UNM**	**Initials**
S1	Feed Water				calcium, magnesium, sodium, potassium, carbonate, bicarbonate, chloride, nitrate, fluoride, sulfate	
S6	Regeneration Fluids				calcium, magnesium, sodium, potassium, carbonate, bicarbonate, chloride, nitrate, fluoride, sulfate	
S7	Regeneration Fluids				calcium, magnesium, sodium, potassium, carbonate, bicarbonate, chloride, nitrate, fluoride, sulfate	
Precipitation bucket after precipitation– no pH adjustment	Supernatant				calcium, magnesium, sodium, potassium, carbonate, bicarbonate, chloride, nitrate, fluoride, sulfate	
Precipitation bucket after precipitation– no pH adjustment	Solid				SEM, EDS (relative elemental composition), XRD (presence of known crystal phases), mass	
Precipitation bucket after precipitation – low pH condition	Solid				SEM, EDS (relative elemental composition), XRD (presence of known crystal phases), mass	
Precipitation bucket after precipitation – high pH condition	Supernatant				calcium, magnesium, sodium, potassium, carbonate, bicarbonate, chloride, nitrate, fluoride, sulfate	
Precipitation bucket after precipitation – high pH condition	Solid				SEM, EDS (relative elemental composition), XRD (presence of known crystal phases), mass	

Week 2

	Date	Time Start	Time - End of Op Cycle	Time - Regen Start
Cycle 2				

Sample Location	Sample Type	Time	Time into cycle	pH	Constituents to measured at UNM	Initials
S1	Feed Water				calcium, magnesium, sodium, potassium, carbonate, bicarbonate, chloride, nitrate, fluoride, sulfate	
Top of SBA column	Resin Sample				carbonate, bicarbonate, chloride, nitrate, fluoride, sulfate, TOC	
S2	Regeneration Fluids		15 ☐			
			20 ☐			
			25 ☐			
			30 ☐			
			35 ☐			
			40 ☐			
			45 ☐			
S3	Regeneration Fluids		15 ☐			
			20 ☐			
			25 ☐			
			30 ☐			
			35 ☐			
			40 ☐			
			45 ☐			
S6	Regeneration Fluids				calcium, magnesium, sodium, potassium, carbonate, bicarbonate, chloride, nitrate, fluoride, sulfate	
S7	Regeneration Fluids				calcium, magnesium, sodium, potassium, carbonate, bicarbonate, chloride, nitrate, fluoride, sulfate	
Precipitation bucket after precipitation– no pH adjustment	Supernatant				calcium, magnesium, sodium, potassium, carbonate, bicarbonate, chloride, nitrate, fluoride, sulfate	
Precipitation bucket after precipitation– no pH adjustment	Solid				SEM, EDS (relative elemental composition), XRD (presence of known crystal phases), mass	
Precipitation bucket after precipitation – low pH condition	Solid				SEM, EDS (relative elemental composition), XRD (presence of known crystal phases), mass	
Precipitation bucket after precipitation – high pH condition	Supernatant				calcium, magnesium, sodium, potassium, carbonate, bicarbonate, chloride, nitrate, fluoride, sulfate	
Precipitation bucket after precipitation – high pH condition	Solid				SEM, EDS (relative elemental composition), XRD (presence of known crystal phases), mass	

Week 2

	Date	Time Start	Time - End of Op Cycle	Time - Regen Start
Cycle 3				

Sample Location	Sample Type	Time	Time into cycle	pH	Constituents to measured at UNM	Initials
S1	Feed Water				calcium, magnesium, sodium, potassium, carbonate, bicarbonate, chloride, nitrate, fluoride, sulfate	
Top of SBA column	Resin Sample				carbonate, bicarbonate, chloride, nitrate, fluoride, sulfate, TOC	
S2	Regeneration Fluids		15 ☐			
			20 ☐			
			25 ☐			
			30 ☐			
			35 ☐			
			40 ☐			
			45 ☐			
S3	Regeneration Fluids		15 ☐			
			20 ☐			
			25 ☐			
			30 ☐			
			35 ☐			
			40 ☐			
			45 ☐			
S6	Regeneration Fluids				calcium, magnesium, sodium, potassium, carbonate, bicarbonate, chloride, nitrate, fluoride, sulfate	
S7	Regeneration Fluids				calcium, magnesium, sodium, potassium, carbonate, bicarbonate, chloride, nitrate, fluoride, sulfate	
Precipitation bucket after precipitation– no pH adjustment	Supernatant				calcium, magnesium, sodium, potassium, carbonate, bicarbonate, chloride, nitrate, fluoride, sulfate	
Precipitation bucket after precipitation– no pH adjustment	Solid				SEM, EDS (relative elemental composition), XRD (presence of known crystal phases), mass	
Precipitation bucket after precipitation – low pH condition	Solid				SEM, EDS (relative elemental composition), XRD (presence of known crystal phases), mass	
Precipitation bucket after precipitation – high pH condition	Supernatant				calcium, magnesium, sodium, potassium, carbonate, bicarbonate, chloride, nitrate, fluoride, sulfate	
Precipitation bucket after precipitation – high pH condition	Solid				SEM, EDS (relative elemental composition), XRD (presence of known crystal phases), mass	

Week 3

	Date	Time Start	Time - End of Op Cycle	Time - Regen Start
Cycle 1				

Sample Location	Sample Type	Time	pH	Constituents to measured at UNM	Initials
S1	Feed Water			calcium, magnesium, sodium, potassium, carbonate, bicarbonate, chloride, nitrate, fluoride, sulfate	
Top of SBA column	Resin Sample			carbonate, bicarbonate, chloride, nitrate, fluoride, sulfate, TOC	
S6	Regeneration Fluids			calcium, magnesium, sodium, potassium, carbonate, bicarbonate, chloride, nitrate, fluoride, sulfate	
S7	Regeneration Fluids			calcium, magnesium, sodium, potassium, carbonate, bicarbonate, chloride, nitrate, fluoride, sulfate	
Precipitation bucket after precipitation– no pH adjustment	Supernatant			calcium, magnesium, sodium, potassium, carbonate, bicarbonate, chloride, nitrate, fluoride, sulfate	
Precipitation bucket after precipitation– no pH adjustment	Solid			SEM, EDS (relative elemental composition), XRD (presence of known crystal phases), mass	
Precipitation bucket after precipitation – low pH condition	Supernatant			calcium, magnesium, sodium, potassium, carbonate, bicarbonate, chloride, nitrate, fluoride, sulfate	
Precipitation bucket after precipitation – low pH condition	Solid			SEM, EDS (relative elemental composition), XRD (presence of known crystal phases), mass	
Precipitation bucket after precipitation – high pH condition	Supernatant			calcium, magnesium, sodium, potassium, carbonate, bicarbonate, chloride, nitrate, fluoride, sulfate	
Precipitation bucket after precipitation – high pH condition	Solid			SEM, EDS (relative elemental composition), XRD (presence of known crystal phases), mass	

Week 3

	Date	Time Start	Time - End of Op Cycle	Time - Regen Start
Cycle 2				

Sample Location	Sample Type	Time	pH	Constituents to measured at UNM	Initials
S1	Feed Water			calcium, magnesium, sodium, potassium, carbonate, bicarbonate, chloride, nitrate, fluoride, sulfate	
Top of SBA column	Resin Sample			carbonate, bicarbonate, chloride, nitrate, fluoride, sulfate, TOC	
S6	Regeneration Fluids			calcium, magnesium, sodium, potassium, carbonate, bicarbonate, chloride, nitrate, fluoride, sulfate	
S7	Regeneration Fluids			calcium, magnesium, sodium, potassium, carbonate, bicarbonate, chloride, nitrate, fluoride, sulfate	
Precipitation bucket after precipitation– no pH adjustment	Supernatant			calcium, magnesium, sodium, potassium, carbonate, bicarbonate, chloride, nitrate, fluoride, sulfate	
Precipitation bucket after precipitation– no pH adjustment	Solid			SEM, EDS (relative elemental composition), XRD (presence of known crystal phases), mass	
Precipitation bucket after precipitation – low pH condition	Supernatant			calcium, magnesium, sodium, potassium, carbonate, bicarbonate, chloride, nitrate, fluoride, sulfate	
Precipitation bucket after precipitation – low pH condition	Solid			SEM, EDS (relative elemental composition), XRD (presence of known crystal phases), mass	
Precipitation bucket after precipitation – high pH condition	Supernatant			calcium, magnesium, sodium, potassium, carbonate, bicarbonate, chloride, nitrate, fluoride, sulfate	
Precipitation bucket after precipitation – high pH condition	Solid			SEM, EDS (relative elemental composition), XRD (presence of known crystal phases), mass	

Week 3

	Date	Time Start	Time - End of Op Cycle	Time - Regen Start
Cycle 3				

Sample Location	Sample Type	Time	pH	Constituents to measured at UNM	Initials
S1	Feed Water			calcium, magnesium, sodium, potassium, carbonate, bicarbonate, chloride, nitrate, fluoride, sulfate	
Top of SBA column	Resin Sample			carbonate, bicarbonate, chloride, nitrate, fluoride, sulfate, TOC	
S6	Regeneration Fluids			calcium, magnesium, sodium, potassium, carbonate, bicarbonate, chloride, nitrate, fluoride, sulfate	
S7	Regeneration Fluids			calcium, magnesium, sodium, potassium, carbonate, bicarbonate, chloride, nitrate, fluoride, sulfate	
Precipitation bucket after precipitation– no pH adjustment	Supernatant			calcium, magnesium, sodium, potassium, carbonate, bicarbonate, chloride, nitrate, fluoride, sulfate	
Precipitation bucket after precipitation– no pH adjustment	Solid			SEM, EDS (relative elemental composition), XRD (presence of known crystal phases), mass	
Precipitation bucket after precipitation – low pH condition	Supernatant			calcium, magnesium, sodium, potassium, carbonate, bicarbonate, chloride, nitrate, fluoride, sulfate	
Precipitation bucket after precipitation – low pH condition	Solid			SEM, EDS (relative elemental composition), XRD (presence of known crystal phases), mass	
Precipitation bucket after precipitation – high pH condition	Supernatant			calcium, magnesium, sodium, potassium, carbonate, bicarbonate, chloride, nitrate, fluoride, sulfate	
Precipitation bucket after precipitation – high pH condition	Solid			SEM, EDS (relative elemental composition), XRD (presence of known crystal phases), mass	

Week 4

	Date	Time Start	Time - End of Op Cycle	Time - Regen Start
Cycle 1				

Sample Location	Sample Type	Time	pH	Constituents to measured at UNM	Initials
S1	Feed Water			calcium, magnesium, sodium, potassium, carbonate, bicarbonate, chloride, nitrate, fluoride, sulfate	
Top of SBA column	Resin Sample			carbonate, bicarbonate, chloride, nitrate, fluoride, sulfate, TOC	
S6	Regeneration Fluids			calcium, magnesium, sodium, potassium, carbonate, bicarbonate, chloride, nitrate, fluoride, sulfate	
S7	Regeneration Fluids			calcium, magnesium, sodium, potassium, carbonate, bicarbonate, chloride, nitrate, fluoride, sulfate	
Precipitation bucket after precipitation– no pH adjustment	Supernatant			calcium, magnesium, sodium, potassium, carbonate, bicarbonate, chloride, nitrate, fluoride, sulfate	
Precipitation bucket after precipitation– no pH adjustment	Solid			SEM, EDS (relative elemental composition), XRD (presence of known crystal phases), mass	
Precipitation bucket after precipitation – low pH condition	Supernatant			calcium, magnesium, sodium, potassium, carbonate, bicarbonate, chloride, nitrate, fluoride, sulfate	
Precipitation bucket after precipitation – low pH condition	Solid			SEM, EDS (relative elemental composition), XRD (presence of known crystal phases), mass	
Precipitation bucket after precipitation – high pH condition	Supernatant			calcium, magnesium, sodium, potassium, carbonate, bicarbonate, chloride, nitrate, fluoride, sulfate	
Precipitation bucket after precipitation – high pH condition	Solid			SEM, EDS (relative elemental composition), XRD (presence of known crystal phases), mass	

Week 4

	Date	Time Start	Time - End of Op Cycle	Time - Regen Start
Cycle 2				

Sample Location	Sample Type	Time	pH	Constituents to measured at UNM	Initials
S1	Feed Water			calcium, magnesium, sodium, potassium, carbonate, bicarbonate, chloride, nitrate, fluoride, sulfate	
Top of SBA column	Resin Sample			carbonate, bicarbonate, chloride, nitrate, fluoride, sulfate, TOC	
S6	Regeneration Fluids			calcium, magnesium, sodium, potassium, carbonate, bicarbonate, chloride, nitrate, fluoride, sulfate	
S7	Regeneration Fluids			calcium, magnesium, sodium, potassium, carbonate, bicarbonate, chloride, nitrate, fluoride, sulfate	
Precipitation bucket after precipitation– no pH adjustment	Supernatant			calcium, magnesium, sodium, potassium, carbonate, bicarbonate, chloride, nitrate, fluoride, sulfate	
Precipitation bucket after precipitation– no pH adjustment	Solid			SEM, EDS (relative elemental composition), XRD (presence of known crystal phases), mass	
Precipitation bucket after precipitation – low pH condition	Supernatant			calcium, magnesium, sodium, potassium, carbonate, bicarbonate, chloride, nitrate, fluoride, sulfate	
Precipitation bucket after precipitation – low pH condition	Solid			SEM, EDS (relative elemental composition), XRD (presence of known crystal phases), mass	
Precipitation bucket after precipitation – high pH condition	Supernatant			calcium, magnesium, sodium, potassium, carbonate, bicarbonate, chloride, nitrate, fluoride, sulfate	
Precipitation bucket after precipitation – high pH condition	Solid			SEM, EDS (relative elemental composition), XRD (presence of known crystal phases), mass	

Week 4

	Date	Time Start	Time - End of Op Cycle	Time - Regen Start
Cycle 3				

Sample Location	Sample Type	Time	pH	Constituents to measured at UNM	Initials
S1	Feed Water			calcium, magnesium, sodium, potassium, carbonate, bicarbonate, chloride, nitrate, fluoride, sulfate	
Top of SBA column	Resin Sample			carbonate, bicarbonate, chloride, nitrate, fluoride, sulfate, TOC	
S6	Regeneration Fluids			calcium, magnesium, sodium, potassium, carbonate, bicarbonate, chloride, nitrate, fluoride, sulfate	
S7	Regeneration Fluids			calcium, magnesium, sodium, potassium, carbonate, bicarbonate, chloride, nitrate, fluoride, sulfate	
Precipitation bucket after precipitation– no pH adjustment	Supernatant			calcium, magnesium, sodium, potassium, carbonate, bicarbonate, chloride, nitrate, fluoride, sulfate	
Precipitation bucket after precipitation– no pH adjustment	Solid			SEM, EDS (relative elemental composition), XRD (presence of known crystal phases), mass	
Precipitation bucket after precipitation – low pH condition	Supernatant			calcium, magnesium, sodium, potassium, carbonate, bicarbonate, chloride, nitrate, fluoride, sulfate	
Precipitation bucket after precipitation – low pH condition	Solid			SEM, EDS (relative elemental composition), XRD (presence of known crystal phases), mass	
Precipitation bucket after precipitation – high pH condition	Supernatant			calcium, magnesium, sodium, potassium, carbonate, bicarbonate, chloride, nitrate, fluoride, sulfate	
Precipitation bucket after precipitation – high pH condition	Solid			SEM, EDS (relative elemental composition), XRD (presence of known crystal phases), mass	

Week 5

	Date	Time Start	Time - End of Op Cycle	Time - Regen Start
Cycle 1				

Sample Location	**Sample Type**	**Time**	**pH**	**Constituents to**	**Initials**
S1	Feed Water			calcium, magnesium, sodium, potassium, carbonate, bicarbonate,	
S6	Regeneration Fluids			calcium, magnesium, sodium, potassium, carbonate, bicarbonate,	
S7	Regeneration Fluids			calcium, magnesium, sodium, potassium, carbonate, bicarbonate,	
Precipitation bucket after precipitation– no pH adjustment	Supernatant			calcium, magnesium, sodium, potassium, carbonate, bicarbonate,	
Precipitation bucket after precipitation– no pH adjustment	Solid			SEM, EDS (relative elemental composition), XRD	
Precipitation bucket after precipitation – low pH condition	Solid			SEM, EDS (relative elemental composition), XRD	
Precipitation bucket after precipitation – high pH condition	Supernatant			calcium, magnesium, sodium, potassium, carbonate, bicarbonate,	
Precipitation bucket after precipitation – high pH condition	Solid			SEM, EDS (relative elemental composition), XRD	

Week 5

	Date	Time Start	Time - End of Op Cycle	Time - Regen Start
Cycle 2				

Sample Location	Sample Type	Time	Time into cycle	pH	Constituents to measured at UNM	Initials
S1	Feed Water				calcium, magnesium, sodium, potassium, carbonate, bicarbonate, chloride, nitrate, fluoride, sulfate	
S2	Regeneration Fluids		15 ☐			
			20 ☐			
			25 ☐			
			30 ☐			
			35 ☐			
			40 ☐			
			45 ☐			
S3	Regeneration Fluids		15 ☐			
			20 ☐			
			25 ☐			
			30 ☐			
			35 ☐			
			40 ☐			
			45 ☐			
S6	Regeneration Fluids				calcium, magnesium, sodium, potassium, carbonate, bicarbonate, chloride, nitrate, fluoride, sulfate	
S7	Regeneration Fluids				calcium, magnesium, sodium, potassium, carbonate, bicarbonate, chloride, nitrate, fluoride, sulfate	
Precipitation bucket after precipitation– no pH adjustment	Supernatant				calcium, magnesium, sodium, potassium, carbonate, bicarbonate, chloride, nitrate, fluoride, sulfate	
Precipitation bucket after precipitation– no pH adjustment	Solid				SEM, EDS (relative elemental composition), XRD (presence of known crystal phases), mass	
Precipitation bucket after precipitation – low pH condition	Solid				SEM, EDS (relative elemental composition), XRD (presence of known crystal phases), mass	
Precipitation bucket after precipitation – high pH condition	Supernatant				calcium, magnesium, sodium, potassium, carbonate, bicarbonate, chloride, nitrate, fluoride, sulfate	
Precipitation bucket after precipitation – high pH condition	Solid				SEM, EDS (relative elemental composition), XRD (presence of known crystal phases), mass	

Week 5

	Date	Time Start	Time - End of Op Cycle	Time - Regen Start
Cycle 3				

Sample Location	Sample Type	Time	Time into cycle	pH	Constituents to measured at UNM	Initials
S1	Feed Water				calcium, magnesium, sodium, potassium, carbonate, bicarbonate, chloride, nitrate, fluoride, sulfate	
S2	Regeneration Fluids		15 ☐			
			20 ☐			
			25 ☐			
			30 ☐			
			35 ☐			
			40 ☐			
			45 ☐			
S3	Regeneration Fluids		15 ☐			
			20 ☐			
			25 ☐			
			30 ☐			
			35 ☐			
			40 ☐			
			45 ☐			
S6	Regeneration Fluids				calcium, magnesium, sodium, potassium, carbonate, bicarbonate, chloride, nitrate, fluoride, sulfate	
S7	Regeneration Fluids				calcium, magnesium, sodium, potassium, carbonate, bicarbonate, chloride, nitrate, fluoride, sulfate	
Precipitation bucket after precipitation– no pH adjustment	Supernatant				calcium, magnesium, sodium, potassium, carbonate, bicarbonate, chloride, nitrate, fluoride, sulfate	
Precipitation bucket after precipitation– no pH adjustment	Solid				SEM, EDS (relative elemental composition), XRD (presence of known crystal phases), mass	
Precipitation bucket after precipitation – low pH condition	Solid				SEM, EDS (relative elemental composition), XRD (presence of known crystal phases), mass	
Precipitation bucket after precipitation – high pH condition	Supernatant				calcium, magnesium, sodium, potassium, carbonate, bicarbonate, chloride, nitrate, fluoride, sulfate	
Precipitation bucket after precipitation – high pH condition	Solid				SEM, EDS (relative elemental composition), XRD (presence of known crystal phases), mass	

Week 6

	Date	Time Start	Time - End of Op Cycle	Time - Regen Start
Cycle 1				

Sample Location	Sample Type	Time	pH	Constituents to measured at UNM	Initials
S1	Feed Water			calcium, magnesium, sodium, potassium, carbonate, bicarbonate, chloride, nitrate, fluoride, sulfate	
S6	Regeneration Fluids			calcium, magnesium, sodium, potassium, carbonate, bicarbonate, chloride, nitrate, fluoride, sulfate	
S7	Regeneration Fluids			calcium, magnesium, sodium, potassium, carbonate, bicarbonate, chloride, nitrate, fluoride, sulfate	
Precipitation bucket after precipitation– no pH adjustment	Supernatant			calcium, magnesium, sodium, potassium, carbonate, bicarbonate, chloride, nitrate, fluoride, sulfate	
Precipitation bucket after precipitation– no pH adjustment	Solid			SEM, EDS (relative elemental composition), XRD (presence of known crystal phases), mass	
Precipitation bucket after precipitation – low pH condition	Supernatant			calcium, magnesium, sodium, potassium, carbonate, bicarbonate, chloride, nitrate, fluoride, sulfate	
Precipitation bucket after precipitation – low pH condition	Solid			SEM, EDS (relative elemental composition), XRD (presence of known crystal phases), mass	
Precipitation bucket after precipitation – high pH condition	Supernatant			calcium, magnesium, sodium, potassium, carbonate, bicarbonate, chloride, nitrate, fluoride, sulfate	
Precipitation bucket after precipitation – high pH condition	Solid			SEM, EDS (relative elemental composition), XRD (presence of known crystal phases), mass	

Week 6

	Date	Time Start	Time - End of Op Cycle	Time - Regen Start
Cycle 2				

Sample Location	**Sample Type**	**Time**	**pH**	**Constituents to measured at UNM**	**Initials**
S1	Feed Water			calcium, magnesium, sodium, potassium, carbonate, bicarbonate, chloride, nitrate, fluoride, sulfate	
S6	Regeneration Fluids			calcium, magnesium, sodium, potassium, carbonate, bicarbonate, chloride, nitrate, fluoride, sulfate	
S7	Regeneration Fluids			calcium, magnesium, sodium, potassium, carbonate, bicarbonate, chloride, nitrate, fluoride, sulfate	
Precipitation bucket after precipitation– no pH adjustment	Supernatant			calcium, magnesium, sodium, potassium, carbonate, bicarbonate, chloride, nitrate, fluoride, sulfate	
Precipitation bucket after precipitation– no pH adjustment	Solid			SEM, EDS (relative elemental composition), XRD (presence of known crystal phases), mass	
Precipitation bucket after precipitation – low pH condition	Supernatant			calcium, magnesium, sodium, potassium, carbonate, bicarbonate, chloride, nitrate, fluoride, sulfate	
Precipitation bucket after precipitation – low pH condition	Solid			SEM, EDS (relative elemental composition), XRD (presence of known crystal phases), mass	
Precipitation bucket after precipitation – high pH condition	Supernatant			calcium, magnesium, sodium, potassium, carbonate, bicarbonate, chloride, nitrate, fluoride, sulfate	
Precipitation bucket after precipitation – high pH condition	Solid			SEM, EDS (relative elemental composition), XRD (presence of known crystal phases), mass	

Week 6

	Date	Time Start	Time - End of Op Cycle	Time - Regen Start
Cycle 3				

Sample Location	Sample Type	Time	pH	Constituents to measured at UNM	Initials
S1	Feed Water			calcium, magnesium, sodium, potassium, carbonate, bicarbonate, chloride, nitrate, fluoride, sulfate	
S6	Regeneration Fluids			calcium, magnesium, sodium, potassium, carbonate, bicarbonate, chloride, nitrate, fluoride, sulfate	
S7	Regeneration Fluids			calcium, magnesium, sodium, potassium, carbonate, bicarbonate, chloride, nitrate, fluoride, sulfate	
Precipitation bucket after precipitation– no pH adjustment	Supernatant			calcium, magnesium, sodium, potassium, carbonate, bicarbonate, chloride, nitrate, fluoride, sulfate	
Precipitation bucket after precipitation– no pH adjustment	Solid			SEM, EDS (relative elemental composition), XRD (presence of known crystal phases), mass	
Precipitation bucket after precipitation – low pH condition	Supernatant			calcium, magnesium, sodium, potassium, carbonate, bicarbonate, chloride, nitrate, fluoride, sulfate	
Precipitation bucket after precipitation – low pH condition	Solid			SEM, EDS (relative elemental composition), XRD (presence of known crystal phases), mass	
Precipitation bucket after precipitation – high pH condition	Supernatant			calcium, magnesium, sodium, potassium, carbonate, bicarbonate, chloride, nitrate, fluoride, sulfate	
Precipitation bucket after precipitation – high pH condition	Solid			SEM, EDS (relative elemental composition), XRD (presence of known crystal phases), mass	

RO Data

Date	Time	Feed Pressure	Concentrate Pressure	Concentrate Flow	Permeate Flow	Feed Temp	Feed Conductivty	Feed pH	Concentrate Temp	Feed Conductivty	Feed pH	Initials
		psi	psi	gpm	gpm	°C	mS/cm		°C	mS/cm		

Appendix D

ESPA-2 Datasheet

NITTO DENKO

HYDRANAUTICS
www.membranes.com
A Nitto Denko Company

Membrane Element ESPA2-LD-4040
(Low Fouling Technology)

Performance:	Permeate Flow:	2,000 gpd (7.57 m^3/d)
	Salt Rejection:	99.6 % (99.4 % minimum)
Type	Configuration:	Low Fouling Spiral Wound
	Membrane Polymer:	Composite Polyamide
	Membrane Active Area:	80 ft^2 (7.43 m^2)
	Feed Spacer:	34 mil (0.864 mm) with biostatic agent
Application Data*	Maximum Applied Pressure:	600 psig (4.16 MPa)
	Maximum Chlorine Concentration:	< 0.1 PPM
	Maximum Operating Temperature:	113 °F (45 °C)
	pH Range, Continuous (Cleaning):	2-11 (1-13)*
	Maximum Feedwater Turbidity:	1.0 NTU
	Maximum Feedwater SDI (15 mins):	5.0
	Maximum Feed Flow:	16 GPM (3.6 m^3/h)
	Minimum Ratio of Concentrate to Permeate Flow for any Element:	5:1
	Maximum Pressure Drop for Each Element:	10 psi

***** The limitations shown here are for general use. For specific projects, operating at more conservative values may ensure the best performance and longest life of the membrane. See Hydranautics Technical Bulletins for more detail on operation limits, cleaning pH, and cleaning temperatures.

Test Conditions

The stated performance is initial (data taken after 30 minutes of operation), based on the following conditions:

1500 PPM NaCl solution
150 psi (1.05 MPa) Applied Pressure
77 °F (25 °C) Operating Temperature
15% Permeate Recovery
6.5 - 7.0 pH Range

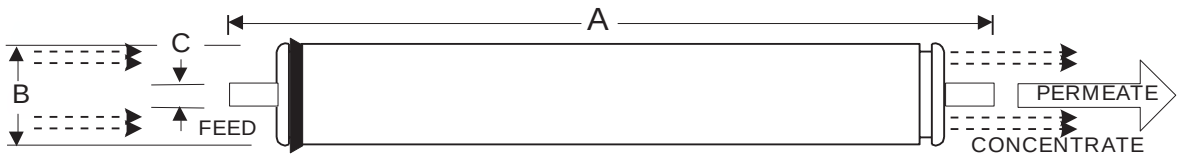

A, inches (mm)	B, inches (mm)	C, inches (mm)	Weight, lbs. (kg)
40.0 (1016)	3.95 (100.3)	0.75 (19.1)	8 (3.6)

Core tube extension = 1.05" (26.7 mm)

Notice: Permeate flow for individual elements may vary + or - 20 percent. All membrane elements are supplied with a brine seal, interconnector, and o-rings. Elements are enclosed in a sealed polyethylene bag containing less than 1.0% sodium meta-bisulfite solution, and then packaged in a cardboard box.

Hydranautics Corporate: 401 Jones Road, Oceanside, CA 92058
1-800-CPA-PURE Phone: 760-901-2500 Fax: 760-901-2578 info@hydranautics.com

Advancing the Science of Water Reuse and Desalination

WATEREUSE RESEARCH

1199 North Fairfax Street, Suite 410
Alexandria, VA 22314 USA
(703) 548-0880
Fax (703) 548-5085
E-mail: Foundation@WateReuse.org
www.WateReuse.org/Foundation